

Mississippi State University

Scholars Junction

Theses and Dissertations

Theses and Dissertations

5-17-2014

Synthesis of Bio-Based Polymers Containing D-Isosorbide by Ring-Opening Metathesis Polymerization

Chinni Yalamanchili

Follow this and additional works at: <https://scholarsjunction.msstate.edu/td>

Recommended Citation

Yalamanchili, Chinni, "Synthesis of Bio-Based Polymers Containing D-Isosorbide by Ring-Opening Metathesis Polymerization" (2014). *Theses and Dissertations*. 4190.
<https://scholarsjunction.msstate.edu/td/4190>

This Graduate Thesis - Open Access is brought to you for free and open access by the Theses and Dissertations at Scholars Junction. It has been accepted for inclusion in Theses and Dissertations by an authorized administrator of Scholars Junction. For more information, please contact scholcomm@msstate.libanswers.com.

Synthesis of bio-based polymers containing D-isosorbide by ring-opening metathesis
polymerization

By

Chinni Yalamanchili

A Thesis
Submitted to the Faculty of
Mississippi State University
in Partial Fulfillment of the Requirements
for the Degree of Master of Science
in Chemistry
in the Department of Chemistry

Mississippi State, Mississippi

May 2014

Copyright by
Chinni Yalamanchili
2014

Synthesis of bio-based polymers containing D-isosorbide by ring-opening metathesis
polymerization

By

Chinni Yalamanchili

Approved:

Gerald Rowland
(Major Professor)

Charles U. Pittman, Jr.
(Director of Thesis)

Keisha B. Walters
(Committee Member)

David Wipf
(Committee Member)

Stephen C. Foster
(Graduate Coordinator)

R. Gregory Dunaway
Professor and Dean
College of Arts & Sciences

Name: Chinni Yalamanchili

Date of Degree: May 17, 2014

Institution: Mississippi State University

Major Field: Chemistry

Major Professor: Gerald Rowland

Title of Study: Synthesis of bio-based polymers containing D-isosorbide by ring-opening metathesis polymerization

Pages in Study: 164

Candidate for Degree of Master of Science

The utilization of renewable sources as alternatives for petroleum and natural gas products has immense commercial, health and global warming significance. D-Isosorbide (**2**) is a bifunctional, polar, chiral and rigid molecule, which is produced from renewable sources. Synthesis of new polymers containing **2** is of interest for polymers and in drug delivery. The aim of the present work is to synthesize various polymers (homo- and copolymers) containing **2** via the olefin metathesis routes, ring-opening metathesis polymerization (ROMP) and acyclic-diene metathesis polymerization (ADMET). *N*-Phenyl-7-oxanorbornene-dicarboximide, and norbornene functionalized onto **2** were used as the monomers for ROMP. These monomers were polymerized using Grubbs' catalysts to generate a series of homo-, co-, block and cross-linked-polymers. These polymers were characterized using GPC, NMR, and IR. In addition, ADMET polymerization of a terminal diolefin-functionalized D-isosorbide (**2**) was also conducted to produce ADMET polymers.

ACKNOWLEDGEMENTS

I would like to acknowledge Dr. Brooks Abel from the University of Southern Mississippi for GPC analysis of polymers and discussions via numerous emails. I would also like to thank Drs. Erson Emiler and Erick Vasquez from Dr. Keisha Walters' lab for help in the GPC, IR and TGA analysis of polymers. I would like to thank Dr. Mei Wang for her generous analysis of monomers using GC-MS and Dr. Satyanarayana Raju Sagi for the HRMS analysis of monomers.

This work is completed only with the support and help of a number of people. To name a few, first, I would like to thank Dr. Rowland for accepting to serve as my Major Professor and Dr. Wipf for serving in my committee. I would like to thank of Dr. Stephen Foster for being so helpful and for his timely emails and letters at various times. This thesis could not be completed without the strong moral support and guidance of Dr. Amar G. Chittiboyina from Ole miss. In addition, I would like to thank my colleagues from Dr. Pittman's group, Drs. Ireshika De Silva, Sabornie Chatterjee, Yingquan Song, and Mr. Martin Mathews for their warm company and help during the course of my stay at MSU. I would like to thank all my friends, roommates and well-wishers who were with me, and backed me during my stay at MSU and currently at Ole miss.

I would like to thank Dr. Walters, who joined the team late, for being my co-adviser and for all her support to make this research work happen. This work would not have completed without the patient, persistent guidance over a course of many years by

Dr. Charles U. Pittman. I could not thank him enough for his extra-ordinary patience and willingness to help me to finish my research and thesis, for the numerous letters to the University officials to maintain my student status and a number of email correspondences and corrections sent by him at various points of time while writing my thesis. Finally, I would like to thank my family for being so supportive during this long period. I have not seen them for many years now.

TABLE OF CONTENTS

ACKNOWLEDGEMENTS	ii
LIST OF TABLES	viii
LIST OF FIGURES	x
LIST OF SCHEMES.....	xiv
ABBREVIATIONS	xvi
LIST OF COMPOUNDS: CHEMICAL NAME AND THEIR ACRONYMS.....	xviii
HOMOPOLYMERS AND COPOLYMERS: NOMENCLATURE AND THEIR ACRONYMS	xix
CHAPTER	
I. SYNTHESIS OF BIO-BASED POLYMERS CONTAINING D-ISOSORBIDE BY RING- OPENING METATHESIS POLYMERIZATION	1
1.1 Background.....	1
1.2 Biomass as an alternative for petroleum.....	1
1.3 D-Isosorbide (2): Structure, nomenclature and properties.....	4
1.3.1 Structure.....	4
1.3.2 Nomenclature and properties.....	5
1.3.3 Isomers of D-isosorbide (2): 1,4:3,6-dianhydrohexitols (DAHs).....	6
1.3.4 Synthesis from biological sources.	7
1.3.5 Applications.	8
1.3.6 Polymers containing D-isosorbide (2).	9
1.4 Olefin metathesis polymerization.	13
1.4.1 Ring-opening metathesis polymerization (ROMP).	14
1.4.2 Acyclic diene metathesis polymerization (ADMET).	21
1.5 Summary.....	24
1.6 GPC basics.....	25
1.6.1 Solvent and hydrodynamic volume.	25
1.6.2 Column calibration: Conventional and universal.	26
1.6.2.1 Conventional calibration.....	26

1.6.2.2	Universal calibration.....	27
1.6.3	Light scattering detector.....	29
1.6.4	GPC measurements in this work.....	30
II.	RESULTS AND DISCUSSION.....	32
2.1	Introduction.....	32
2.2	Starting material.....	32
2.2.1	D-Isosorbide (2).....	32
2.2.2	5-Norbornene-2-carboxylic acid (43) (mixture of <i>endo</i> and <i>exo</i>).....	33
2.3	Synthesis of monomers for ROMP and ADMET polymerizations.....	35
2.3.1	Synthesis of 2- <i>exo</i> -acetyl D-isosorbide (44).....	35
2.3.2	Coupling of D-isosorbide (2) with 5-norbornene-2-carboxylic acid (43).....	37
2.3.2.1	(2- <i>exo</i> -D-Isosorbyl)-5-norbornen-2-carboxylate (NbISB) (46).....	37
2.3.2.2	(2- <i>exo</i> -5- <i>endo</i> -D-Isosorbyl)-di-5-norbornen-2-carboxylate (DiNBISB) (47).....	42
2.3.2.3	[(2- <i>exo</i> -acetyl)-5- <i>endo</i> -D-isosorbyl]-di-5-norbornen-2-carboxylate (AcNbISB) (48).....	48
2.3.3	<i>exo</i> -N-Phenyl-7-oxanorbornene-5, 6-dicarboximide (NbIMPh) 51	49
2.3.4	Diallyl-D-isosorbide (52).....	50
2.4	ROMP of monomers 46-48 and 51 using Grubbs' catalysts.....	54
2.4.1	Homopolymerization.....	54
2.4.1.1	Living polymerization.....	59
2.4.2	Co-polymerization.....	71
2.4.2.1	Random copolymerization.....	71
2.4.2.1.1	Copolymerization of 46 and 51	71
2.4.2.1.2	Crosslinking polymers by random copolymerization of 47 with 31	83
2.4.2.2	Block copolymers.....	86
2.4.2.2.1	Diblock polymers (82 and 84).....	86
2.4.2.2.2	Triblock polymers.....	89
2.5	ADMET polymerization.....	102
2.6	Discussion and conclusions.....	103
III.	EXPERIMENTAL.....	108
3.1	Materials and methods.....	108
3.1.1	Materials.....	108
3.1.2	Methods.....	109
3.1.3	Synthesis of monomers for ROMP and ADMET polymerizations.....	111

3.1.4	Synthesis of (2- <i>exo</i> -D-isosorbyl)-5-norbornen-2-carboxylate NbISB (46) and (2- <i>exo</i> -5- <i>endo</i> -D-isosorbyl)-di-5-norbornen-2-carboxylate DiNbISB (47).	111
3.1.4.1	(2- <i>exo</i> -D-Isosorbyl)-5-norbornen-2-carboxylate (46).	112
3.1.4.2	(2- <i>exo</i> -5- <i>endo</i> -D-Isosorbyl)-di-5-norbornen-2-carboxylate (47).	113
3.1.5	Synthesis of 2- <i>exo</i> -acetyl-D-isosorbide (44) and 2,5-di-acetyl-D-isosorbide (45).	114
3.1.5.1	2- <i>exo</i> -Acetyl-D-isosorbide (44).	115
3.1.6	Synthesis of [(2- <i>exo</i> -acetyl)-5- <i>endo</i> -D-isosorbyl]-di-5-norbornen-2-carboxylate (48).	116
3.1.6.1	[(2- <i>exo</i> -acetyl)-5- <i>endo</i> -D-isosorbyl]-di-5-norbornen-2-carboxylate (AcNbISB) (48).	117
3.1.7	Synthesis of <i>exo</i> -N-phenyl-7-oxanorbornene-5,6-dicarboximide (51).	118
3.1.7.1	<i>exo</i> -N-Phenyl-7-oxanorbornene-5,6-dicarboximide (51).	118
3.1.8	Synthesis of diallyl-D-isosorbide (52).	119
3.1.8.1	Diallyl-D-isosorbide (52).	120
3.1.8.2	2- <i>exo</i> -Allyl-D-isosorbide (53).	120
3.1.8.3	2- <i>endo</i> -Allyl-D-isosorbide (54).	121
3.1.9	Synthesis of dipent-5-enyl-D-isosorbide (55).	121
3.1.9.1	Dipent-5-enyl-D-isosorbide (55).	122
3.1.9.2	2- <i>exo</i> -Pent-5-enyl-D-isosorbide (56).	122
3.1.9.3	5- <i>endo</i> -pentenyl-D-isosorbide (57).	123
3.2	Ring-opening metathesis and acyclic diene metathesis polymerization.	123
3.2.1	Homopolymerization.	123
3.2.1.1	Synthesis of poly[(2- <i>exo</i> -D-isosorbyl)-5-norbornen-2-carboxylate] (poly[NbISB]) (58).	123
3.2.1.1.1	Poly(NbISB) (58).	124
3.2.1.2	Synthesis of poly(NbISB) (59).	124
3.2.1.3	Synthesis of poly(NbISB) (60 to 63).	125
3.2.1.3.1	Poly(NbISB) 60	126
3.2.1.3.2	Polymer 61	126
3.2.1.3.3	Polymer 62	126
3.2.1.3.4	Polymer 63	126
3.2.1.4	Synthesis of poly(NbISB) (64), poly(AcNbISB) (65) and poly(NbIMPh) (66) using Grubbs' II catalyst (27).	127
3.2.1.4.1	Poly(NbISB) 64	128
3.2.1.4.2	Poly(AcNbISB) 65	128
3.2.1.4.3	Poly(NbIMPh) 66	128
3.2.1.5	Synthesis of polymer 67 (Homopolymerization of DiNBISB (47)).	129
3.2.2	Random copolymerization.	130

3.2.2.1 NbISB (46) with NbIMPh (51).....	130
3.2.2.1.1 Using Grubbs' I (26) generation catalyst.....	130
3.2.2.1.1.1 Polymer 68 :.....	131
3.2.2.1.2 In different mole ratios using Grubbs' I (26) generation catalyst.	131
3.2.2.1.3 Poly(NbISB) 69	132
3.2.2.1.4 Poly[(NbISB)- <i>ran</i> -(NbIMPh)] 70	132
3.2.2.1.5 Poly[(NbISB)- <i>ran</i> -(NbIMPh)] 71	133
3.2.2.1.6 Poly[(NbISB)- <i>ran</i> -(NbIMPh)] 72	133
3.2.2.1.7 Poly(NbIMPh) 73	134
3.2.2.2 Copolymerization of NbISB (46) and NbIMPh (51) in different mole ratios using Grubbs' II generation catalyst (27).....	134
3.2.2.2.1 Poly[(NbISB)- <i>ran</i> -(NbIMPh)] 74	135
3.2.2.2.2 Poly[(NbISB)- <i>ran</i> -(NbIMPh)] 75	135
3.2.2.3 Random copolymerization of DiNbISB 47 with norbornene 31	136
3.2.2.3.1 Using Grubbs' I catalyst (26).....	136
3.2.2.4 Random copolymerizations at different 47/31 mole ratios using Grubbs' II catalyst (27).	137
3.2.3 Block polymerizations.	139
3.2.3.1 Diblock polymerizations.	139
3.2.3.1.1 AB-type block copolymer 82 of 46 and 51	139
3.2.3.1.1.1 Polymer poly(NbISB) 81	140
3.2.3.1.1.2 AB-type block polymer 82 of 46 and 51	140
3.2.3.1.2 BA-type block polymer 84 of 46 and 51	141
3.2.3.2.1 Polymer 83	142
3.2.3.2.2 BA-type block polymer 84 of 46 and 51	142
3.2.3.2.3 Triblock polymerization.....	143
3.2.3.3.1 ABA-type block polymer 87	143
3.2.3.3.1.1 Polymer 85	144
3.2.3.3.1.2 Polymer 86	144
3.2.3.3.1.3 ABA-block polymer 87 of 46 and 51	144
3.2.3.3.2 BAB-type block polymer 90 of 46 and 51	145
3.2.3.3.2.1 B-block polymer 88	146
3.2.3.3.2.2 BA-block polymer 89	146
3.2.3.3.2.3 BAB-type triblock polymer 90	147
3.3 ADMET polymerization of diallyl-D-isosorbide (52).....	147

REFERENCES	149
------------------	-----

APPENDIX

A. SPECTRAL DATA OF COMPOUNDS	156
-------------------------------------	-----

LIST OF TABLES

1.1	Physical properties of D-isosorbide (2). ¹¹	6
1.2	Comparison of Grubbs' catalysts used for ROMP. ⁵²	18
2.1	Reaction conditions of the homo-ring-opening metathesis polymerizations of monomers 46 , 47 , 48 and 51 using Grubbs' catalysts at room temperature.	55
2.2	Molecular weights of the homopolymers 58 – 61 prepared from monomer 46 . GPC in THF was employed in comparison with PS standards.	58
2.3	GPC molecular weight comparisons of homopolymers 64 , 65 and 66	58
2.4	Reaction conditions for the random copolymerization of NbISB (46) with NbIMPh (51) at a monomer to catalyst ratio [M]:[C] = 100:1, using Grubbs' catalysts.	74
2.5	Molecular weight measurements of random copolymers 68 to 74 by GPC in THF. These are random copolymers of 46 with 51	76
2.6	Monomer ratios observed in the ¹ H NMR of random copolymers (69 to 75). Polymers 69 to 73 were analyzed in CDCl ₃ while polymers 74 to 75 were analyzed in DMSO- <i>d</i> ₆	77
2.7	Reaction conditions for the random copolymerization of DiNbISB (47) and norbornene (31) at various mole ratios in DCM to generate cross-linked polymers.	84
2.8	Table of calculations to determine the monomer mole ratio of block copolymers using ¹ H NMR integrated regions.	92
2.9	Molecular weight measurements by GPC in THF vs. PS standards for the homopolymers 81 and 85 and block polymers 82 , 84 , 87 , and 90	93
3.1	Monomer ratios and the yields generated in the synthesis of polymers 69 to 73	132

A.2	The processed data for the above GPC trace with the different molecular weights, elution time, peak area, and peak height.	164
-----	--	-----

LIST OF FIGURES

1.1	Utilization of products derived from petroleum and natural gas in various industries and biomass as alternative source for petroleum products. ¹	2
1.2	Sorbitol (1) and its derivatives, including D-isosorbide (2). ¹	3
1.3	Structure and nomenclature ⁷ of D-isosorbide (2).	4
1.4	Structures of 1,4:3,6-dianhydrohexitols (DAHs): D-isosorbide (2), D-isomannide (3), D-isoidide (4).	7
1.5	Schematic representation of synthesis of D-isosorbide (2) from polysaccharides. ¹⁵	8
1.6	1-Vinyl-4-dianhydrohexitol-1,2,3-triazoles (15) used for RAFT polymerization. ²⁷	11
1.7	Examples of various forms of olefin metathesis reactions.	14
1.8	Various architectures accessible via olefin metathesis polymerization. ³²	15
1.9	A general mechanism of a typical ROMP reaction using ruthenium catalysts. ³¹	16
1.10	Amphiphilic poly(macromonomer)- <i>graft</i> -PEG polymer (29) synthesized by Nomura <i>et al.</i> ^{56a}	20
1.11	The mechanism of ADMET polymerization using Grubbs' catalysts. ⁵⁸	23
1.12	Generating a calibration curve using standards with Log(molecular weight on the Y-axis and elution volume on the X-axis).....	27
1.13	Determination of unknown-molecular weight of a sample using conventional calibration curve.	29
2.1	Structure of D-isosorbide (2) and the racemic mixture of both <i>exo</i> and <i>endo</i> isomers of, 5-norbornene-2-carboxylic acid (NbCOOH) (43).	33

2.2	The ^1H NMR (δ 2.5 –4.8) and ^{13}C NMR (δ 92–69) spectra and the spectral assignments ⁷ of D-isosorbide (2) in CDCl_3	34
2.3	The ^1H NMR and ^{13}C NMR spectra of 2- <i>exo</i> -acetyl-D-isosorbide (2AcISB) (44) in CDCl_3	36
2.4	The diastereomers of (2- <i>exo</i> -D-isosorbyl)-5-norbornen-2-carboxylate (NbISB) (46).	38
2.5	The ^1H and ^{13}C NMR spectrum of the 81/91, <i>endo/exo</i> isomeric mixture of (2- <i>exo</i> -D-isosorbyl)-5-norbornen-2-carboxylate (NbISB) (46) in CDCl_3	40
2.6	GC-MS analysis of the isomeric <i>endo/exo</i> mixture of (2- <i>exo</i> -D-isosorbyl)-5-norbornen-2-carboxylate (NbISB) (46).	41
2.7	HRMS spectrum of the isomeric mixture of NbISB (46).	42
2.8	The four possible diastereomers of (2- <i>exo</i> -5- <i>endo</i> -D-isosorbyl)-di-5-norbornen-2-carboxylate (DiNBISB) (47).	44
2.9	The ^1H and ^{13}C NMR spectra of DiNBISB (47).	45
2.10	GC-MS separation and fragmentation patterns of DiNBISB (47) isomers.	46
2.11	MS fragmentation patterns observed for the three peaks GC chromatogram (Figure 2.10) of DiNBISB (47).	47
2.12	HRMS spectrum of DiNBISB (47).	48
2.13	The ^1H and ^{13}C NMR spectra of AcNbISB (48) in CDCl_3	52
2.14	GC-MS spectrum of 81/19 <i>endo/exo</i> AcNbISB (48).	53
2.15	The HRMS spectrum of AcNbISB (48).	53
2.16	^1H NMR spectra of NbISB (46) (at 25 °C) and its ROMP-derived homopolymers poly(NbISB) (58 to 64) (at 70 °C) in $\text{DMSO}-d_6$	65
2.17	^1H NMR spectra of AcNbISB (48) in CDCl_3 at room temperature and poly(NbISB) (65) in $\text{DMSO}-d_6$ at 70 °C.	66
2.18	^1H NMR spectra of NbIMPh (51) and poly(NBIMPh) (66) at room temperature and 70 °C, respectively, using $\text{DMSO}-d_6$ as the solvent.	67

2.19	GPC chromatogram of the polymer 64 , a homopolymer of 46 , synthesized using Grubbs' II catalyst (27).....	68
2.20	GPC chromatogram of the polymer 65 , which is a homopolymer of 48 , synthesized using Grubbs' II catalyst (27).....	69
2.21	GPC chromatogram of the homopolymer of 51 synthesized using Grubbs' II catalyst (27) as the catalyst.	70
2.22	The overlaid ^1H NMR spectra of poly(NbISB) (69) (maroon) and poly(NbIMPh) (73) (blue).....	78
2.23	The stacked ^1H NMR spectra of random copolymers poly[(NbISB)- <i>ran</i> -(NbIMPh)] 69 to 73 (δ 3.0–8.0) in CDCl_3 at room temperature.	79
2.24	The overlaid ^1H NMR spectra of poly(NbISB) (64) and poly(NbIMPh) (66) (blue) in $\text{DMSO}-d_6$ at $70\text{ }^\circ\text{C}$	80
2.25	The ^1H NMR spectra of random copolymers 74 in $\text{DMSO}-d_6$ at $70\text{ }^\circ\text{C}$	81
2.26	The ^1H NMR spectra of random copolymer 75 in $\text{DMSO}-d_6$ at $70\text{ }^\circ\text{C}$	82
2.27	GPC chromatogram of the polymer AB-type block polymer 82	94
2.28	GPC chromatogram of the polymer ABA-type block polymer 87	96
2.29	GPC chromatogram of the polymer BAB-type block polymer 90	97
2.30	^1H NMR spectrum obtained in $\text{DMSO}-d_6$ at $70\text{ }^\circ\text{C}$ (δ 3.2 to 8.0) of AB-type diblock copolymer (82).	98
2.31	^1H NMR spectrum (δ 3.2 to 8.0) of BA-type diblock copolymer (84) obtained in $\text{DMSO}-d_6$ at $70\text{ }^\circ\text{C}$	99
2.32	^1H NMR spectrum obtained in $\text{DMSO}-d_6$ at $70\text{ }^\circ\text{C}$ (δ 3.2 to 8.0) of ABA-type triblock copolymer (87).	100
2.33	^1H NMR spectrum obtained in $\text{DMSO}-d_6$ at $70\text{ }^\circ\text{C}$ (δ 3.2 to 8.0) of BAB triblock copolymer (90).	101
A.1	FT-IR of 2- <i>exo</i> -acetyl-D-isosorbide (2AcISB) (44).	157
A.2	FT-IR spectrum of (2- <i>exo</i> -5- <i>endo</i> -D-isosorbyl)-di-5-norbornen-2-carboxylate (47).	158
A.3	FT-IR spectrum of (2- <i>exo</i> -D-isosorbyl)-5-norbornen-2-carboxylate (NbISB) (46).	159

A.4	FT-IR spectrum of [(2- <i>exo</i> -acetyl)-5- <i>endo</i> -D-isosorbyl]-di-5-norbornen-2-carboxylate (AcNbISB) (48).....	160
A.5	FT-IR spectrum of <i>exo</i> -N-Phenyl-7-oxanorbornene-5,6-dicarboximide (NbIMPh) (51).	161
A.6	TGA analysis of NbISB (64), AcNbISB (65) and NbIMPh (66).	162
A.7	TGA analysis of block polymers AB (82), BA (84), ABA (87) and BAB (90).....	163
A.8	GPC trace of sample, ADMET polymer 52 with 3 peaks identified, and only one peak lies on the calibration curve.....	164

LIST OF SCHEMES

1.1	Synthesis of D-isosorbide-containing poly(ether-ester)s (7) by microwave assisted polycondensation between the diolether of D-isosorbide (5) and terephthaloyl chloride (6). ²⁴	10
1.2	D-Isosorbide (2) containing polyamides (10) synthesized by interfacial polycondensation. ²⁵	11
1.3	Synthesis of poly(1-vinyl-4-dianhydrohexitol-1,2,3-triazole)s (PVDTs) (17) by RAFT polymerization. ²⁷	13
1.4	Random copolymerization of <i>N</i> -cycloalkyl-7-oxanorbornene dicarboximides (30) with norbornene (31) using Grubbs' I (26) and II (27) catalysts to produce polymers (32). ³⁴	21
1.5	Synthesis of ADMET polymer (42) containing D-isosorbide (2).	24
2.1	Acetylation of D-isosorbide (2) to produce 2- <i>exo</i> -acetyl D-isosorbide.	35
2.2	Synthesis of (2- <i>exo</i> -D-isosorbyl)-5-norbornen-2-carboxylate (NbISB) (46) and (2- <i>exo</i> -5- <i>endo</i> -D-isosorbyl)-di-5-norbornen-2-carboxylate (DiNBISB) (47).	37
2.3	Synthesis of [(2- <i>exo</i> -acetyl)-5- <i>endo</i> -D-isosorbyl]-di-5-norbornen-2-carboxylate (AcNbISB) (48).	48
2.4	Synthesis of <i>exo</i> - <i>N</i> -Phenyl-7-oxanorbornene-5,6-dicarboximide (NbIMPh) 51 .	50
2.5	The synthesis of monomers to for acyclic-diene metathesis (ADMET) polymerization from D-isosorbide (2).	51
2.6	Homo-ROMP of monomers NbISB (46) and AcNbISB (48) using Grubbs' catalysts (26 or 27).	56
2.7	Homo-ROMP of monomers NbIMPh (51) and DiNBISB (47) using Grubbs' catalysts (26 or 27).	57
2.8	Random copolymerization of NbISB (46) and NbIMPh (51) using Grubbs' catalysts (26 or 27).	75

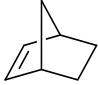
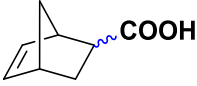
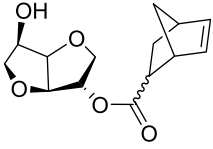
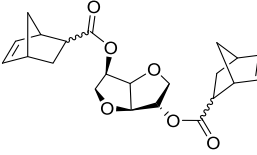
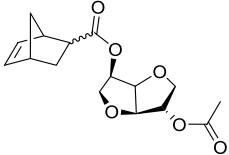
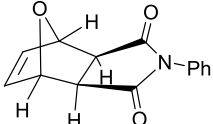
2.9	Random copolymerization of DiNbISB (47) and norbornene (32) using Grubbs' catalysts (26 and 27).	85
2.10	AB-type diblock copolymerization of NbISB (46) followed by NbIMPh (51) using Grubbs' II catalyst (27).....	87
2.11	BA-type diblock copolymerization of NbIMPh (51) followed by NbISB (46) using Grubbs' II catalyst (27).	88
2.12	ABA-type triblock copolymerization of NbISB (51) and NbIMPh (46) using Grubbs' II catalyst (27).	90
2.13	BAB-type triblock copolymerization of NbISB (51) and NbIMPh (46) using Grubbs' II catalyst (27).	91
2.14	GPC chromatogram of the polymer BA-type block polymer 84	95
2.15	ADMET polymerization of 52 using Grubbs' II catalyst (27)	102

ABBREVIATIONS

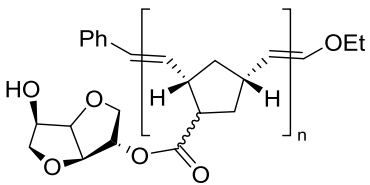
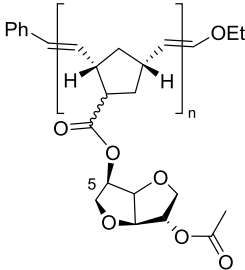
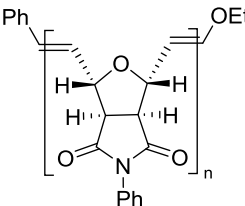
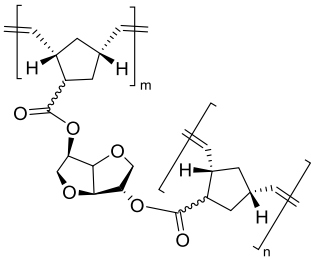
ADMET	Acyclic diene metathesis polymerization
AIBN	Azobisisobutyronitrile
BPA	Bisphenol A
DAH	1,4:3,6-Dianhydrohexitol
DCC	<i>N,N'</i> -Dicyclohexylcarbodiimide
DCM	Dichloromethane
DMAP	4-(Dimethylamino)pyridine
DMF	Dimethylformamide
DP	Degree of polymerization
GC	Gas chromatography
GPC	Gel permeation chromatography
HRMS	High resolution mass spectroscopy
LS	Light scattering
MS	Mass spectroscopy
NMP	<i>N</i> -Methyl pyridine
PDI	Polydispersity index
PMMA	Polymethylmethacrylate
PS	Polystyrene
PVDT	Poly(1-vinyl-4-dianhydrohexitol-1,2,3-triazole)

RAFT	Reversible addition-fragmentation chain transfer
ROMP	Ring opening metathesis polymerization
TGA	Thermogravimetric analysis
THF	Tetrahydrofuran
USM	The University of southern Mississippi
VDT	1-Vinyl-4-dianhydrohexitol-1,2,3-triazole

LIST OF COMPOUNDS: CHEMICAL NAME AND THEIR ACRONYMS.

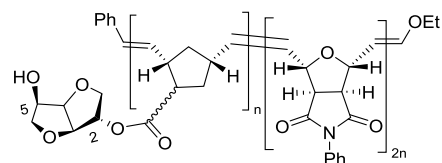
Structure number	Chemical name	Acronym	Structure
31	Norborne	Nb	
43	5-Norbornen-2-carboxylic acid (mixture of <i>exo</i> and <i>endo</i>)	NbCOOH	
46	(2- <i>exo</i> -D-Isosorbyl)-5-norbornen-2-carboxylate (mixture of <i>endo</i> and <i>exo</i>)	NbISB	
47	(2- <i>exo</i> -5- <i>endo</i> -D-Isosorbyl)-di-5-norbornen-2-carboxylate (mixture of four isomers)	DiNbISB	
48	[(2- <i>exo</i> -Acetyl)-5- <i>endo</i> -D-isosorbyl]-di-5-norbornen-2-carboxylate (mixture of <i>endo</i> and <i>exo</i>)	AcNbISB	
51	<i>exo</i> -N-Phenyl-7-oxanorbornene-5,6-dicarboximide	NbIMPh	

HOMOPOLYMERS AND COPOLYMERS: NOMENCLATURE AND THEIR ACRONYMS

Structure number	Scientific name	Acronym	Structure
Homopolymers			
58-64, 81, 85	Poly[(2- <i>exo</i> -D-isosorbyl)-5-norbornen-2-carboxylate]	poly(NbISB)	
65, 83	Poly[(2- <i>exo</i> -acetyl)-5- <i>endo</i> -D-isosorbyl]-di-5-norbornen-2-carboxylate]	poly(AcNbISB)	
66, 83, 88	Poly(<i>exo</i> -N-phenyl-7-oxanorbornene-5,6-dicarboximide)	poly(NbIMPh)	
67	Poly[(2- <i>exo</i> -5- <i>endo</i> -D-isosorbyl)-di-5-norbornen-2-carboxylate]	poly(DiNbISB)	
Random copolymers			

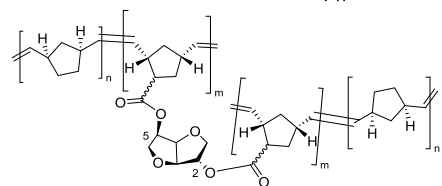
68-75 Poly{[(2-*exo*-D-isosorbyl)-5-norbornen-2-carboxylate]-*random*-[*exo*-N-phenyl-7-oxanorbornene-5,6-dicarboximide]}

poly[(NbISB)-*ran*-(NbIMPh)]



76-80 Poly{[(2-*exo*-5-*endo*-D-isosorbyl)-di-5-norbornen-2-carboxylate]-*random*-[norbornene]}

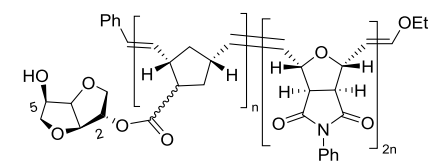
poly[(DiNbISB)-*ran*-(Nb)]



Diblock copolymers

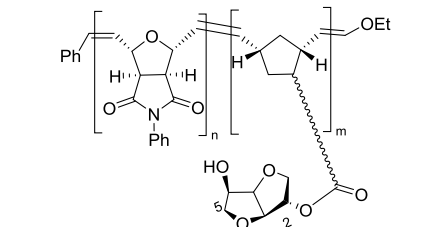
82, 86 Poly[(2-*exo*-D-isosorbyl)-5-norbornen-2-carboxylate]-*block*-poly[*exo*-N-phenyl-7-oxanorbornene-5,6-dicarboximide]

poly(NbISB)-*block*-poly(NbIMPh)



84, 89 Poly[*exo*-N-phenyl-7-oxanorbornene-5,6-dicarboximide]-*block*-poly[2-*exo*-D-isosorbyl)-5-norbornen-2-carboxylate]

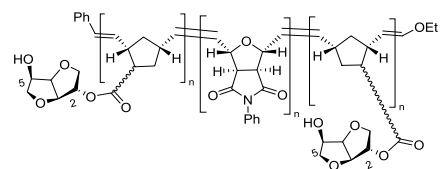
poly(NbIMPh)-*block*-poly(NbISB)]



Triblock copolymers

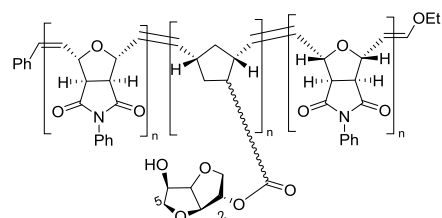
87 Poly{[(2-*exo*-D-isosorbyl)-5-norbornen-2-carboxylate]-*block*-poly[*exo*-N-phenyl-7-oxanorbornene-5,6-dicarboximide]-*block*-poly[(2-*exo*-D-isosorbyl)-5-norbornen-2-carboxylate]}

Poly(NbISB)-*block*-poly(NbIMPh)-*block*-poly(NbISB)



90 Poly[*exo*-N-phenyl-7-oxanorbornene-5,6-dicarboximide]-*block*-poly[(2-*exo*-D-isosorbyl)-5-norbornen-2-carboxylate]-*block*-poly[*exo*-N-phenyl-7-oxanorbornene-5,6-dicarboximide]

Poly(NbIMPh)-*block*-poly(NbISB)-*block*-poly(NbIMPh)



CHAPTER I

SYNTHESIS OF BIO-BASED POLYMERS CONTAINING D-ISOSORBIDE BY RING- OPENING METATHESIS POLYMERIZATION

1.1 Background.

Petroleum- and natural gas-derived products are widely used as raw material in textile, food supply, transportation, housing, recreation, communications and health industries. Chemicals from the petroleum and natural gas industries are catalytically transformed into intermediates, which are used in the synthesis of various products (Figure 1.1). However, the dependence on the petroleum and natural gas products has some shortcomings: they are non-renewable, cause environmental damage and negative health consequences. Hence, a lot of attention has been devoted to alternative, renewable and environment-friendly replacements for petroleum and natural gas products.

1.2 Biomass as an alternative for petroleum.

Biomass (eg: cellulose, sugars etc.,) is considered an alternative renewable source for petroleum- and natural gas-based products. In 2004, the United States Department of Energy (US DOE) published a report with a list of top twelve value-added chemicals from biomass¹ which could be utilized as alternatives for petroleum- and natural gas-based products. Sugars are intermediate platforms, which are produced from the biomass feedstock (Figure 1.1).

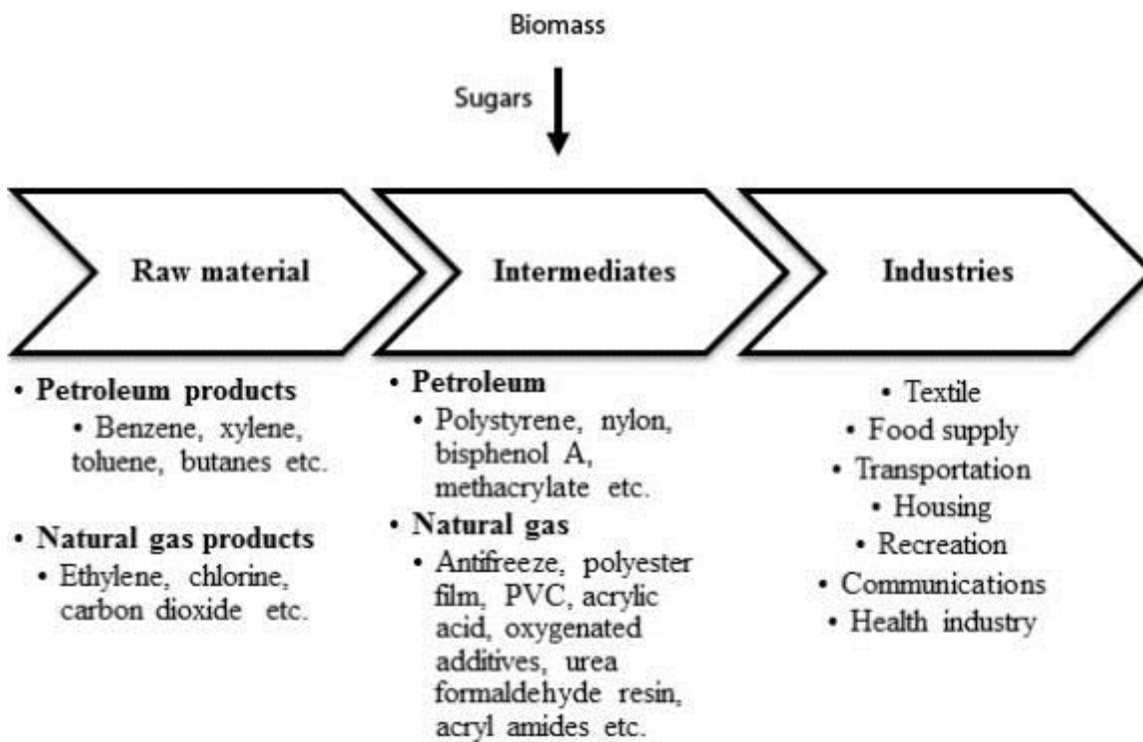


Figure 1.1 Utilization of products derived from petroleum and natural gas in various industries and biomass as alternative source for petroleum products.¹

In the US DOE report,¹ sorbitol (**1**) was named as one of the twelve most promising value-added chemicals from biomass of the potential candidates which can be made from sugars. Glucose can be converted to sorbitol (**1**) by hydrogenation.² An efficient large-scale catalytic hydrogenation of glucose to sorbitol (**1**) is currently a topic of intense research. A list of many catalysts used for the hydrogenation of glucose to sorbitol (**1**) with the sorbitol (**1**) yields was reviewed by Zhang *et al.*² Sorbitol (**1**) is a versatile chemical due to the presence of modifiable hydroxyl functional groups. Various derivatives¹ are obtained from sorbitol (**1**) by three pathways: 1) dehydration to get D-isosorbide (**2**), sorbitans or anhydrosugars; 2) bond cleavage (hydrogenolysis), and 3) direct polymerization.

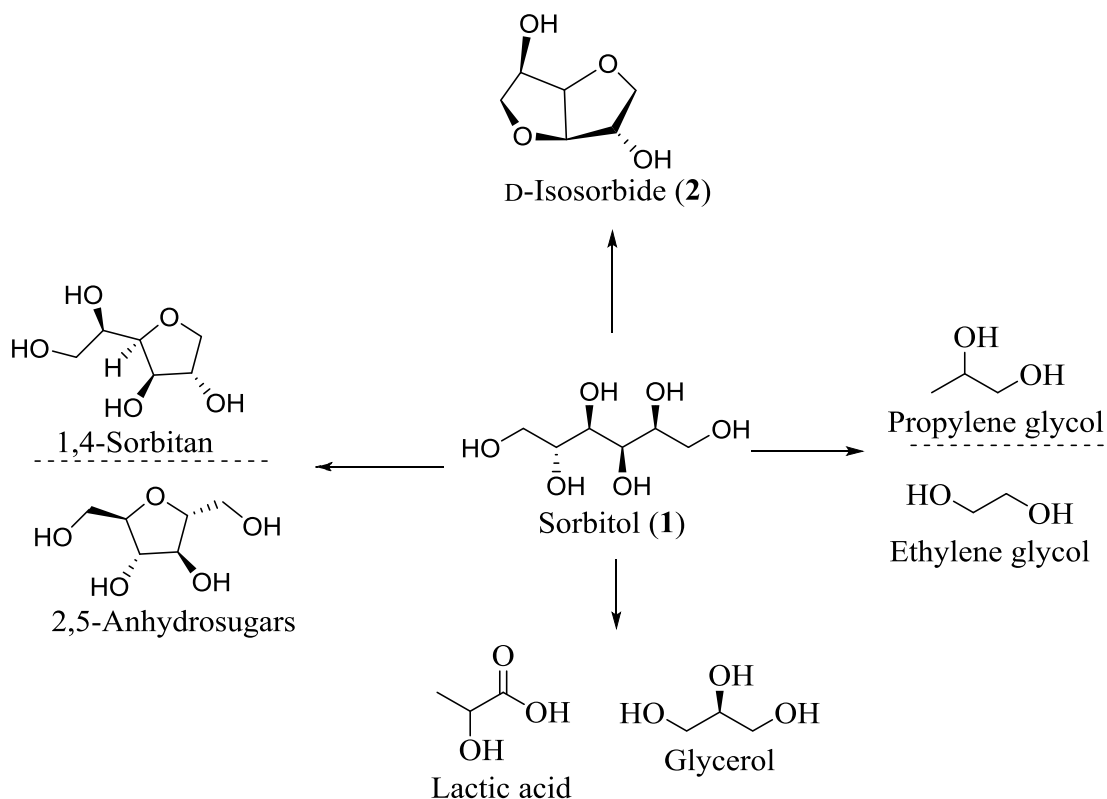
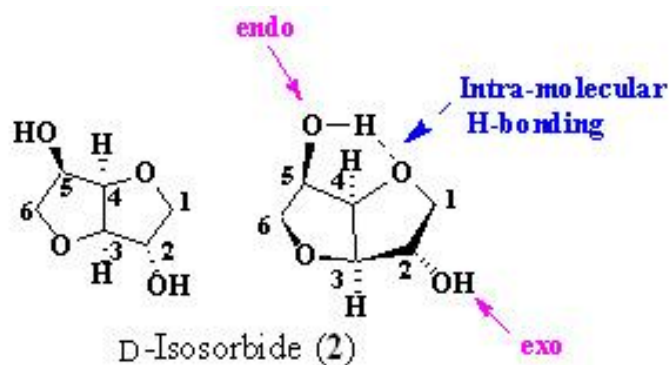


Figure 1.2 Sorbitol (1) and its derivatives, including D-isosorbide (2).¹

Sorbitol (1) and its derivatives are used as food additives³ (sweetener, humectant and excipient), in the production of liquid fuels² (1,2-propanediol, etc.), in catalyst modification⁴ and polymer production. A derivative of sorbitol (1), D-isosorbide (2), has attracted a considerable interest⁵ due to its unique chemical features and possible applications in the polymer and other industries.⁶ Several names of D-isosorbide (2) appear in the literature (Figure 1.3), but D-isosorbide (2) will be used exclusively in this thesis.



Nomenclature type	D-Isosorbide (2)
Sugar derived	1,4:3,6-dianhydro-D-glucitol
Bridged system	(1 <i>R</i> ,4 <i>R</i> ,5 <i>R</i> ,8 <i>S</i>)-2,6-dioxabicyclo[3.3.0]octan-4,8-diol
Fused systems	(3 <i>R</i> ,3 <i>aR</i> ,6 <i>S</i> ,6 <i>aR</i>)-hexahydrofuro[3,2- <i>b</i>]furan-3,6-diol

Numbering

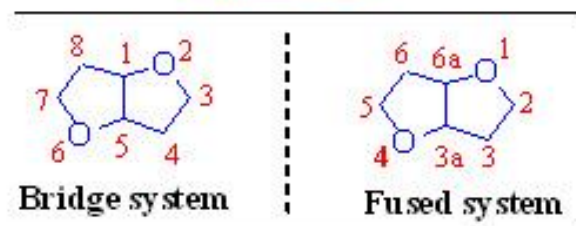


Figure 1.3 Structure and nomenclature⁷ of D-isosorbide (2).

The numbering used in the bridged and the fused nomenclature systems is also shown.

1.3 D-Isosorbide (2): Structure, nomenclature and properties.

1.3.1 Structure.

D-Isosorbide (2), belonging to a class of 1,4:3,6-dianhydrohexitols (DAHs), is synthesized by the double dehydration of sorbitol (1).⁷ It has a fused ring system with two *cis*-connected furan rings at an angle of 120°, giving a V shape (or open-book) (Figure 1.3). It has two secondary hydroxyl groups, one on C2 in the *exo* configuration and the

other on C5 in the *endo* configuration. The C5 (*endo*) hydroxyl group forms an intra-molecular hydrogen bond with the oxygen on the opposite furan ring, whereas the C2 (*exo*) hydroxyl group does not form an intra-molecular hydrogen bond. The nucleophilic character of the C5 hydroxyl group is increased due to hydrogen bonding. Thus, selective tosylation⁸ on the C5 hydroxyl group was performed, despite the greater steric crowding relative to the *exo*-C2 hydroxyl group. Substitution with a more sterically hindered group occurs faster at the less sterically hindered C2-hydroxyl group.

Glycosylation was performed selectively on C5 (*endo*) hydroxyl group of D-isosorbide (**2**) under Koenigs-Knorr conditions using Helferich modification.⁹ **2** was treated with a 1 M equivalent of acetal protected sugar bromide in the presence of silver oxide, and also using mercuric cyanide in both nitromethane and acetonitrile to get predominantly *endo* glycosylated products. Selective etherification of D-isosorbide (**2**) was performed using *N,N'*-dicyclohexylcarbodiimide (DCC) and 4-(dimethylamino) pyridine (DMAP) to produce C2-*exo* (68%), C5-*endo* (8%) and di-substituted (6%) products.¹⁰

1.3.2 Nomenclature and properties.

D-Isosorbide (**2**) is often referred to as 1,4:3,6-dianhydro-D-glucitol as it is derived the through double dehydration of sorbitol (**1**), which in turn is synthesized from D-glucose (Figure 1.5). Because of its structure, D-isosorbide (**2**) can also be named using bridge-system and fused-system nomenclature⁷ (Figure 1.3). It can be named (1*R*,4*R*,5*R*,8*S*)-2,6-dioxabicyclo[3.3.0]octan-4,8-diol according to the bridge-system nomenclature, because it has a dioxabicyclo[3.3.0]octane frame-work. According to the fused-system nomenclature, it can be named (3*R*,3*aR*,6*S*,6*aR*)-hexahydrofuro[3,2-

b]furan-3,6-diol (Figure 1.3). D-Isosorbide (**2**) is heat stable up to 270 °C and acid stable (up to 150 °C in concentrated sulfuric acid). The physical properties of D-isosorbide (**2**) are summarized in Table 1.1.

Table 1.1 Physical properties of D-isosorbide (**2**).¹¹

Melting point	61-64 °C
Boiling point	160 °C
Flash point	> 150 °C
Soluble in	Water, alcohols, dioxane, ketones
Almost insoluble in	Hydrocarbons. esters, ethers

1.3.3 Isomers of D-isosorbide (**2**): 1,4:3,6-dianhydrohexitols (DAHs).

D-Isosorbide (**2**) has two other isomers, namely D-isomannide (**3**) and D-isoidide (**4**) which also belong to the class of 1,4:3,6-dianhydrohexitols (DAHs) (Figure 1.4). They differ in the location of the hydroxyl groups. D-Isomannide (**3**) has both the hydroxyl groups in the *endo* position. In D-isoidide (**4**), the hydroxyl groups are located in the *exo* position. These three DAH isomers (**2-4**) show differences in the physical and chemical properties, such as melting temperatures and reactivities of the hydroxyl groups.^{7, 12}

1,4:3,6-dianhydrohexitols

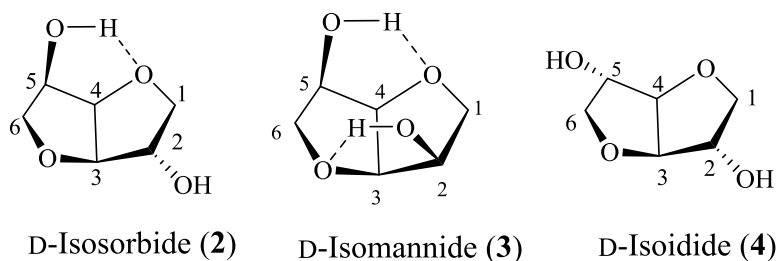


Figure 1.4 Structures of 1,4:3,6-dianhydrohexitols (DAHs): D-isosorbide (2), D-isomannide (3), D-isoidide (4).

1.3.4 Synthesis from biological sources.

D-Isosorbide (2) can be synthesized via dehydration of D-sorbitol to produce 1,4- or 3,6-sorbitans, which upon further dehydration produce D-isosorbide (2). This conversion was performed through treatment with various inorganic acids like HF, H₂SO₄ and HCl at 119 to 135 °C.^{11, 13} This method requires neutralization and separation of dehydration products from the salt solutions. Research efforts are currently underway to produce D-isosorbide (2) in an environmentally benign manner. Zhang *et al.*² summarized the current research progress in the synthesis of D-isosorbide (2) from sorbitol (1). Tin, zirconium and titanium metal phosphates¹⁴ were used as catalysts in the synthesis of D-isosorbide (2) from sorbitol (1), cellulose and lignocelluloses at 410 to 573 °C at 47 to 70 % yields.² Figure 1.5 represents a schematic representation of synthesis of D-isosorbide (2) from biogenic polysaccharides.¹⁵

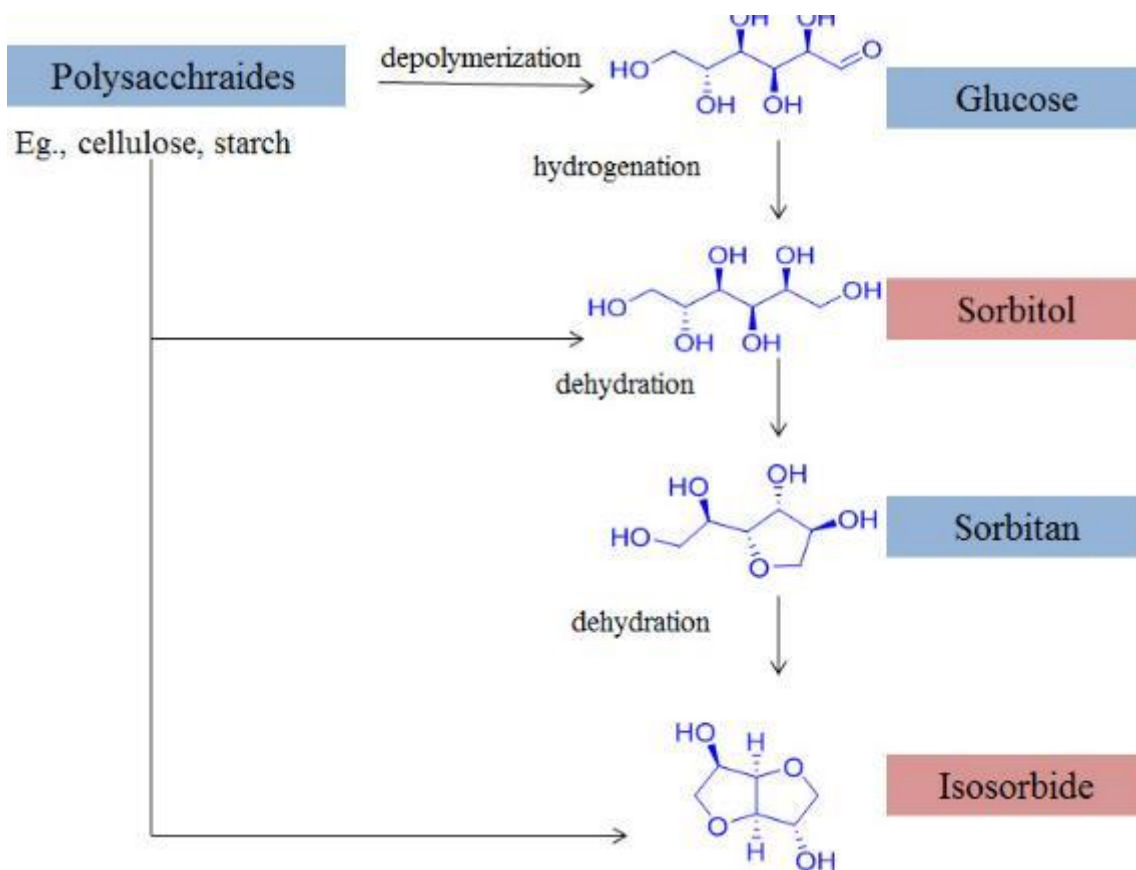


Figure 1.5 Schematic representation of synthesis of D-isosorbide (**2**) from polysaccharides.¹⁵

1.3.5 Applications.

D-Isosorbide (**2**) is being studied for its utilization as a renewable alternative for some petroleum products.¹⁵ Isosorbide nitrates (mono and di) have been used for a few decades in the treatment of heart failure and angina pectoris.¹⁶ Alkyl derivatives of D-isosorbide (**2**) were used as nontoxic solvents in pharmaceutical and cosmetic industries.¹⁷ In addition, compounds derived from D-isosorbide are used as chiral auxiliaries in organic synthesis,¹⁸ due to its rigid structure. For example, D-isosorbide (**2**) and its isomer D-isomannide (**3**) were selectively protected to provide new chiral

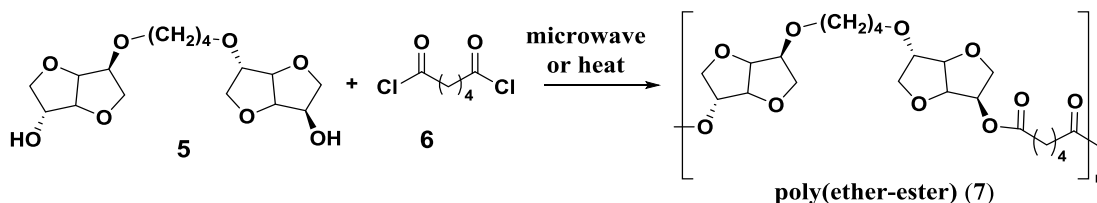
auxialries suitable for the preparation of enantiopure tertiary α -hydroxy acids using organo zinc reagents.¹⁹ D-isosorbide's (**2**) rigid, chiral, and non-toxic nature, was useful in the synthesis of polymers with high glass transition temperatures and/or with special optical properties.²⁰ A wide range of amorphous and semi-crystalline polymers containing D-isosorbide (**2**) were reported in the literature.²⁰⁻²¹ They include polyesters, polyurethanes, polyamides, polycarbonates, polyethers, poly(ester-imide)s, poly(esteramide)s, poly(ether-urethane)s, or polytriazoles.

Like bisphenol A (BPA), D-isosorbide (**2**) has two hydroxyl groups and a rigid architecture. In addition, it is a chiral molecule. It was found to exhibit acceptable thermal and mechanical properties like BPA.²² Hence, it was proposed to be an effective replacement for BPA.²² BPA is widely included in the polymers used in the food, plastic and beverage bottle industries. BPA incorporation influences the toughness of these polymers. Hydrolytic degradation of BPA-containing polycarbonates releases BPA, which is thought to be an estrogen mimic that could be harmful for health.²² Hence, finding effective replacements for BPA is an active field of research with great commercial interest.

1.3.6 Polymers containing D-isosorbide (**2**).

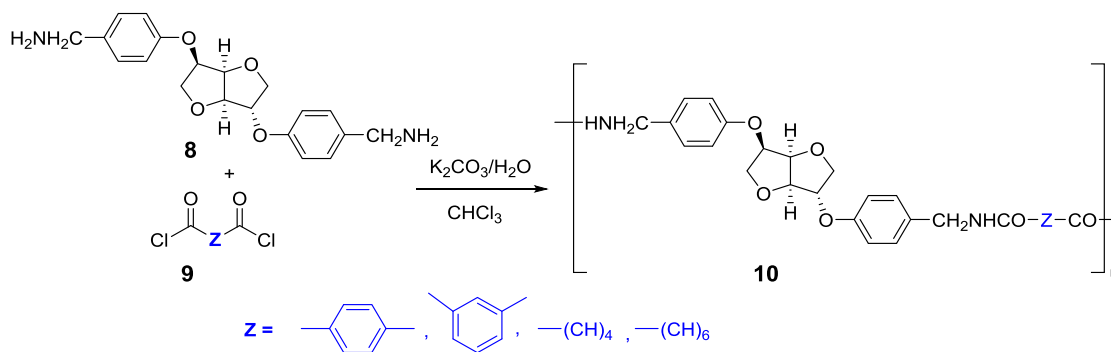
Aliphatic polyesters, furan-containing polyesters, poly(ester-amides)s and poly(ester-carbonate)s have been synthesized by polycondensation using 1,4:3,6-dihydroxyxitol-containing monomers.²³ Their biodegradability ranged from days to years when tested using soil burial degradation tests, active sludge treatment and enzymatic degradation tests. Novel poly(ether-ester)s based on the diol-ether of D-isosorbide (**2**) and adipoyl chloride or terephthaloyl chloride (**6**) were synthesized by

microwave irradiation and conventional heating²⁴ (Scheme 1.1). The microwave reaction proceeded approximately five times faster and produced higher average molecular weights (up to M_w of 8000) compared to conventional heating.



Scheme 1.1 Synthesis of D-isorbide-containing poly(ether-ester)s (**7**) by microwave assisted polycondensation between the diolether of D-isorbide (**5**) and terephthaloyl chloride (**6**).²⁴

Optically active D-isorbide-derived polyamides (**10**) were also synthesized by Bortolussi *et al.*²⁵ The microwave-assisted polycondensation between D-isorbide-derived diacylchloride and different aromatic diamines in the polar organic solvent *N*-methyl pyridine (NMP), produced polymers with inherent viscosities between 0.11 and 0.92 dL/g.²⁵ The interfacial polymerization from an D-isorbide-derived diamine (**8**) with different diacylchlorides (**9**) produced polymers with inherent viscosities in the range 0.21–1.05 dL/g²⁵ (Scheme 1.2). Novel starch-derived polyurethanes²⁶ were synthesized via two routes (polyaddition and polycondensation) to produce polymers with molecular weights between 8000 to 12000 and degrees of polymerization (DP) as high as 70. Poly-addition produced a semi-crystalline polymer with a glass transition temperature (T_g) of 118 °C and a melting range (T_m) of 190-200 °C, whereas polycondensation produced semi-crystalline polymers with T_m of 140-180 °C.²⁶



Scheme 1.2 D-Isorbide (**2**) containing polyamides (**10**) synthesized by interfacial polycondensation.²⁵

Recently, Drockenmuller *et al.*²⁷ reported the synthesis of 1,4:3,6-dianhydrohexitol-containing polymers produced by reversible addition-fragmentation chain transfer (RAFT) polymerization. All the three DAHs (**2**, **3** and **4**) were substituted with 1-vinyl-4-dianhydrohexitol-1,2,3-triazole (VDT) to produce four 1-vinyl-4-dianhydrohexitol-1,2,3-triazoles [**11-14** or (**15**)]. These monomers were used in RAFT polymerizations (Figure 1.6). Monomer **13** has an *exo* VDT substitution on **2** while monomer **14** has *endo* hydroxyl VDT substitution on D-isorbide (**2**).

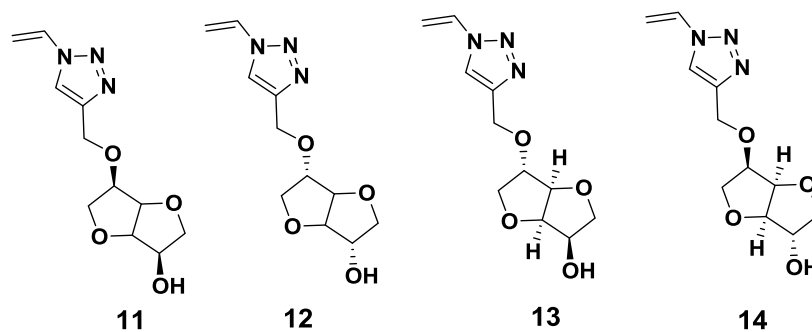
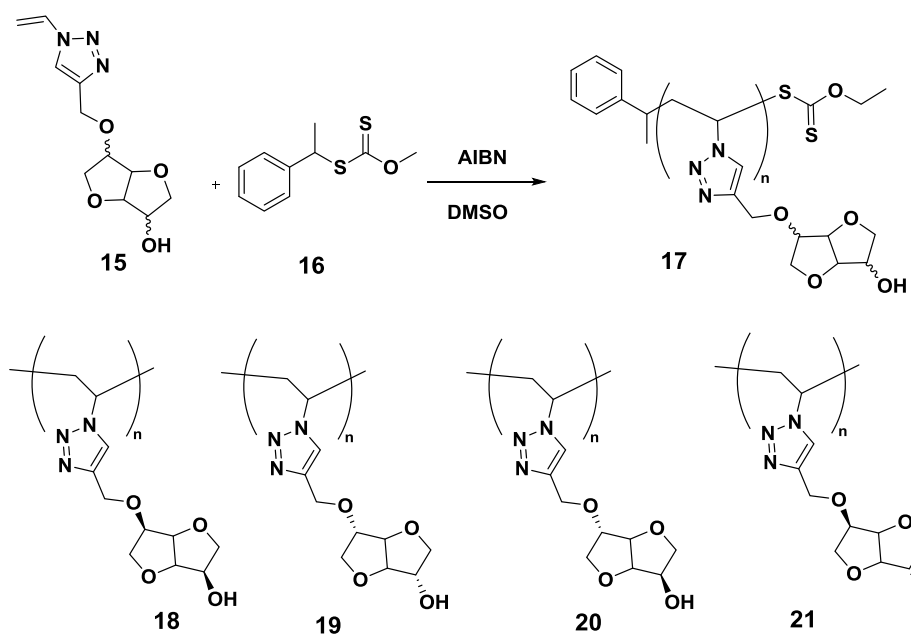


Figure 1.6 1-Vinyl-4-dianhydrohexitol-1,2,3-triazoles (**15**) used for RAFT polymerization.²⁷

These 1-vinyl-4-dianhydrohexitol-1,2,3-triazoles (**15**) were then subjected to RAFT polymerization in DMSO-*d*₆ at 80 °C with *O*-ethyl-*S*-(1-phenylethyl) dithiocarbonate (**16**) as the chain transfer agent and azobisisobutyronitrile (AIBN) (**17**) as a thermal initiator to produce four different poly(1-vinyl-4-dianhydrohexitol-1,2,3-triazole)s (PVDTs) (**18-21**) (Scheme 1.3) with a controlled stereochemistry and with relatively well defined structures. GPC molecular weight analysis indicated a *M*_n of 15–20 kDa and a PDI of ~ 1.5–1.7, relative to polystyrene standards. High PDI was explained not to uncontrolled polymerization, but due to the overestimation with PS calibration. The structure-property relationship of these novel bio-based monomers (**15**) and polymers (**17**) showed a significant influence of the DAH moieties on their physicochemical properties. Monomers **11**, **12** and **14** were viscous liquids, whereas **13** was a crystalline solid. **11**, **12**, and **14** exhibited *T*_g values of -22, -28 and -14 °C whereas **13** exhibited a *T*_m value of 139 °C (no *T*_g value for **13**, as it is a crystalline solid).

D-Isomannide- and D-isoidide-based PVDT-polymers **18** and **19** showed *T*_g values of 49 and 52 °C. Interestingly, D-isosorbide-based PVDT-stereoisomers **20**, and **21** exhibited higher *T*_g's of 71, and 118 °C, respectively, compared to **18** and **19**. Polymers **20** and **21** also showed contrasting solubilities in water. The *endo* substituted product **20** is found to be soluble in water, whereas the *exo* substituted product **21** is insoluble.



Scheme 1.3 Synthesis of poly(1-vinyl-4-dianhydrohexitol-1,2,3-triazole)s (PVDTs) (17) by RAFT polymerization.²⁷

1.4 Olefin metathesis polymerization.

Olefin metathesis is one of the most useful reactions in organic synthetic and polymer chemistry.²⁸ It is performed in many forms²⁹ (Figure 1.7) including cross metathesis (CM), ring-opening metathesis (ROM), ring-closing metathesis (RCM), ring-rearrangement metathesis (RRM), ring-opening metathesis polymerization (ROMP), and acyclic diene metathesis (ADMET) polymerization. ROMP and ADMET polymerizations are used in the synthesis of a number of polymer architectures. ROMP and ADMET produce polymers in a “living” manner (unlike polycondensation or kinetically controlled polymerizations). A living polymer should “proceed without chain transfer or termination.”³⁰ A living polymer should show a linear relationship between the monomer to catalyst mole ratio and the molecular weight of the polymer or exhibit a

linear relationship between the degree of polymerization (DP) (typically measured in terms of number-averaged molecular weight, M_n), monomer molecular weight and monomer consumption.³¹

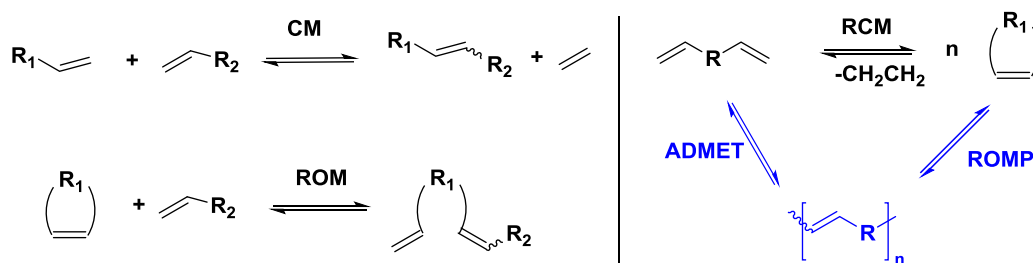


Figure 1.7 Examples of various forms of olefin metathesis reactions.

Cross metathesis (CM), ring-opening metathesis (ROM), ring closing metathesis (RCM), acyclic diene metathesis (ADMET) and ring-opening metathesis polymerization (ROMP).²⁹

1.4.1 Ring-opening metathesis polymerization (ROMP).

Ring-opening metathesis polymerization (ROMP) is a chain-growth polymerization technique where a highly strained ring system containing a carbon-carbon double bond polymerizes in a living manner. With the advent of novel well-defined, commercially available metathesis catalysts, ROMP has become a widely used method for the synthesis of well-defined polymeric materials.³² Homopolymers,³³ random copolymers,³⁴ block copolymers,³⁵ graft copolymers,³⁶ telechelic polymers,³⁷ multi-shaped copolymers,⁴³ amphiphilic polymers,³⁸ alternating copolymers³⁹ and cross-linked copolymers⁴⁰ were all synthesized using ROMP. In addition, new kinds of polymer architectures are also plausible with ROMP³² (Figure 1.8).

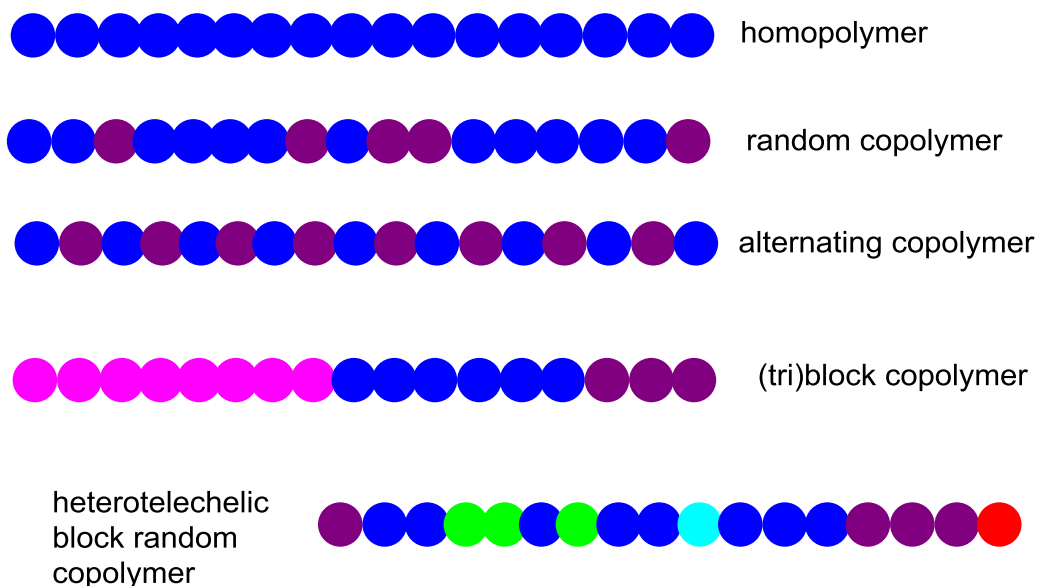


Figure 1.8 Various architectures accessible via olefin metathesis polymerization.³²

ROMP occurs in three stages³¹ (Figure 1.8): initiation, propagation and termination. Initiation occurs through the coordination of the transition-metal alkylidene catalyst complex to a cyclic olefin **22**. This is followed by the [2+2]-cycloaddition to form a four membered metallo-cyclobutane intermediate **23**, which undergoes cycloreversion to form a new metal-alkylidene **24**. This new metal-alkylidene (**24**) acts as a new catalyst and undergoes chain propagation with a new cyclic olefin, which undergoes ring-opening similar to that in the original initiation steps. This propagation cycle goes on until the polymerization ceases due to the depletion of the monomer, or until a reaction equilibrium is reached, or the reaction is terminated by the addition of terminating agents like ethyl vinyl ether or vinyl lactones⁴¹ to produce polymer (**25**).

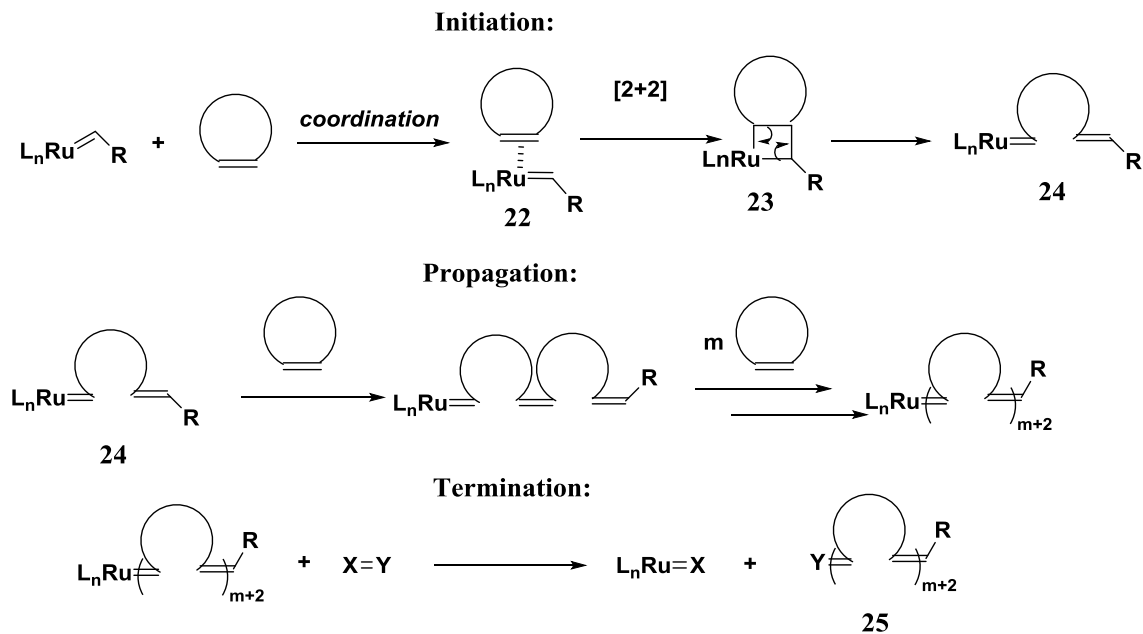


Figure 1.9 A general mechanism of a typical ROMP reaction using ruthenium catalysts.³¹

Grubbs' *et al.*³¹ summarized the characters required for ROMP reaction to be classified as a “living and controlled” reaction. A ROMP must happen by:

- Fast and complete initiation and the rate of initiation should be much greater than the rate of propagation. Thus, all catalyst molecules form initial catalyst-monomer complexes, before propagation advances. This gives the same number of growing chains as there were initiated catalyst molecules. In other words, [growing chains] = [catalyst].
- Chain termination and transfer reactions are relatively slow compared to chain-propagation.⁴² This enables the polymerization happens until the complete consumption of the monomer in the reaction. Chain termination would otherwise result in the quenching of the reaction without the

polymer chain growing completely. Chain transfer reactions, which occur between one growing polymer and another result in high polydispersities or non-uniform molecular weights.

- They should exhibit a linear relationship between the degree of polymerization (DP) and monomer consumption.
- Poly-dispersity index (PDI) < 1.5.

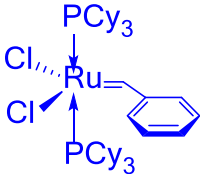
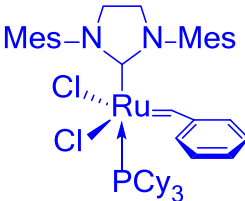
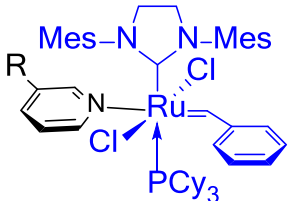
Poly-dispersity index (PDI) = $M_w/M_n = 1 + 1/DP$, where, M_w is the weight-averaged molecular weight, M_n is the number-averaged molecular weight and DP is the degree of polymerization.

Finding efficient and well-defined catalysts for ROMP has been an active field of research since decades.³⁰ According to Grubbs' *et al*,³¹ an ideal-catalyst should “(1) convert to growing polymer chains quantitatively and rapidly (i.e. exhibit fast initiation kinetics), (2) mediate a polymerization without an appreciable amount of (intramolecular or intermolecular) chain transfer or premature termination, (3) react with accessible terminating agents to facilitate selective end-functionalization, (4) display good solubility in common organic solvents (or better: aqueous media), and (5) for practical reasons, show high stability toward moisture, air, and common organic functional groups.”

Catalysts based on titanium,⁴³ tantalum,⁴⁴ tungsten,⁴⁵ and molybdenum⁴⁶ (such as Schrock's well-defined molybdenum and tungsten catalysts) were used in ROMP.³¹ However, they have a low functional group tolerance³¹ (selectivity to bind to olefins compared to other functional groups). The most widely used catalysts currently are based on ruthenium due to their broad functional group tolerance.²⁹ Grubbs' I⁴⁷ (**26**) and Grubbs' II⁴⁸ (**27**) ruthenium-based catalysts are commercially available. Grubbs' III⁴⁹

catalysts (**28a** and **28b**) are generated *insitu* by the reaction of Grubbs' II catalyst (27) with 3-bromopyridine or pyridine. These Grubbs' catalysts differ from each other in their respective rates of initiation or propagation.⁵⁰ Grubbs' I catalyst (**26**) has a faster initiation rate than Grubbs' II catalyst (27), hence the PDI of Grubbs' I catalyst (**26**)-derived polymers are smaller than those from Grubbs' II catalyst (27). Grubbs' II catalyst (27) has a better functional group tolerance than Grubbs' I catalyst (**26**).⁵¹ Grubbs' III catalysts exhibit fast-initiation kinetics³¹ (due to "the labile nature of the pyridine ligands), and extremely high activities in ROMP. **28a** is an ultra-fast acting catalyst while **28b** is a complete-initiation catalyst. In a complete initiation catalyst, each catalyst molecule reacts initiates the ROMP reaction with the monomer. Hence, Grubbs' III catalysts **28** could produce polymers with PDI values close to 1.⁵¹

Table 1.2 Comparison of Grubbs' catalysts used for ROMP.⁵²

 <p>Grubbs' I (26)</p>	 <p>Grubbs' II catalyst (27)</p>	 <p>Grubbs' III catalysts (28) 28a R = Br 28b R = H</p>
Active in protic media without vigorous exclusion of O ₂	Higher functional group tolerance than Grubbs' I	28a Ultra-fast initiating
Better initiation than Grubbs' II (27)	Lower initiation rate than Grubbs' I (26)	28b Complete initiation catalyst
Lower activity compared to Schrock's catalysts ⁵³		

In addition to the choice of initiator, ROMP is influenced by various other factors⁵¹ which include : monomer functionality, solvents and additives, temperature and reaction time. The initiation rate constants of Grubbs' I and Grubbs' II catalysts (**26** and **27**) depend on the dielectric constant of the reaction medium.⁵⁴ “The initiation rate increased by 30% for norbornene polymerization with Grubbs' I and II catalysts (**26** and **27**) when the solvent was changed from toluene ($\epsilon = 2.38$) to DCM ($\epsilon = 8.9$).”⁵¹

A variety of functionalized norbornenes were polymerized via ROMP.^{32, 55} Nomura *et al.*³² synthesized block copolymers containing acetal-protected galactose or ribose using molybdenum-alkylidene and Grubbs' II catalyst (**27**). Removal of the acetal protection produced poly(macromonomer)s containing sugars.⁵⁶ Amphiphilic graft polymers of poly(macromonomer)s with polyethylene glycol (**29**) were also synthesized³² (Figure 1.10). These amphiphilic macromolecules produced micelles (studied by transmission electron microscopy (TEM)). Amphiphilic macromolecules can be used for cellular specific targeting of drugs.³³

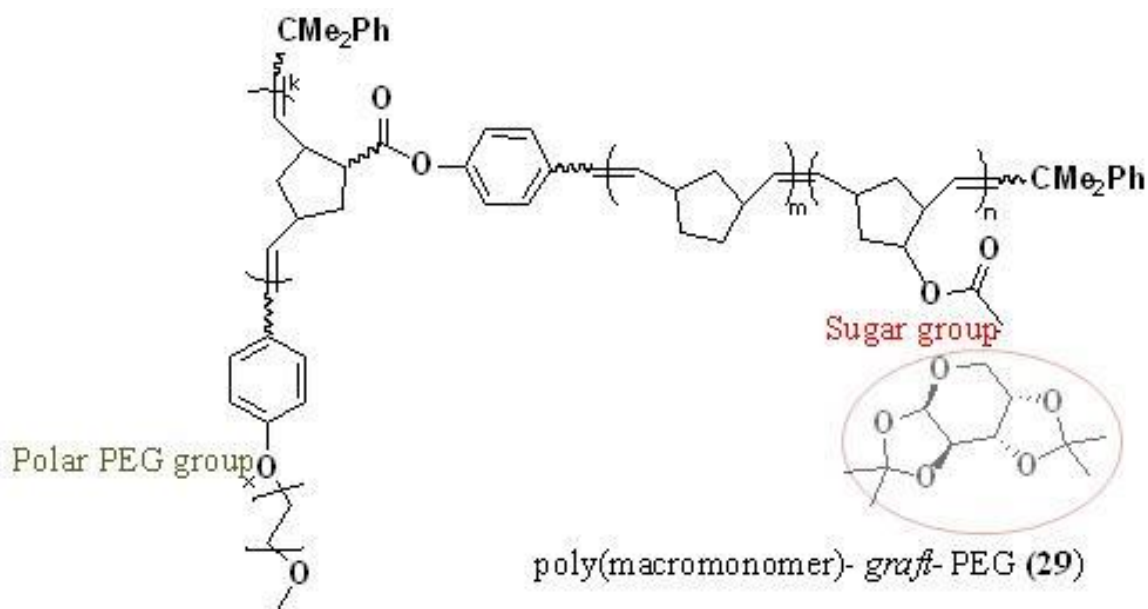
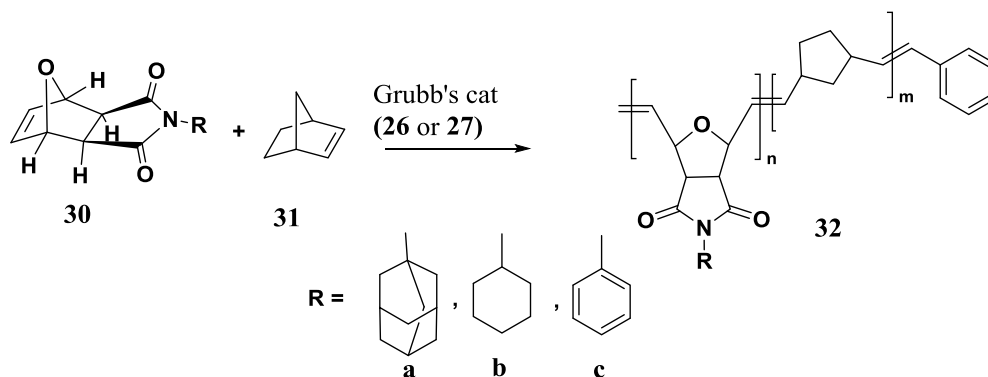


Figure 1.10 Amphiphilic poly(macromonomer)-*graft*-PEG polymer (**29**) synthesized by Nomura *et al.*^{56a}

Polynorbornenes functionalized with carboximide show high thermal resistance, high T_g 's and good mechanical properties.⁵⁷ Polymer membranes of these carboximides exhibited high permselectivity (restriction of permeation of macromolecules across a glomerular capillary wall on the basis of molecular size, charge, and physical configuration) for the separation of H_2 from N_2 , CO_2 , CH_4 and ethylene.⁵⁷ ROMP of *N*-cycloalkyl-7-oxanorbornene dicarboximides (**30**) [alkyl: adamantyl (**a**), cyclohexyl (**b**) and phenyl (**c**)] using Grubbs' I and Grubbs' II catalysts (26 and 27) has been reported.³⁴ Homopolymers having number-average molecular weights (M_n) between 120,000 and 270,000 and PDI 1.2-1.3 were synthesized. Chain transfer and backbiting secondary reactions were claimed to be the reasons for the high PDI. Monomer to catalyst ratios of 1000:1, 4000:1 and 10,000:1 yielded molecular weights of 130,000, 150,000 and 230,000 respectively. Hence, it was concluded that monomers did not polymerize in a purely

living fashion. These are living polymers but as M/C ratio gets larger and molecular weight grows, the secondary reactions have more time to occur and terminations also occur during chain growth increasingly as molecular weight goes up.



Scheme 1.4 Random copolymerization of *N*-cycloalkyl-7-oxanorbornene dicarboximides (**30**) with norbornene (**31**) using Grubbs' I (**26**) and II (**27**) catalysts to produce polymers (**32**).³⁴

Copolymers of *N*-cycloalkyl-7-oxanorbornene dicarboximides (**30**) with norbornene (**31**) in different mole ratios were also synthesized using Grubbs' I and Grubbs' II catalysts (**26** and **27**) (Scheme 1.4). A significant increase in their T_g values was observed compared to that of the homopolymer of norbornene. Grubbs' I catalyst (**26**) yielded copolymers with 70% *trans* vinylene content, whereas Grubbs' II catalyst (**27**) yielded 50% *trans* vinylene content.

1.4.2 Acyclic diene metathesis polymerization (ADMET).

Acyclic diene metathesis polymerization (ADMET) is another living olefin metathesis step-growth polymerization technique widely used for the synthesis of functional polymers. It produces linear polymers with unsaturated polyethylene

backbones from α,ω -dienes. ADMET polymerization (an example is given in Figure 1.11) starts with⁵⁸ the dissociation of the tricyclohexylphosphine from Grubbs' catalyst (**33**) to produce metallo-alkene **34**. Metallo-alkene **34** coordinates with the diene (**35**) which forms a metallo-cyclobutane adduct **36**. Adduct **36** undergoes cyclo-reversion to release ethylene gas, which complexes to ruthenium in the new active metallo-alkene **38** (Figure 1.12). Ethylene gas is then released from **38** and removed from the reaction by the application of vacuum or a constant flow of inert gas. This drives the equilibrium forward. The resulting coordinatively unsaturated active metallo-alkene intermediate either undergoes phosphine re-association to form **39** or undergoes metathesis with a new diene until exhaustion of the starting material or until the chain growth is quenched to obtain high molecular weight polymers (**40**). Release of **40** regenerates coordinatively unsaturated **34** and the cycle can begin again. Polymers containing a variety of functional groups were synthesized using ADMET polymerization and were reviewed recently.⁵⁹

Enholm *et al.*⁶⁰ synthesized carbohydrate-containing polymers by ADMET polymerization using Grubbs' II catalyst (**27**). Terminal diolefin monomers (**41**) were prepared by the reaction of D-ribose, D-isosorbide (**2**) (Scheme 1.5) and D-isomannide (**3**) with 4-pentenoic acid. These monomers were then subjected to ADMET with Grubbs' II catalyst (**27**) to produce polymers containing sugars (eg : **42**). Terminal olefins have the advantage of generating ethylene during ADMET. Ethylene is readily removed allowing the reaction to propagate instead of reversing.

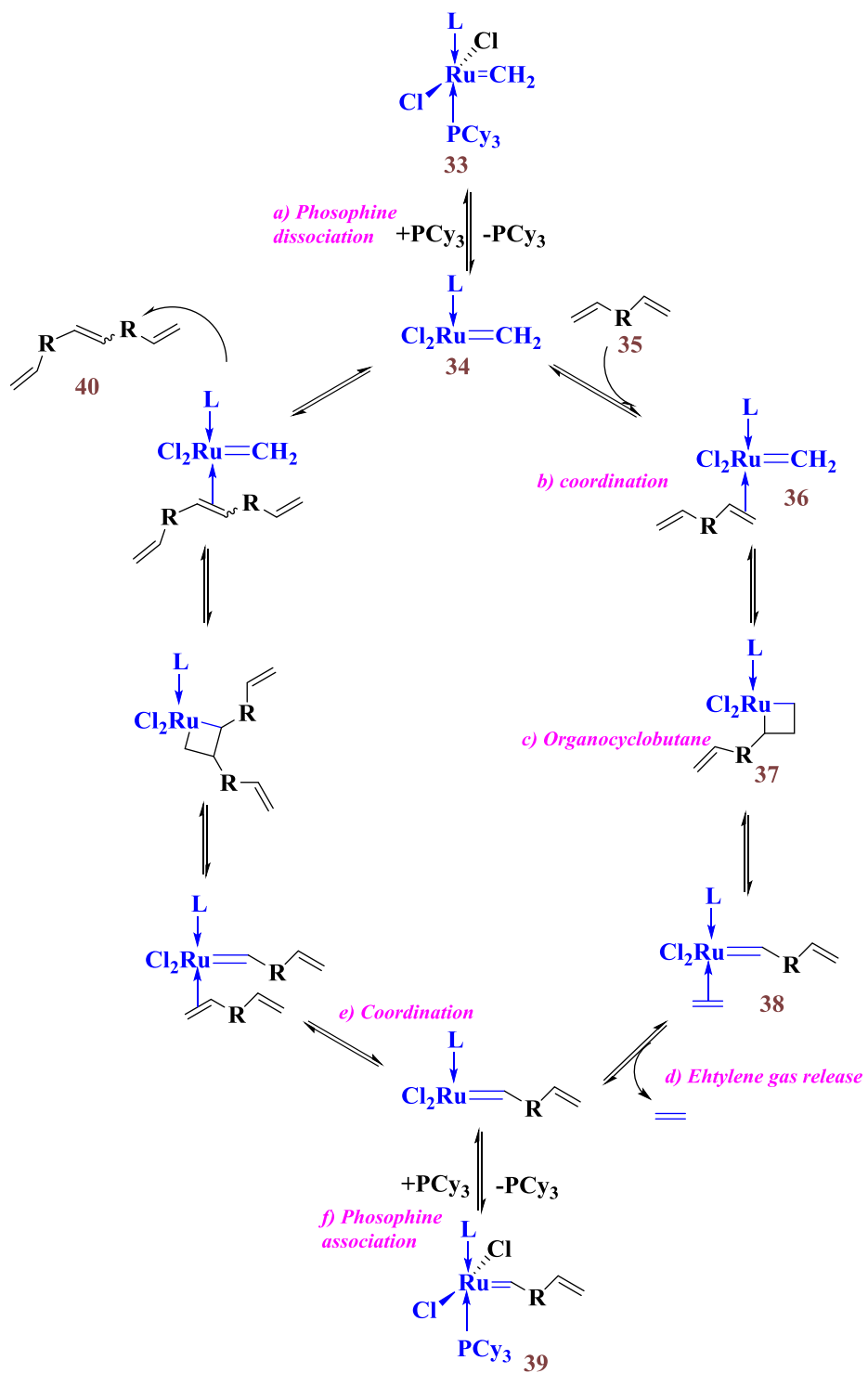
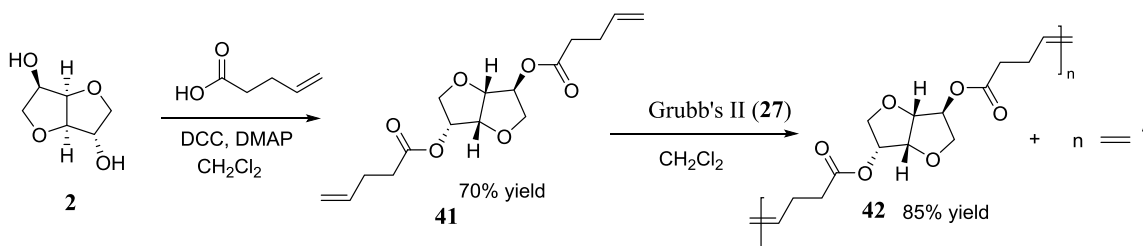


Figure 1.11 The mechanism of ADMET polymerization using Grubbs' catalysts.⁵⁸



Scheme 1.5 Synthesis of ADMET polymer (**42**) containing D-isosorbide (**2**).

1.5 Summary.

The utilization of renewable resources as alternatives for petroleum and natural gas products has immense commercial, and health and global warming significance. D-Isosorbide (**2**) is a bi-functional, polar, chiral and rigid molecule, which is produced from renewable sources. Synthesis of new polymers containing D-isosorbide (**2**) is of interest for polymers and in drug delivery. A number of polymers containing D-isosorbide (**2**) were synthesized and had useful properties. Ring-opening metathesis polymerization (ROMP) and acyclic diene metathesis polymerization (ADMET) are relatively new, yet widely used, polymerization techniques for the synthesis of polymers with different architectures. The aim of the present work is to synthesize various polymers (homo- and copolymers) containing D-isosorbide (**2**) via olefin metathesis routes. Monomers with norbornene (**31**) functionalized onto D-isosorbide (**2**), and *N*-cycloalkyl-7-oxanorbornene dicarboximide were synthesized and then used for ROMP. These monomers were polymerized using Grubbs' catalysts to generate a series of homo-, co-, block and cross-linked-polymers. These polymers were characterized using GPC, NMR, and IR. In addition, ADMET polymerization of a terminal diolefin-functionalized D-isosorbide (**2**) was also conducted to produce ADMET polymers.

1.6 GPC basics.

Polymers contain chains of different molecular weights. The molecular weights of these polymers are indicated by the statistical averages of the polymer molecular weight distribution. They include number-average M_n , weight-average M_w and z-average M_z of the molecular weight distribution (Figure 1.13). Size exclusion chromatography (SEC) otherwise known as gel permeation chromatography (GPC) separates molecules on the basis of their hydrodynamic volume or the size of the molecules rather than their enthalpic interactions with the stationary phase. Thus, high molecular weight fractions elute faster than low molecular weight fractions because larger molecules penetrate fewer pores of the stationary phase and are not held in as many pores for periods that delay elution.

The column is packed with porous particles of a defined pore size. When the polymeric solution is injected into the column, the molecules which are too large to pass through these pores elute faster. The smaller molecules go into a high fraction of the pore volume of the column and are retained longer in the column. As the molecular weight decreases, the elution time increases.

GPC takes into account the molecular size, which is in-turn related to the conformation, swelling and the shape of the molecules. Constant flow rate and baseline stability should be maintained especially when using a refractometer as the detector.

1.6.1 Solvent and hydrodynamic volume.

The hydrodynamic volume of a polymer changes as a function of solvent. Polymer chains become more expanded in a good solvent; hence the hydrodynamic

volume increases for a given molecular weight. The same polymer in a poor solvent, would have more contracted polymer chains hence a lower hydrodynamic volume.

If R_g is the radius of gyration of the polymer, N is the number of bond segments (equal to the degree of polymerization) of the chain and ν is a solvent-constant then $R_g \sim N^\nu$. In a good solvent, $\nu = 3/5$; for a bad solvent $\nu = 1/3$. Therefore, polymer in good solvent has larger size and behaves like a fractal (free) object. In a bad solvent, it behaves like a sphere. In a so-called θ -solvent, where the chain behaves as if it were an ideal chain, $\nu = 1/2$.

1.6.2 Column calibration: Conventional and universal.

1.6.2.1 Conventional calibration.

Calibration of a GPC column is typically made with a series of polymer standards (example: Polystyrene (PS)) with known molecular weights (MW)s and very narrow polydispersities. These polymer standards are first injected into a column and the elution volume (elution volume) of their corresponding peaks is measured. Then a plot of $\text{Log}(\text{MW})$ vs. elution volume gives a calibration curve (Figure 1.11). This calibration curve can be used to identify the molecular weight of the unknown sample as shown in Figure 1.13. The sample whose molecular weight needs to be estimated is injected into the GPC and its elution volume measured. The molecular weight of the unknown sample can be measured using the calibration curve, and the measured elution volume as M_w , M_n or M_z with the help of a concentration detector which shows the amount of polymer present at the detector as a function of elution volume. As the GPC measurements are made based on the hydrodynamic volume, we might assume that the samples have the

same molecular weights as that of standards at that hydrodynamic volume. But normally, this is not the case as different polymers will have various structural features; hence their hydrodynamic volumes for a given molecular weight polymer molecule will be different. Thus, molecular weights measured directly verses standards in this manner should be reported as relative molecular weights, relative to the polystyrene (or other) standards which were employed.

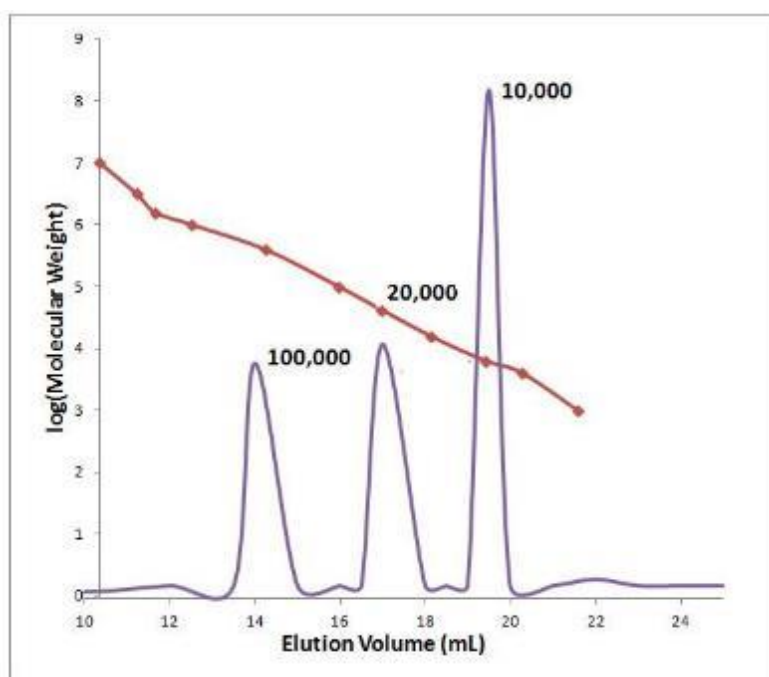


Figure 1.12 Generating a calibration curve using standards with Log(molecular weight on the Y-axis and elution volume on the X-axis.

1.6.2.2 Universal calibration.

Universal calibration is used to determine the absolute molecular weights of the polymers.⁶¹ Universal calibration of the columns is obtained by plotting elution volumes versus the $\text{Log}(M)[\eta]$, rather than $\text{Log } M$ versus elution volume (V_e). Here $[\eta]$ is the

intrinsic viscosity of each polymer standard making up the calibration curve. Then when the sample being studied is injected and one reads where its peak intersects, $\text{Log}(M)[\eta]$ value, that value is divided by the $[\eta]$ of the polymer being studied. By using $\text{Log}(M[\eta])$ in universal calibration, polymers with different chemical compositions all will fall into the same calibration curve.

1. $M[\eta]$ is proportional to the hydrodynamic volume of a polymer in solution.
2. All polymers with same hydrodynamic volume, irrespective of their composition, will elute at the same V_e .

Universal calibration curve is first constructed using standards. The sample is then injected. At each given elution volume, the hydrodynamic volume of the sample, designated by subscript x, is equal to the hydrodynamic volume⁶² of the calibrant.

$$M_{\text{std}} [\eta]_{\text{std}} = M_x [\eta]_x \quad (1.1)$$

From equation 1.1 if the intrinsic viscosity $[\eta]_x$ of the unknown sample is determined, with a known molecular weights M_{std} , and the intrinsic viscosities $[\eta]_{\text{std}}$ of the standards, one can calculate M_x , by: $M_x = M_{\text{std}} [\eta]_{\text{std}} / [\eta]_x$.

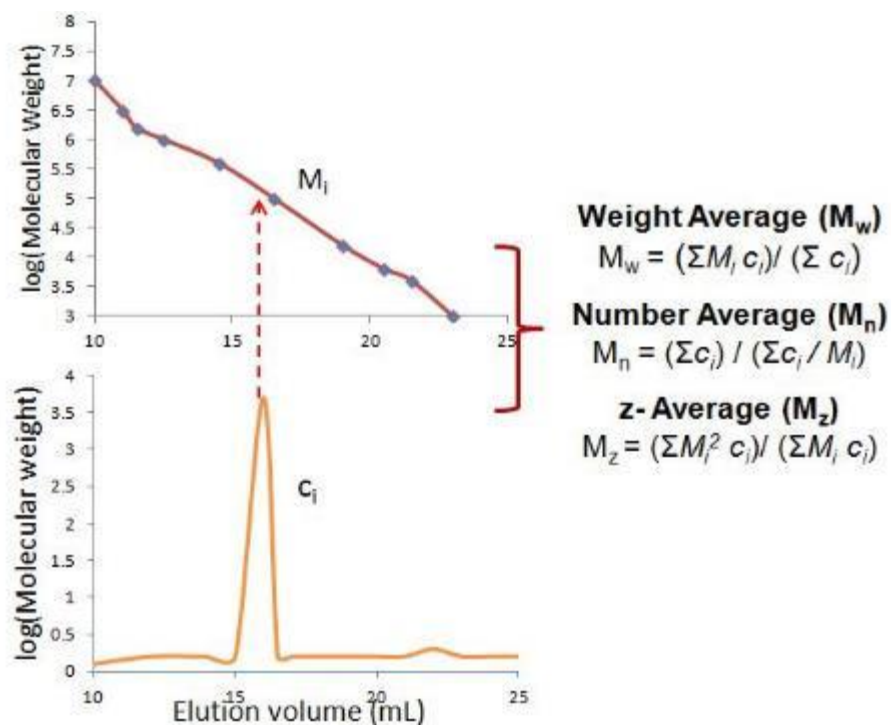


Figure 1.13 Determination of unknown-molecular weight of a sample using conventional calibration curve.

According to the Mark-Houwink relation, $[\eta]_x = KM_x^a$ where K and a are the Mark-Houwink coefficients of the sample. Solving 1.1 for M_x , we arrive at $\text{Log } M_x = [\text{Log}(M_{\text{std}}[\eta]_{\text{std}}) - \text{Log } K] / (a+1)$.

In this way, by knowing the Mark-Houwink coefficients of the standards, one can determine the molecular weights of the unknown by determining the intrinsic viscosity of the sample.

1.6.3 Light scattering detector.

Light scattering detectors employ the light scattering properties of the polymers or particles to determine the molecular size or the molecular weight. Light-scattering

detectors can be employed to determine the *absolute molecular weights* of the polymers. Rayleigh theory describes the relationship between the intensity of the light scattered by a sample and its size and molecular weight by use of Rayleigh equation (simplified form): $KC/R_\theta \propto (1/M_w)$. Here, C = the sample concentration, θ is the measurement angle, R_θ = the Rayleigh ratio (the ratio of the scattered light intensity to incident light intensity) at the measurement angle θ , M_w = Weight average molecular weight, and K is an instrument constant: $K = (4 \pi^2/\lambda_o^4 N_A) (\eta_o \cdot dn/dc)^2$. Here, λ_o is the laser wavelength in a vacuum, N_A is Avogadro's number, η_o is refractive index of the solvent, and dn/dc is the refractive index increment of the sample. Thus, for a sample known dn/dc values, K value can be determined. With the K value known, absolute molecular weights can be determined from the Rayleigh equation, for a known concentration of the sample.

1.6.4 GPC measurements in this work.

In this thesis, the molecular weights were determined using two GPC instruments. In one GPC instrument, (THF-PS) measurements were made using THF as the eluent at 30 °C. The concentration of the polymer fractions was determined using the refractive index (RI) detector. Polystyrene standards were used to get the calibration curves. The elution volumes of these synthesized polymers are compared directly to the elution volume of the polystyrene standards using the calibration curve. The molecular weight of the sample polymers (whose molecular weights are not known) result directly from the PS polymer that has that elution volume. Hence, the molecular weights given from this GPC are based on a direct comparison of the elution volumes of the samples with those of the PS standards. As shown earlier, these molecular weights will not be absolute

values because the polymers being studied do not have equivalent hydrodynamic radii with the PS standards when their molecular weights are the same. Elution volumes are based on hydrodynamic radii. Therefore, the polymer being analyzed will not elute at the same elution volume as a PS standard with the same molecular weight. Thus this method compares relative molecular weight values. For this reason, some of the sample molecular weights were determined at University of Southern Mississippi (USM) using a light scattering detector and dn/dc values.

The GPC instrument at USM (DMF-LS) employed, in DMF as the solvent at 50 °C. This instrument is equipped with a refractive index detector (RI) and a light-scattering (LS) detector. The RI detector determines the concentration of the polymer fraction, while the LS detector uses this concentration value to determine the absolute weight averaged molecular weight of the polymer at that elution volume using the Rayleigh equation. Refractive index detector is used to calculate the number-averaged molecular weight (M_n) and the PDI of the polymers (which are not absolute).

Molecular weight correction: The molecular weight generated for certain polymers analyzed using THF-PS instrument verses PS standards is not absolute but it can be corrected using the absolute M_w values generated by DMF-LS instrument. This correction can be made by dividing the DMF-LS molecular weight with the THF-PS molecular weight.

Molecular weight correction factor = Q factor = $[M_w \text{ from (DMF-LS)}] / [M_w \text{ from (THF-PS)}]$.

CHAPTER II

RESULTS AND DISCUSSION

2.1 Introduction.

Monomers containing polymerizable norbornene or 7-oxo-norbornene functions were synthesized using DCC-DMAP coupling chemistry or as reported in the literature. New compounds were characterized using NMR, FT-IR, GC-MS and HRMS. The monomers were subjected to ring-opening metathesis polymerization (ROMP) using Grubbs' type I or type II catalysts to generate homopolymers, random copolymers or block co- and ter-polymers. The polymers were characterized using ^1H NMR, FT-IR, and GPC methods. TGA analysis was also performed for certain polymers. ADMET polymerization was also attempted on a D-isosorbide-containing di-terminal olefin monomer (**52**).

2.2 Starting material.

2.2.1 D-Isosorbide (**2**).

D-Isosorbide (**2**) is a 1,4:3,6-dianhydrohexitol (DAH) containing two hydroxyl groups, one on C2 in an *exo* conformation and the other on C5 in an *endo* conformation. (Figure 2.1). The NMR chemical shifts of D-isosorbide (**2**) and its various derivatives were summarized in the review of 1,4:3,6-dianhydrohexitols (DAHs) by Stross *et al.*⁷ The ^1H NMR and ^{13}C NMR assignments in this thesis were made for D-isosorbide (**2**)

(Figure 2.2) based on the assignments given in this review. In the ^1H spectrum, the singlet at δ 4.34 is assigned to the proton on C2, and the multiplet observed at δ 4.28 is assigned to the proton on C5. Two doublets observed at δ 2.89 and 2.82 correspond to the protons of the two hydroxyl groups. As reported previously, ^{13}C peaks at δ 76.5 and 72.2 correspond to C2 and C5 were observed (Figure 2.2).

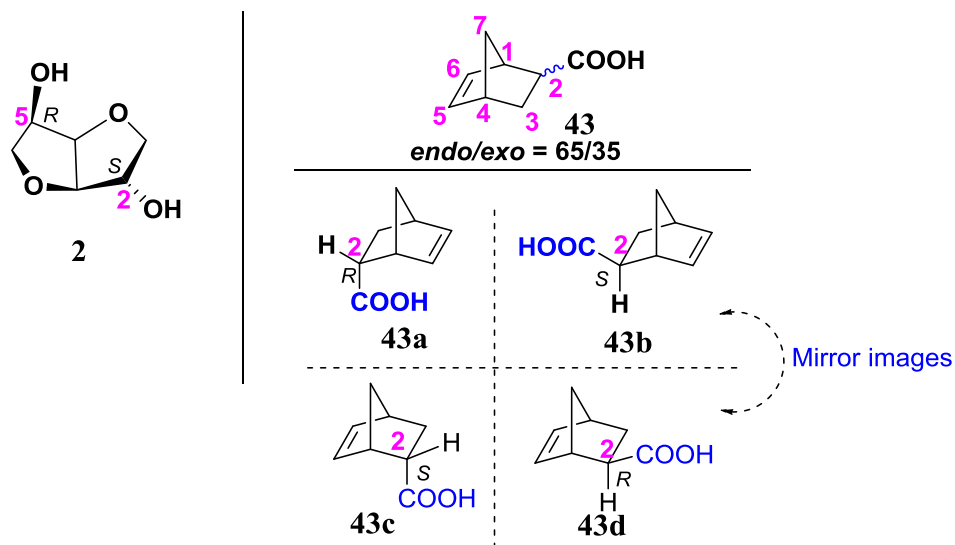


Figure 2.1 Structure of D-isosorbide (**2**) and the racemic mixture of both *exo* and *endo* isomers of, 5-norbornene-2-carboxylic acid (NbCOOH) (**43**).

The ratio of the *endo* (**43a,c**) and the *exo* (**43b,d**) isomers is 65:35 as determined by ^1H NMR.

2.2.2 5-Norbornene-2-carboxylic acid (**43**) (mixture of *endo* and *exo*).

5-Norbornene-2-carboxylic acid (NbCOOH) (**43**) purchased from Sigma-Aldrich (USA) was a mixture of two isomers, with the carboxylic acid group on C2 either in the *exo* or in the *endo* position (Figure 2.1). In the ^1H NMR, two multiplets corresponding to the single C6 vinylic proton were observed at δ 5.9 and 6.1 with an integrated area ratio of 1:0.55, respectively. From this area ratio, the ratio of the *endo* (**43a,c**) and *exo* (**43b,d**)

isomers of NbCOOH (**43**) is 65:35 (*endo* : *exo*). This mixture of isomers was used for the synthesis of monomers for ROMP.

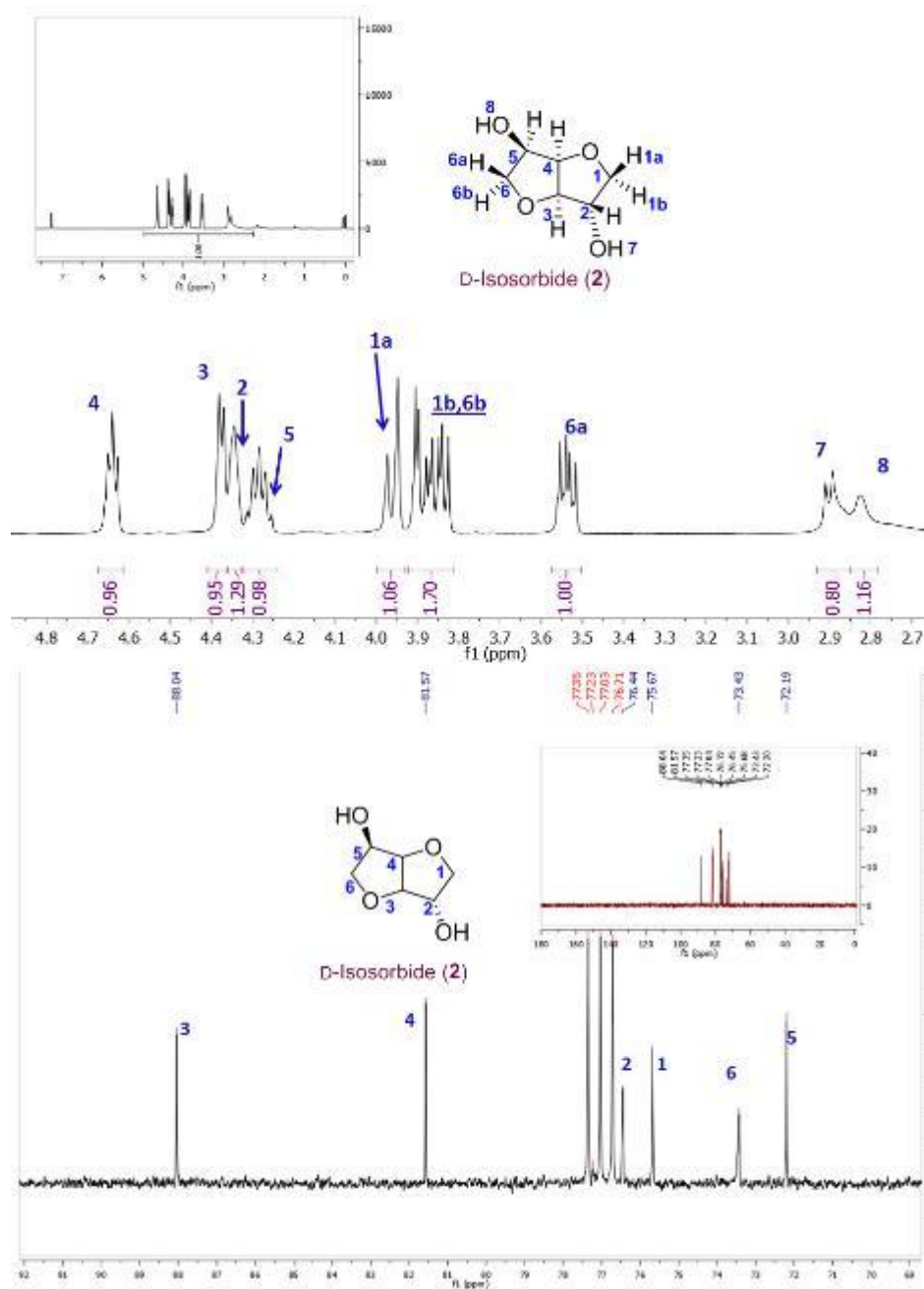


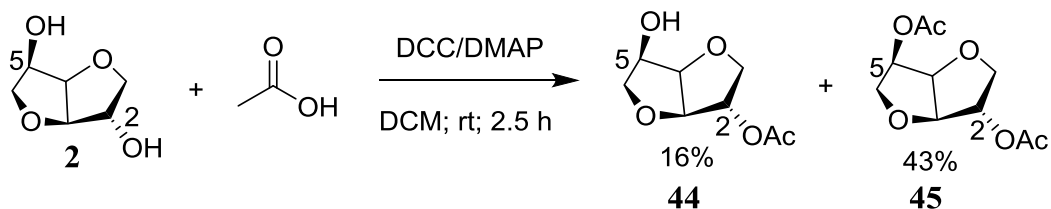
Figure 2.2 The ¹H NMR (δ 2.5 –4.8) and ¹³C NMR (δ 92–69) spectra and the spectral assignments⁷ of D-isosorbide (**2**) in CDCl₃.

The insets in the two spectra show the full NMR spectra of **2**.

2.3 Synthesis of monomers for ROMP and ADMET polymerizations.

2.3.1 Synthesis of 2-*exo*-acetyl D-isosorbide (**44**).

Acetylation of D-isosorbide (**2**) was performed with acetic acid using DCC-DMAP in DCM by stirring at room temperature for 2.5 h to produce the mono- and di-acetylated products, 2-*exo*-acetyl D-isosorbide (**44**) and 2,5 di-acetyl-D-isosorbide (**45**) in 16% and 43% yields, respectively. These products were confirmed using ^1H NMR and IR analysis. The spectral data matched with the previous reports of **44** and **45**.¹⁰



Scheme 2.1 Acetylation of D-isosorbide (**2**) to produce 2-*exo*-acetyl D-isosorbide.

The NMR spectra of **44** (Figure 2.3) was compared with **2** (Figure 2.2) to see the changes in the δ values. The proton on C2 underwent a downfield shift from δ 4.34 in **2** to δ 5.17 in **44**, whereas the proton on C5 of **44** stayed at δ 4.28. Similarly, in ^{13}C NMR spectrum of **44**, the C2 carbon shifted downfield from δ 75.7 in **2** to 78.3. The C5 carbon resonance stayed at 72.2 (as in **2**). This indicates that the acetylation occurred selectively on the C2-*exo* hydroxyl group instead of on C5-*endo* hydroxyl group.

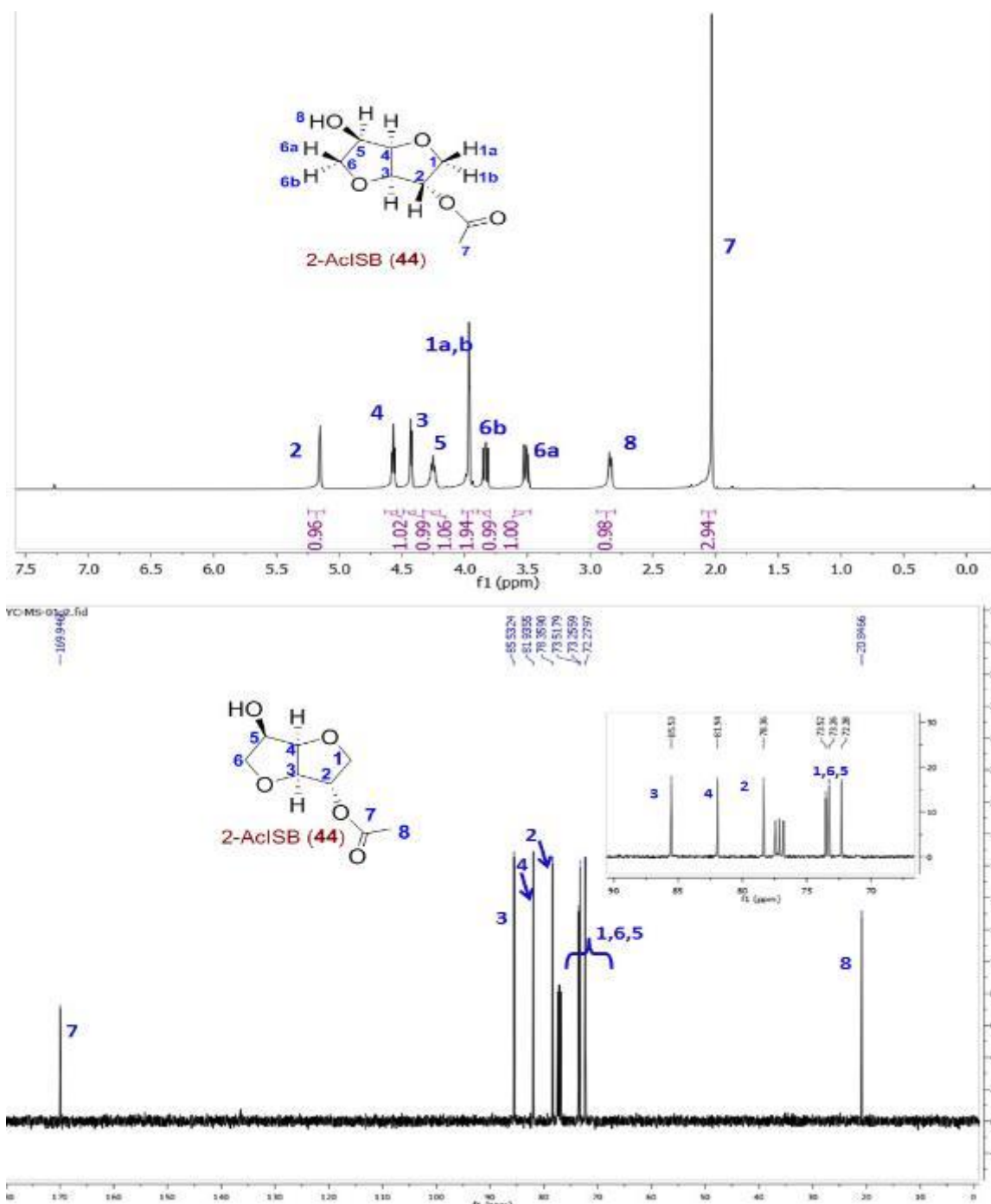
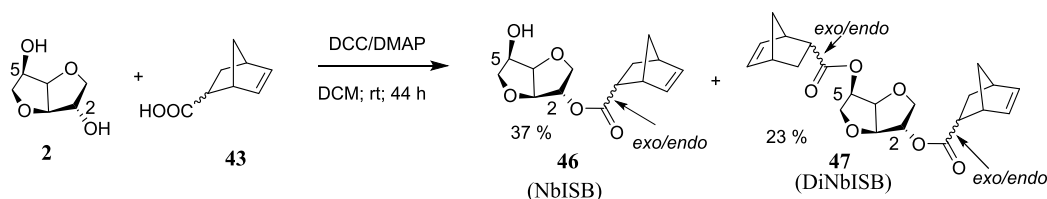


Figure 2.3 The ¹H NMR and ¹³C NMR spectra of 2-*exo*-acetyl-D-isosorbide (2AcISB) (**44**) in CDCl₃.

2.3.2 Coupling of D-isosorbide (**2**) with 5-norbornene-2-carboxylic acid (**43**).

D-Isosorbide (**2**) and 5-norbornene-2-carboxylic acid (**43**) (65:35 mixture of *endo* and *exo*) were coupled using the DCC-DMAP in dry DCM upon stirring for 44 h to generate two products. A mono-substituted product (2-*exo*-D-isosorbyl)-5-norbornen-2-carboxylate (NbISB) (**46**) was generated as a mixture of two isomers in 37% yield. Also, the di-substituted product (2-*exo*-5-*endo*-D-isosorbyl)-di-5-norbornen-2-carboxylate (DiNBISB) (**47**) was also generated as an isomeric mixture at 23 % yield.



Scheme 2.2 Synthesis of (2-*exo*-D-isosorbyl)-5-norbornen-2-carboxylate (NbISB) (**46**) and (2-*exo*-5-*endo*-D-isosorbyl)-di-5-norbornen-2-carboxylate (DiNBISB) (**47**).

2.3.2.1 (2-*exo*-D-Isosorbyl)-5-norbornen-2-carboxylate (NbISB) (**46**).

(2-*exo*-D-Isosorbyl)-5-norbornen-2-carboxylate (NbISB) (**46**) was analyzed using NMR, IR, GC-MS and HRMS. In its ^1H NMR spectrum, a shift in the C2 proton's peak on was observed from δ 4.34 in D-isosorbide (**2**) to δ 5.18. The proton on C5 stayed at δ 4.28 as in D-isosorbide (**2**), indicating a free hydroxyl group was present on C5 (Figure 2.5). The ^{13}C spectrum of **46** indicated a downfield shift had taken place for the C2 carbon (which contains the *exo* OH group) from δ 75.7 in **2** to δ 78.10 in **46**. However, the C5 carbon (which contains the *endo* OH group) of **46** stayed at δ 72.2 (as in **2**). This confirms that the esterification of **43** with **2** occurred selectively on the less sterically

hindered C2-*exo* hydroxyl group in NbISB (**46**). The FT-IR spectrum of **46** exhibited a hydroxyl peak at 3,400 cm⁻¹.

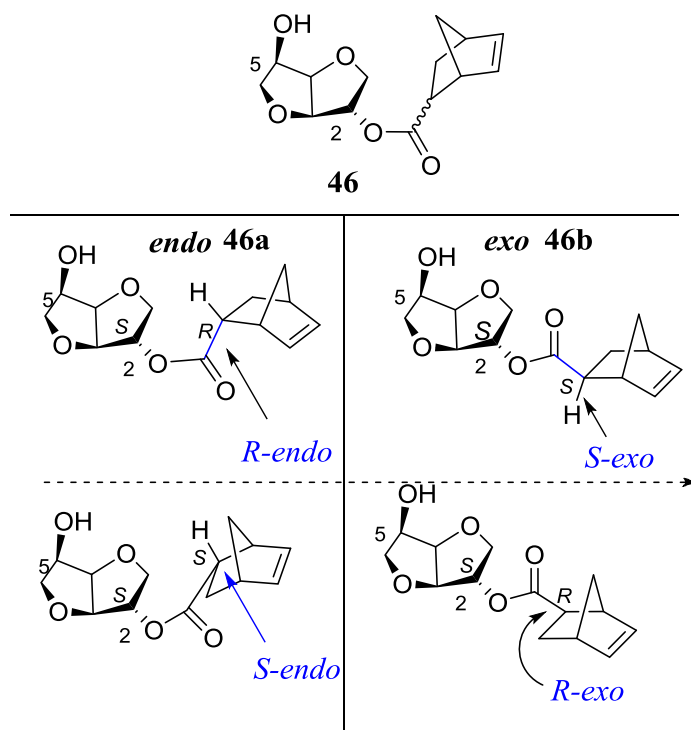


Figure 2.4 The diastereomers of (2-*exo*-D-isosorbityl)-5-norbornen-2-carboxylate (NbISB) (**46**).

The ratio is estimated to be 81:19 *endo* to *exo* by from the peak total ion chromatogram ratios in MS from the two GC peaks in GC-MS.

As shown in the Figure 2.4, there are four possible diastereomers for **46** since the starting carboxylic acid **43** is a 35:65 mixture of *exo* and *endo* isomers and each of the latter can have wither *R* or *S* configurations (eg. enantiomers). The presence of two peaks at δ 5.18 for the proton on C2 at a ratio of 1:0.35 indicated that at least two diastereomers 2-*exo*-D-isosorbityl)-5-norbornen-2-*endo*-carboxylate (**46a**) and (2-*exo*-D-isosorbityl)-5-norbornen-2-*exo*-carboxylate(**46b**) are present in the product at a ratio of 3:1. GC-MS

spectrum (Figure 2.6) showed the presence of two peaks at a total ion chromatogram ratio 81:19, corresponding to the *endo* and *exo* ratio of the two isomers, respectively. The parent ions of the two GC peaks (at $m/e = 266$) have identical mass and identical splitting patterns confirming that they are isomers of each other. HRMS spectra of this enantiomeric mixture (Figure 2.7) confirmed the accurate mass of **46**. $[M+H]^+$ Ion formula $C_{14}H_{19}O_5$; Calculated m/z 267.1227; Obtained m/z 267.1217; Difference (*ppm*) 3.85. $[M+Na]^+$ 289.1033. The main ion observed was the sodium adduct.

The *endo* (norbornene) ester 46a as two diastereomers shown in the left column of Figure 2.4. These are the *S,R-endo* and *S,S-exo* compounds. Likewise, the *exo* (norbornene) ester 46b is a mixture of two diastereomers, *S,S-exo* and *S,R-exo*. The two chromatograph peaks may each contain one or more of the possible diastereomers. This question was not further investigated.

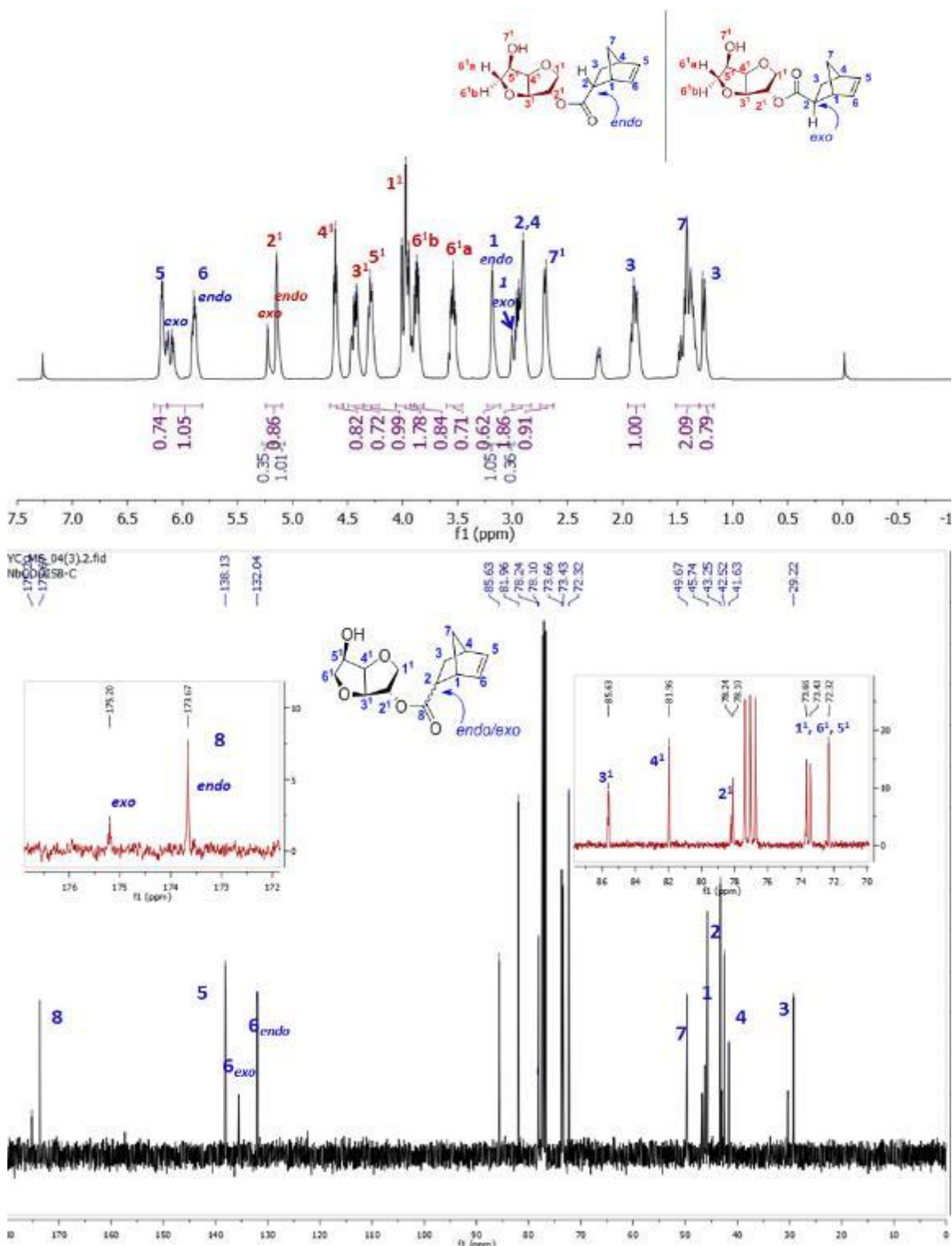


Figure 2.5 The ^1H and ^{13}C NMR spectrum of the 81/91, *endo/exo* isomeric mixture of (2-*exo*-D-isorbyl)-5-norbornen-2-carboxylate (NbISB) (**46**) in CDCl_3 .

The D-isorbyl portion of NbISB is numbered with superscripts.

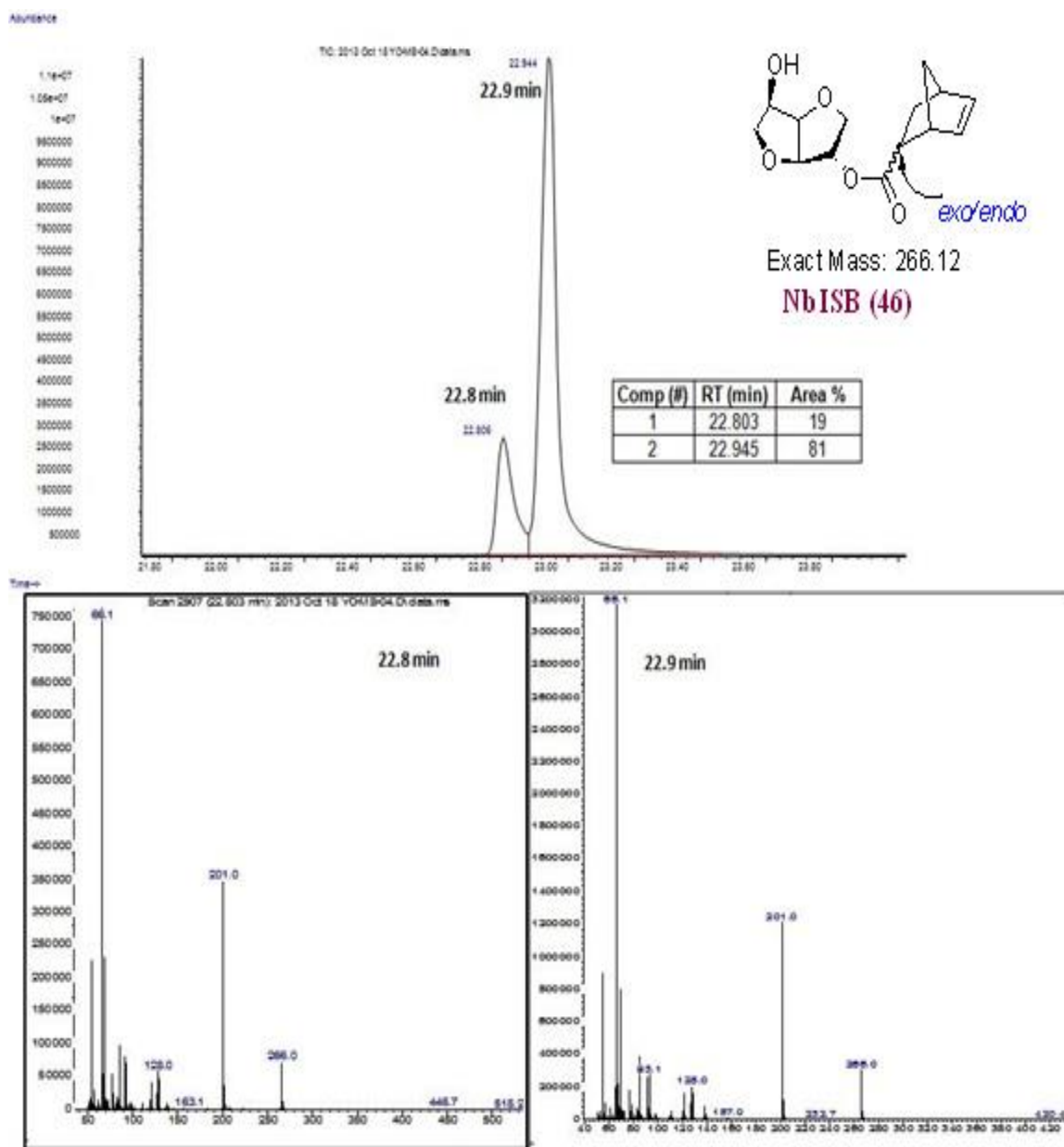


Figure 2.6 GC-MS analysis of the isomeric *endo/exo* mixture of (2-*exo*-D-isosorbyl)-5-norbornen-2-carboxylate (NbISB) (46).

GC indicates the presence of two peaks representing two isomers with an area ratio (total ion current) as 19:81. The parent ions of the two peaks at $m/e = 266$ have identical mass and identical splitting patterns confirming that they are isotopes of each other.

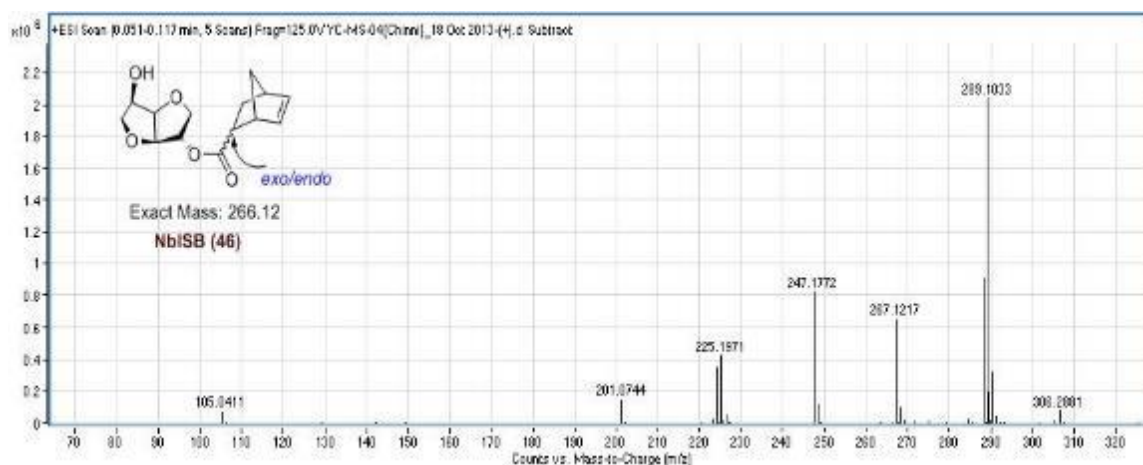


Figure 2.7 HRMS spectrum of the isomeric mixture of NbISB (**46**).

$[M+H]^+$ Ion formula $C_{14}H_{19}O_5$; Calculated m/z 267.1227; Obtained m/z 267.1217; Difference (ppm) 3.85. $[M+Na]^+$ 289.1033. The main ion observed was the sodium adduct.

2.3.2.2 (2-*exo*-5-*endo*-D-Isosorbyl)-di-5-norbornen-2-carboxylate (DiNBISB) (**47**)

The FT-IR spectrum of **47** contained no hydroxyl O-H stretching peaks at 3,400 cm^{-1} . The 1H NMR spectrum (Figure 2.8) of **47** indicated the absence of the hydroxyl protons and the presence of two norbornene units for each D-isosorbide (**2**) unit. The starting NbCOOH (**43**) is a mixture of two isomers (*exo* and *endo*), each of which is a racemic mixture. Both enantiomers of both the *exo* and *endo* isomers can react with either of the two-hydroxyl groups in **2**. Hence, there could be many possible distinct products only four of which are shown in Figure 2.8. Each of the four isomers shown in Figure 2.8 can be written with the other enantiomer of 5-norbornene-2-carboxylic acid having esterified the D-isosorbide. Since the C2 and C5 of D-isosorbide are unique (*exo* and *endo*, respectively and *S* and *R* absolute configuration, respectively this leads to isomeric combinations. However, all of these would simply perform as cross-linking agents in ROMP polymerizations of di-norbornenyl monomers.

The ^1H NMR spectrum of product **47** had two multiplet peaks between δ 5.8 and 6.2 for the two vinylic protons present on the C5 and C6 positions of the two attached norbornene rings (Figure 2.9). Similarly, in the ^{13}C spectrum several minor peaks were observed the region corresponding to the norbornene group. This indicates the presence of more than one isomer in **47**, as expected. The presence of more than a single isomer was confirmed by GC MS analysis, where three different GC peaks (Figure 2.10) with areas 8.5 %, 59.5 % and 32.0 % was observed. Each of these peaks may contain more than one isomer. These peaks have similar mass-fragmentation profiles (Figure 2.11). Hence, it can be concluded that the obtained product is a mixture of many diastereomers. Four such isomers **47a-d** are shown in Figure 2.8. The HRMS spectrum of this isomeric mixture confirmed the mass of the compound was correct for its molecular formula (Figure 2.12). The main ion observed is the sodium adduct of **47**.

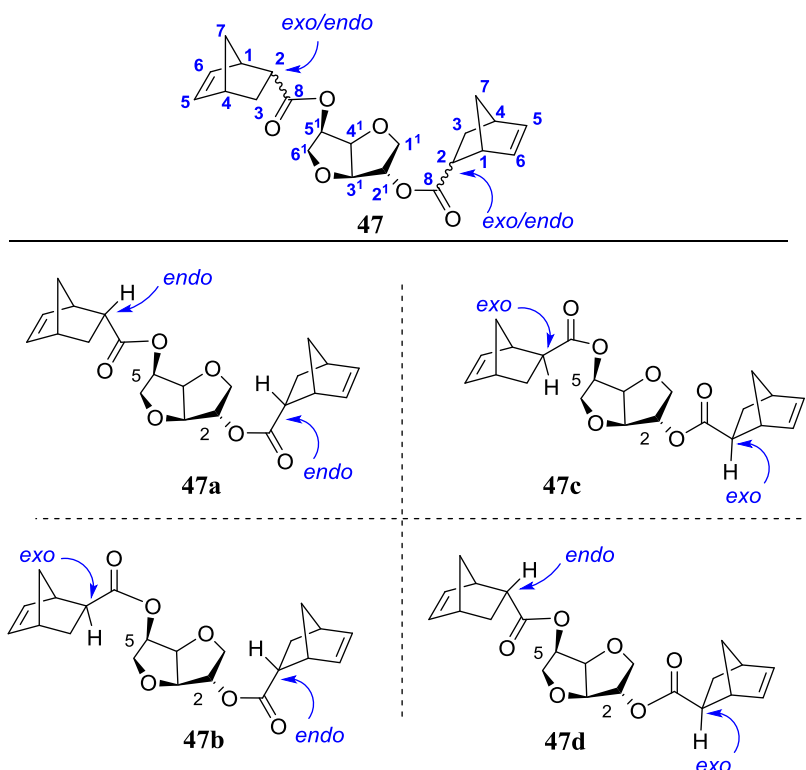


Figure 2.8 The four possible diastereomers of (2-*exo*-5-*endo*-D-isosorbyl)-di-5-norbornene-2-carboxylate (DiNBISB) (**47**).

Each of these could have either (*R*) or (*S*) enantiomer of 5-norbornene-2-carboxylic acid esterified to the C2 and C5 hydroxyl groups of D-isosorbide (**2**) core.

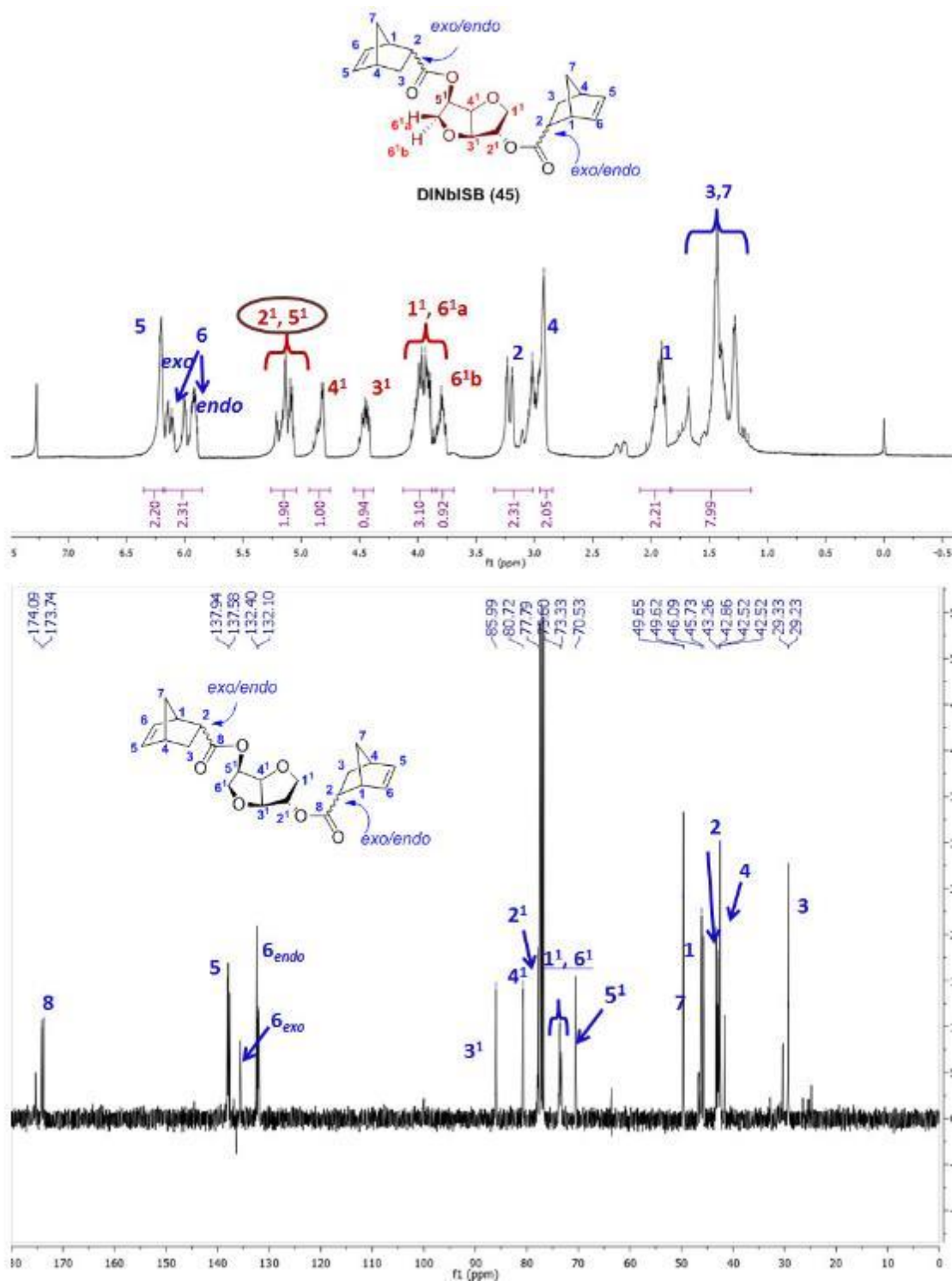


Figure 2.9 The ¹H and ¹³C NMR spectra of DiNbISB (47).

The D-isosorbide portion of DiNbISB is numbered with superscripts.

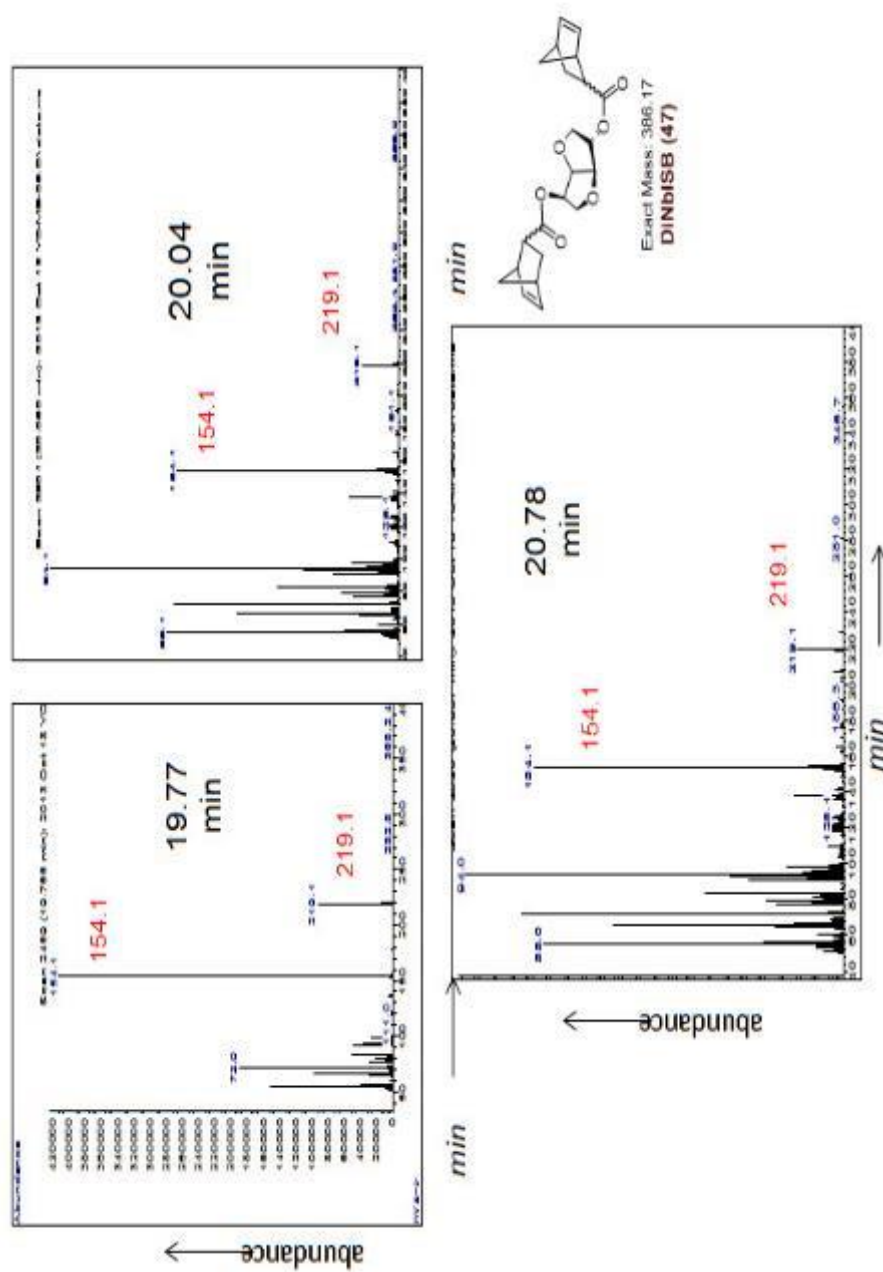


Figure 2.11 MS fragmentation patterns observed for the three peaks GC chromatogram (Figure 2.10) of DiNbISB (47). The peaks at 20.04 and 20.78 min show identical fragmentation pattern, whereas the peak at 19.77 min shows peaks at m/z 154.1 and 219.1 (similar m/z peaks are seen in 20.04 and 20.78 min peaks). This indicates that the three peaks belong to isomers or isomer mixtures. All the three peaks show identical mass fragmentation patterns indicating that they are isomers of each other.

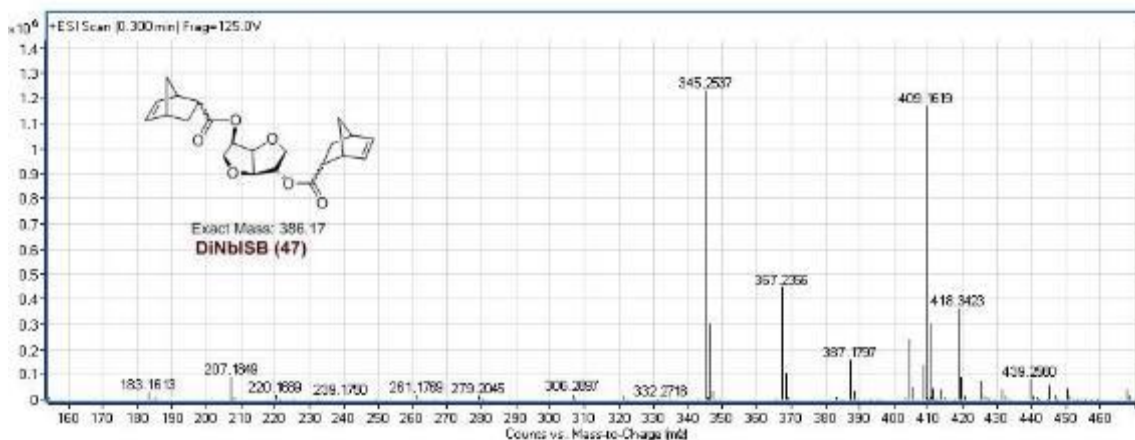
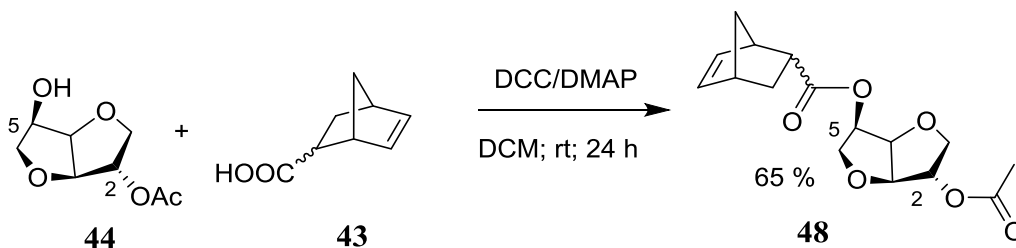


Figure 2.12 HRMS spectrum of DiNbISB (**47**).

$[M+H]^+$ Ion formula $C_{22}H_{27}O_6$; Calculated m/z 387.1802; Obtained m/z 387.1797; Difference (ppm) 1.17. $[M+Na]^+$ 409.1620. The main ion observed was the sodium adduct.

2.3.2.3 [(2-*exo*-acetyl)-5-*endo*-D-isosorbyl]-di-5-norbornen-2-carboxylate (AcNbISB) (**48**).

2-*exo*-Acetyl-D-isosorbide (**2-7**) was coupled with 5-norbornene-2-carboxylic acid (**43**) (mixture of *endo* and *exo*) using DCC-DMAP to produce [(2-*exo*-acetyl)-5-*endo*-D-isosorbyl]-di-5-norbornen-2-carboxylate (AcNbISB) (**48**) as a mixture of two sets of diastereomers (*exo R*, *exo S* and *endo R*, *endo S*) when esterification occurred at the C5 (*R* configuration) *endo* hydroxyl group (Scheme 2.3). The yield was 65% based on **44**.



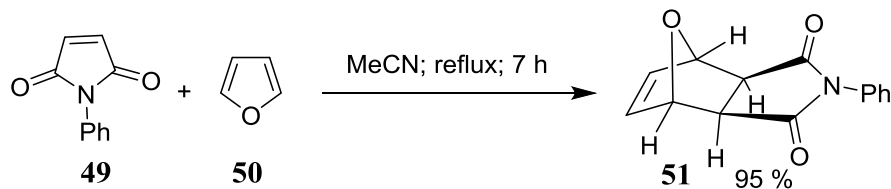
Scheme 2.3 Synthesis of [(2-*exo*-acetyl)-5-*endo*-D-isosorbyl]-di-5-norbornen-2-carboxylate (AcNbISB) (**48**).

The FT-IR spectrum of **48** contained no hydroxyl O-H stretching at 3,400 cm⁻¹, which indicates both hydroxyl groups in **48** were substituted. The ¹H NMR spectrum of **48** (Figure 2.13) exhibited chemical shifts of the protons on C2 and C5 at δ 5.16 and 5.07. This represents downfield shifts compared to δ 4.34 and 4.24 for the protons on C2 and C5 of D-isosorbide (**2**). The ¹³C spectrum showed peaks at δ 78.01 and 70.6 corresponding to carbons C2 and C5. This represents a down field shift of the C2 proton (against δ 75.7 for C2 in **2**) and an up field shift of the C5 proton (against δ 72.2 for the same in **2**). A singlet resonance corresponding to the three-acetyl protons was observed at δ 2.08. This confirms both hydroxyl groups in **48** were substituted. The product **48** was also expected to be an unequal mixture of two sets of diastereomers (four total compounds). This was confirmed by the presence of smaller NMR resonances adjacent to those (both ¹H and ¹³C) in the norbornene region of the spectra. The presence of more than a single isomer was confirmed by GC MS analysis, where three different GC peaks (Figure 2.14) were observed with areas 12, 12.4 and 75.6 %. These three peaks have similar fragmentation patterns. Also one of those peaks contains more than one isomer. HRMS spectrum confirmed that the molecular ion had the formula C₁₆H₂₀O₆ as expected for **47**. [M+H]⁺ Ion formula C₁₆H₂₁O₆; Calculated *m/z* 309.1333; Obtained *m/z* 309.1335; Difference (*ppm*) 0.57. [M+Na]⁺ 331.1156. The main ion observed was the sodium adduct.

2.3.3 *exo*-N-Phenyl-7-oxanorbornene-5, 6-dicarboximide (NbIMPh) **51**.

The compound *exo*-N-Phenyl-7-oxanorbornene-5, 6-dicarboximide (NbIMPh) **51** was synthesized as reported in the literature.^{34, 63} *N*-Phenylmaleimide was refluxed with

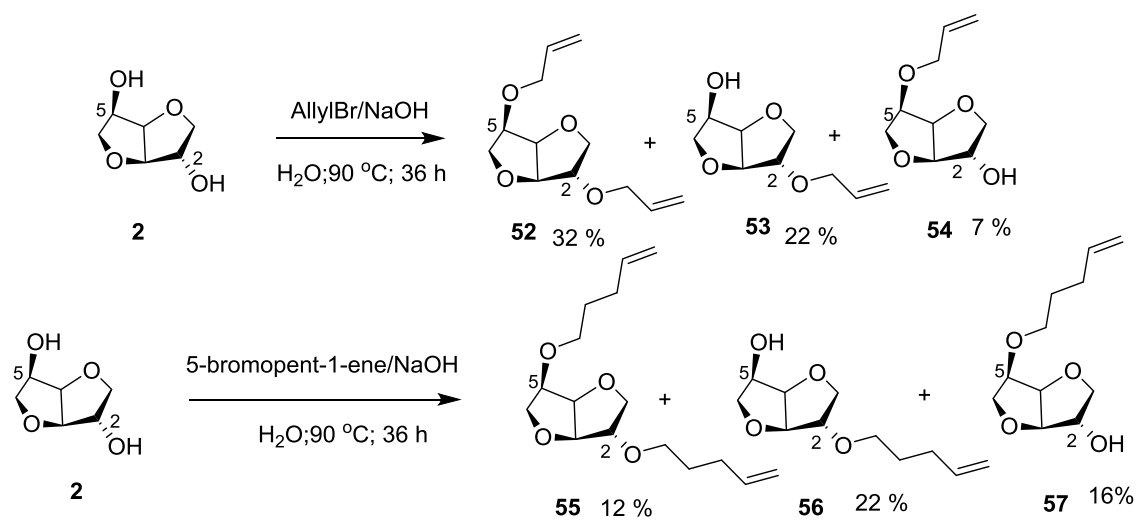
furan for 7 h to generate **51** in 78 % yield. The structure of **51** was confirmed by ^1H NMR and IR spectra. ^1H NMR indicated that the product **51** is not a mixture (due the absence of splitting in the protons at δ 6.61, 5.25 and 3.0. MP (164-165 $^{\circ}\text{C}$) of **51** confirmed that the product is an *exo* isomer (as in the literature³⁴).



Scheme 2.4 Synthesis of *exo*-N-Phenyl-7-oxanorbornene-5,6-dicarboximide (NbIMPh) **51**.

2.3.4 Diallyl-D-isosorbide (**52**).

Diallyl-D-isosorbide (**52**) was synthesized as reported in the literature⁶⁴ by refluxing allyl bromide and D-isosorbide (**2**) in aqueous NaOH at 90 $^{\circ}\text{C}$ for 36 h. A 32% yield was obtained based on D-isosorbide (**2**). **52** was utilized as a monomer for ADMET polymerization reactions. Dipentenyl-D-isosorbide (**55**) was also synthesized using this same procedure used to synthesize **52** to generate **55**, but now at a lower yield (12 %) compared to that of **52** (32 %), perhaps due to low water solubility of 5-bromopent-1-ene.



Scheme 2.5 The synthesis of monomers to for acyclic-diene metathesis (ADMET) polymerization from D-isosorbide (**2**).

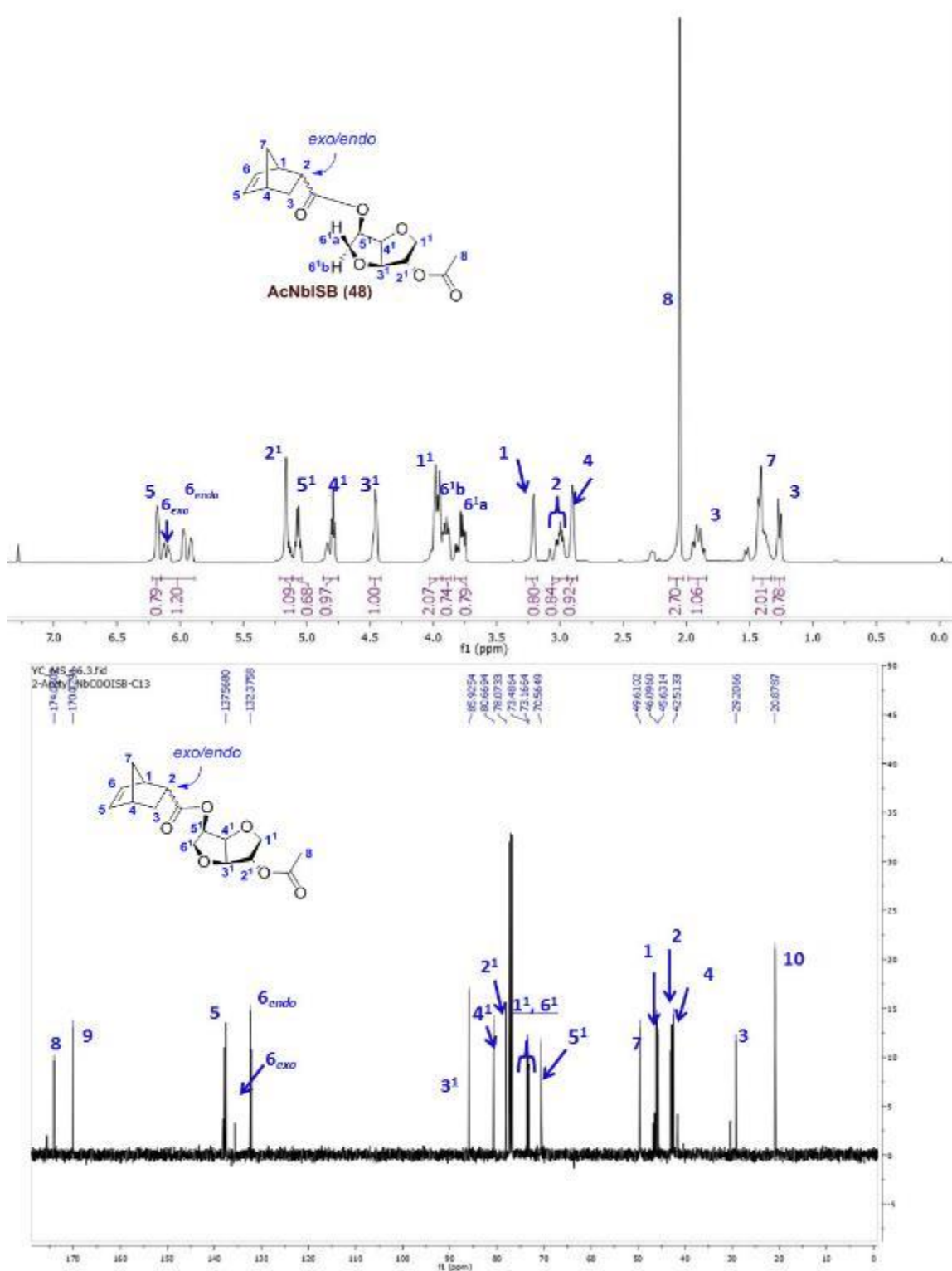


Figure 2.13 The ¹H and ¹³C NMR spectra of AcNbISB (**48**) in CDCl₃.

The D-isosorbide portion of AcNbISB is numbered with superscripts.

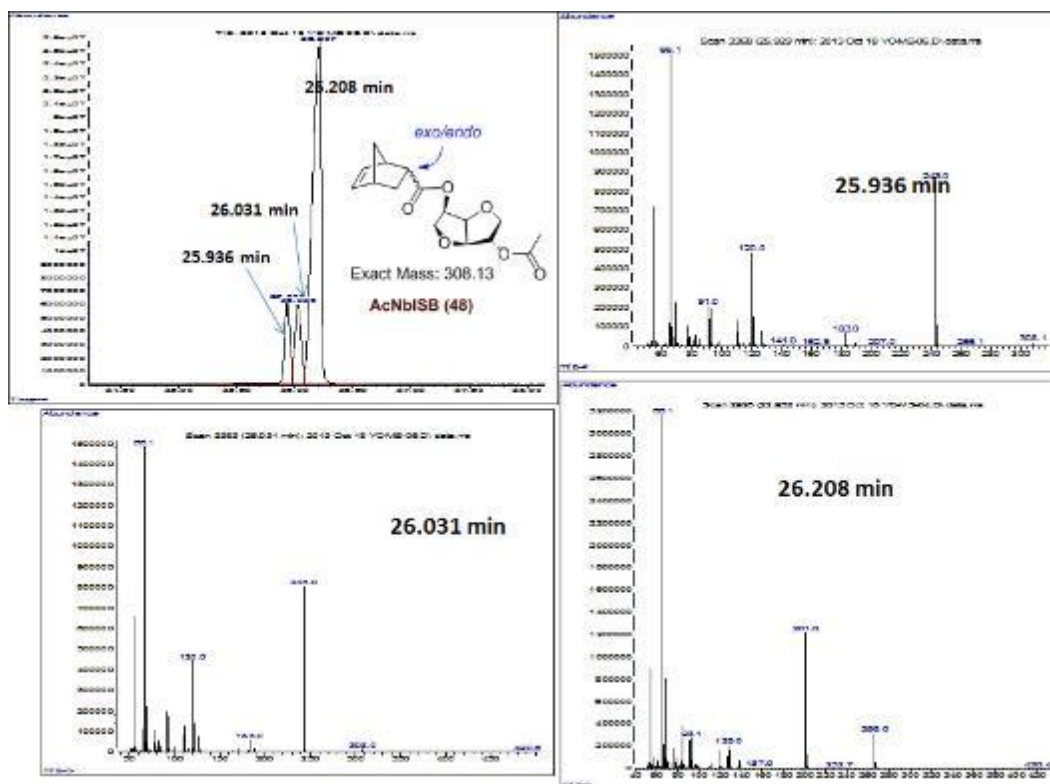


Figure 2.14 GC-MS spectrum of 81/19 *endo/exo* AcNbISB (**48**).

All three peaks showed the molecular ion peak at m/z 308.13. Hence, they are isomers of each other.

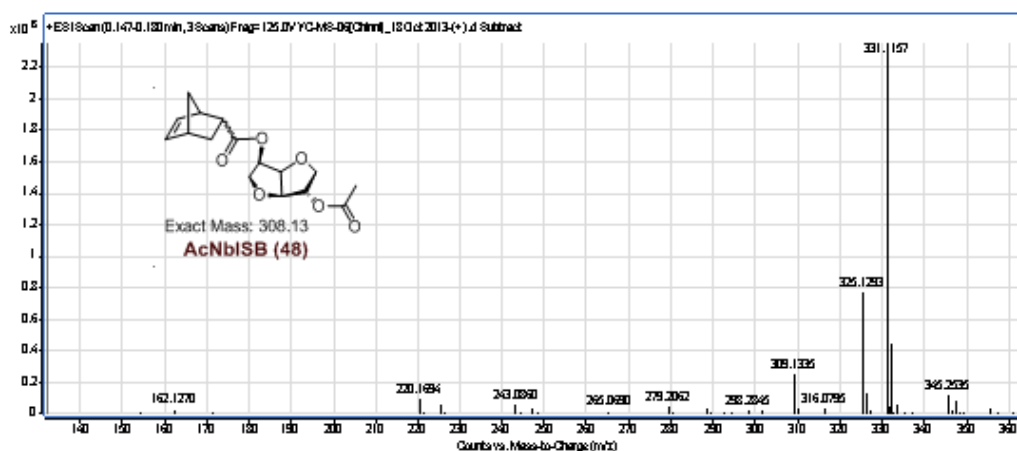


Figure 2.15 The HRMS spectrum of AcNbISB (**48**).

$[M+H]^+$ Ion formula $C_{16}H_{21}O_6$; Calculated m/z 309.1333; Obtained m/z 309.1335; Difference (ppm) 0.57. $[M+Na]^+$ 331.1156. The main ion observed was the sodium adduct.

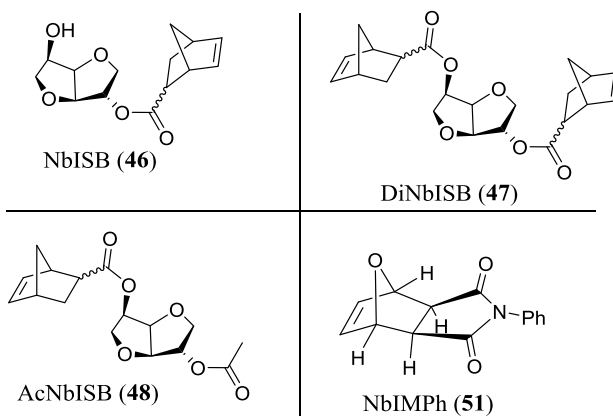
2.4 ROMP of monomers **46-48** and **51** using Grubbs' catalysts.

Four monomers NbISB (**46**), AcNbISB (**48**), DiNbISB (**47**) and NbIMPh (**51**) were synthesized for use in ROMP studies. Norbornene (**31**) was used as a comonomer in some ROMP reactions to make copolymers. Monomers **46**, **47**, and **51** are crystalline solids, whereas monomer **48** is a viscous liquid. The catalysts used were Grubbs' I (**26**) and II (**27**) catalysts. All polymerization reactions were quenched using ethyl vinyl ether and all polymers were precipitated in methanol.

2.4.1 Homopolymerization.

The reaction conditions used for the homopolymerizations of the monomers **46**, **48**, **51** and **47** to generate polymers **58-64**, **65**, **66** and **67**, respectively, are summarized in Table 2.1 and the reactions are shown in Schemes 2.6 and 2.7. The GPC-determined molecular weight measurements of all the homopolymers are summarized in Table 2.2 and 2.3. All the polymers were analyzed using proton NMR (Figure 2.16 to 2.18), IR and GPC. The GPC chromatograms of **65**, **66** and **67** are shown in Figures 2.19 to 2.21.

Table 2.1 Reaction conditions of the homo-ring-opening metathesis polymerizations of monomers **46**, **47**, **48** and **51** using Grubbs' catalysts at room temperature.



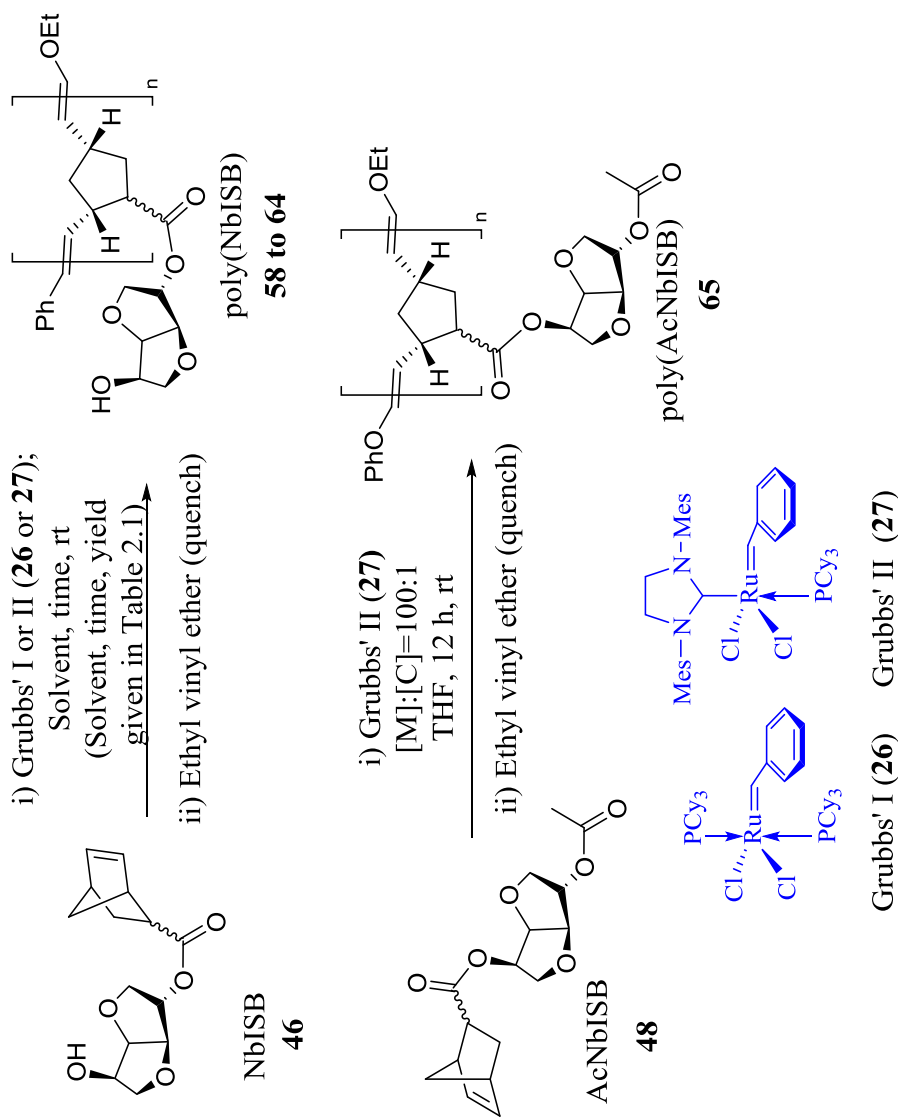
Monomer	Solvent	Catalyst ^a	[M]:[C]	Molarity (M) ^b	Time (h)	Polymer	Yield ^c (%)
46	THF	Grubbs' I	100:1	0.683	~48	58	92
46	THF	Grubbs' I	100:1	1.87	~240	59	95
46	THF	Grubbs' II	50:1	0.141	40	60	95
46	THF	Grubbs' II	100:1	0.141	40	61	90
46	THF	Grubbs' II	200:1	0.141	40	62	03
46	THF	Grubbs' II	500:1	0.141	40	63	10
46	THF	Grubbs' II	100:1	0.33	12	64	94
48	THF	Grubbs' II	100:1	0.33	12	65	100
51	THF	Grubbs' II	100:1	0.33	12	66	96
47	DCM	Grubbs' I	100:1	0.69	20	67	100

^aGrubbs' I = bis(tricyclohexylphosphine)benzylidene ruthenium(IV) chloride (**26**).

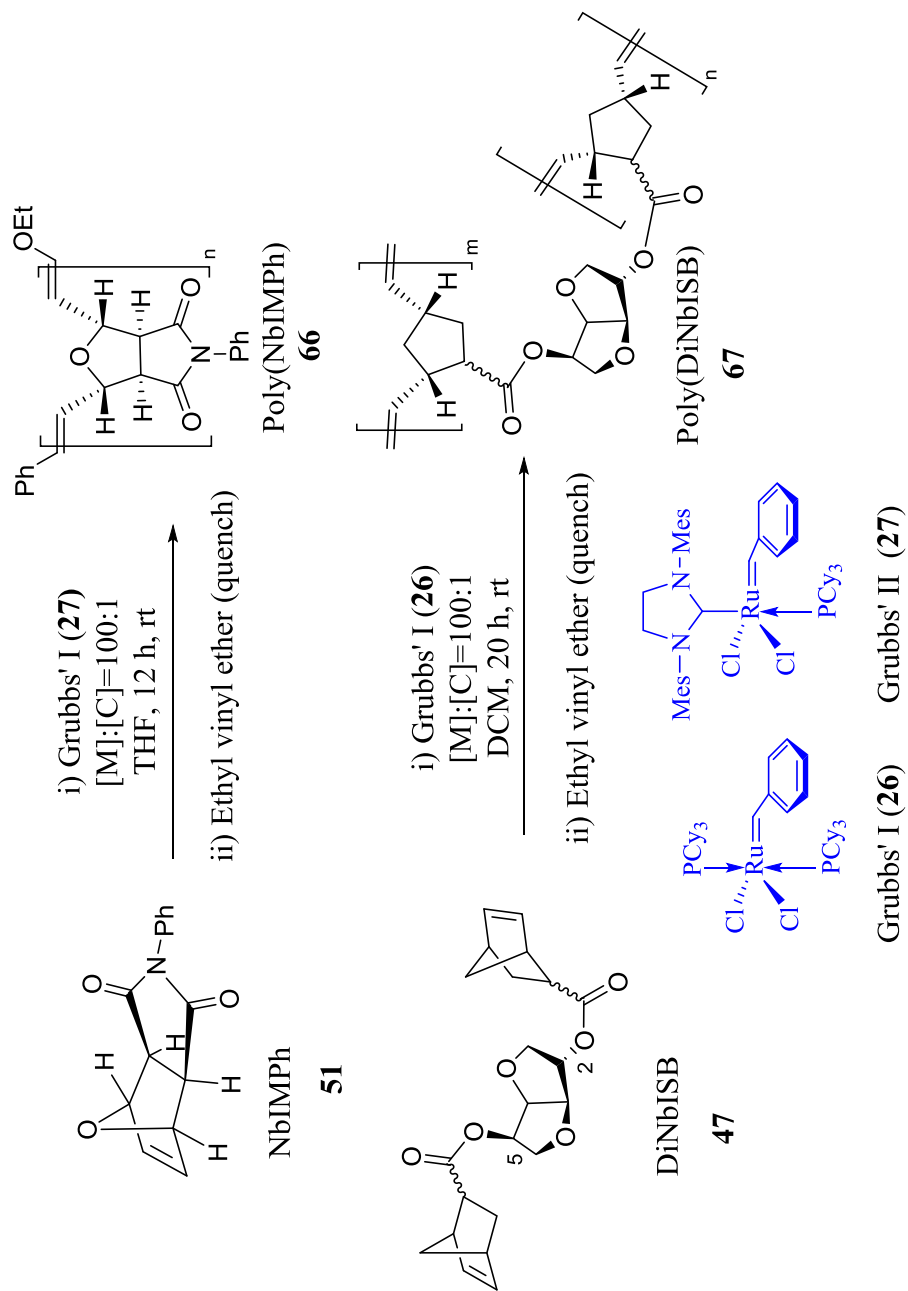
Grubbs' II = (1,3-bis(2,4,6-trimethylphenyl)-2-imidazolidinylidene)dichloro(phenylmethylene)(tricyclohexylphosphine) ruthenium (**27**).

^bBased on the initial monomer concentration in the reaction.

^cBased on the polymer weight obtained from the monomer weight charged.



Scheme 2.6 Homo-ROMP of monomers NbISB (**46**) and AcNbISB (**48**) using Grubbs' catalysts (**26** or **27**).



Scheme 2.7 Homo-ROMP of monomers NbIMPh (**51**) and DiNbISB (**47**) using Grubbs' catalysts (**26** or **27**).

Table 2.2 Molecular weights of the homopolymers **58** – **61** prepared from monomer **46**. GPC in THF was employed in comparison with PS standards.

Polymer ^a	GPC in THF ^a					Corrected M _w ^d
	M _n	M _w	M _z	PDI	DP ^c	
58	28,457	40,914	53,096	1.44	107	122,742
59	35,352	48,355	65,418	1.37	133	145,065
60	66,103	181,350	489,937	2.74	249	544,050
61	39,565 ^b	70,092 ^b	105,040 ^b	1.77 ^b	148 ^b	- ^b

^a Homopolymers **62** and **63** were insoluble in THF, and polymer **67** is a cross-linked polymer; Hence, their molecular weights could not be determined.

^b Polymer **61** was only partially soluble in THF. Thus, it could not be readily compared to molecular weights determined in DMF where it was soluble.

^c Calculated based on the Q-factor = ~ 3; derived from the ratio (LS-M_w)/(RI-PS-M_w) where LS-M_w is the weight-averaged molecular weight obtained from the Light scattering detector. RI-PS-M_w is the weight-averaged molecular weight obtained

Table 2.3 GPC molecular weight comparisons of homopolymers **64**, **65** and **66**.

Monomer used	Polymer	GPC Solvent	Solubility ^a	GPC ^b				
				M _n	M _w	M _z	PDI	DP
46	64	THF	Soluble ^a	52,273	199,002	799,378	3.81	197
		DMF	Soluble	134,128	612,666	2,050,000	4.57	504
48	65	THF	Insoluble	NA ^c	NA ^c	NA ^c	NA ^c	NA ^c
		DMF	Soluble	418,759	1,150,000	3,230,000	2.75	1,574
51	66^e	THF	Partly soluble	48,093 ^d	83,735 ^d	123,376 ^d	1.74 ^d	NA ^d
		DMF	Soluble	641,686	1,080,000	17,780,000	1.68	2,412

GPC measurements were performed in THF using PS standards and in DMF with LS detector. All the polymers are synthesized using Grubbs' II catalyst (**27**) in dry degassed THF at [M]:[C]= 100:1, stirred at rt for 12 h.

^a All the polymers had some fine undissolved particles left in the solvent which were filtered using 0.45 nm filter before injection into GPC.

^b Molecular weights determined by GPC in THF relative to PS at MSU, and in DMF using LS detector at USM.

^c Not available because the polymer is insoluble in THF which was used for GPC molecular weight measurements.

^d Poorly soluble in THF used for this GPC measurement. Hence, the measurement is not an accurate representation of the complete sample synthesized.

^e During the polymerization, to completely dissolve the undissolved monomer, reaction mixture containing Grubbs' II catalyst (**27**) was heated a little. GPC in DMF showed peaks at high elution volume indicating the presence of residual monomer.

The ROMP of NbISB (**46**) was first attempted in THF using Grubbs' I catalyst (**26**) with a monomer to catalyst mole ratio $[M]:[C] = 100:1$. Two polymers **58** and **59** were synthesized in high yields (92 % and 95%, respectively) by stirring at room temperature. The FT-IR spectrum of homopolymer **58** showed O-H stretching at $3,400\text{ cm}^{-1}$. Norbornene vinyl proton resonances at $\delta\ 5.7\text{--}6.2$, present in **46**, were absent in the ^1H NMR spectrum of polymer **58** and new vinylic proton resonances were observed at $\delta\ 5.2\text{--}5.6$ due to vinyl protons present along the backbone of the polymer. This disappearance of the norbornene vinyl protons was observed for the polymers produced by ROMP of the monomers **46**, **48** and **51** (Table 2.1). The NMR assignments for NbISB (**46**) and its homopolymers poly(NbISB) (**58-64**) are shown in the Figure 2.16.

2.4.1.1 Living polymerization.

Homopolymerizations of **46** were also performed using Grubbs' II catalyst (**27**) at monomer to catalyst ratios of 50:1, 100:1, 200:1 and 500:1 with an initial monomer (**46**) molarity of 0.141 M and a reaction time of 40 h. All the polymers were precipitated into methanol producing poly(NbISB) **60-63**. The yields were high for the polymers synthesized at the low $[M]:[C]$ ratios of 50:1 and 100:1 (**60** and **61**). However, for $[M]:[C] > 200:1$ polymerizations resulted in very low yields of polymers **62** and **63**. The molecular weights were generated by GPC versus PS standards in THF for homopolymers **60** and **61**. These are given in Table 2.2. Values of M_n 66,000, PDI 2.74 and DP 249 were found for **60**. Polymer **61** was only partially soluble in THF. Hence, GPC measurements were made using the soluble fraction of the polymer after filtering the insoluble fraction.

One aim of using a series of [M]:[C] ratios is to determine if the polymerization is an ideal “living polymerization” with no termination until it is quenched. However, full analysis requires “absolute molecular weights” and polymers which are completely soluble in the GPC solvent. The partial solubility of the polymers **61**, **62** and **63** in THF (solvent used for GPC molecular weight determination) prevented a rigorous assessment. The yields of the polymerization were also very low at the high [M]:[C] ratios. The high polydispersities (PDI) and the high values of the degree of polymerization (DP) of the molecular weights are “reasonably” consistent with a situation where living polymerization occurred but it was ideal. Either (1) only a fraction of catalyst molecules initiated chains or (2) living growth occurred with significant chain transfer and reaction between growing chain ends and already formed polymer chains

The GPC analysis of poly(NbISB) **58** to **61** (Table 2.2) indicate high PDIs compared to those generated in normal ROMP polymerizations. However, these molecular weight determinations were made by direct comparison with PS standards. Measurements by GPC are based on the hydrodynamic radii of the polymer samples compared with those of the standards. However, the poly(NbISB)s will most likely have entirely different hydrodynamic volumes when compared to the same molecular weight polystyrene (PS) standards. This would mean that at the same elution volume, poly(NbISB) and PS have entirely different molecular weights. Thus, this molecular weight approximation would obviously be inaccurate.

Such measurements for a series of poly(NbISB)s would show their relative molecular weights, but not absolute molecular weight and PDI values. These could be corrected with the use of absolute M_w values generated using LS-detector through a

correction factor. This is called a Q-factor. A correction factor of ~ 3 was generated for poly(NbISB) **64** versus PS values. This value is generated by dividing the LS-derived molecular weight value of **64** with the molecular weight measurement in THF relative to PS (Table 2.3). The Q-factor-corrected molecular weight indicates an approximately threefold difference in the M_w values of **58** - **61** measured in THF (and detected by RI) compared to those measured in DMF using a light scattering detector. This is a result of two factors. First, the structure of the two polymers differs. Therefore, even if they had exactly the same hydrodynamic interaction with the two solvents (which they don't), the amount of poly(NbISB) mass versus PS mass would differ in the same volume of the polymers coil in solution. Secondly, the solvents swell different polymers to different degrees in the same solvent. It is possible that the more polar poly(NbISP) would tend to have a tighter coiling in THF versus PS. If true, this would tend to put more poly(NbISB) mass within a given polymer's hydrodynamic radii than for PS in THF.

The polymer poly(NbISB) would also have a larger hydrodynamic volume in DMF solvent compared to that in THF. Accurate conclusions about the DP and PDI could not be made for the polymers **58** to **61** because, the calibration was performed using PS standards; the Q-factor correction resulted only in the corrected M_w values. Absolute M_n and M_z values were not available to be used to get Q values to compare with those from M_w measurements. However, the M_n and M_z values determined in DMF (versus those determined in THF) could be used to give crude approximations of Q that are not as reliable as those from M_w . but they are not as reliable. This is because M_n and M_z values are not directly given by light scattering measurements. Hence, the DP (measured using M_n) and the PDI (uses M_n) of these polymers could not be estimated as

accurately. However, it is obvious that high molecular weight polymers with broad PDIs were generated. That is absolutely confirmed by this work.

Homopolymerization of monomers **46**, **48** and **52** were each performed using Grubbs' II catalyst at a [M]:[C] ratio of 100:1. Polymers **64**, **65**, **66** were generated in very high yields. These polymers were analyzed using NMR, IR and GPC. NMR assignments of these polymers are shown in Figures 2.15 to 2.18. Polymers **64** and **65** are generated by the ROMP of **46** and **48**, respectively. **46** has a free hydroxyl group and the norbornene function substituted on the C2-*exo* oxygen of D-isosorbide while, **48** does not have any free hydroxyl group. The C2-hydroxyl group in **48** is acetylated, while the C5-hydroxyl group is esterified with NbCOOH (**31**). These polymers **64** and **65** differ in the physical properties. **64** is a thick green colored transparent globular film, while **65** is a thick maroon transparent film. **64** is partially soluble in THF, while **65** is insoluble in THF. **66** is partially soluble in chloroform. **64**, **65**, and **66** were soluble in DMSO. Hence, DMSO-*d*₆ was used as the solvent for the proton NMR spectroscopic determinations. One more reason for using DMSO-*d*₆ is that it has a high boiling point (low vapor pressure) for high temperature NMR spectrometric determinations. Figures 2.18, 2.19 and 2.20 show the proton NMR spectral assignments of the polymers **64** and **65** and **66** in comparison with their monomer **46**, **48** and **52**, respectively. TGA of **64**, **65** and **66** is shown in Figure A.6.

Molecular weights of **64**, **65**, and **66** were determined using GPC in THF with PS standard and in DMF using a light scattering detector. The results are summarized in Table 2.3. All the polymers showed high PDIs and DPs. Polymer **64** showed an M_w value of 199,002 relative to PS-standards (in THF); while an M_w value of 612,666 was obtained

for **64** using GPC instrument equipped with LS detector (in DMF). The LS-detector obtained values are absolute. This absolute M_w value obtained from LS was used for the determination of the correction factor (Q) of ~ 3 for the GPC measurements in THF for the polymer **64**.

$$\begin{aligned} \text{Correction factor Q for poly(NbISB)} &= (M_w\text{-value from DMF/LS})/(M_w \text{ from THF/PS}) \\ &= (612,666)_{\text{DMF/LS}}/(199,002)_{\text{THF/PS}} = \sim 3. \end{aligned} \quad (2.1)$$

This correction factor $Q \sim 3$ for poly(NbISB) can be used for the determination of corrected weight-averaged molecular weights of polymers **58** to **61**. These Q-corrected M_w values for **58** to **61** are given in Table 2.2. The Q-factor- M_w correction was also made for polymer **69** in Table 2.5.

The GPC analyses of polymers **64**, **65** and **66** in DMF are shown in Figures 2.18, 2.19 and 2.20, respectively. These spectra are plotted with elution volume on the x-axis and overlaid detector peaks (RI- red and LS-black) on the y-axis. The chromatograms also contain graph with a plot which is an overlay of Log MW (black) and normalized weight fraction (purple) on the x-axis and elution volume on the y-axis. If the columns used in these GPC experiments are separating the polymers properly, i.e., in a linear fashion, then the Log MW trace should be linear across the normalized weight fraction.

A linear separation from high to low molecular weight polymers was indeed observed for polymers **64**, **65** and **66**. For polymer **64**, however, there is a vertical jump was seen in the Log MW graph at around 14.5 mL (Figure 2.18). This is normally observed in highly polydisperse samples (according to Dr.Brooks Abel from the University of Southern Mississippi). For polymer **65**, the normalized weight fraction curve has crossed the elution volume (Figure 2.19). This indicates that the polymer is a

very high molecular weight polymer. In the RI-LS chromatogram of polymer **66** (Figure 2.19), a mysterious peak was observed at a high elution volume of 20 mL. The high elution volume of this peak indicates that it belongs to a small molecule. This peak could be due to the presence of an unreacted monomer in the polymer. **51** was not completely soluble in the solvent (THF) used for the ROMP reaction. In order to dissolve the monomer, the reaction mixture (with the catalyst **27**) was heated slightly using a heat gun. This resulted in the immediate precipitation of a white colored polymer. The slight heating of the reaction mixture with **51** should have increased the ROMP reaction-rate. But some part of the monomer was left undissolved. This undissolved monomer **51** might be the peak obtained at the elution volume of 20 min Figure 2.20.

Cross-linked polymer **67**: ROMP of DiNbISB **47** was performed using Grubbs' I catalyst (**26**) in DCM and stirring using magnetic stirrer at room temperature (Scheme 2.7) (Table 2.1). After 2-3 h, upon checking, the magnetic stirrer stopped stirring and a highly cross-linked polymer gel **67** was generated. This cross-linked polymer was insoluble in THF, DMF and other organic solvents. The polymer was characterized using FT-IR. An absence of O-H stretching at $3,400\text{ cm}^{-1}$ indicated that the polymer does not have any hydroxyl groups. A solvent-absorption test was performed for **67** using DCM as a solvent. After soaking for 24 h and removing the surface solvent with a paper towel, an increase in the weight of about of 5% w/w was measured. This is not a significant amount of solvent absorption.

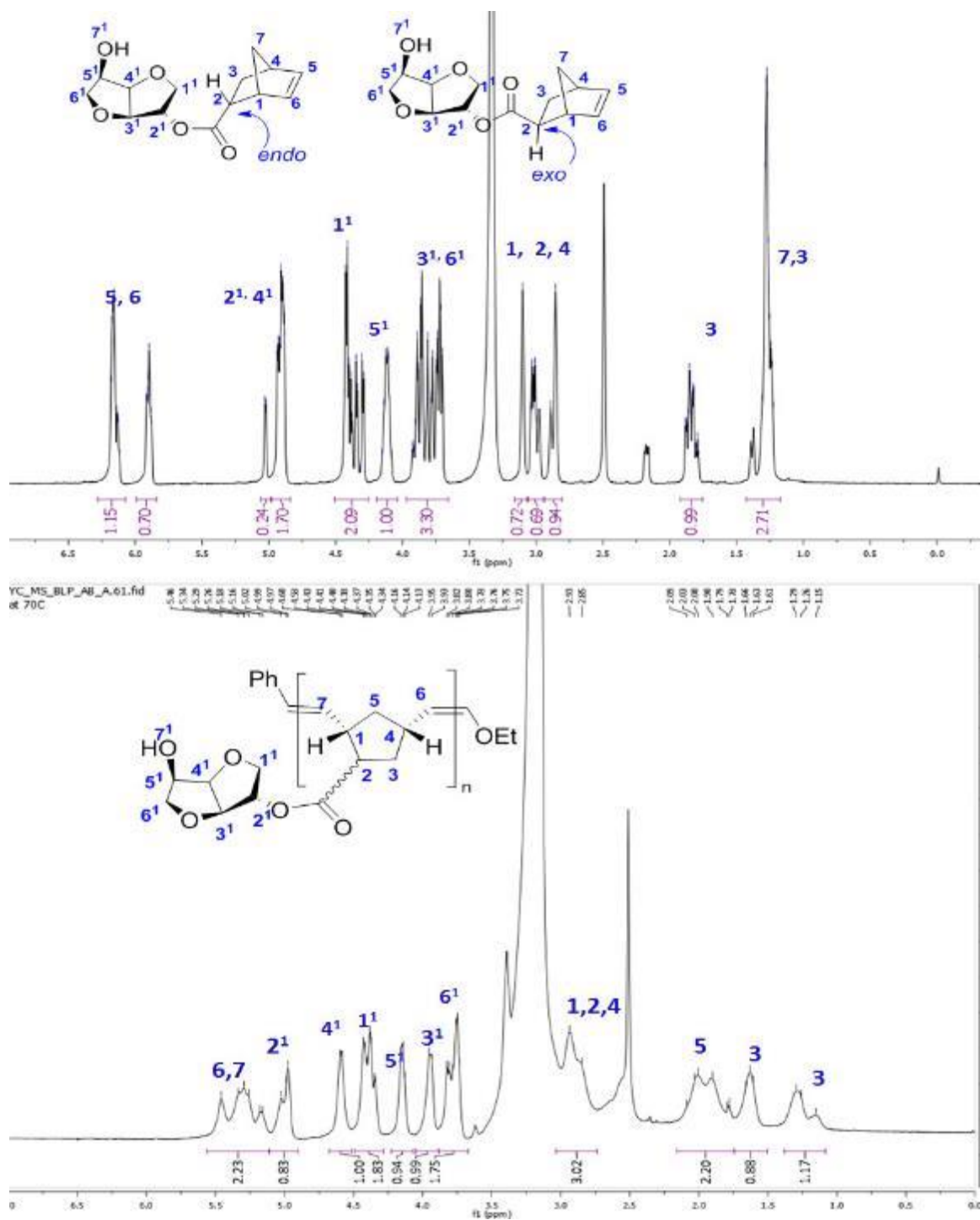


Figure 2.16 ^1H NMR spectra of NbISB (**46**) (at 25 °C) and its ROMP-derived homopolymers poly(NbISB) (**58** to **64**) (at 70 °C) in $\text{DMSO-}d_6$.

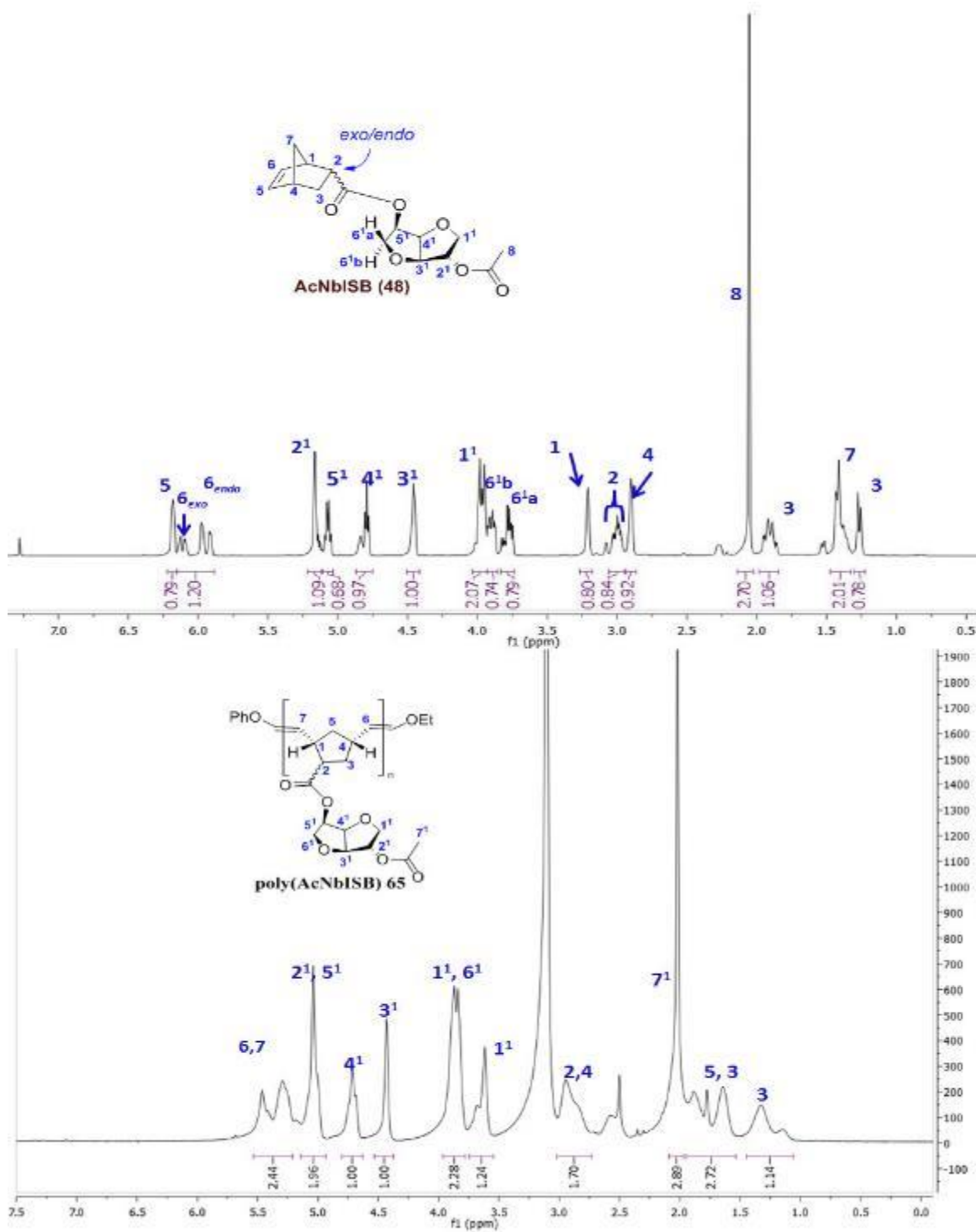


Figure 2.17 ^1H NMR spectra of AcNbISB (48) in CDCl_3 at room temperature and poly(NbISB) (65) in $\text{DMSO}-d_6$ at 70°C .

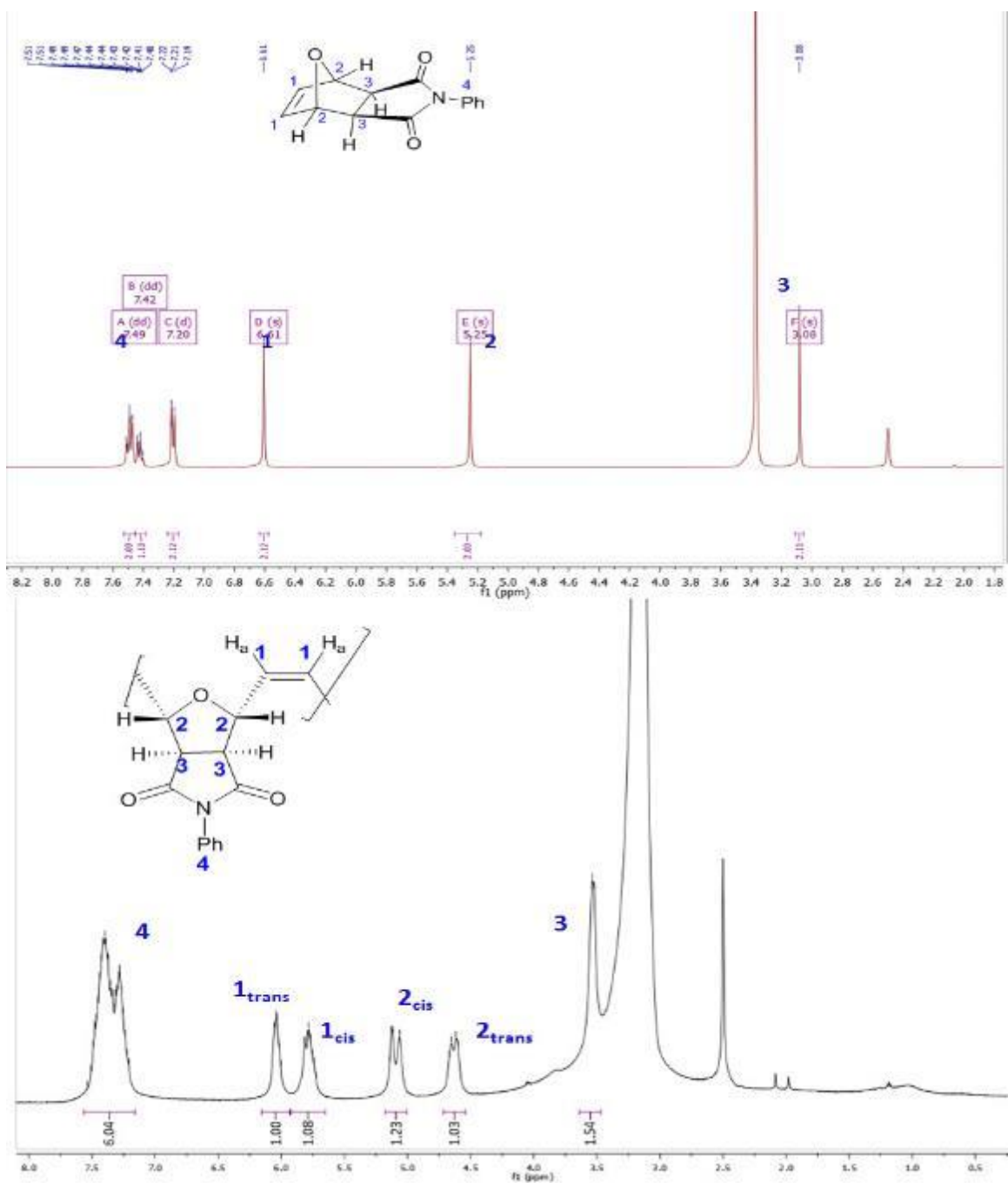


Figure 2.18 ^1H NMR spectra of NbIMPh (**51**) and poly(NBIMPh) (**66**) at room temperature and 70 °C, respectively, using $\text{DMSO-}d_6$ as the solvent.

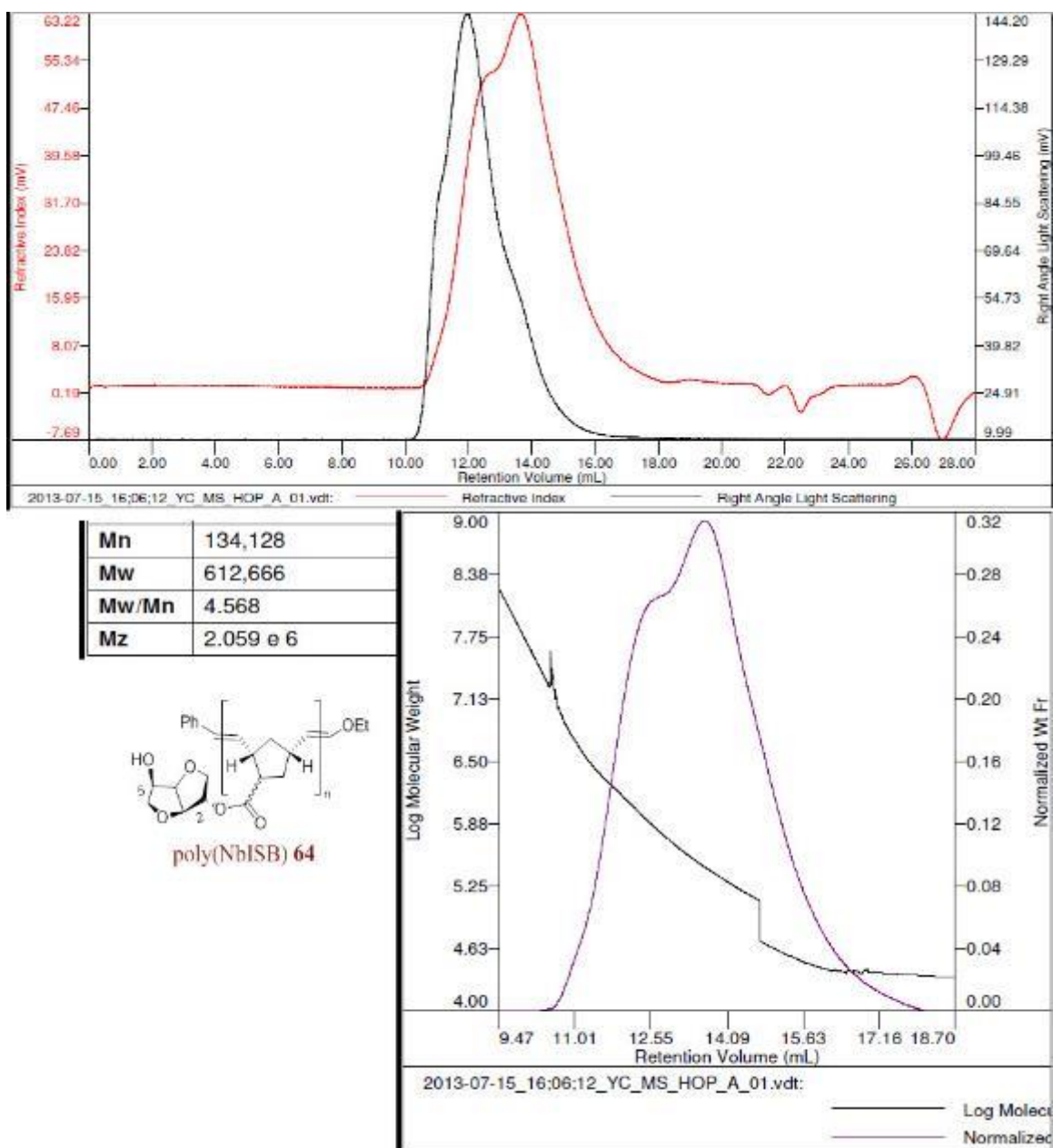


Figure 2.19 GPC chromatogram of the polymer **64**, a homopolymer of **46**, synthesized using Grubbs' II catalyst (**27**).

The chromatogram in the top has overlaid RI (red) and LS (black) peaks against elution volume. The overlay is made without the baseline correction. The chromatogram in the bottom is an overlay of Log MW (black) and normalized weight fraction (purple) vs. retention volume. If the columns are separating the polymers properly, i.e., in a linear fashion, then the Log MW trace should be linear across the normalized weight fraction. **Note:** There is a linear separation from high to low molecular weight polymers. However, there is a vertical jump seen in the Log MW at around 14.5 mL. This is normally observed in highly polydisperse samples and does not hurt the reliability of this analysis.

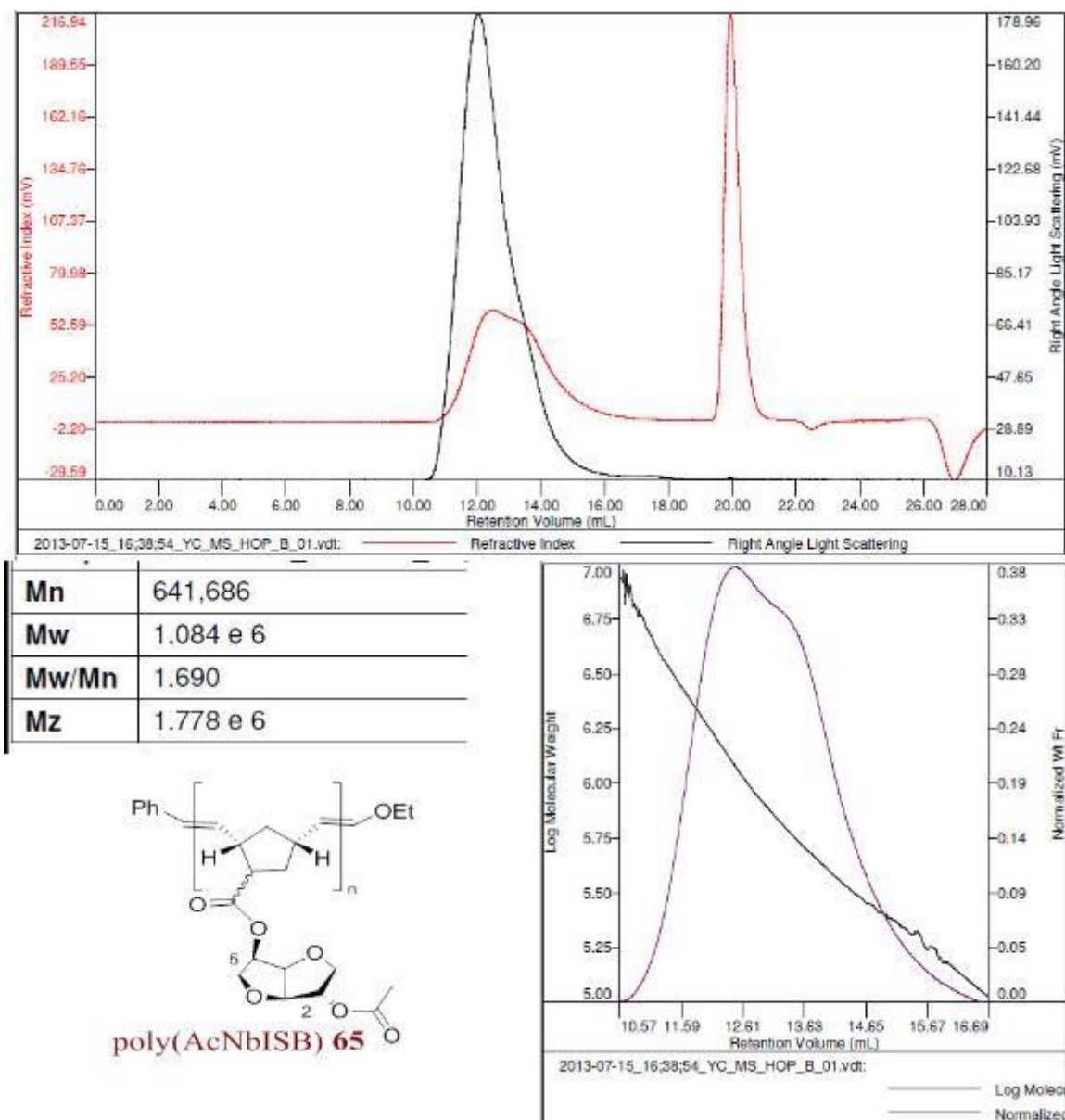


Figure 2.20 GPC chromatogram of the polymer **65**, which is a homopolymer of **48**, synthesized using Grubbs' II catalyst (**27**).

The chromatogram in the top has an overlaid RI (red) and LS (black) peaks against elution volume. The overlay is made without the baseline correction. The chromatogram in the bottom is an overlay of Log MW (black) and normalized weight fraction (purple) vs. retention volume. If the columns are separating the polymers properly, i.e., in a linear fashion, then the Log MW trace should be linear across the normalized weight fraction. Note that there is a linear separation from high to low molecular weight polymers. The normalized weight fraction curve has crossed the elution volume indicating that the polymer is a very high molecular weight polymer.

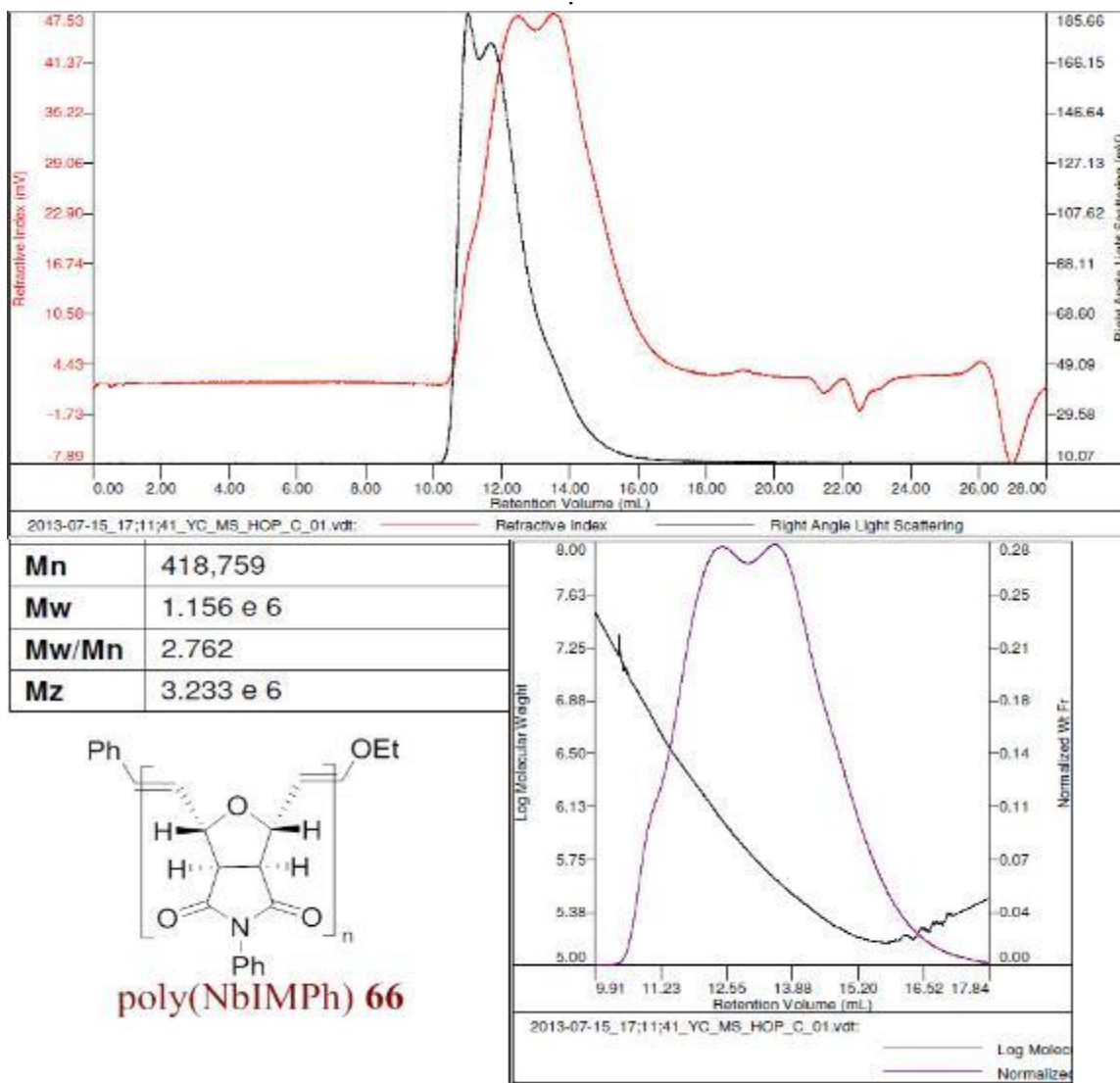


Figure 2.21 GPC chromatogram of the homopolymer of **51** synthesized using Grubbs' II catalyst (**27**) as the catalyst.

The chromatogram in the top has overlaid RI (red) and LS (black) peaks against elution volume. The overlay is made without the baseline correction. The chromatogram in the bottom is an overlay of Log MW (black) and normalized weight fraction (purple) vs. retention volume. If the columns are separating the polymers properly, i.e., in a linear fashion, then the Log MW trace should be linear across the normalized weight fraction. Note that there is a linear separation from high to low molecular weight polymers. Note that there is a narrow peak at high elution volume (at 20 ml) this could be due to the presence of unreacted monomer.

2.4.2 Co-polymerization.

2.4.2.1 Random copolymerization.

2.4.2.1.1 Copolymerization of **46** and **51**.

With initial success in the ROMP of **46**, the copolymerization of **46** with NbIMPh (**51**) was attempted. An initial attempt to co-polymerization of **46** with **51** was made at a mole ratio of 3:1 using Grubbs' II catalyst (**27**) and THF. A colorless amorphous polymer **68** was generated upon precipitation in methanol at 45 % yields. The poor solubility of **51** in THF may be the reason for the poor yields for the polymer **68**.

A series of random copolymerizations of **46** with **51** were then attempted using Grubbs' I and Grubbs' II catalysts (**26** and **27**) at a [M]:[C] of 100:1 at various **46** : **51** mole ratios to generate polymers **69** to **75** in good yields (Scheme 2.8). The reaction conditions and the yields for the synthesis of these random copolymers **69** to **75** are shown in Table 2.4.

Polymers **69** to **75** were analyzed using GPC in THF. The polymers **69** to **73** were synthesized using Grubbs' I catalyst (**26**). Polymers **69** to **73** had M_n values between 16,000 to 32,000, and PDI values between 1.46 and 1.77 in comparison with PS standards (Table 2.5). Polymers **74** and **75** were synthesized using Grubbs' II catalyst (**27**) by stirring at room temperature for 10 h. **74** was analyzed by GPC in THF (soluble in THF), while **75** was insoluble in THF. Hence, GPC could not be run for polymer **75**. Polymer **74** had a M_n of 66,879 and a PDI of 2.8 relative to PS standards. The molecular weights obtained here are not absolute molecular weights since they were obtained from the PS calibration curves. In principle, GPC measurements are based on the hydrodynamic volume of polymers rather than molecular weights. The hydrodynamic

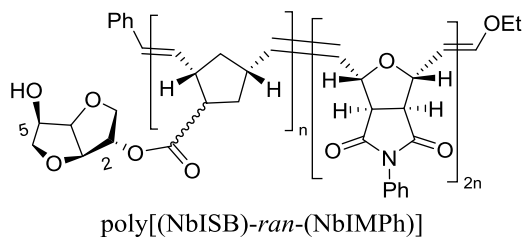
volumes of these random copolymers would certainly be different from those of PS standards used in the generation of the calibration curve. Hence, the molecular weights obtained are only relative to PS standards. GPC instruments equipped with the light scattering detector or the viscosity detector can be employed to obtain an absolute molecular weight. From the PDI values of **69** to **73**, and **74** and **75**, it can be concluded that Grubbs' I catalyst (**26**) produced polymers with lower PDIs when compared to polymers made using Grubbs' II catalyst (**27**). All polymers **69** to **75** were also analyzed using proton NMR. **69** to **73** were analyzed in CDCl₃, whereas polymers **74** and **75** were analyzed in DMSO-*d*₆. Proton NMR spectra was employed to obtain the monomer composition of copolymers.

The first step in determining the monomer composition of the polymers is to identify the non-over-lapping ¹H resonances between the spectra of the two homopolymers in a particular solvent. Then the proton spectra of the copolymers **69** and **73** were analyzed using CDCl₃ and an overlay of the two spectra was analyzed (Figure 2.21). This procedure indicates the presence of three regions where the peaks from monomers **46** and **51** units in the polymers **69** and **73** do not overlap with each other. The regions from δ 7.55 – 7.10 contain the five phenyl protons from monomer **51** in polymer **73**, and δ 4.5 – 3.75 contains protons on the C1, C3, C5 and C6 of D-isosorbide of monomer **46** in polymer **69**. These regions have only these protons and did not overlap with any other proton resonances. Thus, area integration values of these regions of the spectra could be used to quantify the **46/51** molar composition of these polymers. The peak at δ 3.5, which belongs to one proton on C6 of the D-isosorbide portion of **69**, is normalized to 1.0, and the peak at δ 3.25, which belongs to the two protons of **73** is

normalized to 2.0. Normalizing the peak region from δ 7.55 to 7.10 gave an integration value of 5.65, and the peak region from δ 5.6 to 6.2 gave a value of 5.58. These values were employed to calculate the **46:51** mole compositions of polymers **70** to **73**. Table 2.6 summarizes the calculated monomer ratios of random copolymers **70** to **73**. From the integration ratio calculations, **70** and **72** had monomer ratios comparable to those of the initial feed monomer mole ratios, while **72** showed a substantially different monomer ratio than expected from the feed ratio (**46:51** observed 1:1.88; initial 1:3). The stacked proton NMR spectra of **69** to **73** (region δ =3.0 to 8.0) are shown in Figure 2.19.

Polymers **74** and **75** were analyzed in DMSO- d_6 at 70 °C using proton NMR instead of in CDCl₃ which was used for **69** - **73**. To find the non-overlapping regions belonging to the monomers **46** and **51** of the polymers of **74** and **75** in DMSO- d_6 , the NMR spectra of **64** and **66** was used. From the overlapped spectra (Figure 2.23), the non-overlapping regions for both monomers were found to be at δ 7.00 – 7.60, δ 6.2 – 5.6 and δ 7.00 – 7.60. By normalizing the peak at δ 4.6 to 1 (**64**) and the peak at δ 6.1 to 1 (**66**), area integration values of 6.04, 2.08, 5.51 were obtained for the following regions δ 7.00 - 7.60, δ 6.2 - 5.6 and δ 7.00 - 7.60, respectively. These area integration values were used to calculate the monomer composition ratios in **74** and **75** (Table 2.16). The NMR spectra (δ 3 to 8) of **74** and **75** are shown in Figure 2.24 and Figure 2.25. A monomer ratio (**46:51**) of 4.4:1 was observed (theoretical 3:1) in **74** and 1:5.8 was observed for **75** (theoretical: 1:3).

Table 2.4 Reaction conditions for the random copolymerization of NbISB (**46**) with NbIMPh (**51**) at a monomer to catalyst ratio [M]:[C] =100:1, using Grubbs' catalysts.



68 -75

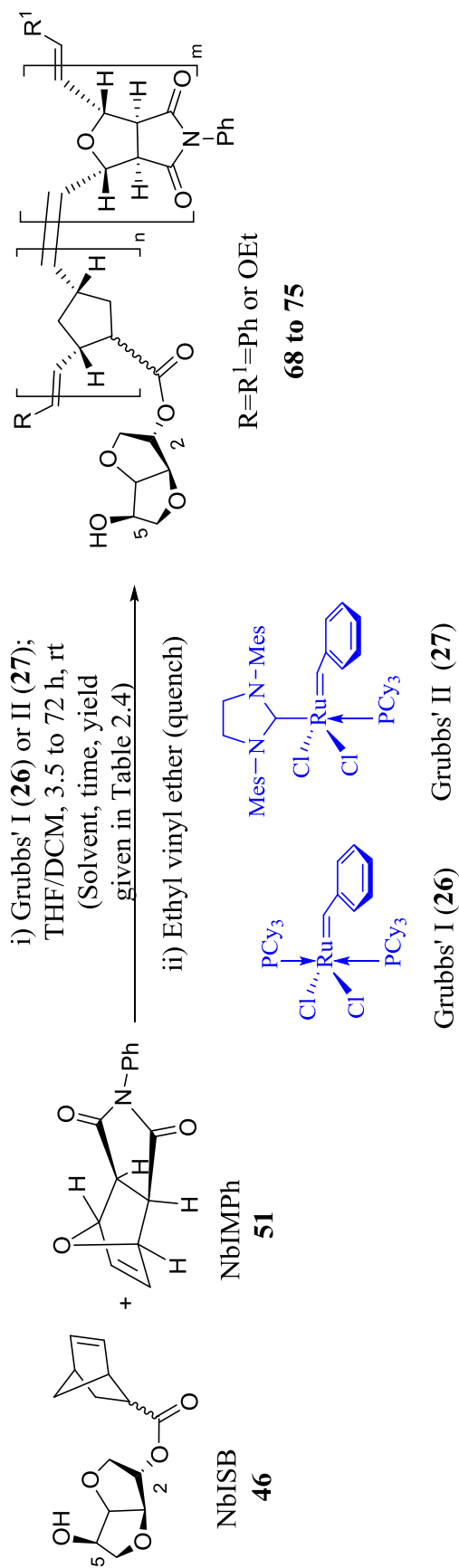
Monomer ratio (46:51) ^a	Solvent	Catalyst ^b	Molarity ^c	Time (h)	Polymer	Yield ^d (%)
03:01	THF	Grubbs' I	0.228	3.5	68	45
100:00	DCM	Grubbs' I	0.294	72	69	78
75:25	DCM	Grubbs' I	0.294	72	70	98
50:50	DCM	Grubbs' I	0.294	72	71	69
25:75	DCM	Grubbs' I	0.213	72	72	89
0:100	DCM	Grubbs' I	0.213	72	73	70
03:01	THF+DCM (1:1.25)	Grubbs' II	0.13	10	74	100
01:03	THF+DCM (1:1.25)	Grubbs' II	0.13	10	75	96

^a NbISB (**46**) : NbIMPh (**51**).

^b Grubbs' I = bis(tricyclohexylphosphine)benzylidene ruthenium(IV) chloride (**26**)
Grubbs' II = (1,3-bis(2,4,6-trimethylphenyl)-2-midazolinyldiene)dichloro(phenylmethylene)(tricyclohexylphosphine) ruthenium (**27**).

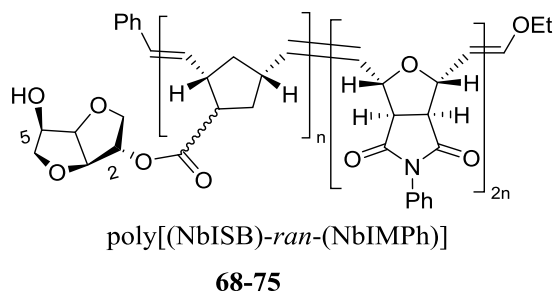
^c Molarity calculated based on the initial monomer concentration in the reaction.

^d Based on the polymer weight obtained from the monomer weight charged.



Scheme 2.8 Random copolymerization of NbISB (**46**) and NbIMPh (**51**) using Grubbs' catalysts (**26** or **27**).

Table 2.5 Molecular weight measurements of random copolymers **68** to **74** by GPC in THF. These are random copolymers of **46** with **51**.



Polymer ^a	GPC in THF ^b				Monomer ratio		Absolute M _w ^c
	M _n	M _w	M _z	PDI	Theoretical	Observed	
68	17,461	26,685	35,420	1.53	1:3		
69	16,864	26,758	37,213	1.59	1:0	1:0	80,274
70	23,246	33,854	44,382	1.46	3:1	2.99:1	-
71	14,089	21,583	29,275	1.53	1:1	1.22:1	-
72	24,726	39,620	55,129	1.6	1:3	1:1.88	-
73	32,422	57,260	89,656	1.77	0:1	0:1	-
74	66,879	186,940	594,521	2.8	3:1	4.4:1	-
75^a	-	-	-	-	1:3	1:5.77	-

^a Polymer **75** was insoluble in THF; could not be analyzed by GPC in THF.

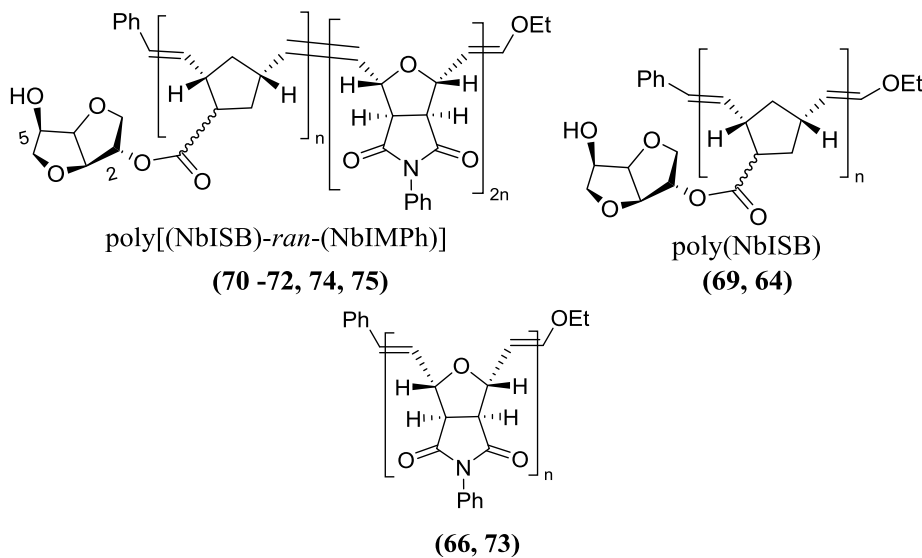
^b Molecular weights relative to PS calibration.

^c Mole ratio of the monomers **46:51** used in the reaction.

^d Obtained by ¹H NMR area integrations using CDCl₃ or DMSO-*d*₆ at 70 °C.

^e Obtained from the Q-factor correction ~ 3 obtained from Table 2.3 for poly(NbISB)

Table 2.6 Monomer ratios observed in the ^1H NMR of random copolymers (**69** to **75**). Polymers **69** to **73** were analyzed in CDCl_3 while polymers **74** to **75** were analyzed in $\text{DMSO}-d_6$.



Monomer ratio ^a	Polymer	Integration value		Monomer mole ratio	
		δ 4.50 – 3.75	δ 7.55 – 7.10	Observed	Theoretical ^c
1:0	69^b	5.58	0	1:0	1:0
75:25	70	17.48	5.65	3.13:1	3:1
50:50	71	6.47	5.65	1.16:1	1:1
25:75	72	2.58	5.65	1:2.17	1:3
0:1	73^b	0	5.65	0:1	0:1
1:0	64^b	5.5	0	1:0	1:0
0:1	66^b	0	6.04	0:1	0:1
3:1	74	5.5	1.39	4.4:1	3:1
1:3	75	5.5	34.9	1:5.8	1:3

^a NbISB: NbIMPh (**46:51**).

^b These are homopolymers. The integration values of these homopolymers were used to determine the composition of the random copolymers.

^c Calculated based on the initial monomer mole ratio in the reaction mixture.

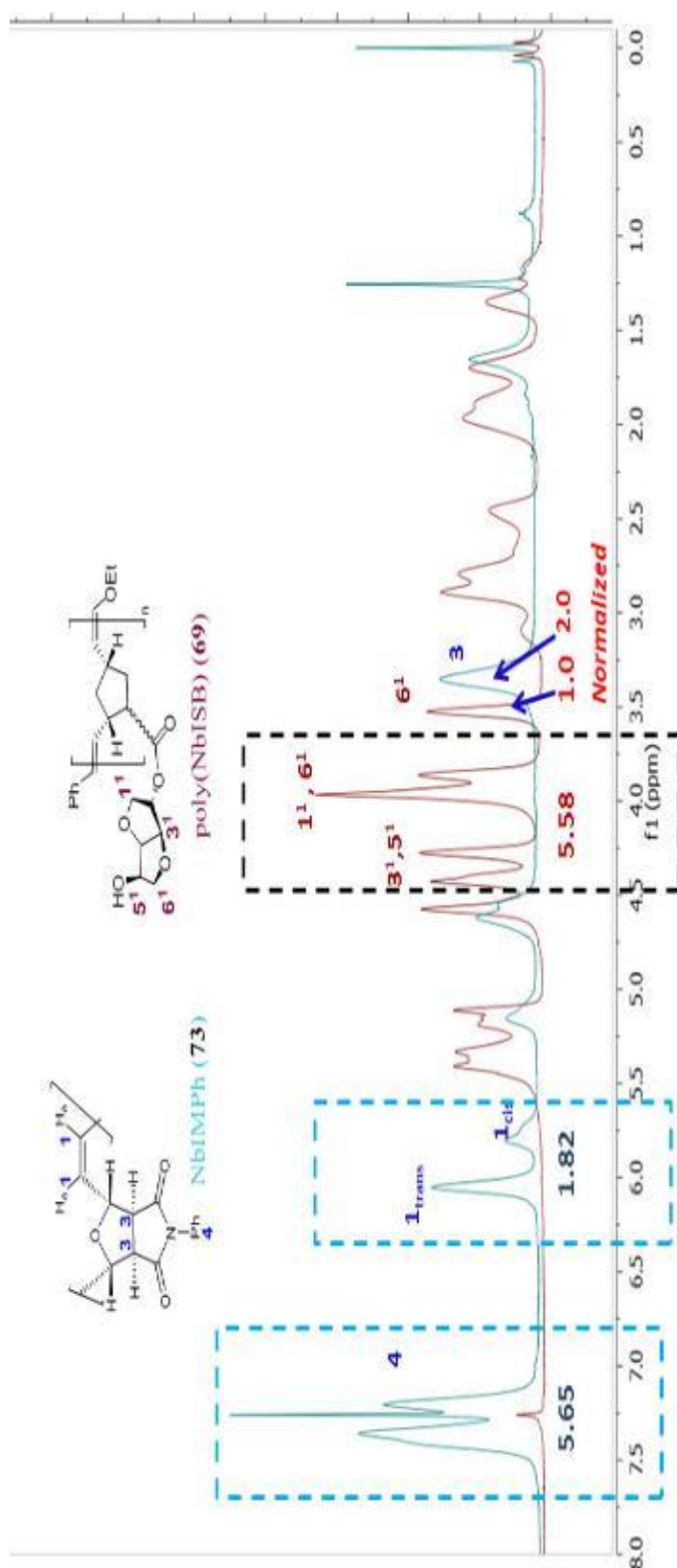


Figure 2.22 The overlaid ^1H NMR spectra of poly(NbISB) (69) (maroon) and poly(NbIMPh) (73) (blue).

The spectral regions δ 7.55–7.10 for 73 and 4.5–3.75 for 69 are the regions with no protons from one spectrum which occur in the same region as proton resonances from the other spectrum. After normalization, these regions have integration ratios of 5.65, and 6.98 for the homopolymers 69, and 73, respectively and are used for copolymer composition determinations in polymers 70 to 72.

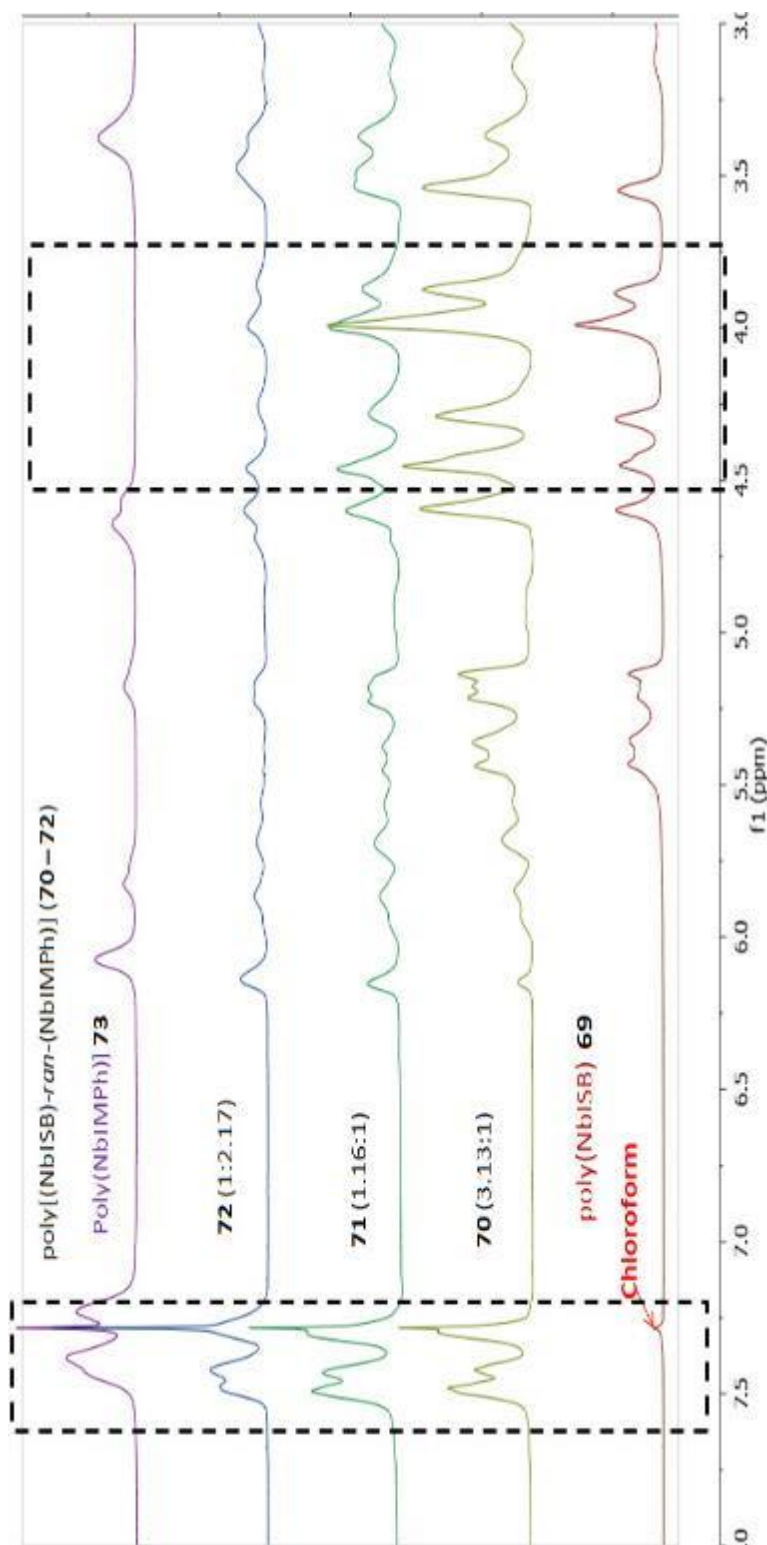


Figure 2.23 The stacked ^1H NMR spectra of random copolymers poly[(NbISB)-*ran*-(NbIMPh)] **69** to **73** (δ 3.0–8.0) in CDCl_3 at room temperature.

The boxed region δ 3.75 to 4.5 belongs to the protons of NbISB only, while the boxed region δ 7.2 to 7.6 belongs to the protons of NbIMPh only. The brackets beside the polymer numbers indicate the observed monomer ratio NbISB to NbIMPh in random copolymers **70**, **71** and **72**.

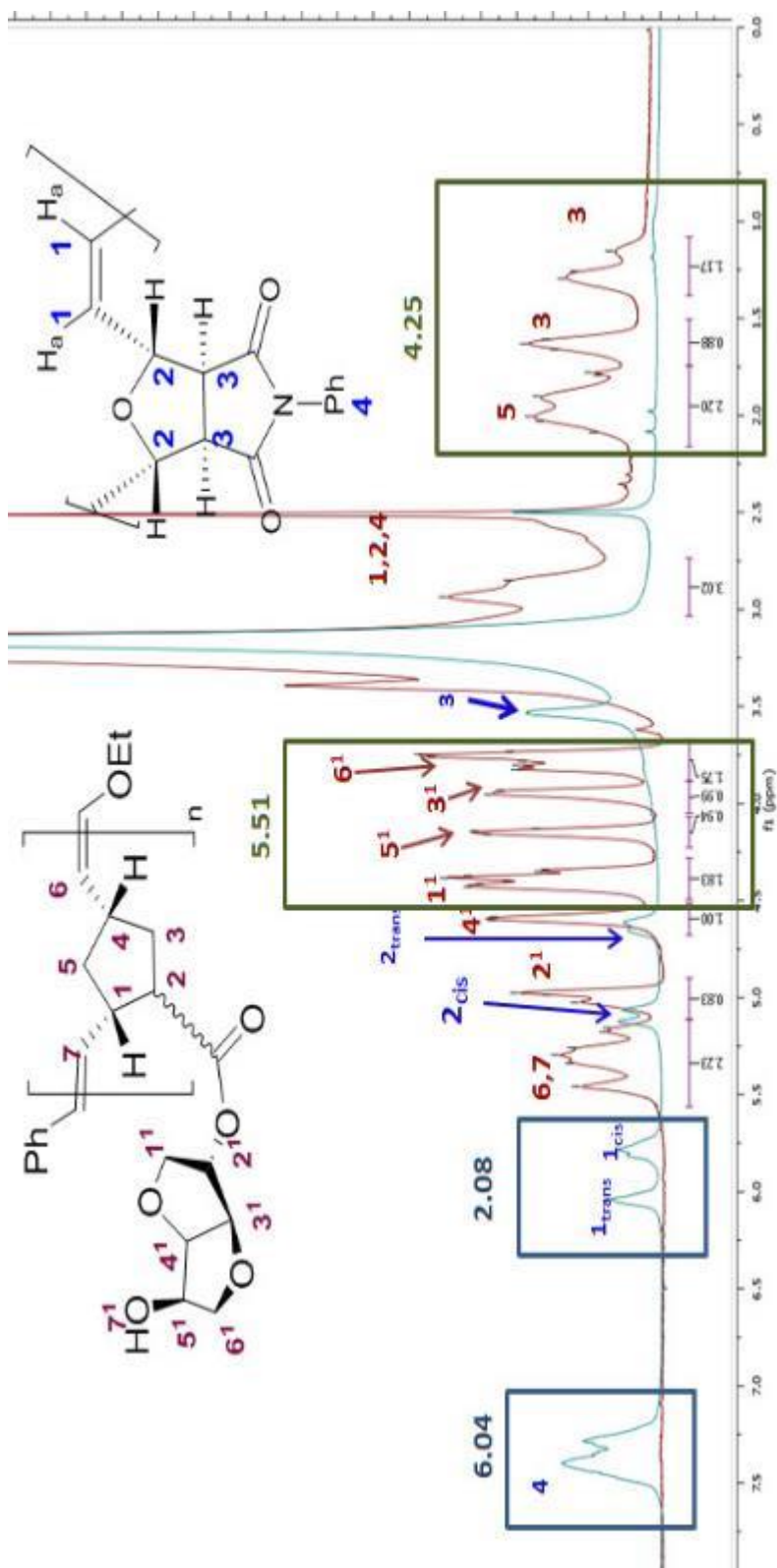


Figure 2.24 The overlaid ^1H NMR spectra of poly(NbISB) (64) and poly(NbIMPh) (66) in $\text{DMSO-}d_6$ at $70\text{ }^\circ\text{C}$.

Poly(NbISB) (64) (maroon) showed resonances from δ 4.49 – 3.68, and 2.14 – 1.06 that did not overlap with resonances of 66. These peaks belong to the protons on C1, C2, C5 and C6. They give normalized integration values of 5.50 and 4.26, respectively, when the resonance at δ 4.6 belonging to C4 is normalized to 1.0. Poly(NbIMPh) (66) peaks at δ 7.0 – 7.40, and 6.16 – 5.66 but poly(NbISB) (64) has no resonances in these regions. These regions exhibit the aromatic and vinylic protons of poly(NbIMPh) and had normalized integration values of 6.04 and 2.08, respectively when the resonance at δ 6.1 is normalized to 1.0.

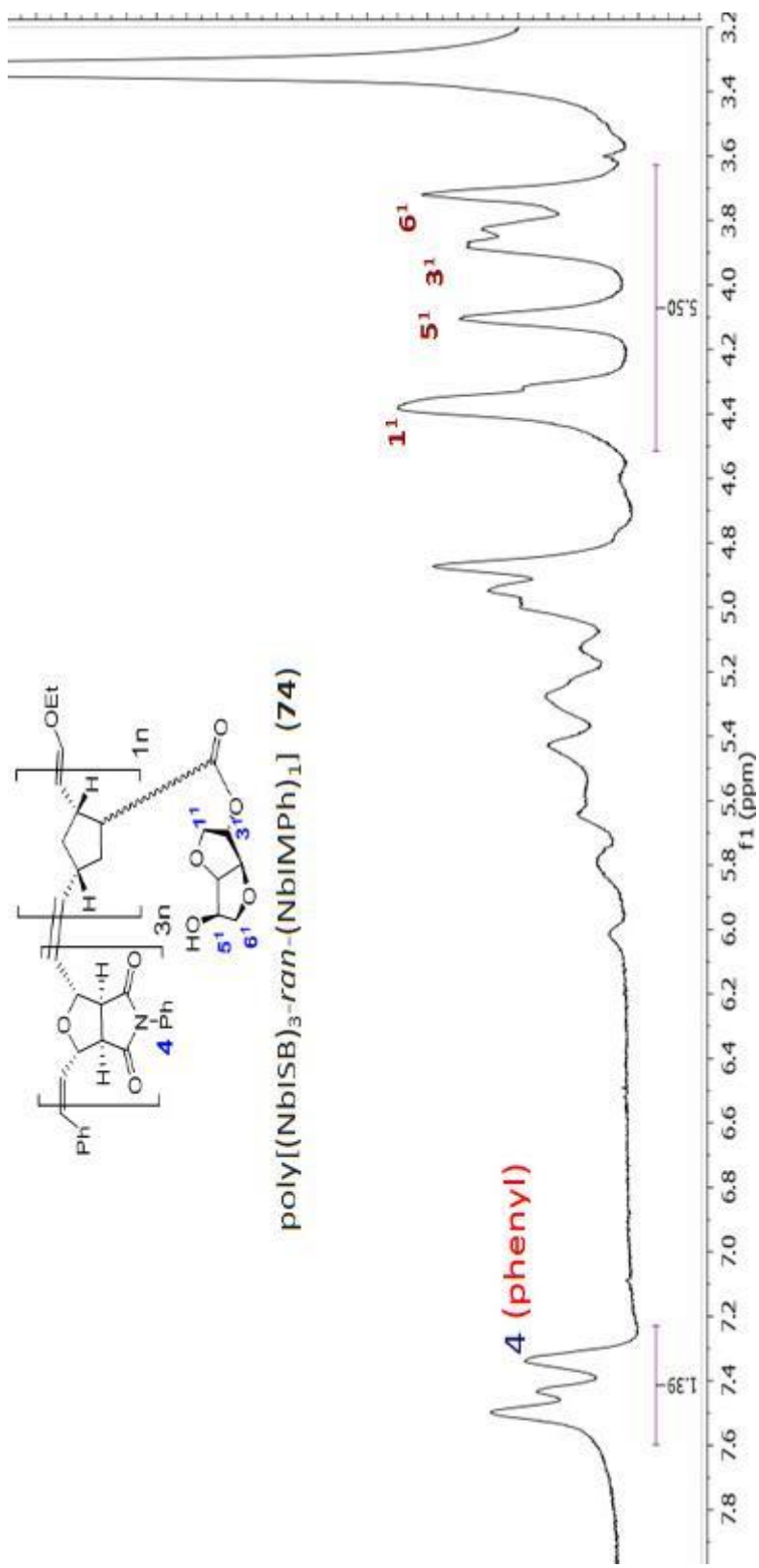


Figure 2.25 The ¹H NMR spectra of random copolymers **74** in DMSO-*d*₆ at 70 °C.

The spectral region from 3.2 to 8.0 is shown. Summing the areas at δ 3.5 to 4.5 and δ 7.2 to 7.6 polymer **74** had a normalized integration area ratio of 3:0.76, respectively (monomer feed ratio (**46**):(**51**) = 3:1).

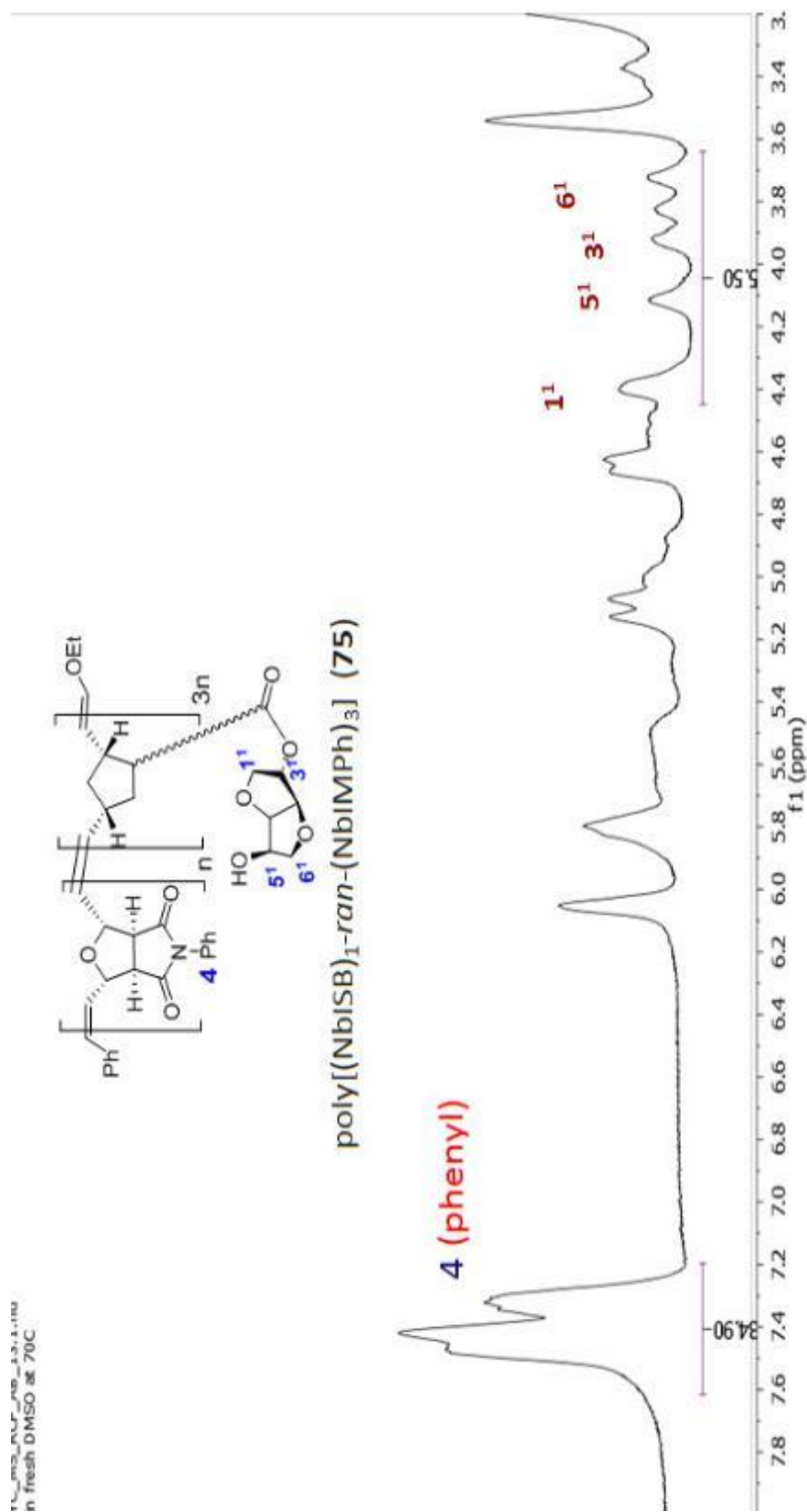


Figure 2.26 The $^1\text{H NMR}$ spectra of random copolymer **75** in $\text{DMSO}-d_6$ at 70°C .

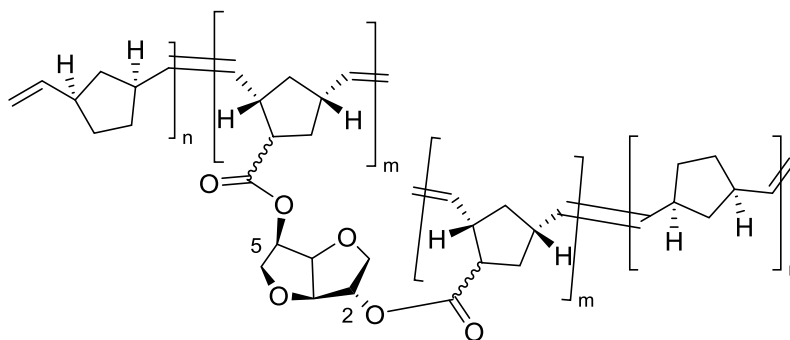
Summing the areas At δ 3.5 to 4.5 and δ 7.2 to 7.6, the polymer **75** had a normalized integration ratio of 1:6.34 when compared to monomer feed ratio (**46**):(**51**) = 1:3.

2.4.2.1.2 Crosslinking polymers by random copolymerization of **47** with **31**.

Random copolymerization of DiNbISB (**47**) and norbornene (**31**) at various mole ratios in DCM generated cross-linked polymers. The reaction conditions and the yields were summarized in Table 2.7 while the Scheme 2.9 shows the synthesis of these random cross-linked copolymers.

Polymers **76** to **80** were generated. These polymers were very hard yet brittle in nature and insoluble in organic solvents. Catalyst **26** was used to generate **76**, whereas **27** was used to generate **77** to **80**. Various mole ratios of **47:31** were employed in the synthesis of these polymers. Since crosslinking builds up during polymerization, gel formation occurred in the reactions generating **77** to **80** (Table 2.7). The polymer **80** which has the maximum norbornene content formed gel within 1 min, whereas the polymer **77** produced the gel in 20 minutes. All the polymers were analyzed using FT-IR.

Table 2.7 Reaction conditions for the random copolymerization of DiNbISB (**47**) and norbornene (**31**) at various mole ratios in DCM to generate cross-linked polymers.



76 to 80

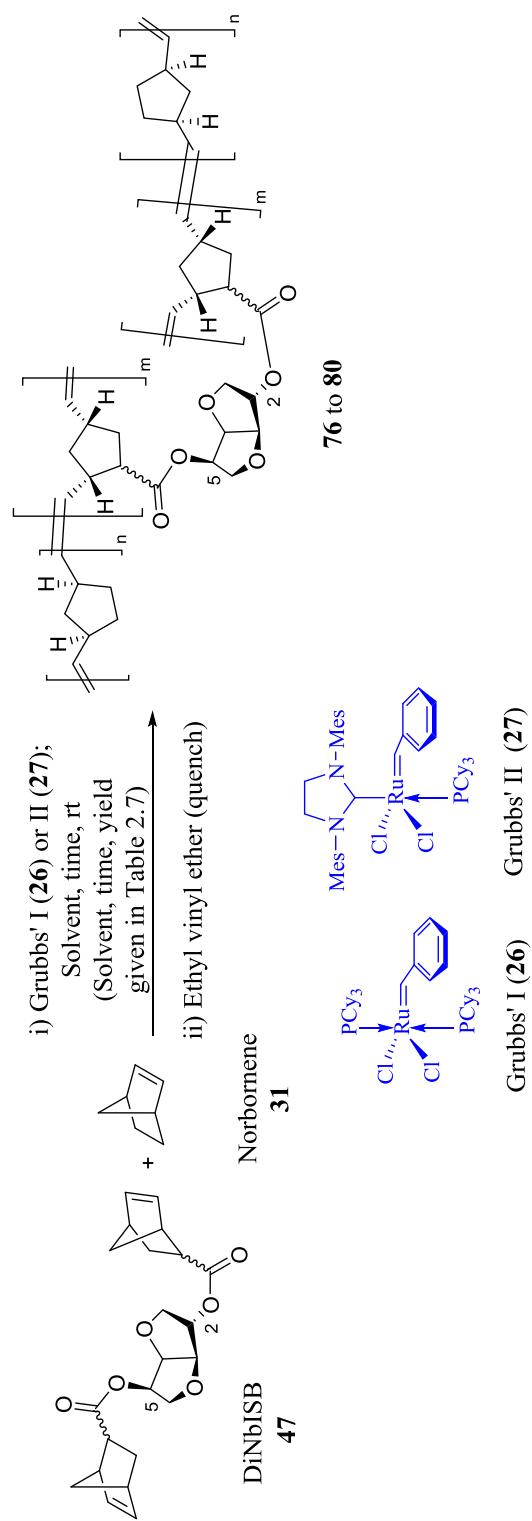
Polymer	Monomer ratio of 47:31 ^a	Catalyst ^b	[M]:[C]	M ^c [47]+[31]	Gel time (min)	Time (h)
76	1:10	Grubbs' I	1000:1	1.81	Not checked	1 h
77	100:00	Grubbs' II	200:1	0.5	20	6 h
78	93:07	Grubbs' II	200:1	0.5	10–15	6 h
79	66:33	Grubbs' II	200:1	0.5	3	6 h
80	33:66	Grubbs' II	200:1	0.5	1	6 h

The yields are approximated as 100% since no mass loss occurred in the synthesis of these highly cross-linked materials.

^a Mole ratio of DiNbISB: norbornene (**47:31**).

^b Grubbs' I = bis(tricyclohexylphosphine)benzylidene ruthenium(IV) chloride (**26**); Grubbs' II = (1,3-bis(2,4,6-trimethylphenyl)-2-imidazolidinylidene)dichloro(phenylmethylene)(tricyclohexylphosphine) ruthenium (**27**).

^c Molarity was calculated based on the combined monomer concentrations of monomers **47** and **31** in the reaction.



Scheme 2.9 Random copolymerization of DiNbISB (**47**) and norbornene (**32**) using Grubbs' catalysts (**26** and **27**).

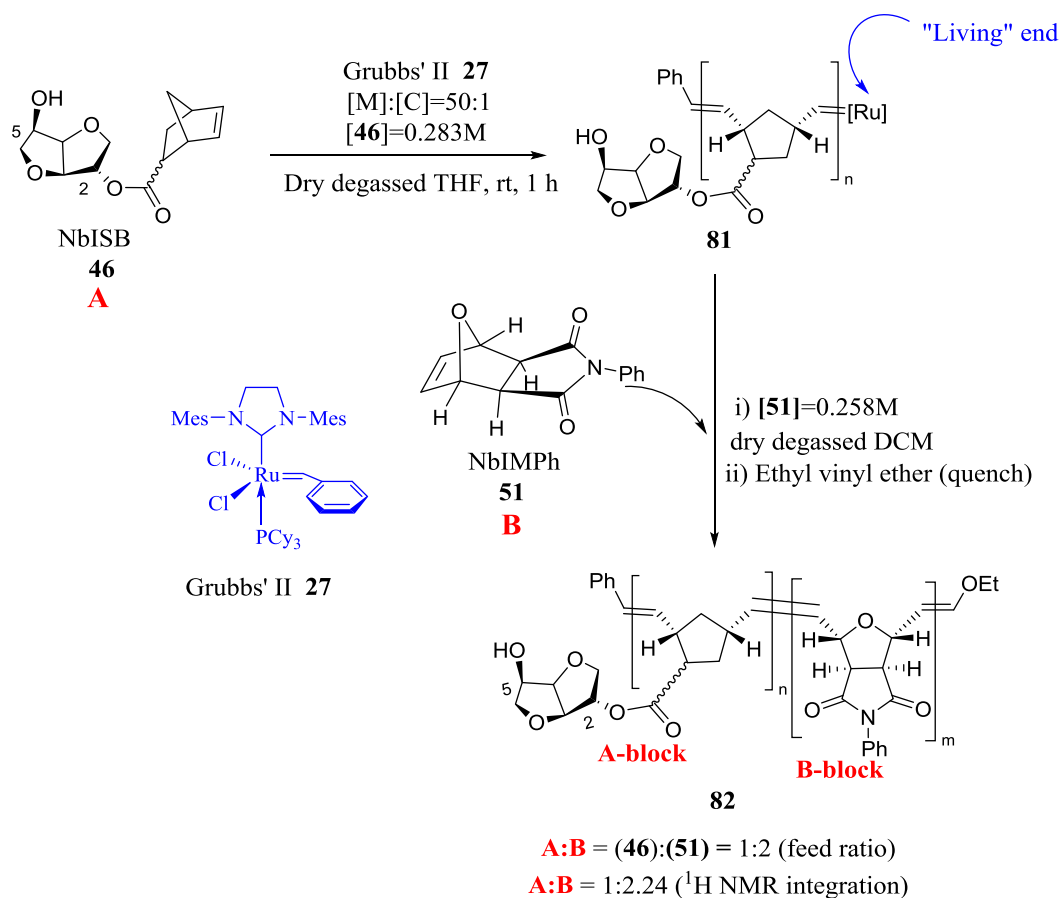
2.4.2.2 Block copolymers.

A series of AB-type, BA-type, ABA and BAB- blockpolymers were synthesized. Monomer **46** was designated as A while monomer **51** was designated as B. All the di- and triblock polymers (**82**, **84**, **87** and **90**) were analyzed using NMR and GPC. The composition ratio of **46** to **51** in these polymers was determined using NMR. The calculations for the block-ratio determination of these block polymers are provided in Table 2.8. The GPC traces of these block polymers is shown in Figures 2.26 to 2.29. The TGA of blockpolymers **82**, **84**, **87** and **90** is shown in Figure A.7.

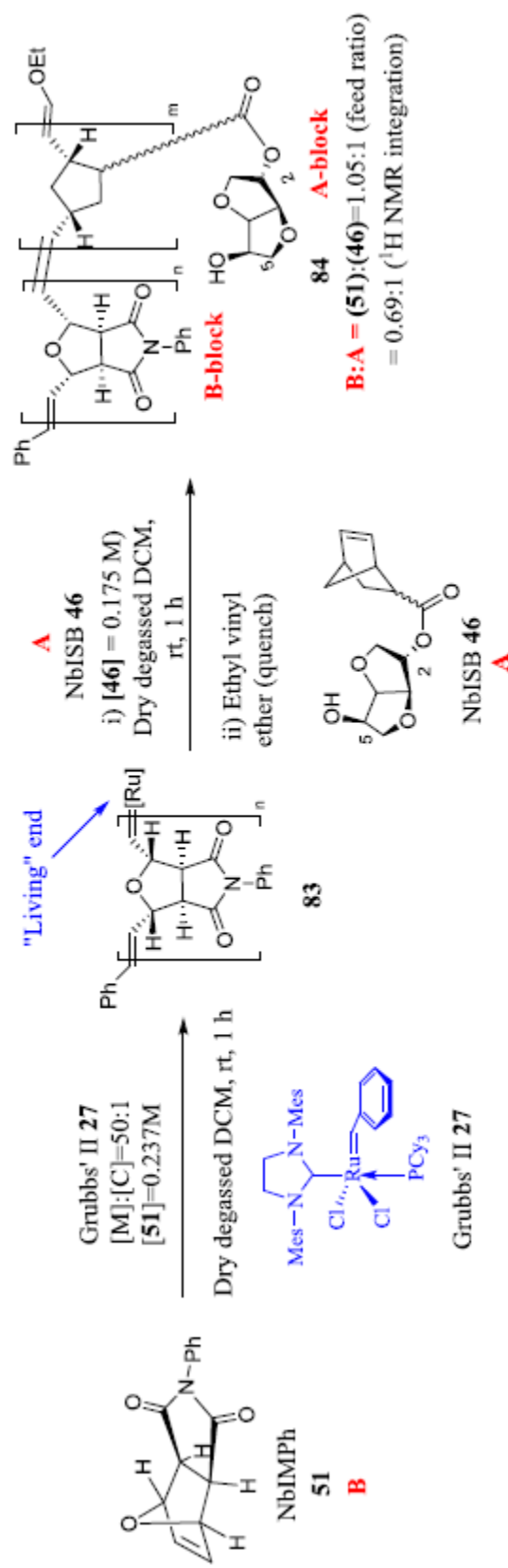
2.4.2.2.1 Diblock polymers (**82** and **84**).

AB (**82**) and BA (**84**) type diblock polymers (Schemes 2.10 and 2.11) were synthesized from **46** and **51** using Grubbs' II catalyst (**27**) at [M] to [C] ratios of 50:1. AB-type polymer **82** was synthesized (Scheme 2.10) using Grubb's II catalyst (**27**) at a monomer to catalyst ratio of 50:1 Monomer A is first polymerized with **27**. After 1 h, the living polymer of monomer A was formed. Then monomer B (mole ratio of A:B = 1:2) was added and the reaction mixture was stirred for 8 h. The reaction was then quenched using excess ethyl vinyl ether. The polymeric solution was precipitated into methanol, filtered and dried overnight at 40 °C under vacuum (3 - 4 mm Hg) to generate **82**. **82** was analyzed using NMR, IR and GPC. The proton NMR spectrum of **82** (Figure 2.31) had peak area integration ratios of 1:2.24 for A: B (**46:51**) after normalization (Figure 2.24). The monomer feed ratio of A to B is 1:2. The block-ratio calculations are shown in Table 2.8. GPC analysis of **82** in DMF indicated a very high molecular weight (M_w of 1,139,000 and a PDI of 1.9) (Table 2.9).

BA-diblock polymer **84** was synthesized by a procedure similar to that of AB-type polymer. The initial monomer used was monomer B (**51**), generating a living polymer within 1 h, followed by the addition of the second monomer A (**46**) (Scheme 2.11). The proton NMR spectrum of **84** (Figure 2.32) had peak area integration ratios of 1:0.69 for A:B (**46**:**51**) after normalization. The monomer feed ratio of **46** to **51** was 1:1.05. GPC analysis of **84** in DMF indicated very high absolute molecular weight (M_w of 903,903 and a PDI of 1.65).



Scheme 2.10 AB-type diblock copolymerization of NbISB (**46**) followed by NbIMPh (**51**) using Grubbs' II catalyst (**27**).

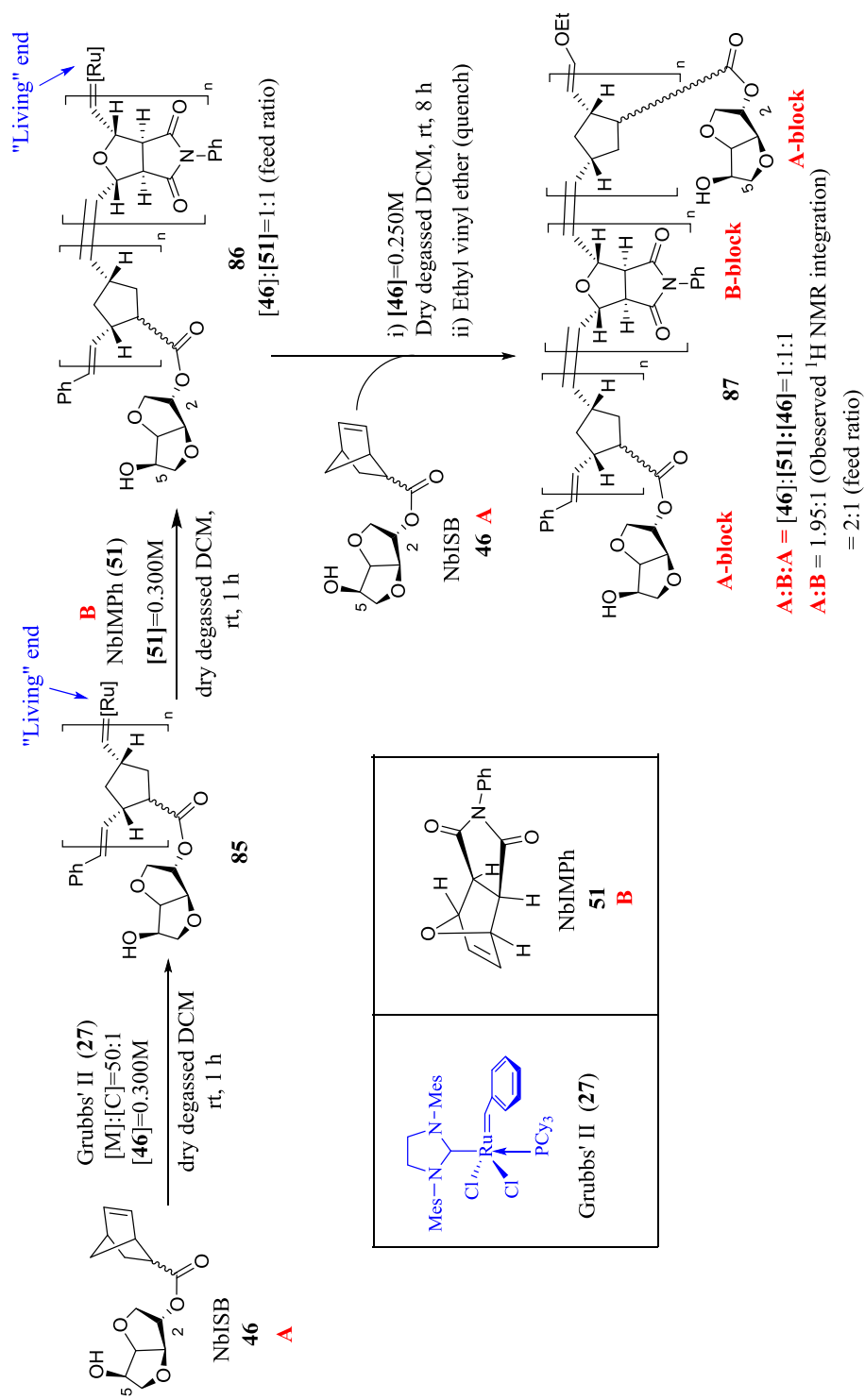


Scheme 2.11 BA-type diblock copolymerization of NbIMPh (**51**) followed by NbISB (**46**) using Grubbs' II catalyst (**27**).

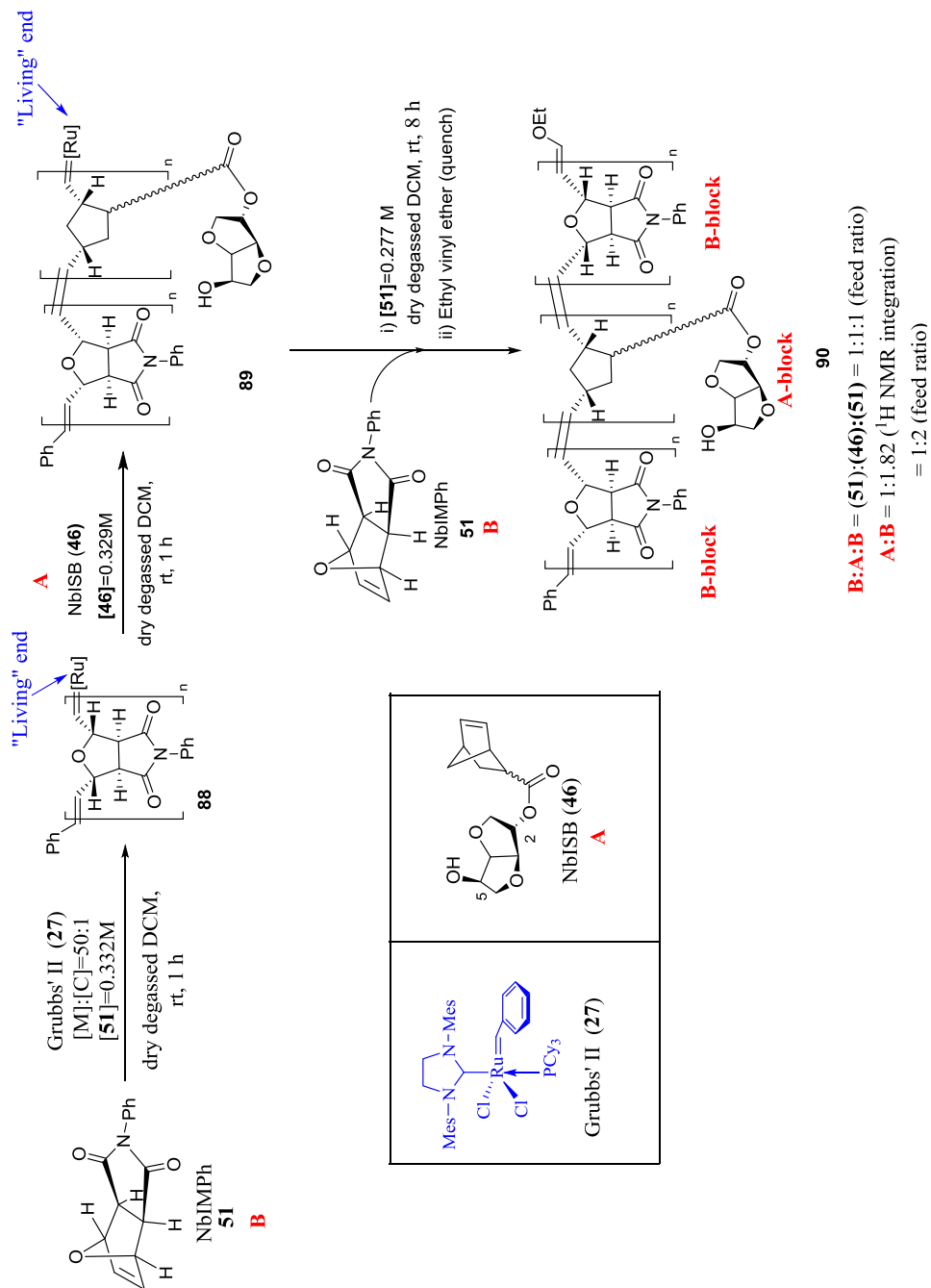
2.4.2.2.2 Triblock polymers

ABA and BAB triblock polymers **87** and **90** were also synthesized using Grubbs' II catalyst (**27**) and monomers **46** (A) and **51** (B) at an initial [M]:[C] of 50:1. In the synthesis of ABA block polymer **87**, Monomer A (**46**) was initiated with **27** to produce a living polymer; after 1 h monomer B (**51**) was added to the living polymer of A and the reaction solution was stirred for 1 h giving AB living polymer. After 1 h, monomer A **46** was again added to the AB-living polymer. After stirring for 8 h, the reaction was quenched using excess ethyl vinyl ether and the polymer was precipitated in methanol giving ABA-blockpolymer **87**. **87** was analyzed using NMR, IR and GPC in DMF. Integrating the proton NMR spectrum of **87** (Figure 2.31) gave peak area ratios, after normalization, of 1.95:1 for A:B (**46:51**). The A:B feed ratio was 2:1. A molecular weight of M_w of 399,107 and a PDI of 4.0 were observed by GPC analysis in DMF for **87**. GPC traces (Figure 2.29) showed a hump in the chromatogram with Log MW (black) overlaid with normalized weight fraction curve vs. retention volume. This hump is characteristic of highly polydisperse samples (according to Dr. Brooks Abel from USM). However, this hump does not affect the absolute molecular weight determinations by GPC.

BAB polymer **90** was synthesized by a procedure similar to the ABA polymer synthesis except that the initial monomer polymerized was monomer B (**51**), the second monomer added was A (**46**), followed by adding more B (**51**) (Scheme 2.13). The proton NMR spectrum (Figure 2.34), after normalization showed peak area integration ratios of 1:1.82 for A:B (**46:51**), regions of **90**. The **46:51** feed ratio was 1:2. GPC analysis of **90** in DMF confirmed **90** had a high molecular weight with M_w of 944,267 and a PDI of 2.0. GPC traces of **90** are shown in Figure 2.30.



Scheme 2.12 ABA-type triblock copolymerization of NbISB (51) and NbIMPh (46) using Grubbs' II catalyst (27).



Scheme 2.13 BAB-type triblock copolymerization of NbISB (51) and NbIMPh (46) using Grubbs' II catalyst (27).

Table 2.8 Table of calculations to determine the monomer mole ratio of block copolymers using ¹H NMR integrated regions.

Polymer	Integration value			Block ratio calculation ^c		Block ratios (A:B)	
	A	B		A	B	Practical ^d	Theoretical ^e
	(δ 4.49-3.68) ^a	(δ 7.40-7.0) ^b	(δ 6.25 – 5.5) ^b	(δ 4.49-3.68) ^{integration} /5.5	Sum /8.12		
Homo A or B	5.5	6.04	2.08	-	-	-	-
82 (AB)	5.5	12.96	5.27	1	2.25	1:2.24	1:2
84 (BA)	5.5	4.05	1.52	1	0.69	1:0.69	1:1.05
87 (ABA)	5.5	3.13	1.06	1	0.52	1.95:1	2:1
90 (BAB)	5.5	10.81	4.01	1	1.83	1:1.82	1:2

Blocks of Polymers poly(NbISB) are designated as A, while blocks of poly(NbIMPh) are designated as B. The proton NMR overlay of the A and B and the normalizations are detailed in Figure 2.24.

^a For poly(NbISB) (A), an integration value of 5.5 was observed between □ 4.49 – 3.68 for C1, C3, C5 and C6 (represents five) protons.

^b For poly(NbIMPh) B, an integration sum of 8.12 was obtained between □ 7.40-7.0 and □ 6.25 – 5.5 which represent 7 protons

^c Block ratios of the copolymers 82, 84, 87 and 90 were calculated by dividing the integration value of A by 5.5 and the integration value of B by 8.12.

^d Measured from the block ratio calculations of A and B.

^e Initial monomer ratios of A and B used in the synthesis.

Table 2.9 Molecular weight measurements by GPC in THF vs. PS standards for the homopolymers **81** and **85** and block polymers **82**, **84**, **87**, and **90**.

Polymer ^a	Solvent	Solubility ^b	GPC molecular weights				(A:B) Block ratios ^c		Monomer (A+B) MW ^d	DP ^f
			M _n	M _w	M _z	PDI	Theoretical	Observed		
81 (A)	THF	Soluble	35,840	78,853	174,018	2.20	1:0	1:0	266	135
	DMF	Soluble	Not measured							
82 (AB)	THF	Partly soluble	43,373 ^e	98,688 ^e	292,879 ^e	2.28 ^e	1:2	1:2.24	805	54
	DMF	Soluble	597,254	1,139,000	1,731,000	1.90				742
84 (BA)	THF	Insoluble	Not measured				1:1.05	1:0.69	432	
	DMF	Soluble	539535	903903	1,379,000	1.65				1249
85 (A)	THF	Soluble	85,059	297,735	1,570,854	3.50	1:0	1:0	266	320
	DMF	Soluble	Not measured							
87 (ABA)	THF	Partly soluble	36,722 ^e	73,882 ^e	197,773 ^e	2.01 ^e	2:1	1.95:1	760	48
	DMF	Soluble	106,093	399,107	1,180,000	4.0				140
90 (BAB)	THF	Partly soluble	47,892 ^e	90,924 ^e	174,252 ^e	1.9 ^e	1:2	1:1.82	704.6	68
	DMF	Soluble	568,258	944,267	1,391,000	2.0				806

These were synthesized by ROMP using Grubbs' II catalyst (**27**) at monomer to catalyst ratio ([M]:[C]) 50:1. Several of the polymers are not completely soluble in THF. Polymer poly(NbISB) is designated as A, while polymer poly(NbIMPh) is designated as B.

^a Molecular weights were not determined for polymers **83**, **86**, **88** and **89** due to the of adequate sample amounts.

^b All the polymers had some fine un-dissolved particles left in the solvent which were filtered using 0.45 nm filter before injection.

^c Measured by ¹H NMR area integrations of samples measured at 70 oC in CDCl₃ or DMSO-d₆.

^d Sum of the observed monomer ratio of A multiplied by 266 and the observed monomer ratio of B multiplied by 241.

^e Calculated by dividing M_n with monomer molecular weight.

^f Poorly soluble in THF used for this GPC measurement. Hence, this measurement does not accurately represent the synthesized polymer.

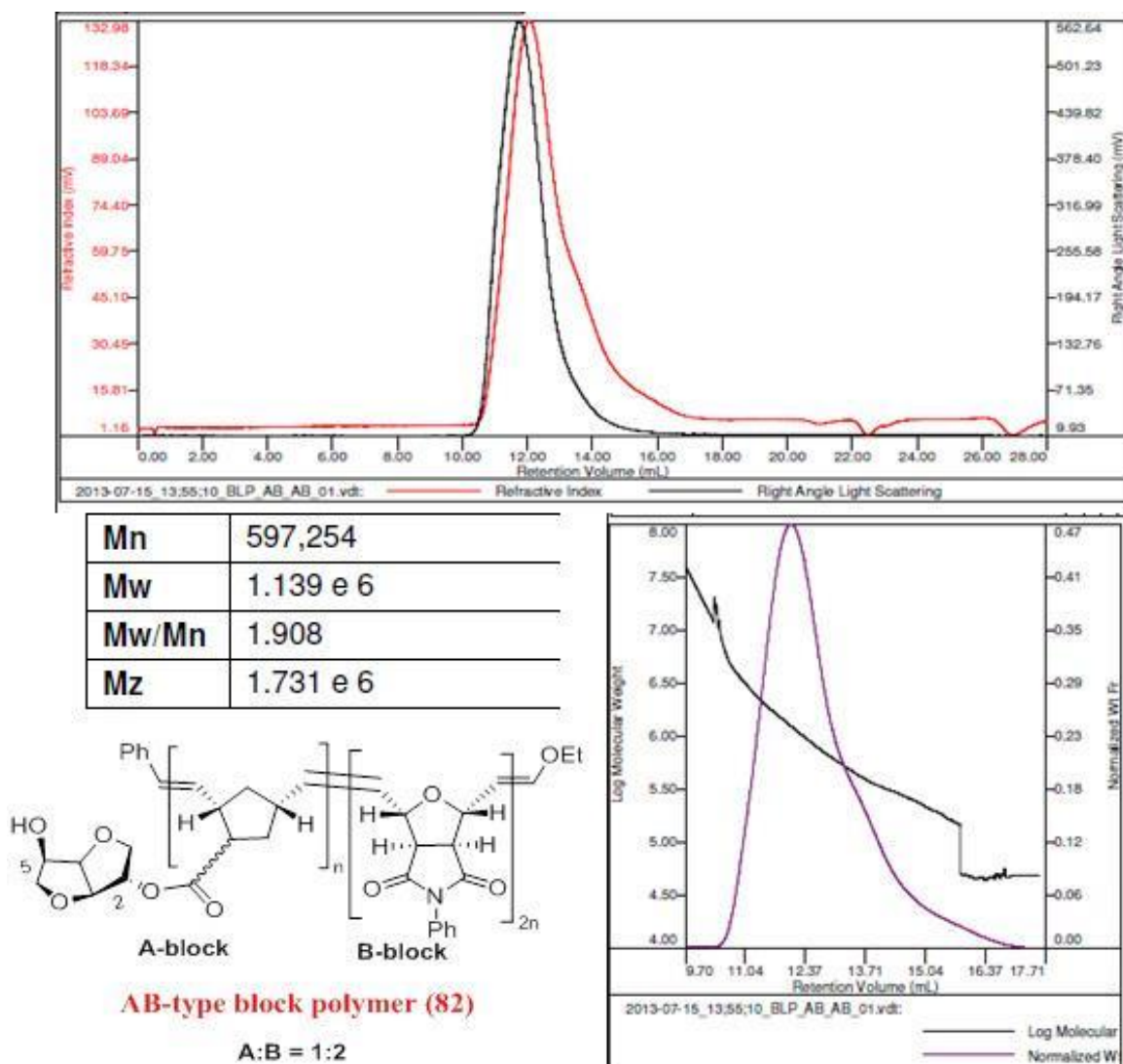
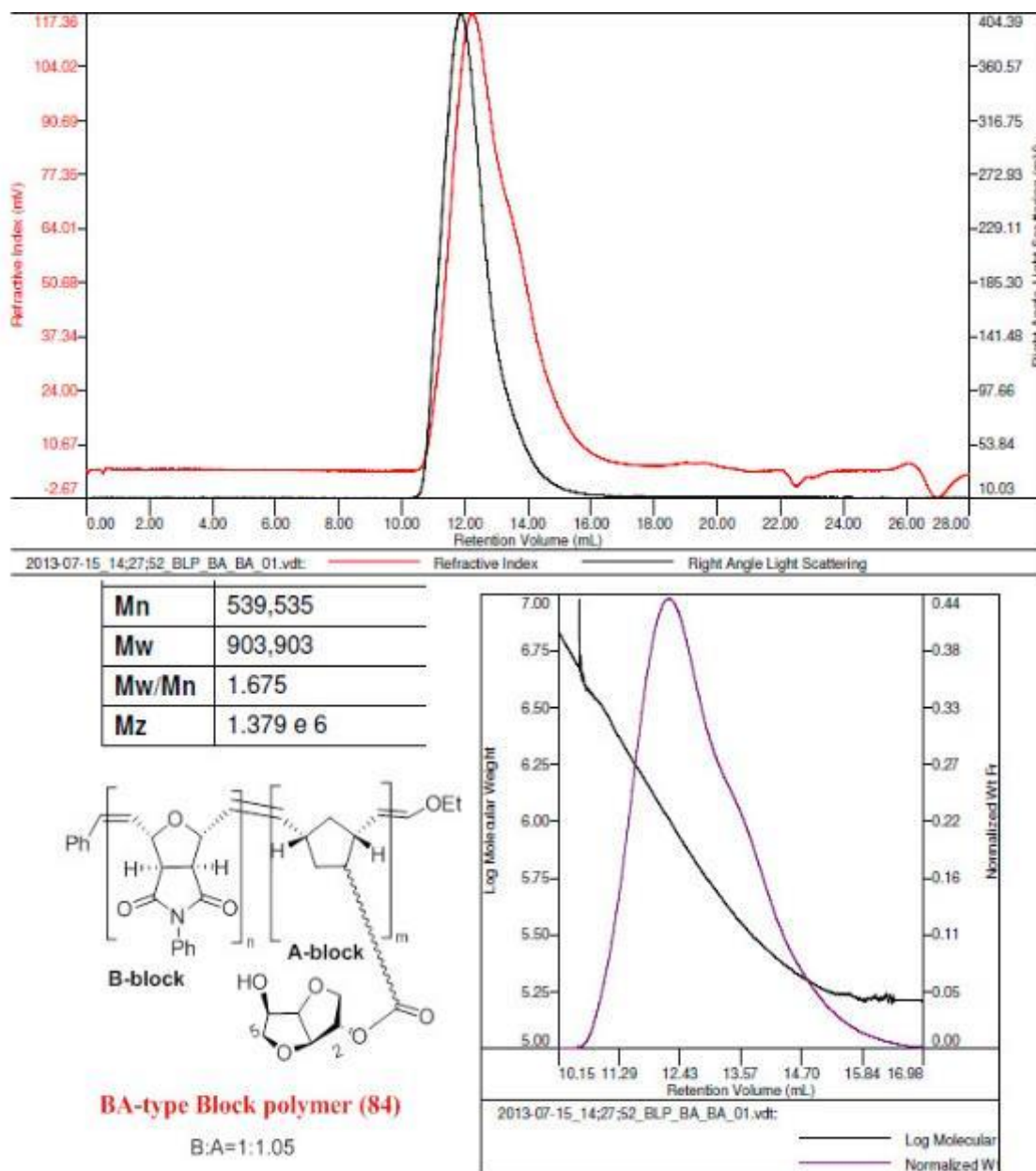


Figure 2.27 GPC chromatogram of the polymer AB-type block polymer **82**.

The chromatogram in the top has an overlaid RI (red) and LS (black) peaks against elution volume. The overlay is made without the baseline correction. The chromatogram in the bottom is an overlay of Log MW (black) and normalized weight fraction (purple) vs. retention volume. If the columns are separating the polymers properly, i.e., in a linear fashion, then the Log MW trace should be linear across the normalized weight fraction. Note that there is a linear separation from high to low molecular weight polymers.



Scheme 2.14 GPC chromatogram of the polymer BA-type block polymer **84**.

The chromatogram in the top has an overlaid RI (red) and LS (black) peaks against elution volume. The overlay is made without the baseline correction. The chromatogram in the bottom is an overlay of Log MW (black) and normalized weight fraction (purple) vs. retention volume. If the columns are separating the polymers properly, i.e., in a linear fashion, then the Log MW trace should be linear across the normalized weight fraction. Note that there is a linear separation from high to low molecular weight polymers.

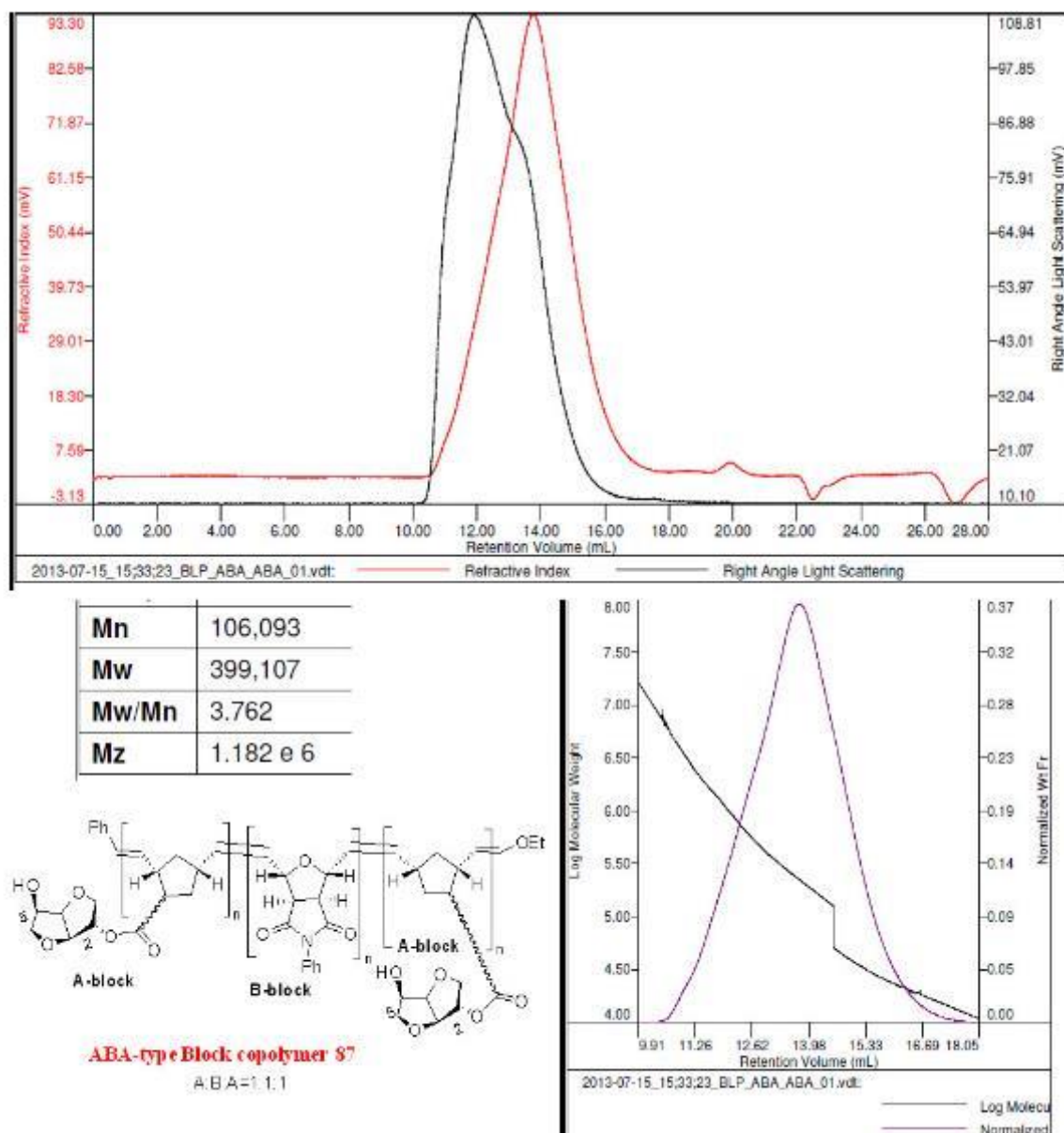


Figure 2.28 GPC chromatogram of the polymer ABA-type block polymer **87**.

The chromatogram in the top has an overlaid RI (red) and LS (black) peaks against elution volume. The overlay is made without the baseline correction. The chromatogram in the bottom is an overlay of Log MW (black) vs. normalized weight fraction (purple). If the columns are separating the polymers properly, i.e., in a linear fashion, then the Log MW trace should be linear across the normalized weight fraction. Note that there is a linear separation from high to low molecular weight polymers. There is a sudden hump seen for Log MW curve at about 14 min which is seen in highly polydisperse polymers. However, this doesn't effect the absolute molecular weight determinations.

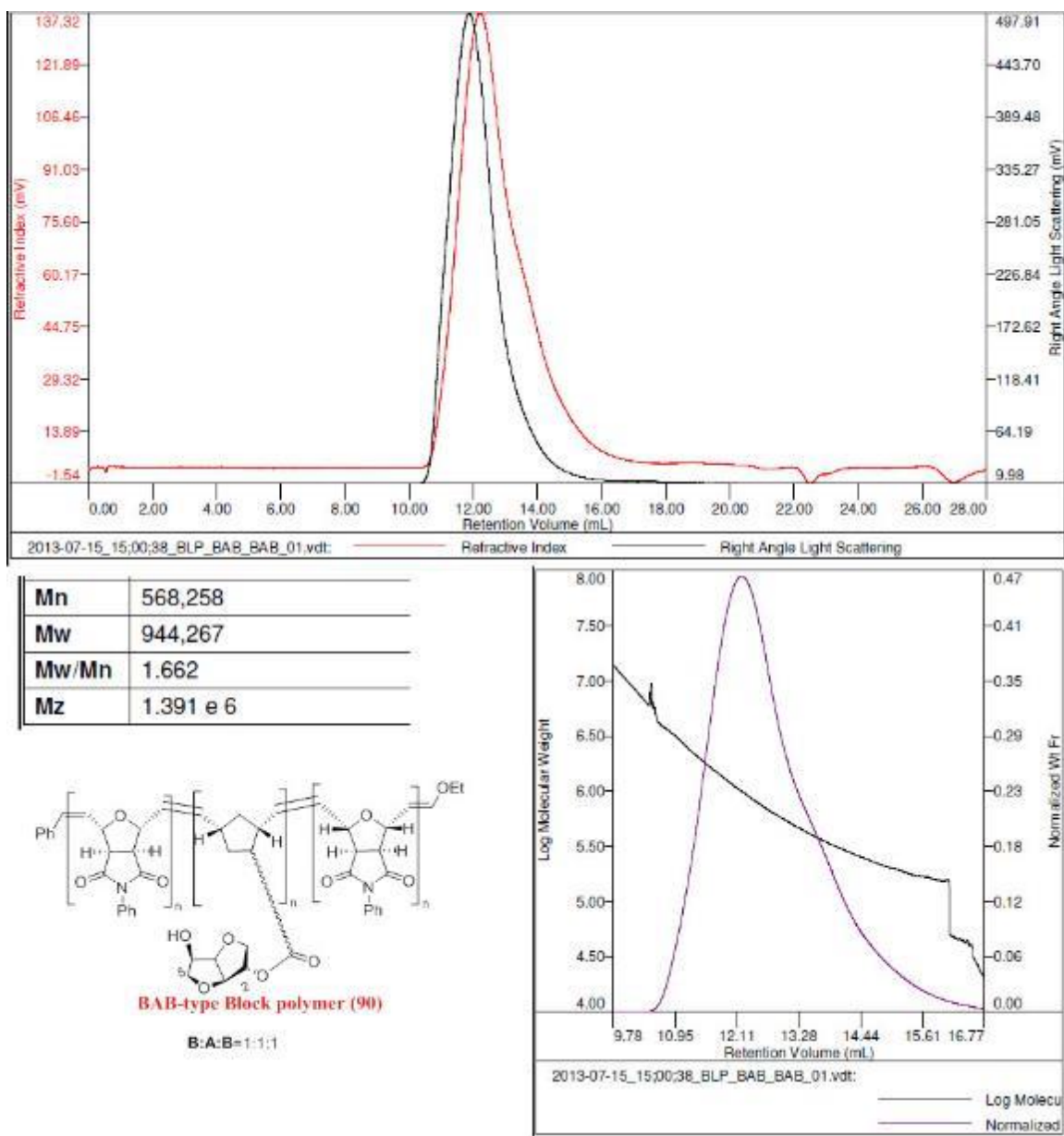


Figure 2.29 GPC chromatogram of the polymer BAB-type block polymer **90**.

The chromatogram in the top has an overlaid RI (red) and LS (black) peaks against elution volume. The overlay is made without the baseline correction. The chromatogram in the bottom is an overlay of Log MW (black) and normalized weight fraction (purple) vs. retention volume. If the columns are separating the polymers properly, i.e., in a linear fashion, then the Log MW trace should be linear across the normalized weight fraction. Note that there is a linear separation from high to low molecular weight polymers.

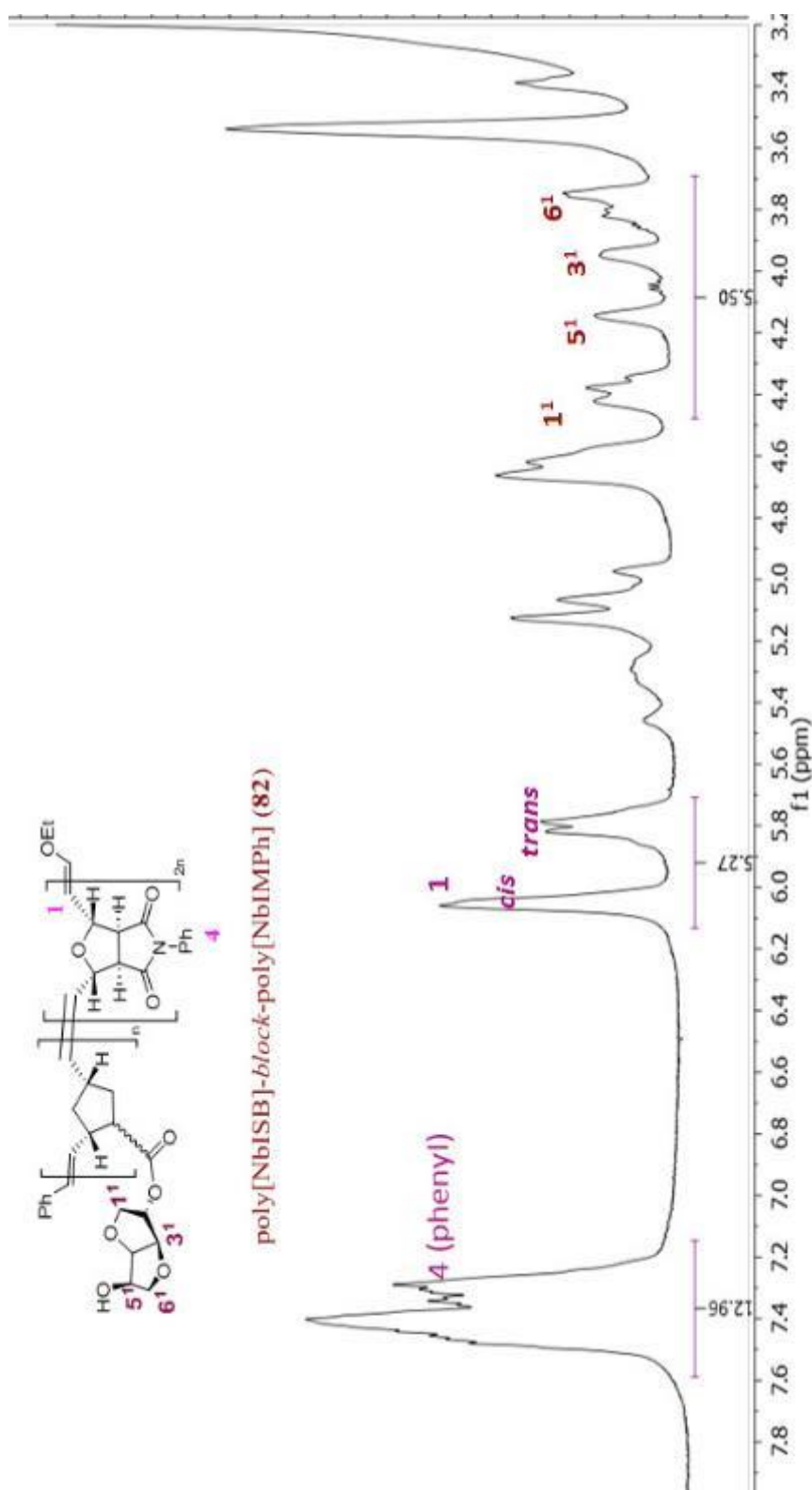


Figure 2.30 ^1H NMR spectrum obtained in DMSO- d_6 at 70 °C (δ 3.2 to 8.0) of AB-type diblock copolymer (82).

The area integration ratios of the three spectral regions (δ 7.6–7.2, 6.16–5.66, and 4.49–3.5) indicate that this block polymer contains an A block of **46** and the B block of **51** at a **46:51** mole ratio of 1 : 2.24 (theoretical = 1:2).

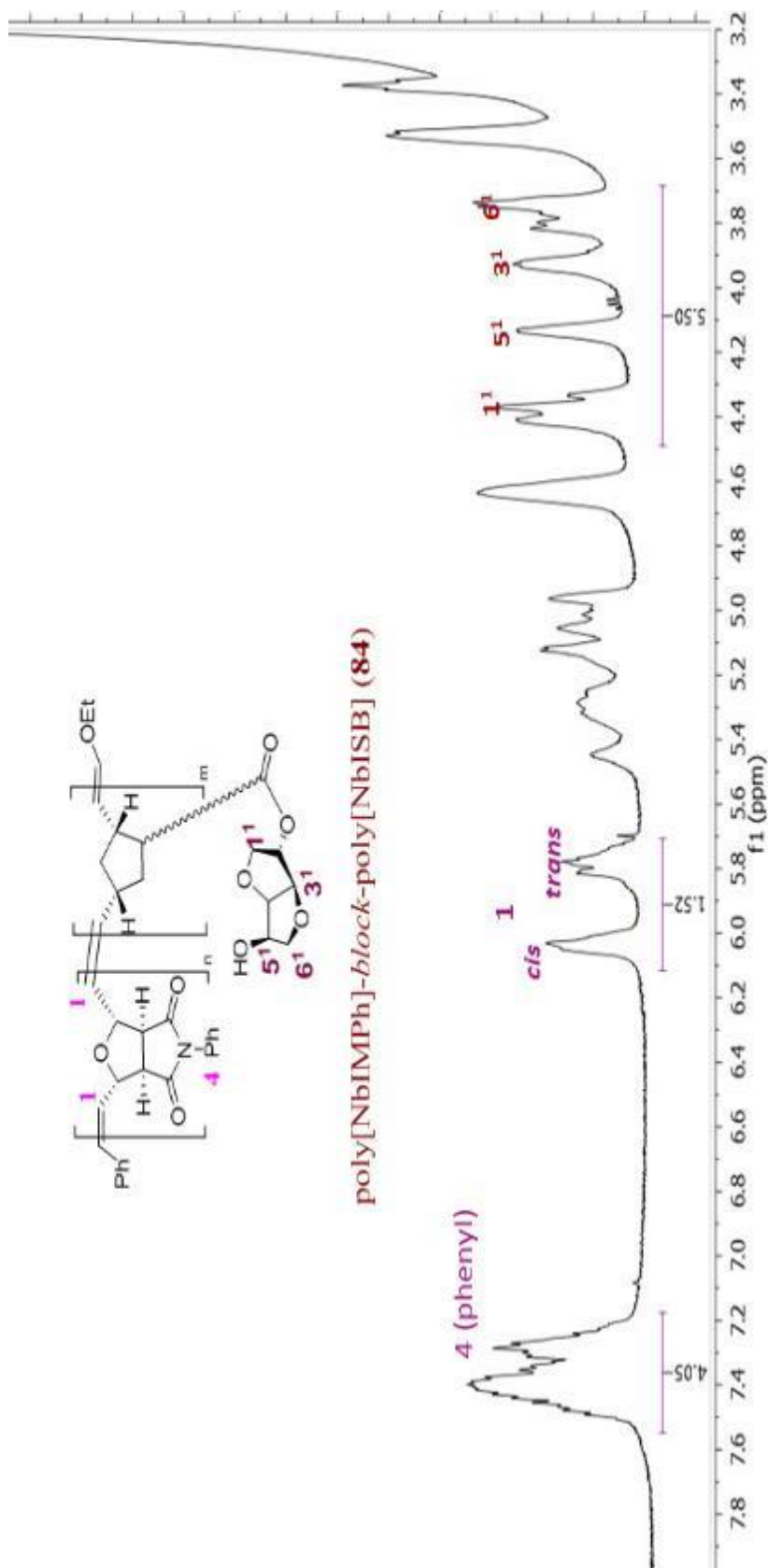


Figure 2.31 ^1H NMR spectrum (δ 3.2 to 8.0) of BA-type diblock copolymer (**84**) obtained in DMSO- d_6 at 70 °C.

The area integration ratios of the three spectral regions (δ 7.6–7.2, 6.16–5.66, and 4.49–3.5) indicate that this block polymer has an A block of **46** and a B block of **51** at a mole ratio of 46:51 (theoretical = 1:1.05).

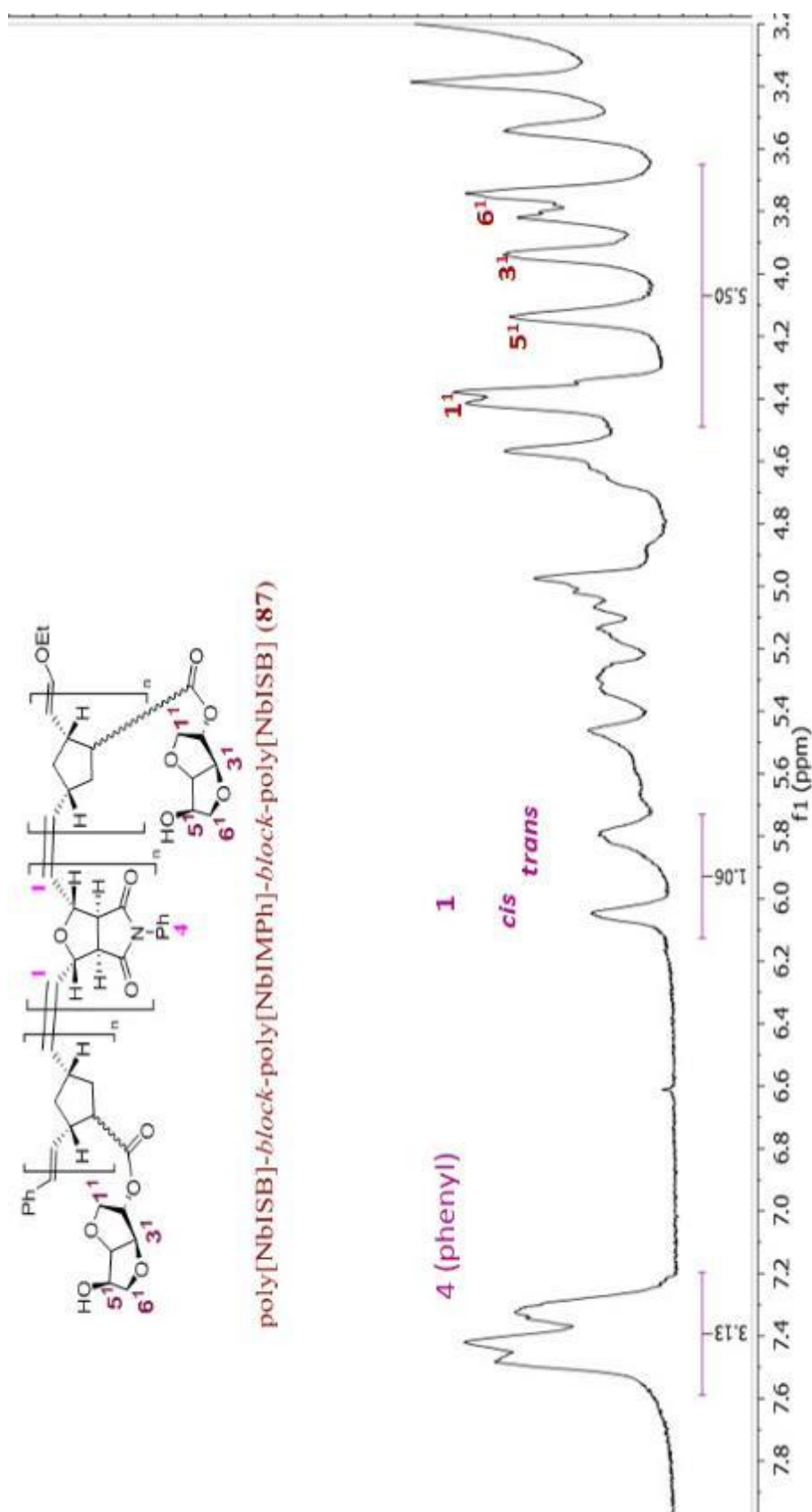


Figure 2.32 ^1H NMR spectrum obtained in DMSO- d_6 at 70 °C (δ 3.2 to 8.0) of ABA-type triblock copolymer (**87**).

The area integration ratios of the three spectral regions (δ 7.6–7.2, 6.16–5.66, and 4.49–3.5) indicate that this block polymer contains an A block of **46** and aB block of **51** at a mole ratio of **46:51** of 1.95: 1 (theoretical = 1:2).

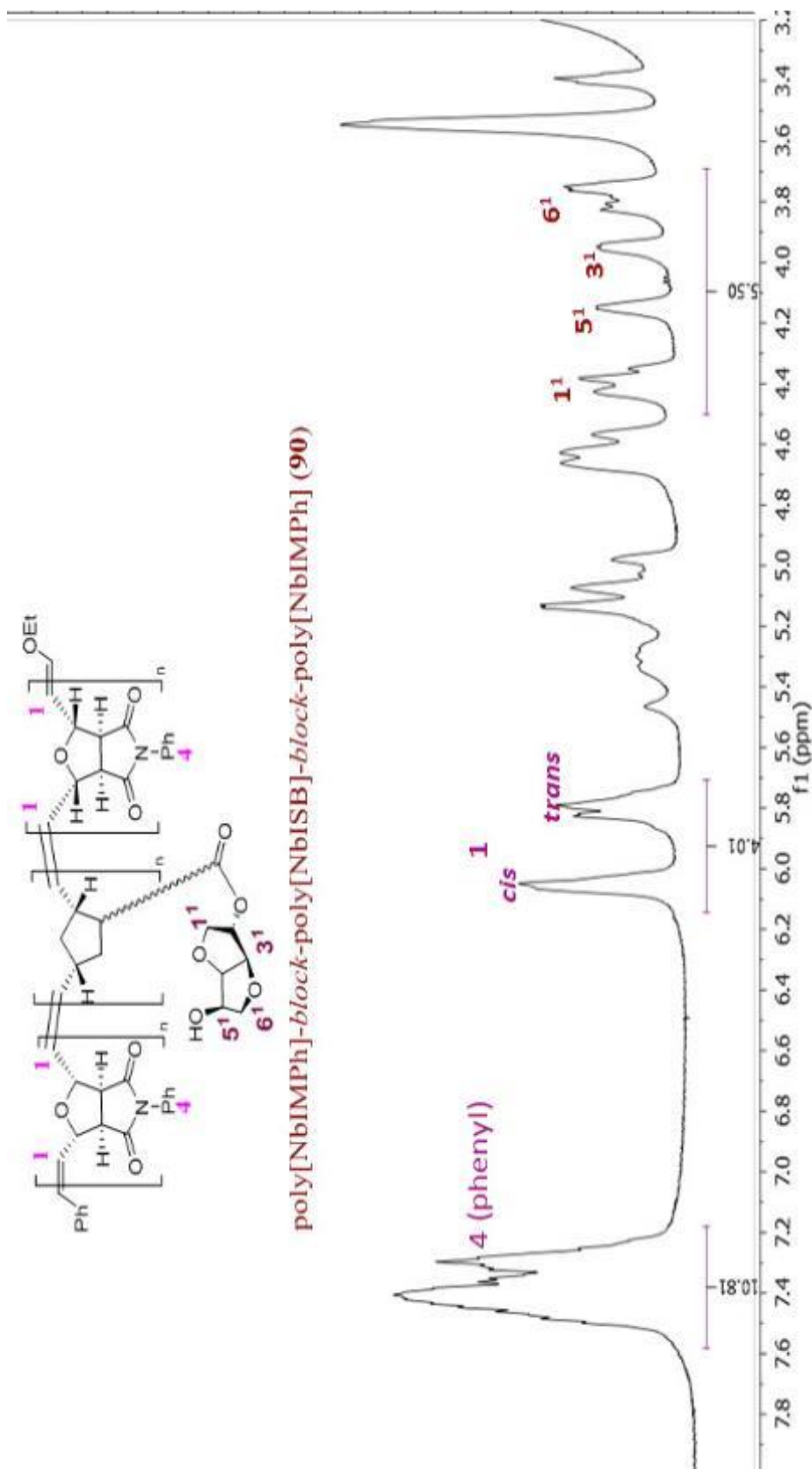
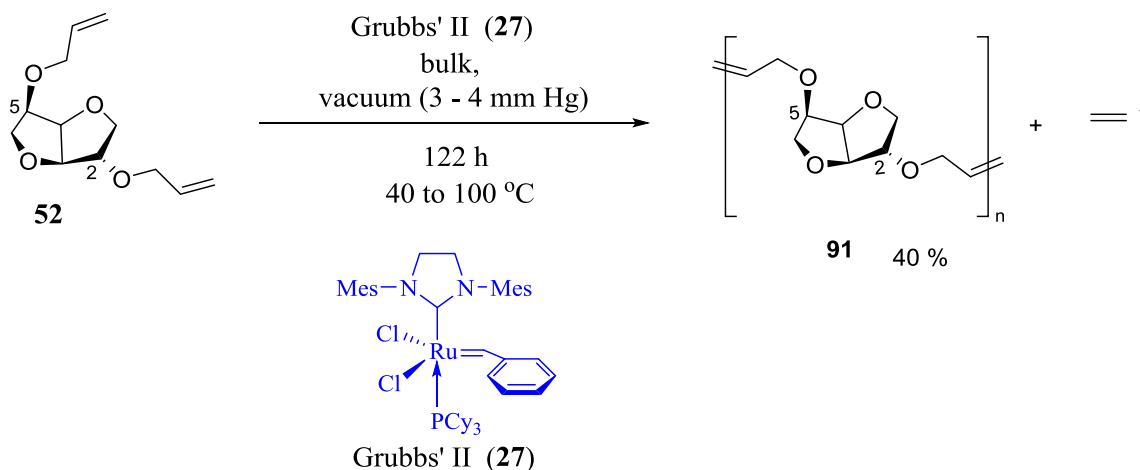


Figure 2.33 ^1H NMR spectrum obtained in $\text{DMSO}-d_6$ at 70°C (δ 3.2 to 8.0) of BAB triblock copolymer (90).

The area integration ratios of the three spectral regions (δ 7.6–7.2, 6.16–5.66, and 4.49–3.5) indicate that this block polymer contains an A block of **46** and a B block of **51** at a **46:51** mole ratio of 1:1.82 (theoretical = 1:2).

2.5 ADMET polymerization.



Scheme 2.15 ADMET polymerization of **52** using Grubbs' II catalyst (**27**)

The diallyl substituted D-isosorbide (**52**) was subjected to ADMET polymerization using catalyst **27**. The reaction was performed for 122 h. at a temperature ranging from 40 to 100 °C in a Schlenk flask. Ethylene gas bubbled from the reaction. High vacuum was applied during the reaction course to remove the evolved ethylene gas from the reaction, to move the equilibrium forward. The temperature was maintained at 40 C for the first 8 h, then it was raised to 80 °C and stirred for 13 h and further raised to 100 °C and stirred for 88 h. After the reaction was quenched with ethyl vinyl ether to precipitate the polymer product, the reaction solution was added into cold pentane. A honey-colored viscous polymer was generated. The proton NMR spectrum of the polymer contained no terminal vinylic protons at δ 6.2 to 5.8 (4H), or vinylic protons at δ 5.4 to 5.20. Instead, new vinylic protons in the region δ 6.0 to 6.25 were observed. GPC analysis of the polymer indicated a M_n of only 1194 and a DP of 5 (Figure A.6). Hence,

high molecular weights were not obtained from ADMET under the conditions used. One reason for the low yields may be due to the cyclization of the terminal alkenes in **52** to produce cyclic products or due to the formation of cyclic-oligomers which may not participate in the ADMET reaction.

2.6 Discussion and conclusions.

A series of monomers containing D-isosorbide **2** functionalized with norbornene were synthesized. These compounds, NbISB **46**, DiNbISB **47**, AcNbISB **48**, along with an already reported monomer NbIMPh (**51**) were used as the monomers for ROMP.

Homopolymerization: First, the synthesis of a series of homopolymers of NbISB was performed using Grubbs' I and Grubbs' II catalysts (**26** and **27**). This yielded polymers **58** to **63**, respectively. GPC molecular weight determinations of these in THF showed M_n between 28,000 to 40,000, relative to PS standards. Homopolymerization of di-functional **47** yielded a highly cross-linked polymer **67** which is insoluble in organic solvents.

Homopolymerization of the monomers **46**, **48** and **51** were also conducted using catalyst **27** to yield polymers poly(NbISB) **64**, poly(AcNbISB) **65** and poly(NbIMPh) **66**. The polymers **64** and **65** had different physical characteristics. Polymer **64** has a greenish color, whereas **65** had a maroon color (**66** is a colorless polymer). Absolute molecular weights of polymers **64** to **66** were determined using GPC with LS detector in DMF. **64** was also analyzed using GPC in THF. The weight averaged molecular weight (M_w) obtained for **64** using LS detector in DMF (DMF-LS) was 612,666 (absolute), whereas the M_w in THF relative to PS (THF-PS) was 199,002. Using these two molecular weight measurements, a conversion factor Q was calculated by dividing the $M_{w(DMF-LS)}$ value with

the $M_{w(\text{THF-PS})}$ value. This yielded a Q-factor of ~ 3 . This Q-factor was used to correct the THF-PS-derived molecular weights of poly(NbISB) (**58** to **61**) (Table 2.2). A Q-factor of ~ 3 for poly(NbISB) suggests that this polymer has a more contracted architecture in THF compared to PS standards, thus resulting in a reduced hydrodynamic volume; while, in DMF expands its hydrodynamic volume. In addition, the molecular weights determined in THF are relative to PS standards. PS contains a different chemical structure when compared to poly(NbISB). This difference in the chemical structures between the two polymers makes the molecular weight determinations inaccurate. This has been reported in the literature in the synthesis functionalized norbornene polymers.^{27, 34, 65}

Random copolymerization: Random copolymerization of different mole ratios of **46** and **51** was performed using catalysts **26** and **27**. Catalyst **26** yielded homopolymers **69** and **73** and random copolymers **70** to **72** which have M_w values in THF between 26,000 to 58,000, relative to PS standards, whereas **27** yielded polymer **74** with a M_w values in THF 186,000 relative to PS standards. The monomer ratio in these random copolymers was determined by using proton NMR, by integrating the chemical shift regions of the proton peaks specific to these two monomers (Table 2.6). Random copolymers **69** to **73** were synthesized by using catalyst **26** had monomer ratios comparable to that of their initial monomer feed ratios. The polymers synthesized using catalyst **27** had greater deviations from the initial monomer feed ratio (Table 2.5). The high PDI values of these polymers could be due to the improper estimation of the polymer molecular weights as these molecular weights are relative to PS standards.⁶⁵

Similar random copolymerizations were performed by using **47** and **31** in different feed ratios. These co-polymerizations produced highly cross-linked hard

polymers **76** to **80**. All these polymers produced gels within 20 min from the start of the reaction.

Block polymerizations: Block polymerization was performed with NbISB (A) (**46**) and NbIMPh (B) (**51**) using Grubbs' II catalyst (**27**) at an initial monomer to catalyst ratio of 50:1. AB- and BA- type diblock polymers (**82** and **84**) and ABA- and BAB- type triblocks (**87** and **90**) were synthesized. The physical characteristics of these blocks were also different from each other. AB-diblock (**82**) was a granular powder; BA-diblock (**84**) was an amorphous polymer. ABA-triblock (**87**) is a colorless powder, whereas BAB-triblock (**90**) was an amorphous polymer. The ratio of the two monomers A and B in these blocks was determined using proton NMR (Table 2.9). The observed monomer ratios of A and B were found to be similar to that of the initial monomer feed ratios. Hence, the synthesized polymers in-fact have block-type architecture in them. However, the exact composition of these blocks and proof of block architecture could not be confirmed by only performing the proton NMR integrations.

These block polymers were also analyzed using GPC in DMF-LS and showed very high molecular weights. PDI values of < 2.0 were observed for AB (**82**), BA (**84**) and BAB (**90**) type polymers. ABA had a PDI of 4.0. . The aliquots (weights) of blocks A, B, AB and BA (**81**, **83**, **85**, **86**, **88**, **90**) taken out during the synthesis of these polymers, The weights of the recovered polymers obtained from these aliquots were very low to determine their molecular weights using GPC in DMF. Having the molecular weights of these blocks would have given a better understanding of the block ratios of these polymers. The high molecular weights, high PDIs and DPs can be due to the drop wise addition of the catalysts into the monomers solutions during the block polymer

synthesis. The catalyst being added over time will start out different chains growing at different times and at those times different amts. of monomer are left. Hence, different chains grow for different times to different lengths and this enlarges PDI and it allows some polymers to have molecular weights. > Monomer to catalyst ratio predictions. Thus high PDI values are seen for these block polymers and in some cases for homopolymers. If the catalyst was added all together instead of dropwise, this could have resulted block polymers with lower PDI values. The catalyst **27** used in the synthesis of block polymers has a slow initiation rate relative to **26**.⁵¹ This slow initiation rate of **27** could initiate fewer chains than the no. of catalyst molecules added and lead to molecular weights > Monomer to catalyst predictions. This poor initiation relative to propagation would cause the monomers to be initiated at different times (some monomers earlier than the other monomers). The monomer fraction which is initiated earlier would then propagate earlier than the monomer fraction which is initiated later. This would result in polymers with different chain lengths at a given point of time and the resulting polymer will have broad PDIs. In addition, with increased reaction time periods and increased molecular weights of the growing polymer chains, there is an increased probability for catalyst decomposition, chain termination, and chain transfer reactions to occur. These chain termination and chain transfer reactions³¹ at various stages of polymer growth would result in polymers with different chain lengths, hence, could be contributing factors for the high PDI and DP values of the block and random copolymers.

Two monomers for ADMET polymerization, diallyl-D-isosorbide (**52**) and dipent-5-enyl-D-isosorbide (**55**) were synthesized. Sterically these two monomers differ from each other due to their different structural features; hence their reactivities with the

catalysts would differ from each other. The possibility for the steric hindrance in the diallyl-case (**52**) when the coordination and metallocycle formation is more versus the dipentenyl (**55**) case. Also, there is a possibility for coordination of oxygen atoms in the diallyl monomer (**52**) to Ru during the mechanism which would slow or shut down the catalyst. This coordination could be related to a far higher frequency factor of O encountering Ru in the diallyl vs. di pentenyl case. ADMET polymerization was performed for **52** was performed but could not be performed for **55** due to lower yields in the latter case. **52** resulted in polymers with very low molecular weights. This could be due to the formation of cyclic oligomers and due its steric and structural features as discussed above.

In conclusion, a series of homo-, random-, block- and cross-linked polymers containing D-isosorbide (**2**) were synthesized and characterized using GPC and NMR. The DSC and TGA analysis (Figures A.6 and A.7) of these polymers is performed and the interpretation is yet to be made. Further testing of their mechanical properties, micelle formation could verify their utility as alternatives for petroleum-based products in polymer industry and in drug-delivery.

CHAPTER III

EXPERIMENTAL

3.1 Materials and methods.

3.1.1 Materials.

D-isosorbide (**2**), 5-Norbornene-2-carboxylic acid (**43**) (predominantly *endo* isomer, 97% pure), and allyl bromide were purchased from Alfa Aesar. *N*-Phenylmaleimide, 4-(dimethylamino)pyridine (DMAP), *N,N'*-dicyclohexylcarbodiimide (DCC), ethyl vinyl ether, norbornene and anhydrous methanol were also purchased from Sigma Aldrich and used as received. DCM and acetonitrile were dried over calcium hydride, and distilled.

The Grubbs' type I generation catalyst, bis(tricyclohexylphosphine)benzylidene ruthenium(IV) chloride (**26**), and the Grubbs' II generation catalyst, (1,3-bis(2,4,6-trimethylphenyl)-2-imidazolidinylidene)dichloro(phenylmethylene)(tricyclohexyl phosphine)ruthenium (**27**) were purchased from Sigma Aldrich. Tetrahydrofuran (THF) was distilled from sodium benzophenone ketyl prior to use. Degassing of the reactions was performed by three freeze-pump and thaw cycles using liquid nitrogen as the coolant. All ROMPs were carried out under N₂ or Ar. All the glassware was dried by heating in an oven at 120 °C before using.

3.1.2 Methods.

IR spectra were recorded using a universal attenuated total reflection sampling accessory with a diamond (attenuated total reflectance) ATR on an Agilent Cary 630 FT-IR spectrometer.

^1H (400 MHz) and ^{13}C (100 MHz) NMR spectra were recorded on American Varian Mercury Plus 400 NMR spectrometers. ^1H (500 MHz) and ^{13}C (126 MHz) NMR spectra were recorded in CDCl_3 or $\text{DMSO}-d_6$ solutions on a Bruker AVANCE DRX spectrometer at room temperature or at 70 °C for certain polymers wherever indicated. Chemical shifts are referenced to the residual solvent signal (CDCl_3 : δ H 7.26 , δ C 77.1; $\text{DMSO}-d_6$ δ H 2.5). Splitting patterns are designed as “s, d, t, q, and m”; these symbols indicate “singlet, doublet, triplet, quartet, and multiplet,” respectively. Coupling constants, J , were reported in Hertz (Hz).

Accurate masses were obtained with a high resolution ESIMS (Agilent 6200 Series, ESI source model #G1969A equipped with TOF, Agilent Technologies). The positive-ionization mode was employed with a capillary voltage of 4000 V. Nitrogen was used as the nebulizing gas (30 psi) as well as the drying gas at 11 L/min at a temperature of 350 °C. The voltage of the photo multiplier tube (PMT), fragmentor, and skimmer were set at 850, 100, and 60 V, respectively. Full-scan mass spectra were acquired from m/z 100–1000. Data acquisition and processing was done using Analyst QS software (Agilent Technologies).

GC analyses were performed with an Agilent 7890A GC and an Agilent 5975C Inert XL mass selective detector, equipped with an Agilent 7693 autosampler. The injector temperature was set to 250 °C. The oven temperature program was as follows:

initial temperature was 45 °C (held for 2 min), then 1.5 °C/min programmed to 100 °C, 2 °C/min programmed to 200 °C, and 10 °C/min programmed to the final temperature of 280 °C (held for 30 min). The column used for the analysis was an Agilent HP-5MS GC capillary column (30 m × 0.25 mm × 0.25 μm). The electron-impact ion source was set to 70 eV. The mass spectrometer was scanned from 40 to 550 amu. ChemStation software was used for acquisition, processing, and calibration of the GC-MS data.

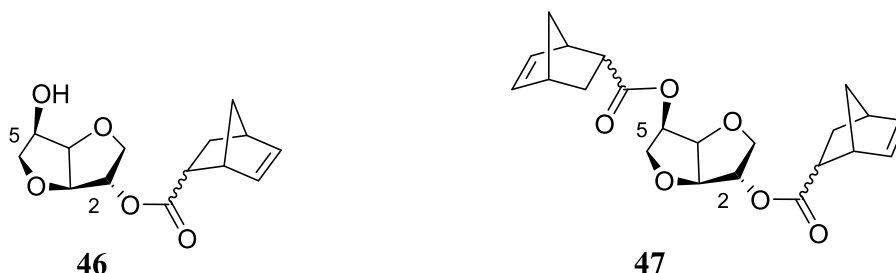
Gel permeation chromatography (GPC) was performed using two instruments. Certain polymers soluble in THF were analyzed in a Waters GPC instrument, equipped with a Waters 717 plus auto-sampler, a Waters 1515 isocratic HPLC pump, a column heater, Waters Styragel HR 5E (effective resolution 2K to 4 M) and 4E (effective resolution 50 K to 100 K) columns, and a guard column. A Waters 2414 refractive index detector was employed. This system was operated at 0.3 mL/min flow rate at 30 °C using Optima THF as the eluting solvent. Polystyrene (PS) standards were used for direct molecular weight calibrations. Hence, the molecular weights given from GPC are based on a direct comparison of the elution volumes of the samples with those of the PS standards. These values are not absolute values because the polymers being studied do not have equivalent hydrodynamic radii with PS when their molecular weights are the same. Elution volumes are determined based on hydrodynamic radii, therefore the polymer being analyzed will not elute at the same elution volume as a PS standard with the same molecular weight.

GPC was also performed, using DMF as the eluent, for some polymers insoluble in THF and some THF-soluble polymers. Samples were prepared at a concentration of about 14 – 16 mg/mL and an injection volume of 50 μL was employed. The DMF eluent

(0.02 M LiBr) was used at a flow rate of 1.0 mL/min in combination with 1 x Agilent Polar Gel-M Guard column, 2 x Agilent Polar Gel-M 300 x 7.5 mm columns, a Viscotek-TDA 302 (RI, viscosity, 7 mW 90° and 7° true low angle light scattering detectors (670 nm)) at 50 °C equipped with an Agilent 1100 series isocratic pump and Agilent 1100 series autosampler. The dn/dc of each polymer detected using light scattering was determined in DMF at 50 °C using a Viscotek refractometer and Omnisec 4.2 software. Among the molecular weights obtained using light scattering, the weight-averaged molecular weight (M_w) is an absolute molecular weight determination, whereas the number-averaged molecular weight (M_n) and Z-averaged molecular weight (M_z) are calculated based on the weight averaged molecular weights.

3.1.3 Synthesis of monomers for ROMP and ADMET polymerizations.

3.1.4 Synthesis of (2-*exo*-D-isosorbyl)-5-norbornen-2-carboxylate NbISB (**46**) and (2-*exo*-5-*endo*-D-isosorbyl)-di-5-norbornen-2-carboxylate DiNbISB (**47**).

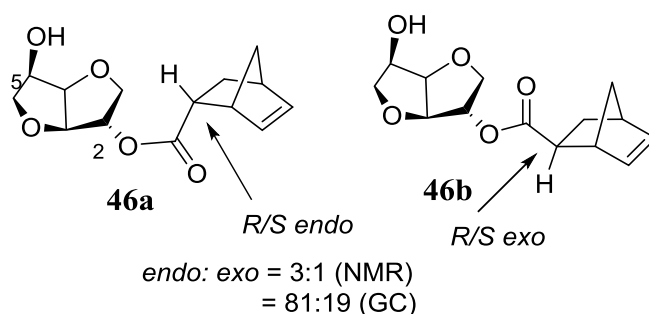


D-Isosorbide (**2**) (0.54 g, 3.60 mmol) and 5-norbornene-2-carboxylic acid (**43**) (0.49 g, 3.67 mmol of 65/35 *endo/exo* ratio) were dissolved in dry DCM. The solution was cooled to 0 °C and *N,N'*-dicyclohexylcarbodiimide (DCC) (0.85 g, 4.14 mmol) and *N,N'*-dimethylaminopyridine (DMAP) (4 mg, 1.14 mmol) were added with stirring. A white crystalline precipitate of *N,N'*-dicyclohexylurea was formed immediately. The

disappearance of D-isosorbide (**2**) was monitored by TLC (60:40 ethyl acetate: hexane) using phosphomolybdic acid in methanol as the stain

After 44 h the reaction mixture was filtered and extracted with 2M aqueous HCl (2x50 mL) and aqueous NaHCO₃ (2x50 mL). Additional urea precipitated again from the solution and it was filtered. The reaction mixture was dried over anhydrous Na₂SO₄, concentrated under vacuum and separated using silica gel column chromatography to separate **46** (0.35 g, 1.35 mmol, 37%) and **47** (0.24 g, 0.82 mmol, 23 %). GC-MS showed three peaks with peak areas of 8.5, 59.5 and 32 percent for the diastereomers of DiNbISB (**47**) and a ratio of 19 and 81% for the diastereomers of **46**. HRMS confirmed the mass of these compounds via accurate mass measurements.

3.1.4.1 (2-*exo*-D-Isosorbyl)-5-norbornen-2-carboxylate (**46**).



Colorless crystalline solid.

R_f = ~ 0.30-0.35 (60:40 v/v, ethyl acetate: hexane); Small minor spots were observed below and above the major spot in TLC, indicating the presence of multiple compounds; mp = 84-88 °C.

¹H NMR (400 MHz, CDCl₃) δ 6.18 (m, 1H), 6.14 – 5.82 (m, 1H), 5.18 (m, 1H), 4.61 (m, 1H), 4.43 (m, 1H), 4.29 (m, 1H), 4.06 – 3.89 (m, 2H), 3.87 (m, 1H), 3.54 (m, 1H), 3.18 (s, 1H), 3.00 – 2.83 (m, 2H), 2.71 (m, 1H), 1.89 (m, 1H), 1.52 – 1.30 (m, 2H),

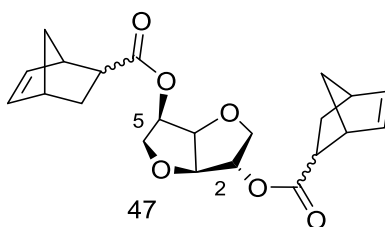
1.26 (m, 1H). All the proton peaks are labeled as multiplets because no conclusive splitting pattern observed at all the regions (as compound **46** is a mixture of isomers). Two peaks with integration ratio of 1.0:0.35 were observed at δ 5.0 to 5.1 and δ 3.25 - 2.95.

^{13}C NMR (101 MHz, CDCl_3) δ 175.20, 173.67, 138.13, 132.04, 85.63, 85.59, 81.96, 78.25, 78.10, 73.72, 73.66, 73.43, 73.41, 72.32, 49.68, 49.67, 49.62, 46.76, 46.65, 46.25, 45.74, 43.25, 43.01, 42.97, 42.54, 41.63, 41.63, 30.39, 30.32, 29.28, 29.22. All the carbon peaks are reported including a number of small peaks corresponding to the carbons of minor isomers.

IR (neat, cm^{-1}): 3425, 2971, 2941, 2874, 1724.1, 1660, 1591, 1406, 1357.8, 133.0, 1269, 1173, 1109, 1068, 1044, 1010, 965, 910, 866, 833, 775.

HRMS data of the isomeric mixture: $[\text{M}+\text{H}]^+$ Ion formula: $\text{C}_{14}\text{H}_{19}\text{O}_5$; Calculated m/z : 267.1227; Observed m/z : 267.1217; Difference (ppm) 3.85. $[\text{M}+\text{Na}]^+$: 289.1033. The main ion observed was the sodium adduct.

3.1.4.2 (2-*exo*-5-*endo*-D-Isosorbyl)-di-5-norbornen-2-carboxylate (**47**)



Colorless crystalline solid.

$R_f = \sim 0.60$ -0.65 (ethyl acetate: hexane = 6:4); Small minor spots were observed below/above the major spot in TLC, indicating the presence of multiple compounds. mp = 68-70 $^{\circ}\text{C}$.

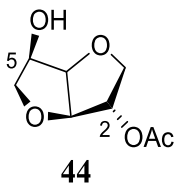
^1H NMR (400 MHz, CDCl_3) δ 6.35 – 6.17 (m, 2H), 6.19 – 5.85 (m, 2H), 5.26 – 5.04 (m, 2H), 4.84 (m, 1H), 4.45 (m, 1H), 3.96 (m, 3H), 3.81 (m, 1H), 3.35 – 3.01 (m, 2H), 2.93 (m, 2H), 1.92 (m, 2H), 1.83 – 1.14 (m, 8H). All the peaks were labeled multiplets because no conclusive splitting pattern observed (as the compound is a mixture of isomers)

^{13}C NMR (101 MHz, CDCl_3) δ 175.26, 174.10, 173.74, 138.15, 138.10, 138.05, 137.94, 137.87, 137.85, 137.58, 135.59, 135.54, 132.40, 132.21, 132.10, 132.01, 85.99, 85.99, 80.72, 77.79, 76.77, 73.72, 73.60, 73.36, 70.53, 52.42, 49.65, 49.62, 46.65, 46.27, 46.09, 45.73, 43.26, 42.86, 42.52, 42.52, 41.65, 41.61, 30.32, 29.33, 29.23. A number of small carbon peaks belonging to the minor isomers were observed adjacent to the major isomers. All the major and minor peaks were reported here.

IR (neat, cm^{-1}): 2967.4, 2937.3, 2872.1, 1725.9, 1652.8, 1541.8, 1448.0, 1332.1, 1268.0, 116.7, 1091.3, 1023.1, 910.8, 835.7, 771.8, 708.3.

HRMS data of the isomeric mixture: $[\text{M}+\text{H}]^+$ Ion formula: $\text{C}_{22}\text{H}_{27}\text{O}_6$; Calculated m/z : 387.1802; Observed m/z : 387.1797; Difference (ppm) 1.17. $[\text{M}+\text{Na}]^+$: 409.1620. The main ion observed was the sodium adduct.

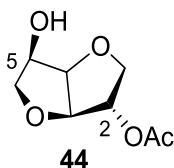
3.1.5 Synthesis of 2-*exo*-acetyl-D-isosorbide (**44**) and 2,5-di-acetyl-D-isosorbide (**45**).



D-Isosorbide (**2**) (5g, 34 mmol) and acetic acid (2.28g, 37.64 mmol) were dissolved in 75 mL of dry DCM and cooled to 0 °C. To this, N,N' -

dicyclohexylcarbodiimide (7.766 g, 37.64 mmol) and *N,N'*-dimethylaminopyridine (42 mg, 0.3421 mmol) were added with stirring. A white crystalline precipitate of *N,N'*-dicyclohexylurea was formed immediately. The course of the reaction was monitored by TLC (4:6 v/v ethyl acetate: hexane) to follow the disappearance of **1**. After 2.5 h. the reaction mixture was filtered to remove *N,N'*-dicyclohexylurea and the filtrate was washed with water (30 mL), 5% aqueous acetic acid (30 mL), dried over anhydrous MgSO₄, evaporated under vacuum and the resulting crude product was separated by silica gel column chromatography to produce 2,5-di-acetyl-D-isosorbide (**45**) (2.77 g, 14.7 mmol, 43%) and 2-*exo*-acetyl-D-isosorbide (**46**) (1.12 g, 6 mmol, 16%).

3.1.5.1 2-*exo*-Acetyl-D-isosorbide (**44**).



Colorless crystalline solid.

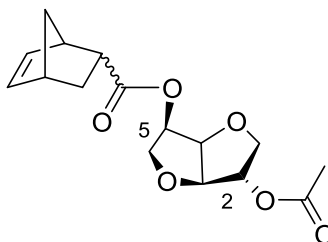
R_f = 0.4 (ethyl acetate: hexane = 40:60); mp = 74-75 °C.

¹H NMR (400 MHz, CDCl₃) δ 5.15 (m, 1H), 4.57 (t, J = 4.9 Hz, 1H), 4.43 (d, J = 4.4 Hz, 1H), 4.25 (m, 1H), 3.96 (m, 2H), 3.83 (dd, J = 9.4, 6.0 Hz, 1H), 3.51 (dd, J = 9.4, 6.1 Hz, 1H), 2.84 (m, 1H), 2.03 (s, 3H).

¹³C NMR (101 MHz, CDCl₃) δ 169.95, 85.53, 81.94, 78.36, 73.52, 73.26, 72.28, 20.85.

IR (neat, cm⁻¹) 3402.1, 2923.5, 2884.7, 1729.9, 1625.9, 1572.0, 1434.1, 1375.0, 1299.5, 1251.1, 1124.3, 1086.9, 1045.5, 1009.2, 987.6, 916.0, 887.3, 829.7, 760.2.

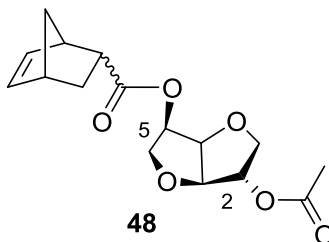
3.1.6 Synthesis of [(2-*exo*-acetyl)-5-*endo*-D-isosorbyl]-di-5-norbornen-2-carboxylate (48).



48

2-*exo*-Acetyl-D-isosorbide **44** (1.2 g, 6.38 mmol) and 5-norbornene-2-carboxylic acid (0.969 g, 7.01 mmol, *endo/exo* ratio of 65/35) were dissolved in dry DCM. The solution was cooled to 0 °C and *N,N'*-dicyclohexylcarbodiimide (1.44 g, 7.01 mmol) and *N,N'*-dimethylaminopyridine (23 mg, 0.21 mmol) dissolved in 10 mL DCM were added with stirring. A white crystalline precipitate of *N,N'*-dicyclohexylurea was formed immediately. After 24 h the reaction mixture was filtered and extracted with 2M aqueous HCl (2x50 mL) and aqueous NaHCO₃ (2x50 mL). More urea was precipitated and it was filtered. The reaction mixture was dried over anhydrous Na₂SO₄, concentrated under vacuum and separated using silica gel column to generate [(2-*exo*-acetyl)-5-*endo*-D-isosorbyl]-di-5-norbornen-2-carboxylate (**48**) (1.3 g, 4.2 mmol, 65%). GC-MS separated three peaks of peak area ratios of 12, 12.5 and 75.5 percent for diastereomers of AcNbISB (**48**).

3.1.6.1 [(2-*exo*-acetyl)-5-*endo*-D-isosorbyl]-di-5-norbornen-2-carboxylate (AcNbISB) (48).



Colorless viscous liquid.

$R_f = \sim 0.3$ (ethyl acetate: hexane) = 40:60. Small minor spots were observed below/above the major spot in TLC, indicating the presence of multiple compounds.

^1H NMR (400 MHz, CDCl_3) δ 6.18 (m, 1H), 6.15 – 5.88 (m, 1H), 5.16 (m, 1H), 5.07 (m, 1H), 4.81 (m, 1H), 4.46 (m, 1H), 4.03 – 3.93 (m, 2H), 3.90 (m, 1H), 3.77 (m, 1H), 3.21 (m, 1H), 3.00 (m, 1H), 2.90 (m, 1H), 2.14 – 2.02 (m, 3H), 1.90 (m, 1H), 1.47 – 1.33 (m, 2H), 1.26 (d, $J = 8.2$ Hz, 1H). All the peaks contained a broad base were obtained. Broad peaks are due to the presence of isomers in the compound. All the peaks are labeled as multiplets.

^{13}C NMR (101 MHz, CDCl_3) δ 175.64, 175.56, 174.05, 170.03, 170.01, 138.16, 138.11, 137.85, 137.57, 135.64, 135.57, 132.38, 132.21, 85.93, 85.90, 80.75, 80.67, 78.09, 78.07, 73.63, 73.49, 73.31, 73.17, 70.61, 70.56, 49.61, 46.85, 46.47, 46.39, 46.25, 46.10, 45.63, 43.06, 42.91, 42.84, 42.77, 42.51, 42.48, 41.64, 41.60, 30.49, 30.35, 29.33, 29.21, 20.88. A number of minor peaks were seen adjacent to the major peaks indicating the compound is a mixture of isomers. All the large and small peaks are reported here.

Hence, the total number of peaks is more than that is expected for a single isomer.

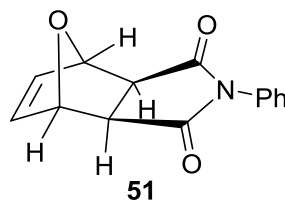
IR (neat, cm^{-1}): 2974, 1732, 1447, 1368, 1335, 1230, 1168, 1091, 1018, 987, 912, 860.2, 836, 772.

HRMS data of the isomeric mixture: $[M+H]^+$ Ion formula $C_{16}H_{21}O_6$; Calculated m/z : 309.1333; Observed m/z : 309.1335; Difference (ppm) 0.57. $[M+Na]^+$ 331.1156. The main ion observed was the sodium adduct.

3.1.7 Synthesis of *exo*-*N*-phenyl-7-oxanorbornene-5,6-dicarboximide (**51**).

The synthesis of *exo*-*N*-phenyl-7-oxanorbornene-5,6-dicarboximide (**51**) was performed as reported in the literature procedure.⁶⁶ A round-bottomed flask (100 mL) equipped with a magnetic stirring bar, a heating mantle, a reflux condenser was charged with a solution of *N*-phenylmaleimide (3 g, 17 mmol) in MeCN (10 mL). Following the addition of excess furan (3 mL), the stirred solution was heated at reflux for 5 h. Then the reaction mixture was cooled to room temperature and then a colorless solid precipitated. The material was filtered and washed with MeCN (200 mL). The filtrate solution was concentrated to afford more of the product, which was also filtered and washed with MeCN (100 mL). The combined solid portions were dried under vacuum (3 mm Hg) at room temperature over-night to afford *exo*-*N*-phenyl-7-oxanorbornene-5,6-dicarboximide (**51**) (3.2 g, 13 mmol, 78%).

3.1.7.1 *exo*-*N*-Phenyl-7-oxanorbornene-5,6-dicarboximide (**51**).

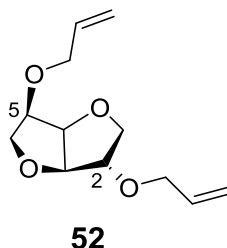


Colorless crystalline solid; mp = 163 - 165 °C; reported 164 - 165 °C.

1H NMR (400 MHz, $DMSO-d_6$) δ 7.54 – 7.45 (m, 2H), 7.42 (t, $J = 7.4$ Hz, 1H), 7.20 (d, $J = 7.5$ Hz, 2H), 6.61 (s, 2H), 5.25 (s, 2H), 3.08 (s, 2H).

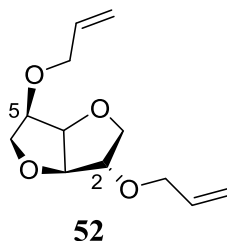
IR (neat, cm^{-1}): 3064, 3021, 3003, 1773, 1701, 1593, 1492, 1375, 1284.4, 1182, 1143, 1085, 1057, 1012, 936, 910, 871, 850, 808, 770, 710.

3.1.8 Synthesis of diallyl-D-isosorbide (**52**)



Synthesis of diallyl-D-isosorbide (**52**) was carried out as reported in the literature.⁶⁴ D-Isosorbide (**2**) (4.0 g, 27.3 mmol) and sodium hydroxide (2.63 g, 65.7 mmol) were weighed and dissolved in 14 mL distilled water, in a 50 mL round bottomed flask equipped with condenser. To this solution, allyl bromide (7.95 g, 5.69 mL, 65 mmol) was added and the solution was stirred at 90 °C for 36 h. The reaction was monitored by TLC using 4:6 ethyl acetate and hexane as the eluant and iodine on silica gel was used as the staining agent. After 36 h, the reaction mixture was acidified with 2M aqueous HCl to pH 1 and the products were extracted with ethyl acetate (3x30 mL). The combined organic layer was extracted with brine solution (2x15 mL), dried over anhydrous MgSO_4 and the solvent was evaporated under vacuum. The crude product was purified using silica gel column chromatography giving diallyl-D-isosorbide (**52**) (2.0 g, 8.9 mmol, 32%), 2-*exo*-allyl-D-isosorbide (**53**) (1.127 g, 6.1 mmol, 22%) and 5-*endo*-allyl-D-isosorbide (**54**) (0.33 g, 1.8 mmol, 6.7%)

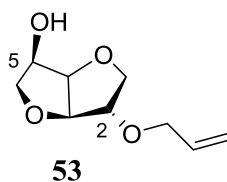
3.1.8.1 Diallyl-D-isosorbide (52).



Colorless viscous liquid

^1H NMR (300 MHz, CDCl_3) δ 5.99 – 5.77 (m, 2H), 5.29 (dq, J = 5.3, 1.6 Hz, 1H), 5.23 (dq, J = 5.3, 1.6 Hz, 1H), 5.18 (dq, J = 4.3, 1.4 Hz, 1H), 5.15 (dq, J = 4.3, 1.4 Hz, 1H), 4.58 – 4.62 (m, 1H), 4.70- 4.68 (m, 1H), 4.10 -4.25 (m, 1H), 3.95 - 4.05 (m, 5H), 3.96 – 3.86 (m, 3H), 3.50 – 3.60 (m, 1H), .

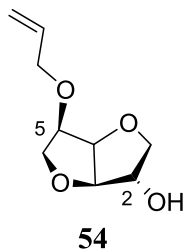
3.1.8.2 2-*exo*-Allyl-D-isosorbide (53).



Colorless viscous liquid.

^1H NMR (300 MHz, CDCl_3) δ 5.70 - 5.90 (m, 1H), 5.31 – 5.07 (m, 2H), 4.50 – 4.60 (m, 1H), 4.35 – 4.45 (m, 1H), 4.15 – 4.25 (m, 1H), 4.07 – 3.89 (m, 4H), 3.70 – 3.85 (m, 2H), 3.35 – 3.50 (m, 1H), 3.29 – 2.85 (m, 1H).

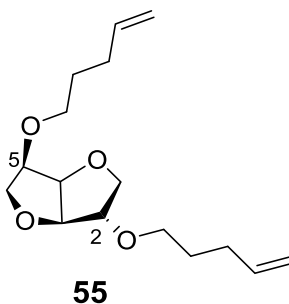
3.1.8.3 2-endo-Allyl-D-isosorbide (**54**).



Colorless viscous liquid

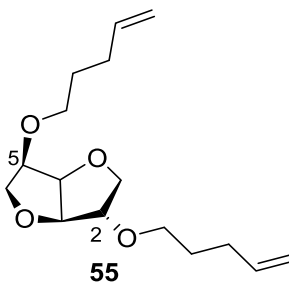
^1H NMR (300 MHz, CDCl_3) δ 5.75 – 5.95 (m, 1H), 5.32 – 5.08 (m, 2H), 4.60 (t, J = 4.4 Hz, 1H), 4.35 (d, J = 4.2 Hz, 1H), 4.23 – 4.17 (m, 1H), 4.05 – 4.15 (m, 1H), 4.04 – 3.93 (m, 2H), 3.92 – 3.79 (m, 3H), 3.74 – 3.56 (s, 1H), 3.45 – 3.55 (m, 1H).

3.1.9 Synthesis of dipent-5-enyl-D-isosorbide (**55**).



Synthesis of dipent-5-enyl-D-isosorbide (**54**) was performed using the same procedure reported for the synthesis of diallyl Isosorbide (**52**). Isosorbide (**2**) (0.5 g, 3.42 mmol), NaOH (0.32 g, 7.9 mmol) and 5-bromopent-1-ene (1.1 g, 7.53 mmol) were used for the reaction. Compounds dipent-5-enyl-D-isosorbide (**55**) (0.11 g, 0.4 mmol, 11.7%), 2-*exo*-pentenyl-D-isosorbide (2-18) (0.159g, 0.741mmol, 21.6%) 5-*endo*-pent-5-enyl-D-isosorbide (**57**) (0.12 g, 0.54 mmol, 15.8%) were isolated.

3.1.9.1 Dipent-5-enyl-D-isosorbide (55).

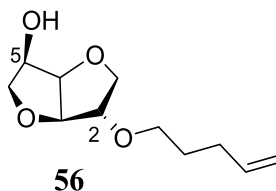


Colorless liquid.

^1H NMR (300 MHz, CDCl_3) δ 5.88 – 5.63 (m, 2H), 5.08 – 4.87 (m, 4H), 4.60 (t, J = 4.2 Hz, 1H), 4.47 (d, J = 4.3 Hz, 1H), 4.02 – 3.83 (m, 5H), 3.72 – 3.36 (m, 5H), 2.20 – 2.00 (m, 4H), 1.80 – 1.53 (m, 4H).

IR (neat, cm^{-1}): 3075, 2934, 2868, 1731, 1640, 1445, 1370, 1321, 1209, 1075, 1015, 910, 834, 776.

3.1.9.2 2-*exo*-Pent-5-enyl-D-isosorbide (56).

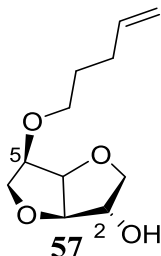


Colorless liquid.

^1H NMR (300 MHz, $\text{DMSO}-d_6$) δ 5.90 – 5.70 (m, 1H), 5.06 – 4.89 (m, 2H), 4.90 – 4.70 (m, 1H), 4.38 – 4.28 (m, 2H), 4.14 – 3.98 (m, 1H), 3.87 – 3.63 (m, 4H), 3.38 – 3.45 (m, 2H), 3.32 – 3.20 (m, 1H), 2.11 – 1.95 (m, 2H), 1.56 (dt, 2H).

IR (neat, cm^{-1}): 3439, 3077, 2935, 2869, 1726, 1640, 1405, 1640, 1405, 1337, 1194, 1113, 1073, 1048, 1008, 967, 913, 867, 832, 776.

3.1.9.3 5-endo-pentenyl-D-isosorbide (57).



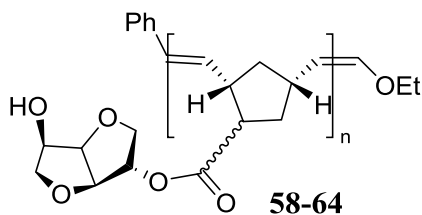
Colorless liquid.

^1H NMR (300 MHz, $\text{DMSO}-d_6$) δ 5.90 - 5.75 (m, 1H), 5.20 – 4.90 (m, 2H), 5.01 – 4.88 (m, 1H), 4.53 (t, $J = 4.3$ Hz, 1H), 4.25 (d, $J = 4.2$ Hz, 1H), 4.05 – 4.00 (m, 1H), 3.95 - 3.85 (m, 1H), 3.82 – 3.63 (m, 3H), 3.60 – 3.50 (m, 1H), 3.42 – 3.38 (m, 1H), 3.55 – 3.25 (m, 1H), 2.55 – 3.45 (m, 1H), 2.10 – 1.99 (m, 2H), 1.64 – 1.47 (m, 2H).

3.2 Ring-opening metathesis and acyclic diene metathesis polymerization.

3.2.1 Homopolymerization.

3.2.1.1 Synthesis of poly[(2-*exo*-D-isosorbyl)-5-norbornen-2-carboxylate] (poly[NbISB]) (58).



To a solution of NbISB **46** (1.82 g, 6.84 mmol) dissolved in 10 mL dry degassed THF, a 10 mL THF solution of Grubbs' first generation catalyst, bis(tricyclohexylphosphine)benzylidene ruthenium(IV) chloride (**26**) ($0.056\text{ g}, 6.8 \times 10^{-2}$ mmol) was added in a $[\text{M}]/[\text{C}]$ ratio of 100:1. After 1 h the reaction mixture became viscous due to the polymerization of NbISB. THF (3 mL) was added to dilute the viscous polymeric solution and to enable stirring. After 2 days, the reaction was quenched using

excess (0.1 mL) ethyl vinyl ether. The polymer solution was precipitated twice from THF into methanol (100 mL) to generate a sticky, grey solid. The synthesized polymer was then dried over-night at 40 °C under vacuum to generate an amorphous, grayish, thick translucent film of poly(NbISB) (**58**).

3.2.1.1.1 Poly(NbISB) (**58**).

Amorphous grayish thick translucent film.

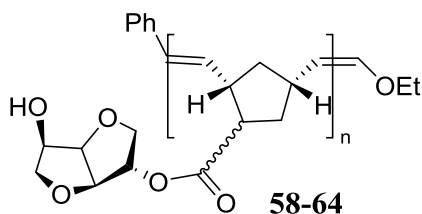
Yield (% w/w) = 92% (1.67 g); GPC analysis results in THF: $M_n = 28,457$, $M_w = 40,914$, $M_z = 53,096$, PDI = 1.44, DP = 107; by direct comparison with PS standards.

LS-corrected $M_w = 122,742$; Q-factor = ~ 3 .

^1H NMR (500 MHz, $\text{DMSO}-d_6$) δ 5.56 – 5.11 (m, 2H), 5.00 (m, 1H), 4.68 – 4.51 (m, 1H), 4.49 – 4.28 (m, 2H), 4.23 – 4.07 (m, 1H), 3.94 (m, 1H), 3.77 (m, 2H), 2.89 (m, 3H), 2.16 – 1.74 (m, 2H), 1.74 – 1.51 (m, 1H), 1.22 (m, 1H).

IR (neat, cm^{-1}): 3450, 293, 3867, 1725, 1633, 1455, 1367, 1166, 1073, 1044, 1009, 968, 868, 830, 743.

3.2.1.2 Synthesis of poly(NbISB) (**59**).



Monomer NbISB **46** (1.00g, 3.76 mmol) was dissolved in 3 mL dry degassed THF. Grubbs' first generation catalyst, bis(tricyclohexylphosphine) benzylidene ruthenium(IV) chloride (**26**) (0.046 g, 3.76×10^{-2} mmol) was dissolved in 7 mL THF. This solution was added to the monomer solution and the combined solution was stirred

at room temperature for about 10 days. The reaction was then quenched using excess (0.1 mL) ethyl vinyl ether. The polymer solution was then precipitated from THF twice into methanol (100 mL) to generate a sticky, grey solid. The synthesized polymer was then dried over-night at 40 °C under vacuum to generate a dark grey colored stretchy amorphous polymer poly(NbISB) (**59**).

Yield (% w/w) = 95 % (0.95 g).

GPC analysis results (in THF) : $M_n = 35,352$, $M_w = 48,355$, $M_z = 65,418$ and PDI = 1.37, DP = 133 at M_n ; by direct comparison with PS standards.

^1H NMR (300 MHz, CDCl_3): same as polymer **58**.

IR (neat, cm^{-1}): 3450, 293, 3867, 1725, 1633, 1455, 1367, 1166, 1073, 1044, 1008, 968, 868, 830, 743.

3.2.1.3 Synthesis of poly(NbISB) (**60** to **63**).

Monomer **46** (150 mg, 0.564 mmol) was weighed separately into four round bottomed flasks. Then 3 mL dry, degassed THF was added into each flask to dissolve **46**. Various amounts of Grubbs' II generation catalyst, (1,3-bis(2,4,6-trimethylphenyl)-2-imidazolidinylidene)dichloro(phenylmethylene)(tricyclohexylphosphine)ruthenium (**27**) (9.6 mg, 0.01 mmol), (4.8 mg, 0.005 mmol), (2.4 mg, 0.0025 mmol), (1.2 mg, 0.0125 mmol) were each dissolved in 1 mL THF and then these solutions were individually added dropwise to one each of the five flasks. Then all five reaction solutions were allowed to stir for 40 h under argon. The reactions were quenched with excess ethyl vinyl ether (0.1 mL), concentrated by rotary evaporation, followed by individual precipitation into 25 mL of methanol. The precipitates generated were separated and dried over-night at 40 °C under vacuum to generate poly(NbISB)s **60** to **63**.

^1H NMR and IR of **60** to **63** are same as that of poly(NbISB) **58**.

3.2.1.3.1 Poly(NbISB) 60.

Grayish, transparent, hard and thick film.

Yield (% w/w) = 95 % (142 mg).

GPC analysis results (in THF): $M_n = 66,103$, $M_w = 181,350$, $M_z = 489,937$, PDI = 2.7, DP= 249 at M_n ; by direct comparison with PS standards.

3.2.1.3.2 Polymer 61.

Transparent thick lumps.

Yield (% w/w) = 90 % (134 mg).

GPC analysis results (in THF- partially soluble): $M_n = 39,565$, $M_w = 70,092$, $M_z = 105,040$, PDI = 1.77 and DP= 148 at M_n ; by direct comparison with PS standards.

3.2.1.3.3 Polymer 62.

Transparent hard film.

Yield (% w/w) = 3 % (4 mg).

GPC analysis was not performed due to the lack of sufficient sample for GPC analysis.

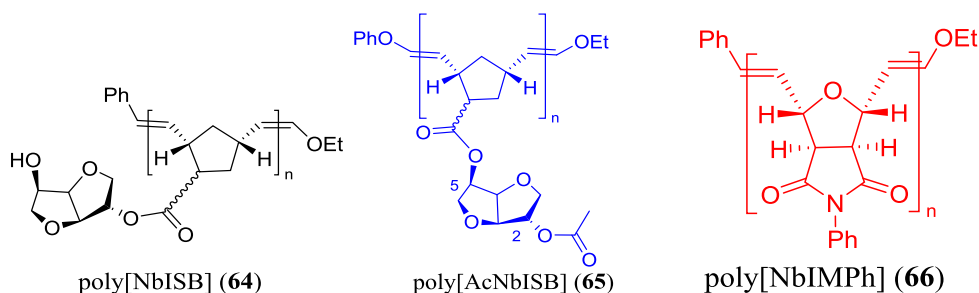
3.2.1.3.4 Polymer 63.

Transparent soft film.

Yield (% w/w) = 10 % (15 mg).

GPC analysis was not performed due to an inadequate amount of sample.

3.2.1.4 Synthesis of poly(NbISB) (**64**), poly(AcNbISB) (**65**) and poly(NbIMPh) (**66**) using Grubbs' II catalyst (**27**).



Monomers NbISB **46** (0.266 g, 1mmol), AcNbISB **48** (0.241g, 1mmol) and NbIMPh **51** (0.308 g, 1mmol) were individually weighed into three separate round bottomed flasks. Then 2 mL of dry degassed THF was added to each flask, followed by the addition of Grubbs' second generation catalyst, (1,3-bis(2,4,6-trimethylphenyl)-2-imidazolidinylidene)dichloro(phenylmethylene)(tricyclohexylphosphine)ruthenium (**27**) (8.5 g, 0.01 mmol) in 1 mL THF to the reaction solution. All solutions were stirred at room temperature under argon. After 12 h, the reactions were quenched by the dropwise addition of excess ethyl vinyl ether (0.1 mL), concentrated by rotary evaporation, and precipitated from THF into 50 mL methanol. The synthesized precipitates were separated and dried over-night under vacuum at 40 °C to generate polymers poly(NbISB) **64** (95%), poly(AcNbISB) **65** (100%) and poly(NbIMPh) **66** (96%).

Note: The monomer NbIMPh **51** was not completely soluble in the added volume of THF. In order to dissolve it, the monomer solution with the catalyst already added was warmed using a heat gun. Upon heating, the monomer was dissolved and the polymerization was activated and immediately produced a white colored polymer precipitate.

3.2.1.4.1 Poly(NbISB) 64.

Slightly greenish-thick globular films.

Yield (% w/w) = 94 % (250 mg).

^1H NMR and IR spectra are the same as those of polymer **58**.

GPC analysis results (in THF) : $M_n=52,273$, $M_w=199,002$, $M_z=799,378$, PDI =3.81, DP = 197 at M_n ; by direct comparison with PS standards.

GPC analysis results (in DMF): $M_n=134,128$, $M_w=612,666$, $M_z=2,050,000$, PDI = 4.57, DP = 504 at M_n ; with light scattering detector, M_w absolute.

3.2.1.4.2 Poly(AcNbISB) 65.

Grayish globular films.

Yield (% w/w) =100 % (244 mg).

^1H NMR (500 MHz, DMSO- d_6) δ 5.54 – 5.21 (m, 2H), 5.02 (m, 2H), 4.80 – 4.63 (m, 1H), 4.43 (m, 1H), 3.87 (m, 2H), 3.74 – 3.54 (m, 1H), 3.02 – 2.73 (m, 2H), 2.02 (s, 3H), 1.95 – 1.54 (m, 3H), 1.35 (m, 1H).

IR (neat, cm^{-1}): 2938, 2873, 1727, 1446, 1367, 1229, 1166, 1090, 1016, 980, 858, 752.

GPC (in THF): Not performed (Insoluble).

GPC analysis results (in DMF): $M_n=418,759$, $M_w=1,150,000$, $M_z=3,230,000$, PDI=2.57, DP = 1,574 at M_n ; with light scattering detector, M_w absolute.

3.2.1.4.3 Poly(NbIMPh) 66.

Colorless thick lumps.

Yield (% w/w) = 96 % (297 mg).

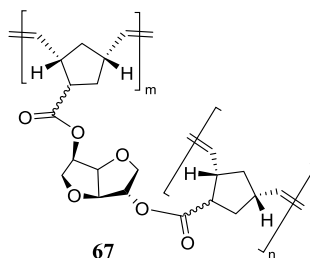
^1H NMR (500 MHz, $\text{DMSO-}d_6$) δ 7.40 (m, 6H), 6.16 – 5.93 (m, 1H), 5.77 (m, 1H), 5.18 – 5.01 (m, 1H), 4.72 – 4.54 (m, 1H), 3.64 – 3.47 (m, 2H).

IR (neat, cm^{-1}): 1779, 1704, 1596, 1495, 1373, 1174, 1058, 1013, 966, 908, 740.2, 690.

GPC analysis results (poorly soluble in THF): M_n = 48,093, M_w = 83,735, M_z = 123,376; PDI = 1.74 and DP = 1.74 at M_n ; by direct comparison with PS standards.

GPC analysis results (DMF at 50 $^{\circ}\text{C}$): M_n = 641,686, M_w = 1,080,000, M_z = 17,780,000, PDI = 1.68, DP = 2,412 at M_n ; with light scattering detector, M_w absolute.

3.2.1.5 Synthesis of polymer **67** (Homopolymerization of DiNBISB (**47**)).



DiNBISB **47** (0.4 g, 1.03 mmol) was dissolved in 1 mL DCM. Grubbs' I generation catalyst, bis(tricyclohexylphosphine)benzylidene ruthenium(IV) chloride (**26**) (9 mg, 0.01 mmol) was dissolved in 0.5 mL DCM and then added to the reaction solution. This was stirred magnetically under nitrogen. After 20 h, a jelly like maroon colored polymer was formed with the magnetic stirrer was trapped within one word the mass and stopped stirring. Ethyl vinyl ether (0.05 mL) was added to quench the reaction followed by the addition of DCM (4 mL) in order to dissolve the product. However, the polymer was not soluble. The generated polymer was dried at 40 $^{\circ}\text{C}$ under vacuum to constant weight to get highly brittle maroon colored crystals.

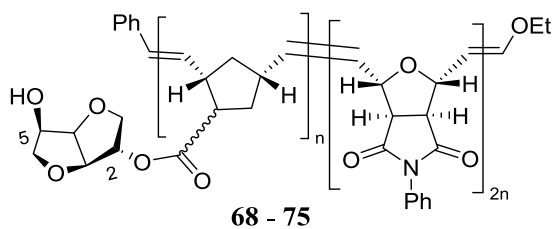
The isolated yield of the polymer was approximated as 100% (0.4 g) as there is no detected mass loss in the reaction. **67** is a highly cross-linked polymer, insoluble in organic solvents. Hence, NMR solution spectra or GPC determined molecular weights could not be generated. A solvent swelling absorption test was performed by soaking **67** in DCM for 1 day, followed by wiping DCM from the polymer surface using tissue paper. Then the final weight was measured.

Solvent absorption (g) = Final weight - Initial weight (g) = 0.4560 - .4037 = 0.053g (4.69%). This is a very small amount of imbibed solvent.

IR (neat, cm^{-1}): 2932, 3857, 1731, 1657, 1505, 1450, 1366, 1160, 1092, 968, 890, 835.7, 745, 713.

3.2.2 Random copolymerization.

3.2.2.1 NbISB (**46**) with NbIMPh (**51**).



3.2.2.1.1 Using Grubbs' I (**26**) generation catalyst.

Monomers NbISB (**46**) (500 g, 1.9 mmol) and NbIMPh (**51**) (0.151 g; 0.63mmol) (**47:51** = 3:1) were dissolved in 10 mL of dry THF. Grubbs' I generation catalyst, bis(tricyclohexylphosphine)benzylidene ruthenium(IV) chloride (**26**) (20.6 mg, 0.00251 mmol) dissolved in THF (1 mL) was added to the monomer mixture and allowed stir at room temperature. After 3.5 h, the resulting polymer was quenched with excess ethyl vinyl ether (0.5 mL) and precipitated from THF into methanol (50 mL) to generate a

white sticky precipitate. The precipitate was dissolved in DCM and re-precipitated in methanol (50 mL). The precipitated polymer was dried over-night at 40 °C under vacuum to generate a colorless solid lump of **68**.

3.2.2.1.1.1 Polymer **68**:

Colorless solid lump.

Yield (% w/w) = 45% (225 mg).

GPC analysis results (in THF): $M_n = 17,461$, $M_w = 26,685$, $M_z = 35,420$, PDI = 1.53, by direct comparison with PS standards.

^1H NMR analysis: Not performed.

IR (neat, cm^{-1}): 3422, 2941, 2867, 1713, 1496, 1456, 1373, 1169, 1075, 1045, 1009, 967, 869, 830, 744, 692.

3.2.2.1.1.2 In different mole ratios using Grubbs' I (**26**) generation catalyst.

Monomers **46** and **51** were weighed into five different round bottomed flasks at different mole ratios (see table **1**). In the first three flasks, a 0.294 M monomer solution was prepared by the addition of 2.6 mL of dry DCM. To the next two flasks, 3.6 mL of DCM was added to generate 0.23M solutions of the combined monomers.

A solution of Grubbs' first generation catalyst **26** was prepared (5 mL of 10 mg/mL). To all five of the monomer solutions, 0.8 mL of 10 mg/mL catalyst **26**, bis(tricyclohexylphosphine)benzylidineruthenium(IV)chloride (**26**) (8 mg, 0.01 mmol) was added. The solutions were stirred at room temperature for 3 days using a magnetic stirrer. The five resulting living polymerizations were quenched by the dropwise addition to each of excess ethyl vinyl ether (0.1 mL). The crude polymers were precipitated twice

from DCM into methanol (50 mL) and dried under vacuum over-night at 40 °C to generate five polymers **69** to **73**.

Table 3.1 Monomer ratios and the yields generated in the synthesis of polymers **69** to **73**

Polymers	Mole ratio	Weight ratio [47:51] (mg)	Molarity (47 + 51)	Yield (%w/w)
69	1:00	266:0	0.294	78
70	0.75:0.25	199:60	0.294	98
71	0.5:0.5	133:120	0.294	69
72	0.25:0.75	66:180	0.23	89
73	0:01	0:240	0.23	70

3.2.2.1.3 Poly(NbISB) **69**.

Grey thick translucent film.

Yield (% w/w) = 78% (207 mg).

¹H NMR (400 MHz, CDCl₃) δ 5.60 – 5.28 (m, 2H), 5.28 – 5.02 (m, 1H), 4.66 – 3.75 (m, 7H), 3.65 – 3.42 (m, 1H), 3.23 – 2.67 (m, 3H), 2.59 – 2.33 (m, 1H), 2.06 – 1.93 (m, 1H), 1.78 (m, 2H), 1.46 – 1.24 (m, 1H).

IR (neat, cm⁻¹): 3444, 2926, 2859, 1715, 1490, 1456, 1373, 1261, 1160, 1075, 1043, 1011, 967, 867, 801, 744.

GPC analysis results (in THF): M_n = 16,864, M_w = 26,758, M_z = 37,213, PDI = 1.59; by direct comparison with PS standards.

3.2.2.1.4 Poly[(NbISB)-*ran*-(NbIMPh)] **70**.

Grey thick translucent lumps.

Yield (% w/w) = 98% (254 mg).

^1H NMR (400 MHz, CDCl_3) δ 7.55 – 7.12 (m, 5H), 6.16 – 5.75 (m, 2H), 5.71 – 5.03 (m, 10H), 4.49 – 3.75 (m, 17H), 3.61 – 3.26 (m, 6H), 3.21 – 2.32 (m, 13H), 2.25 – 1.57 (m, 11H), 1.57 – 0.98 (m, 5H).

IR (neat, cm^{-1}): 3449, 2933, 2869, 1712, 1497, 1457, 1374, 1167, 1070, 1044, 1009, 966, 916, 868, 831, 742.

GPC analysis results (in THF): $M_n = 23,246$, $M_w = 33,854$, $M_z = 37,213$, PDI = 1.46; by direct comparison with PS standards.

3.2.2.1.5 Poly[(NbISB)-*ran*-(NbIMPh)] 71.

Colorless fine powder.

Yield (% w/w) = 69% (175 mg).

^1H NMR (400 MHz, CDCl_3) δ 7.55 – 7.10 (m, 5H), 6.20 – 4.79 (m, 6H), 4.58 (s, 2H), 4.50 – 3.70 (m, 6H), 3.59 – 2.30 (m, 8H), 2.20 – 1.16 (m, 6H).

IR (neat, cm^{-1}): 3428, 2945, 2873, 1780, 1713, 1497, 1457, 1374, 1174, 1077, 1047, 1010, 967, 913, 870, 832, 742.

GPC analysis results (in THF): $M_n = 14,089$, $M_w = 21,583$, $M_z = 29,275$, PDI = 1.53; by direct comparison with PS standards.

3.2.2.1.6 Poly[(NbISB)-*ran*-(NbIMPh)] 72.

Colorless fine powder.

Yield (% w/w) = 89% (219 mg).

^1H NMR (400 MHz, CDCl_3) δ 7.55 – 7.10 (m, 5H), 6.21 – 4.79 (m, 4H), 4.62 (m, 1H), 4.12 (m, 3H), 3.68 – 2.39 (m, 4H), 1.74 (m, 4H).

IR (neat, cm^{-1}): 3452, 2946, 2870, 1780, 1711, 1497, 1457, 1375, 1176, 1047, 1011, 967, 910, 742.

GPC analysis results (in THF): $M_n = 24,726$, $M_w = 39,620$, $M_z = 55,129$, PDI = 1.60; by direct comparison with PS standards.

3.2.2.1.7 Poly(NbIMPh) **73**.

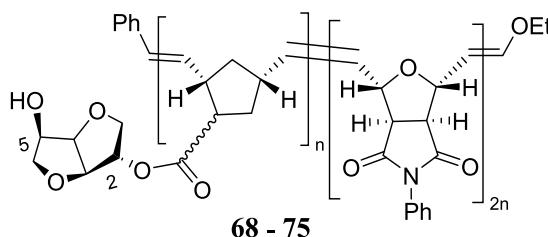
Grey fine powder.

Yield (% w/w) = 70 % (168 mg).

GPC analysis results (in THF) : $M_n = 32,442$, $M_w = 57,260$, $M_z = 89,656$, PDI = 1.77; by direct comparison with PS standards.

^1H NMR and IR spectra were the same as **66**.

3.2.2.2 Copolymerization of NbISB (**46**) and NbIMPh (**51**) in different mole ratios using Grubbs' II generation catalyst (**27**).



NbISB **46** (266 mg, 1mmol) and NbIMPh **51** (80 mg, 0.3mmol) [Mixture I] , and **46** (88 mg, 0.3mmol) and **51** (241 mg, 1mmol) [Mixture II] were placed in two separate round-bottomed flasks and then each was dissolved into a solution of dry, degassed THF (4 mL) and dry, degassed DCM (5 mL). Grubbs' second generation catalyst, (1,3-bis(2,4,6-trimethylphenyl)-2-imidazolidinylidene)dichloro(phenylmethylene)-(tricyclohexylphosphine)ruthenium (**27**) (11 mg, 0.013mmol) dissolved in 1 mL dry, degassed THF was added dropwise to both the flasks. These two solutions were stirred at

room temperature for 10 h under argon. Then the reactions were quenched with excess ethyl vinyl ether (0.1 mL) and concentrated by rotary evaporation. The crude products were precipitated into methanol (75 mL). The precipitated polymers **74** and **75** were filtered and dried under vacuum at 40 °C for 12 h.

3.2.2.2.1 Poly[(NbISB)-*ran*-(NbIMPh)] 74.

Yield (% w/w) = 100% (351 mg).

¹H NMR (500 MHz, DMSO-*d*₆) δ 7.60 – 7.23 (m, 5H), 6.02 (s, 1H), 5.80 (s, 1H), 5.54 (m, 9H), 5.21 (m, 3H), 5.07 – 4.73 (m, 7H), 4.51 – 3.63 (m, 24H), 3.30 – 2.57 (m, 8H), 2.13 – 1.38 (m, 11H), 1.24 (s, 5H), 1.11 (s, 1H).

IR (neat, cm⁻¹): 3436, 2941, 2870, 1713, 1496, 1456, 1371, 1168, 1073, 1045, 1009, 967, 869, 830, 743, 692.

GPC analysis results: M_n = 66,879, M_w = 186,940, M_z = 594,524 and PDI = 2.80; by direct comparison with PS standards.

3.2.2.2.2 Poly[(NbISB)-*ran*-(NbIMPh)] 75

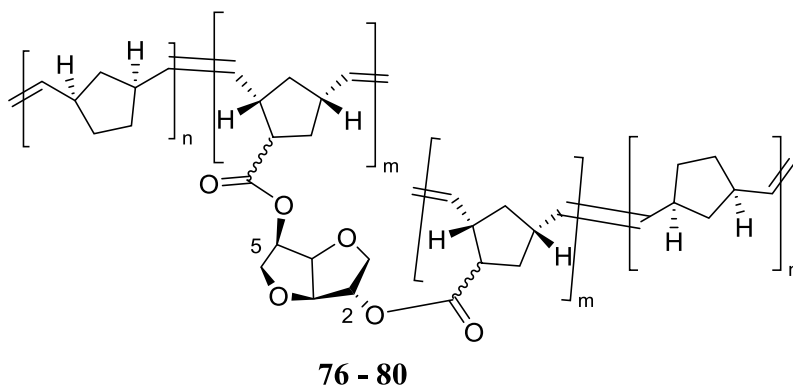
Yield (% w/w) = 96% (317 mg)

¹H NMR (500 MHz, DMSO-*d*₆) δ 7.66 – 7.19 (m, 35H), 6.17 – 5.97 (m, 5H), 5.81 (m, 6H), 5.66 – 5.39 (m, 6H), 5.10 (m, 5H), 4.63 (s, 7H), 4.40 (s, 6H), 3.54 (s, 8H), 1.98 (s, 1H), 1.79 – 1.08 (m, 3H).

IR (neat, cm⁻¹): same as **74**.

GPC analysis was not performed (Insoluble in THF).

3.2.2.3 Random copolymerization of DiNbISB **47** with norbornene **31**.



3.2.2.3.1 Using Grubbs' I catalyst (**26**).

Norbornene (**31**) (250 mg, 2.6 mmol) and bi-functional monomer DiNbISB (**47**) (100 mg, 0.25 mmol) were dissolved in 1.6 mL dry DCM under nitrogen. Grubbs' first generation catalyst, bis(tricyclohexylphosphine)benzylideneruthenium(IV) chloride (**26**) (2.411 mg, 0.0029 mmol), dissolved in 1 mL dry DCM, was added and the resulting solution was stirred at room temperature. After 1 h, a solid gel was present and the magnetic stirrer stopped. Ethyl vinyl ether (0.05 mL) was added to quench the reaction, DCM (4 mL) was added to try dissolve the gel. However, this cross-linked polymer was not soluble. It was dried at 40 °C under vacuum to constant weight to give a hard maroon-colored solid material **76**.

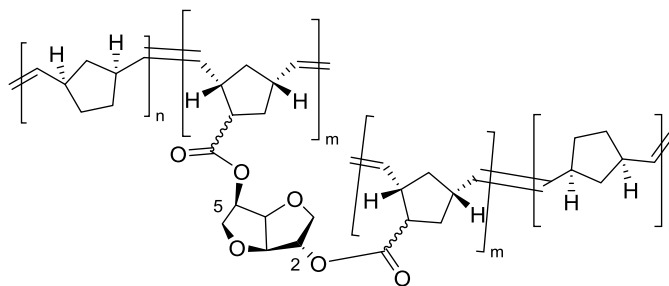
The isolated polymer **76** was approximated as 100% (0.4 g). Polymer **67** is a highly cross-linked polymer, insoluble in organic solvents. Hence, solution NMR analysis or GPC molecular weight determinations could not be performed.

Polymer **76**.

Maroon colored hard solid.

IR (neat, cm^{-1}): 2931, 2856, 1733, 1701, 1657, 1507, 1448, 1366, 1211, 1159, 1093, 966, 890, 733.

3.2.2.4 Random copolymerizations at different **47/31** mole ratios using Grubbs' II catalyst (**27**).



Monomers DiNbISB **47** and norbornene **31** were weighed in four different mole ratios (total of 2.0 mmol of combined monomers) and dissolved in 3 mL DCM to generate solution I [**47** (722 mg, 2 mmol)], solution II [**47** (718 mg, 1.86 mmol), **31** (13 mg, 0.14mmol)], solution III [**47** (509.74 mg, 1.31 mmol), **31** (13 mg, 0.68 mmol)], solution IV [**47** (254 mg, 0.65 mmol), **31** (126 mg, 1.34 mmol)]. Grubbs' second generation catalyst, (1,3-bis(2,4,6-trimethylphenyl)-2-imidazolidinylidene)dichloro (phenylmethylene)(tricyclohexylphosphine) ruthenium (**27**) (8.5 mg, 0.01 mmol) dissolved in DCM (1 mL) was added to each of these monomer solutions. Then they were stirred at room temperature.

Each polymer solution (I to IV) produced a gel at different times. Solution IV produced a gel within one minute, solution III in 3-4 minute, solution II in 10 - 15 min and solution I in 20 minutes. Dry degassed DCM (2 mL) was added to each solution and they were allowed to stir for 6 h at room temperature. The reactions were quenched with

ethyl vinyl ether (0.1 mL). Then the polymers washed with methanol (10 mL) and dried at 40 °C under vacuum for 12 h to get polymers **77** to **80**.

Polymer **77**.

Hard black solid.

Yield (% w/w) = 99.7 % (770 mg).

IR (neat, cm^{-1}): 2930, 2855, 1731, 1670, 1658, 1500, 1451, 1368, 1213, 1161, 1092, 1052, 968, 891, 736.

Polymer **78**.

Yield (% w/w) = 100 % (733 mg).

IR (neat, cm^{-1}): 2930, 2855, 1730, 1698, 1656, 1499, 1499, 1367, 1211, 1212, 1091, 967, 890, 734.

Polymer **79**.

Glassy-hard transparent polymer.

Yield (% w/w) = 100% (576 mg).

IR (neat, cm^{-1}): 2931, 2858, 1732, 1700, 1657, 1504, 1500, 1367, 1211, 1160, 1092, 967, 891, 733.

Polymer **80**.

Glassy transparent polymer.

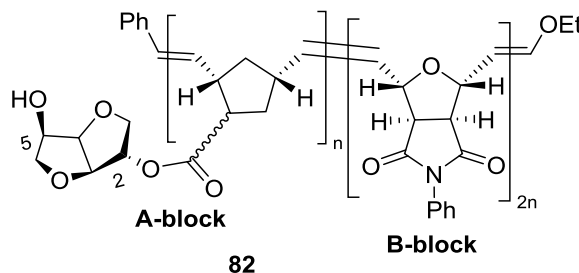
Yield (% w/w) = 100 % (379 mg).

IR (neat, cm^{-1}): 2931, 2856, 1733, 1701, 1657, 1507, 1448, 1366, 1211, 1159, 1093, 966, 890, 733.

3.2.3 Block polymerizations.

3.2.3.1 Diblock polymerizations.

3.2.3.1.1 AB-type block copolymer **82** of **46** and **51**.



Monomer NbISB **46** (377 mg, 1.42mmol) was dissolved in dry, degassed THF (5 mL). Grubbs' second generation catalyst, (1,3-bis(2,4,6-trimethyl phenyl)-2-imidazolidinylidene)dichloro(phenylmethylene)(tricyclohexylphosphine) ruthenium (**27**) (24.11 mg, 0.0284 mmol) dissolved in THF (2 mL) was added dropwise. This solution was added to the solution of **46** and stirred at room temperature for 1h under argon to form a living polymer of **46**. Monomer **51** (683 mg, 2.83 mmol) dissolved in dry, degassed DCM (11 mL) was then added dropwise to the living polymer solution, generating a cloudy white solution. This was stirred at room temperature for 8h. Then this reaction was quenched by dropwise addition of excess ethyl vinyl ether (0.5 mL), concentrated by rotary evaporation and precipitated into methanol (150 mL) to generate diblock polymer **82**. A small aliquot (about 0.5 mL) of the living polymer **46** solution was taken out once before the addition of monomer **51**. This was also quenched in excess ethyl vinyl ether (0.1 mL) and washed in methanol (10 mL) to generate polymer **81**. This polymer is the starting A block of AB-diblock copolymer **82**. Both the polymers were filtered using a Buchner funnel and dried over-night under vacuum at 40 °C to provide A-block polymer **81** and AB-block polymer **82**.

3.2.3.1.1.1 Polymer poly(NbISB) **81**.

Translucent grey solid.

Yield (% w/w) = 47 mg.

GPC analysis results (in THF): $M_n = 35,840$, $M_w = 78,853$, $M_z = 174,018$, PDI =

2.2 and DP = 135 at M_n ; by direct comparison with PS standards.

Estimated absolute $M_w = 236,559$ using (Q-factor = ~ 3.0 ; calculated using **64**).

GPC analysis could not be performed in DMF due to the lack of sufficient sample for GPC analysis.

^1H NMR and IR spectra: These were the same as those of polymer **58**.

3.2.3.1.1.2 AB-type block polymer **82** of **46** and **51**.

Colorless-fluffy powdered granules.

Yield (% w/w) = 92% (0.925 g).

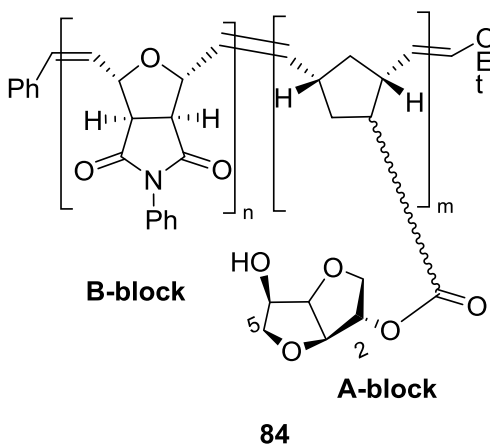
GPC analysis results (very poorly soluble in THF): $M_n = 43,373$, $M_w = 98,688$, $M_z = 292,879$, PDI = 2.01 and DP = 54 at M_n ; by direct comparison with PS standards.

GPC analysis results (in DMF): $M_n = 597,254$, $M_w = 1,139,000$, $M_z = 1,731,000$, PDI = 1.9, and DP = 742 at M_n ; with light scattering detector, M_w absolute.

^1H NMR (500 MHz, DMSO- d_6) δ 7.38 (m, 13H), 6.13 – 5.71 (m, 5H), 5.39 – 4.93 (m, 5H), 4.64 (m, 3H), 4.48 – 3.69 (m, 6H), 3.67 – 3.47 (m, 6H), 3.40 (m, 1H), 2.93 (s, 1H), 2.15 – 1.04 (m, 5H).

IR (neat, cm^{-1}): 3424, 2941, 2868, 1780, 1709, 1496, 1456, 1372, 1171, 1046, 1009, 967, 908, 833, 740, 690.

3.2.3.2 BA-type block polymer **84** of **46** and **51**.



Monomer **51** (400 mg, 1.65 mmol) was dissolved in dry, degassed DCM (7 mL). To this solution, Grubbs' second generation catalyst, (1,3-bis(2,4,6-trimethylphenyl)-2-imidazolidinylidene)dichloro(phenylmethylene)(tricyclohexylphosphine)ruthenium (**27**) (28 mg, 0.033 mmol) dissolved in DCM (1 mL) was added dropwise. This solution was stirred at room temperature for 1h under argon. To this living homopolymer of **51** solution, the second monomer NbISB **46** (463 mg, 1.74mmol) dissolved in DCM (10 mL) was added dropwise. The solution was then stirred at room temperature for 8 h. The reaction mixture was then quenched by the dropwise addition of excess ethyl vinyl ether (0.5 mL), concentrated by rotary evaporation and precipitated into methanol (150 mL) to generate a white fluffy BA-type diblock copolymer **84**. A small aliquot (0.5 mL) of the living polymer **51** was taken out once before the addition of monomer **46**. This was also quenched in excess ethyl vinyl ether (0.1 mL), and washed in methanol (10 mL) to generate a colorless globular polymer **83**. This polymer is the starting B block of BA-diblock copolymer **84**. Both polymers were filtered in a Buchner funnel and dried overnight under vacuum at 40 °C to generate a white fluffy polymers **83** and **84**.

3.2.3.2.1 Polymer 83.

Colorless fluffy polymer.

Yield = 15 mg.

GPC (in THF): Not performed (insoluble in THF).

GPC (in DMF): Not performed due to the lack of sufficient sample for GPC analysis.

^1H NMR and IR spectra: These were the same as those of polymer 66.

3.2.3.2.2 BA-type block polymer 84 of 46 and 51.

Slight grayish-powder with lumps.

Yield (% w/w) = 99% (840 mg).

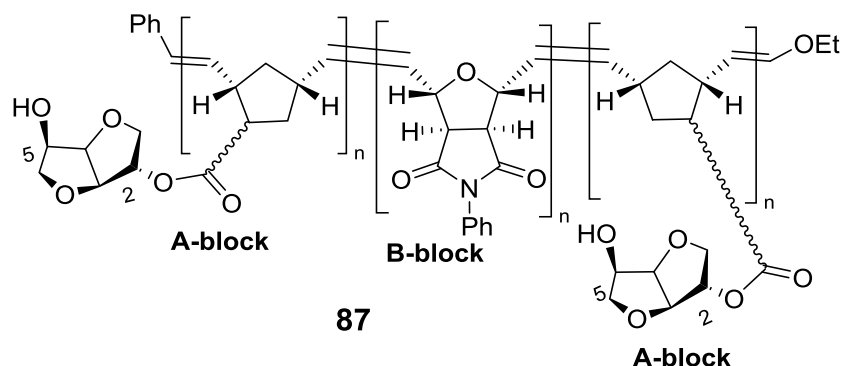
^1H NMR (500 MHz, $\text{DMSO}-d_6$) δ 7.37 (m, 4H), 6.12 – 5.71 (m, 2H), 5.57 – 4.86 (m, 3H), 4.64 (d, J = 13.2 Hz, 1H), 4.49 – 3.68 (m, 6H), 3.66 – 3.34 (m, 6H), 2.88 (m, 1H), 2.17 – 1.03 (m, 5H).

IR (neat, cm^{-1}): 3448, 2944, 2874, 1778, 1710, 1496, 1377, 1172, 1073, 1045, 1010, 969, 912, 871, 832, 742, 691.

GPC analysis results (in DMF): M_n = 539,535, M_w = 903,903, M_z = 1,379,000, PDI = 1.65, DP = 135 at M_n ; with light scattering detector, M_w absolute.

3.2.3.3 Triblock polymerization.

3.2.3.3.1 ABA-type block polymer **87**.



Monomer **46** (400 mg, 1.50 mmol) was dissolved in DCM (5 mL). To this solution, Grubbs' second generation catalyst, (1,3-bis(2,4,6-trimethylphenyl)-2-imidazolidinylidene)dichloro(phenylmethylene)(tricyclohexylphosphine)ruthenium (**27**) (26 mg, 0.03 mmol) dissolved in DCM (1 mL) was added dropwise. This solution was stirred at room temperature for 1 h under argon. To this living homopolymer, monomer **51** (362 mg, 1.50 mmol) dissolved in DCM (5 mL) was added dropwise to get a cloudy, white solution and stirred at room temperature for 1 h to generate the diblock living polymer. To this living diblock copolymer, monomer **46** (400 mg, 1.50 mmol) dissolved in DCM (6 mL) was added dropwise and stirred at room temperature for 16 h. The reaction mixture was then quenched by the dropwise addition of excess ethyl vinyl ether (1 mL), concentrated by rotary evaporation, and precipitated into methanol (150 mL) to generate a white fluffy ABA-triblock polymer **87**. Small aliquots (approx. 0.5 mL) of the living polymer solutions were sampled before the addition of the second (**46**) and third (**51**) monomers and quenched with the addition of ethyl vinyl ether (0.1 mL) and washed in methanol (10 mL) to generate polymers to get A-block and AB-block polymers, **85**,

and **86**, respectively. All the polymers were filtered in a Buchner funnel and dried overnight under vacuum at 40 °C to get white colored polymers **85**, **86** and **87**.

3.2.3.3.1.1 Polymer **85**.

Grey translucent solid.

Yield = 13 mg.;

GPC analysis results (in THF): $M_n = 85,059$, $M_w = 297,735$, $M_z = 1,570,854$ PDI = 3.5 and DP = 320 at M_n ; by direct comparison with PS standards.

Estimated absolute $M_w = 893,206$ using Q-factor (~ 3.0 ; calculated using **64**).

GPC (in DMF): Not performed due to the lack of adequate amount of sample.

^1H NMR and IR spectra: These were the same as those of polymer **58**.

3.2.3.3.1.2 Polymer **86**.

Colorless fluffy powder.

Yield = 47 mg.

GPC analysis: Not performed (insoluble in THF).

GPC (in DMF): Not performed due to the lack of adequate amount of sample.

3.2.3.3.1.3 ABA-block polymer **87** of **46** and **51**.

Colorless fine powder.

Yield (% w/w) = 54 % (616 mg).

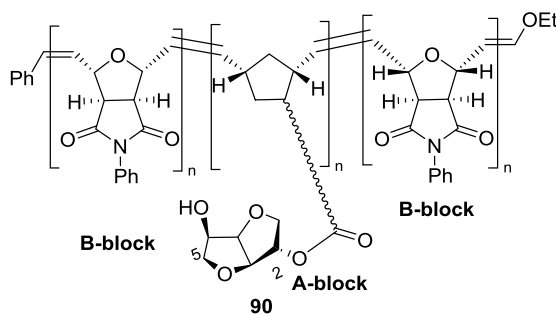
^1H NMR (500 MHz, DMSO- d_6) δ 7.39 (m, 3H), 5.92 (m, 1H), 5.70 – 4.82 (m, 4H), 4.57 (s, 1H), 4.49 – 3.65 (m, 6H), 3.64 – 3.29 (m, 1H), 2.93 (s, 1H), 2.21 – 1.13 (m, 2H).

IR (neat, cm^{-1}): 3475, 2843, 2871, 1780. 1710., 1497, 1456., 1374, 1172, 1046, 1009, 968, 911, 832, 741., 691..

GPC analysis results (very poorly soluble in THF): $M_n = 36,722$, $M_w = 73,882$, $M_z = 197,773$, PDI = 2.01 and DP = 48 at M_n ; by direct comparison with PS standards.

GPC analysis results (in DMF): $M_n = 106,093$, $M_w = 399,107$, $M_z = 1,180,000$, PDI = 4.0 and DP = 140 at M_n ; with light scattering detector, M_w absolute.

3.2.3.3.2 BAB-type block polymer **90** of **46** and **51**.



NbIMPh (**51**) (400 mg, 1.65 mmol) was dissolved in DCM (5 mL). To this solution, Grubbs' second generation catalyst, (1,3-bis(2,4,6-trimethylphenyl)-2-imidazolidinylidene)dichloro(phenylmethylene)(tricyclohexylphosphine) ruthenium (**27**) (26 mg, 0.03 mmol) dissolved in DCM (1 mL) was added dropwise. This solution was stirred at room temperature for 1 h under argon to generate polymer **88**. To this living polymer of **51**, the second monomer NbISB (**46**) (438 mg, 1.65 mmol) dissolved in DCM (5 mL) was added dropwise. The solution became cloudy white. This solution was then stirred for one more hour at room temperature to generate BA-type living polymer. To this living BA-diblock copolymer, monomer **51** (438 mg, 1.65 mmol) dissolved DCM (5 mL) was added dropwise and stirred at room temperature for 16 h. Then, the solution was quenched by the dropwise addition of excess ethyl vinyl ether (1 mL), concentrated by rotary evaporation and precipitated into methanol (150 mL) to generate white, fluffy BAB-triblock copolymer **90**.

Small aliquots (approx. 0.5 mL) of the polymer solution were taken out before the addition of the second **46** and third **51** monomers. Each of these polymers were quenched with the addition of ethyl vinyl ether (0.1 mL) and washed in methanol (10 mL) to generate polymers B-block **88** and BA-block **89**. All the polymers were filtered in a Buchner funnel and dried over-night under vacuum at 40 °C to generate white polymers **88** to **90**.

3.2.3.3.2.1 B-block polymer **88**.

Colorless transparent powder.

Yield (% w/w) = 11 mg.

GPC analysis: Not performed (insoluble in THF).

GPC (in DMF): Not performed due to the lack of adequate amount of sample.

¹H NMR and IR spectra were the same as **66**.

IR (neat, cm⁻¹): 1780.4, 1707.8, 1569.9, 1495.7, 1371.8, 1174.5, 1058.5, 1007.2, 966.5, 906.4, 739.8, 689.3.

3.2.3.3.2.2 BA-block polymer **89**.

Colorless granules.

Yield (% w/w) = 11 mg.

GPC analysis: Not performed (insoluble in THF).

GPC (in DMF): Not performed due to the lack of adequate amount of sample.

IR (neat, cm⁻¹): 3473, 2861, 1781, 1709, 1597, 1496, 1373, 1176, 1059, 1010, 967, 907.5, 740, 690.

3.2.3.3.2.3 BAB-type triblock polymer **90**.

Colorless thick lumps.

Yield (% w/w) = 1.10 g.

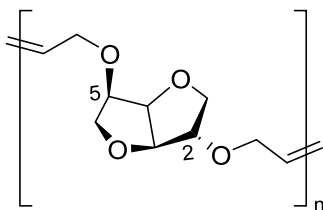
^1H NMR (500 MHz, $\text{DMSO-}d_6$) δ 7.58 – 7.18 (m, 11H), 6.14 – 5.71 (m, 4H), 5.55 – 4.87 (m, 5H), 4.78 – 4.53 (m, 3H), 4.50 – 3.69 (m, 6H), 3.47 (m, 5H), 2.89 (m, 1H), 2.14 – 1.15 (m, 5H).

IR (neat, cm^{-1}): 3424, 2942, 2865, 1781, 1711, 1496, 1374, 1174, 1047, 1009, 968, 908, 833, 741, 690.

GPC analysis results (very poorly soluble in THF): $M_n = 47,892$, $M_w = 90,924$, $M_z = 174,252$, PDI = 1.9 and DP = 68 at M_n ; by direct comparison with PS standards.

GPC analysis results (in DMF): $M_n = 568,258$, $M_w = 944,267$, $M_z = 1,391,000$, PDI = 2.0 and DP = 806 at M_n ; with light scattering detector, M_w absolute.

3.3 ADMET polymerization of diallyl-D-isosorbide (**52**).



90

Diallyl-D-isosorbide (**52**) (0.26 g, 1.165 mmol) was weighed in a Schlenk tube and was subjected to three cycles of freeze-thaw cycles over 1.5 h. To this bulk monomer **52**, Grubbs' II catalyst (**27**) (1mg, 1.17×10^{-3} mmol, $[M]/[C] = 1000:1$) was added and attached to the Schlenk line. The solution was then stirred under N_2 at 40 °C for 1 h. Gas bubbles were observed in the gas bubble tube. After 1 h, vacuum (3 – 4 mm Hg) was applied and the reaction mixture was allowed to stir for 7 h (to remove the released

ethylene) at 40 °C. Then the temperature was increased to 80 °C and the solution was stirred further for 13 h under vacuum (3-4 mm Hg). Then, the temperature was raised to 100 °C and the reaction was stirred under high vacuum for 88 h. The reaction was monitored using proton NMR. After a total of 122 h, the reaction was quenched using ethyl vinyl ether (100 μ L). The polymer was dissolved in 1 mL DCM and precipitated thrice in excess cold pentane (10 mL). A honey colored viscous liquid precipitate and dried under vacuum (3-4 mm Hg) to provide polymer **90** at about 40 % (yield w/w).

Polymer 91.

Honey colored viscous precipitate.

Yield (% w/w) = 40 % (90 mg).

^1H NMR (300 MHz, CDCl_3) δ 6.31 – 5.90 (m, 2H), 5.02 – 4.81 (m, 1H), 4.80 – 4.63 (m, 1H), 4.63 – 4.39 (m, 3H), 4.39 – 4.18 (m, 2H), 4.16 – 3.35 (m, 7H).

GPC analysis (in THF): M_n = 1194, M_w = 2899, M_z = 6442, PDI = 2.4 and = 5.4 at M_n ; relative to polystyrene standards. Three peaks were observed by GPC, but only one peak was observed within the calibration range of the column. The remaining two low molecular weight peaks could be oligomers or the starting material.

REFERENCES

1. Werpy, T.; Petersen, G.; Aden, A.; Bozell, J.; Holladay, J.; Manheim, A.; Eliot, D.; Lasure, L.; Jones, S., Top value added chemicals from biomass. *U.S. Department of Energy: Oak Ridge, TN*, **2004**, 1.
2. Zhang, J., Advances in the catalytic production and utilization of sorbitol. *Industrial & Engineering Chemistry Research* **2013**, 52 (34), 11799-11815.
3. Ramírez-López, C. A.; Ochoa-Gómez, J. R.; Gil-Río, S.; Gómez-Jiménez-Aberasturi, O.; Torrecilla-Soria, J., Chemicals from biomass: synthesis of lactic acid by alkaline hydrothermal conversion of sorbitol. *Journal of Chemical Technology & Biotechnology* **2011**, 86 (6), 867-874.
4. (a) Siqueira, J. L. P.; Carlos, I. A., Effect of adding sorbitol to the electroplating solution on the process of depositing lead on copper and the morphology of the film produced. *J. Power Sources* **2007**, 166 (2), 519-525; (b) Liu, H.; Chaudhary, D.; Yusa, S.-i.; Tade, M. O., Preparation and characterization of sorbitol modified nanoclay with high amylose bionanocomposites. *Carbohydr. Polym.* **2011**, 85 (1), 97-104; (c) Hong, J.; Marceau, E.; Khodakov, A. Y.; Griboval-Constant, A.; La Fontaine, C.; Villain, F.; Briois, V.; Chernavskii, P. A., Impact of sorbitol addition on the structure and performance of silica-supported cobalt catalysts for Fischer-Tropsch synthesis. *Catal. Today* **2011**, 175 (1), 528-533; (d) Jean-Marie, A.; Griboval-Constant, A.; Khodakov, A. Y.; Diehl, F., Influence of sub-stoichiometric sorbitol addition modes on the structure and catalytic performance of alumina-supported cobalt Fischer Tropsch catalysts. *Catal. Today* **2011**, 171 (1), 180-185.
5. Kricheldorf, H. R., Sugar diols as building blocks of polycondensates. *Journal of Macromolecular Science, Part C* **1997**, 37 (4), 599-631.
6. (a) Gohil, R. M., Properties and strain hardening character of polyethylene terephthalate containing Isosorbide. *Polymer Engineering & Science* **2009**, 49 (3), 544-553; (b) Zhu, Y.; Durand, M.; Molinier, V.; Aubry, J.-M., Isosorbide as a novel polar head derived from renewable resources. Application to the design of short-chain amphiphiles with hydrotropic properties. *Green Chemistry* **2008**, 10 (5), 532-540.
7. Stoss, P.; Hemmer, R.; Derek, H., 1,4:3,6-Dianhydrohexitols. In *Adv. Carbohydr. Chem. Biochem.*, Academic Press: 1991; Vol. Volume 49, pp 93-173.

8. Lemieux, R. U.; McInnes, A. G., The Preferential Tosylation of the endo-5-Hydroxyl Group of 1,4:3,6-Dianhydro-D-Glucitol. *Can. J. Chem.* **1960**, *38* (1), 136-140.
9. Claffey, D. J.; Casey, M. F.; Finan, P. A., Glycosylation of 1,4:3,6-dianhydro-d-glucitol (isosorbide). *Carbohydr. Res.* **2004**, *339* (14), 2433-2440.
10. Cekovic, Z., Selective esterification of 1,4:3,6-dianhydro-D-glucitol. *Synthesis (Stuttgart)* **1989**, (8), 610.
11. Fleche, G.; Huchette, M., Isosorbide. Preparation, properties and chemistry. *Starch-Stärke* **1986**, *38* (1), 26-30.
12. Fleche, G., Isosorbide. Preparation, properties and chemistry. *Starch-Stärke* **1986**, *38* (1), 26-30.
13. Defaye, J.; Gabelle, A.; Pedersen, C., Acyloxonium ions in the high-yielding synthesis of oxolanes from alditols, hexoses, and hexonolactones catalysed by carylic acids in anhydrous hydrogen fluoride. *Carbohydr. Res.* **1990**, *205* (0), 191-202.
14. Gu, M.; Yu, D.; Zhang, H.; Sun, P.; Huang, H., Metal (IV) phosphates as solid catalysts for selective dehydration of sorbitol to Isosorbide. *Catal. Lett.* **2009**, *133* (1-2), 214-220.
15. Rose, M., Isosorbide as a renewable platform chemical for versatile applications-quo vadis? *ChemSusChem* **2012**, *5* (1), 167-176.
16. Obach, R. S., Trend Analysis of a Database of Intravenous Pharmacokinetic Parameters in Humans for 670 Drug Compounds. *Drug Metabolism and Disposition* **2008**, *36* (7), 1385-1405.
17. Dederen, Dimethyl isosorbide, a novel pharmaceutical solvent. *Expo. - Congr. Int. Technol. Pharm., 3rd* **1983**, *5*, 335.
18. Enholm, E. J.; Cottone, J. S., Highly diastereoselective radical cyclizations on soluble ring opening metathesis supports. *Org. Lett.* **2001**, *3* (24), 3959-3962.
19. Loupy, A.; Monteux, D., Isomannide and isosorbide as new chiral auxiliaries for the stereoselective synthesis of tertiary α -hydroxy acids. *Tetrahedron* **2002**, *58* (8), 1541-1549.
20. Chatti, S., Cyclic and noncyclic polycarbonates of isosorbide (1, 4: 3, 6-dianhydro-d-glucitol). *Macromolecules* **2006**, *39* (26), 9064.

21. (a) Fenouillot, F.; Rousseau, A.; Colomines, G.; Saint-Loup, R.; Pascault, J. P., Polymers from renewable 1,4:3,6-dianhydrohexitols (isosorbide, isomannide and isoidide): A review. *Prog. Polym. Sci.* **2010**, *35* (5), 578-622; (b) Ben Abderrazak, H.; Fildier, A.; Marque, S.; Prim, D.; Ben Romdhane, H.; Kricheldorf, H. R.; Chatti, S., Cyclic and non cyclic aliphatic-aromatic polyesters derived from biomass: Study of structures by MALDI-ToF and NMR. *Eur. Polym. J.* **2012**, *47* (11), 2097-2110; (c) Bersot, J. C.; Jacquel, N.; Saint-Loup, R.; Fuertes, P.; Rousseau, A.; Pascault, J. P.; Spitz, R.; Fenouillot, F.; Monteil, V., Efficiency increase of poly(ethylene terephthalate-co-isosorbide terephthalate) Synthesis using bimetallic catalytic systems. *Macromol. Chem. Phys.* **2011**, *212* (19), 2114-2120; (d) He, X. Z.; Xiao, L. J.; Zhang, B. Y.; Xiao, W. Q., Synthesis and characterization of side chain liquid crystalline elastomers containing cholesterol. *J. Appl. Polym. Sci.* **2005**, *98* (1), 383-390; (e) Kricheldorf, H. R.; Sun, S. J.; Chen, C. P.; Chang, T. C., Polymers of carbonic acid. XXIV. Photoreactive, nematic or cholesteric polycarbonates derived from hydroquinone-4-hydroxybenzoate 4,4'-dihydroxychalcone and isosorbide. *J. Polym. Sci., Part A: Polym. Chem.* **1997**, *35* (9), 1611-1619.
22. Nelson, A. M. M., A perspective on emerging polymer technologies for bisphenol-A replacement. *Polym. Int.* **2012**, *61* (10), 1485-1491.
23. (a) Okada, M.; Aoi, K., Biodegradable polymers from 1,4:3,6-dianhydro-D-glucitol (Isosorbide) and its related compounds. *Current Trends in Polymer Science* **2002**, *7*, 57-70; (b) Yokoe, M.; Aoi, K.; Okada, M., Biodegradable polymers based on renewable resources VIII. Environmental and enzymatic degradability of copolycarbonates containing 1, 4: 3, 6-dianhydrohexitols. *J. Appl. Polym. Sci.* **2005**, *98* (4), 1679-1687.
24. Chatti, S.; Bortolussi, M.; Bogdal, D.; Blais, J. C.; Loupy, A., Synthesis and properties of new poly(ether-ester)s containing aliphatic diol based on isosorbide. Effects of the microwave-assisted polycondensation. *Eur. Polym. J.* **2006**, *42* (2), 410-424.
25. Caouthar, A., Synthesis and characterization of new polyamides derived from di (4-cyanophenyl) isosorbide. *Eur. Polym. J.* **2007**, *43* (1), 220.
26. Bachmann, F.; Reimer, J.; Ruppenstein, M.; Thiem, J., Synthesis of a novel starch derived AB-type polyurethane. *Macromol. Rapid Commun.* **1998**, *19* (1), 21-26.
27. Beghdadi, S.; Abdelhedi Miladi, I.; Ben Romdhane, H.; Bernard, J.; Drockenmuller, E., RAFT Polymerization of Bio-Based 1-Vinyl-4-dianhydrohexitol-1, 2, 3-triazole Stereoisomers Obtained via Click Chemistry. *Biomacromolecules* **2012**, *13* (12), 4138-4145.

28. (a) Schuster, M.; Blechert, S., Olefin metathesis in organic chemistry. *Angewandte Chemie International Edition in English* **1997**, *36* (19), 2036-2056; (b) Grubbs, R. H., Olefin-metathesis catalysts for the preparation of molecules and materials (Nobel lecture). *Angew. Chem. Int. Ed.* **2006**, *45* (23), 3760-3765.
29. Trnka, T. M.; Grubbs, R. H., The development of L₂X₂RuCHR olefin metathesis catalysts: An organometallic success story. *Acc. Chem. Res.* **2001**, *34* (1), 18-29.
30. Darling, T. R.; Davis, T. P.; Fryd, M.; Gridnev, A. A.; Haddleton, D. M.; Ittel, S. D.; Matheson, R. R.; Moad, G.; Rizzardo, E., Living polymerization: Rationale for uniform terminology. *J. Polym. Sci., Part A: Polym. Chem.* **2000**, *38* (10), 1706-1708.
31. Bielawski, C. W.; Grubbs, R. H., Living ring-opening metathesis polymerization. *Prog. Polym. Sci.* **2007**, *32* (1), 1-29.
32. Leitgeb, A.; Wappel, J.; Slugovc, C., The ROMP toolbox upgraded. *Polymer* **2010**, *51* (14), 2927-2946.
33. Fuchter, M. J.; Vesper, B. J.; Murphy, K. A.; Collins, H. A.; Phillips, D.; Barrett, A. G. M.; Hoffman, B. M., ROM polymerization-capture-release strategy for the chromatography-free synthesis of novel unsymmetrical porphyrazines. *The Journal of organic chemistry* **2005**, *70* (7), 2793-2802.
34. Vargas, J.; Colin, E. S.; Tlenkopatchev, M. A., Ring-opening metathesis polymerization (ROMP) of *N*-cycloalkyl-7-oxanorbornene dicarboximides by well-defined ruthenium initiators. *Eur. Polym. J.* **2004**, *40* (7), 1325-1335.
35. (a) Sutthasupa, S.; Sanda, F.; Masuda, T., Copolymerization of amino acid functionalized norbornene monomers. Synthesis of amphiphilic block copolymers forming reverse micelles. *Macromolecules* **2008**, *41* (2), 305-311; (b) Runge, M. B.; Lipscomb, C. E.; Ditzler, L. R.; Mahanthappa, M. K.; Tivanski, A. V.; Bowden, N. B., Investigation of the assembly of comb block copolymers in the solid state. *Macromolecules* **2008**, *41* (20), 7687-7694.
36. Hilf, S.; Kilbinger, A. F. M., An all-ROMP route to graft copolymers. *Macromol. Rapid Commun.* **2007**, *28* (11), 1225-1230.
37. Allcock, H. R.; de Denu, C. R.; Prange, R.; Laredo, W. R., Synthesis of norbornenyl telechelic polyphosphazenes and ring-opening metathesis polymerization reactions. *Macromolecules* **2001**, *34* (9), 2757-2765.
38. Colak, S.; Nelson, C. F.; Nußlein, K.; Tew, G. N., Hydrophilic modifications of an amphiphilic polynorbornene and the effects on its hemolytic and antibacterial activity. *Biomacromolecules* **2009**, *10* (2), 353-359.

39. Sutthasupa, S.; Shiotsuki, M.; Masuda, T.; Sanda, F., Alternating ring-opening metathesis copolymerization of amino acid derived norbornenemonomers carrying nonprotected carboxy and amino groups based on acid-base interaction. *J. Am. Chem. Soc.* **2009**, *131* (30), 10546-10551.
40. Liaw, D.-J.; Tsai, J.-S.; Wu, P.-L., Polynorbornene with cross-linkable side chains via ring-opening metathesis polymerization. *Macromolecules* **2000**, *33* (19), 6925-6929.
41. Hilf, S.; Grubbs, R. H.; Kilbinger, A. F. M., End capping ring-opening olefin metathesis polymerization polymers with vinyl lactones. *J. Am. Chem. Soc.* **2008**, *130* (33), 11040-11048.
42. Wu, Z.; Benedicto, A. D.; Grubbs, R. H., Living ring-opening metathesis polymerization of bicyclo[3.2.0]heptene catalyzed by a ruthenium alkylidene complex. *Macromolecules* **1993**, *26* (18), 4975-4977.
43. Risse, W.; Grubbs, R. H., Block and graft copolymers by living ring-opening olefin metathesis polymerization. *J. Mol. Catal.* **1991**, *65* (1-2), 211-217.
44. Schrock, R. R.; Fellmann, J. D., Multiple metal-carbon bonds. 8. Preparation, characterization, and mechanism of formation of the tantalum and niobium neopentylidene complexes, $M(CH_2CMe_3)_3(CHCMe_3)$. *J. Am. Chem. Soc.* **1978**, *100* (11), 3359-3370.
45. Klavetter, F. L.; Grubbs, R. H., Polycyclooctatetraene (polyacetylene): synthesis and properties. *J. Am. Chem. Soc.* **1988**, *110* (23), 7807-7813.
46. Schrock, R. R.; Murdzek, J. S.; Bazan, G. C.; Robbins, J.; DiMare, M.; O'Regan, M., Synthesis of molybdenum imido alkylidene complexes and some reactions involving acyclic olefins. *J. Am. Chem. Soc.* **1990**, *112* (10), 3875-3886.
47. (a) Schwab, P.; France, M. B.; Ziller, J. W.; Grubbs, R. H., A Series of well-defined metathesis catalysts: Synthesis of $[RuCl_2(=CHR')(PR_3)_2]$ and its reactions. *Angewandte Chemie International Edition in English* **1995**, *34* (18), 2039-2041;
(b) Schwab, P.; Grubbs, R. H.; Ziller, J. W., Synthesis and applications of $RuCl_2(CHR')(PR_3)_2$: The influence of the alkylidene moiety on metathesis activity. *J. Am. Chem. Soc.* **1996**, *118* (1), 100-110.
48. Bielawski, C. W.; Grubbs, R. H., Highly efficient ring-opening metathesis polymerization (ROMP) using new ruthenium catalysts containing-heterocyclic carbene ligands. *Angew. Chem.* **2000**, *112* (16), 3025-3028.

49. (a) Sanford, M. S.; Love, J. A.; Grubbs, R. H., A versatile precursor for the synthesis of new ruthenium olefin metathesis catalysts. *Organometallics* **2001**, *20* (25), 5314-5318; (b) Love, J. A.; Morgan, J. P.; Trnka, T. M.; Grubbs, R. H., A practical and highly active ruthenium based catalyst that effects the cross metathesis of acrylonitrile. *Angew. Chem. Int. Ed.* **2002**, *41* (21), 4035-4037.
50. Slugovc, C., Ring opening metathesis polymerisation in donor solvents. *Chemical Communications (Cambridge, England)* **2002**, (21), 2572-2573.
51. Slugovc, C., The ring opening metathesis polymerisation toolbox. *Macromolecular Rapid Communications*. **2004**, *25* (14), 1283-1297.
52. Slugovc, C., The ring opening metathesis polymerisation toolbox. *Macromol. Rapid Commun.* **2004**, *25* (14), 1283-1297.
53. Nguyen, S. T.; Grubbs, R. H.; Ziller, J. W., Syntheses and activities of new single-component, ruthenium-based olefin metathesis catalysts. *J. Am. Chem. Soc.* **1993**, *115* (21), 9858-9859.
54. Sanford, M. S. S., New insights into the mechanism of ruthenium-catalyzed olefin metathesis reactions. *J. Am. Chem. Soc.* **2001**, *123* (4), 749-750.
55. Espinosa, L. M., Organometallics and renewables olefin metathesis of renewable platform Chemicals. *Topics in Organometallic Chemistry* **2012**, *39*, 1-44.
56. (a) Murphy, J. J.; Furusho, H.; Paton, R. M.; Nomura, K., Precise synthesis of poly(macromonomer)s containing sugars by repetitive ROMP and their attachments to Poly(ethylene glycol): Synthesis, TEM analysis and their properties as amphiphilic block fragments. *Chemistry – A European Journal* **2007**, *13* (32), 8985-8997; (b) Murphy, J. J. J., Precise synthesis of poly(macromonomer)s containing sugars by repetitive ring-opening metathesis polymerisation. *Chemical communications (Cambridge, England)* **2005**, (32), 4080.
57. Tlenkopatchev, M. A.; Vargas, J.; Lapez-Gonzalez, M. D. M.; Riande, E., Gas transport in polymers prepared via metathesis copolymerization of *exo-N*-phenyl-7-oxanorbornene-5,6-dicarboximide and norbornene. *Macromolecules* **2003**, *36* (22), 8483-8488.
58. Lehman, S. E.; Wagener, K. B., Comparison of the kinetics of acyclic diene metathesis promoted by Grubbs ruthenium olefin metathesis catalysts. *Macromolecules* **2002**, *35* (1), 48-53.

59. (a) Opper, K. L.; Wagener, K. B., ADMET: Metathesis polycondensation. *J. Polym. Sci., Part A: Polym. Chem.* **2011**, *49* (4), 821-831; (b) Mutlu, H.; de Espinosa, L. M.; Meier, M. A. R., Acyclic diene metathesis: a versatile tool for the construction of defined polymer architectures. *Chem. Soc. Rev.* **2011**, *40* (3), 1404-1445.
60. Enholm, E. J., Acyclic diene metathesis reactions of carbohydrates. *Synlett* **2009**, (15), 2539.
61. Grubisic, Z.; Rempp, P.; Benoit, H., A universal calibration for gel permeation chromatography. *Journal of Polymer Science Part B: Polymer Letters* **1967**, *5* (9), 753-759.
62. Hill, S. J., Handbook of HPLC *Appl. Organomet. Chem.* **2000**, *14* (2), 130-131.
63. Ravikumar, V. T.; Kumar, R. K.; Olsen, P.; Moore, M. N.; Carty, R. L.; Andrade, M.; Gorman, D.; Zhu, X.; Cedillo, I.; Wang, Z.; Mendez, L.; Scozzari, A. N.; Aguirre, G.; Somanathan, R.; Berneels, S., UnyLinker: An efficient and scaleable synthesis of oligonucleotides utilizing a universal linker molecule: A novel approach to enhance the purity of drugs. *Organic Process Research & Development* **2008**, *12* (3), 399-410.
64. Abenham, D., Selective alkylations of 1,4:3,6-dianhydro-d-glucitol (isosorbide). *Carbohydr. Res.* **1994**, *261* (2), 255-266.
65. Guillaneuf, Y.; Castignolles, P., Using apparent molecular weight from SEC in controlled/living polymerization and kinetics of polymerization. *J. Polym. Sci., Part A: Polym. Chem.* **2008**, *46* (3), 897-911.
66. Ravikumar, V. T.; Krishna Kumar, R.; Zhu, X., Convenient large-scale synthesis of universal solid support. *Synth. Commun.* **2006**, *36* (16), 2269-2274.

APPENDIX A
SPECTRAL DATA OF COMPOUNDS

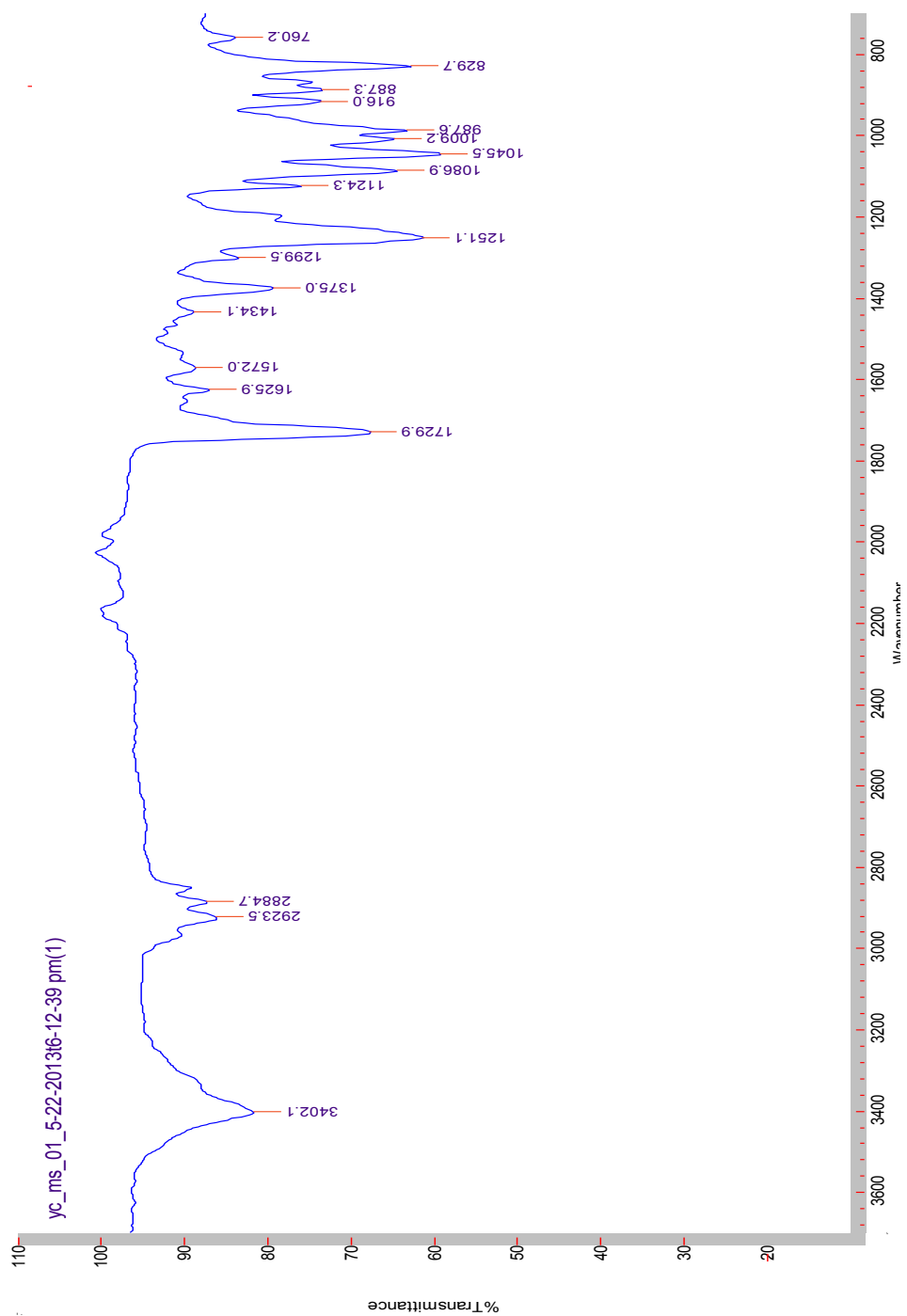
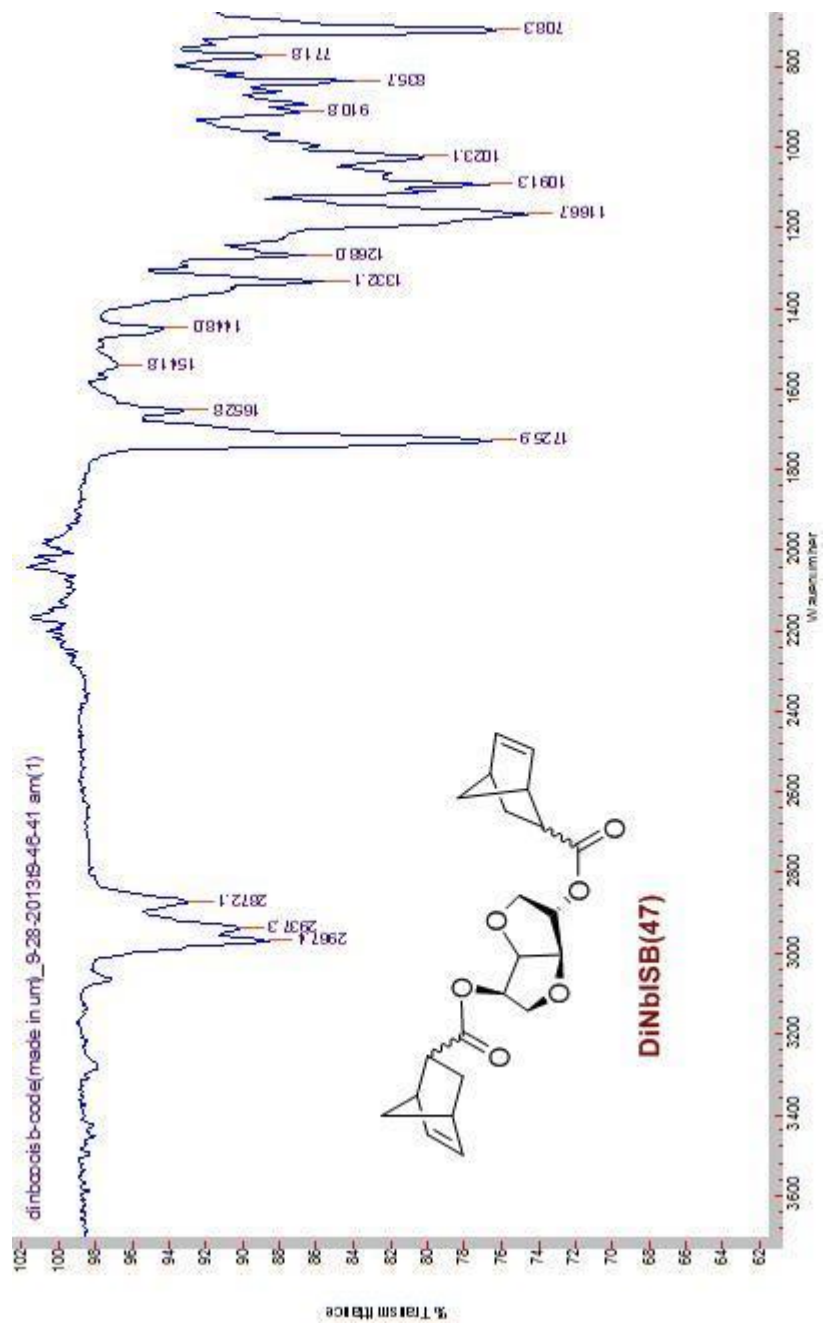


Figure A.1 FT-IR of 2-exo-acetyl-D-isosorbide (2AcISB) (**44**).



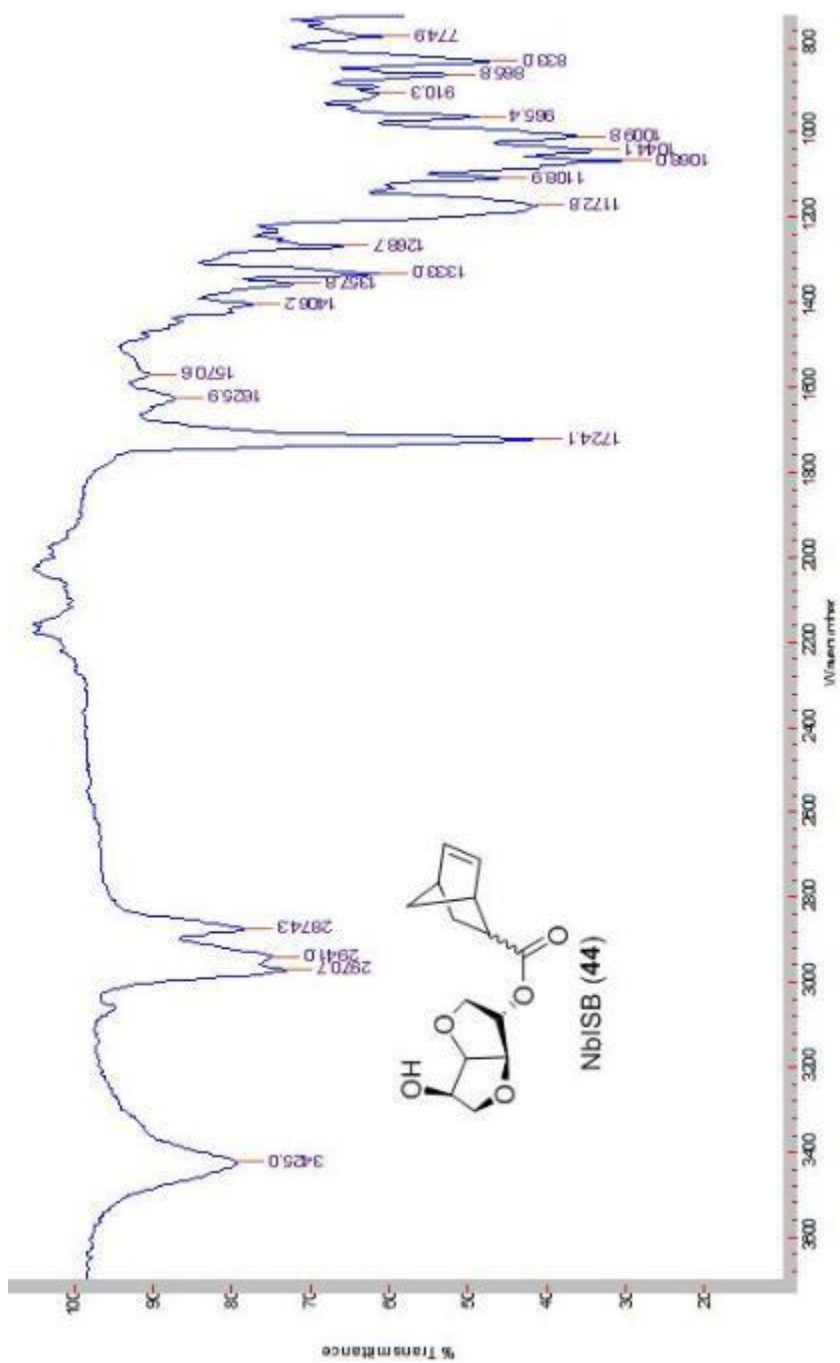


Figure A.3 FT-IR spectrum of (2-exo-D-isosorbyl)-5-norbomen-2-carboxylate (NbISB) (46).

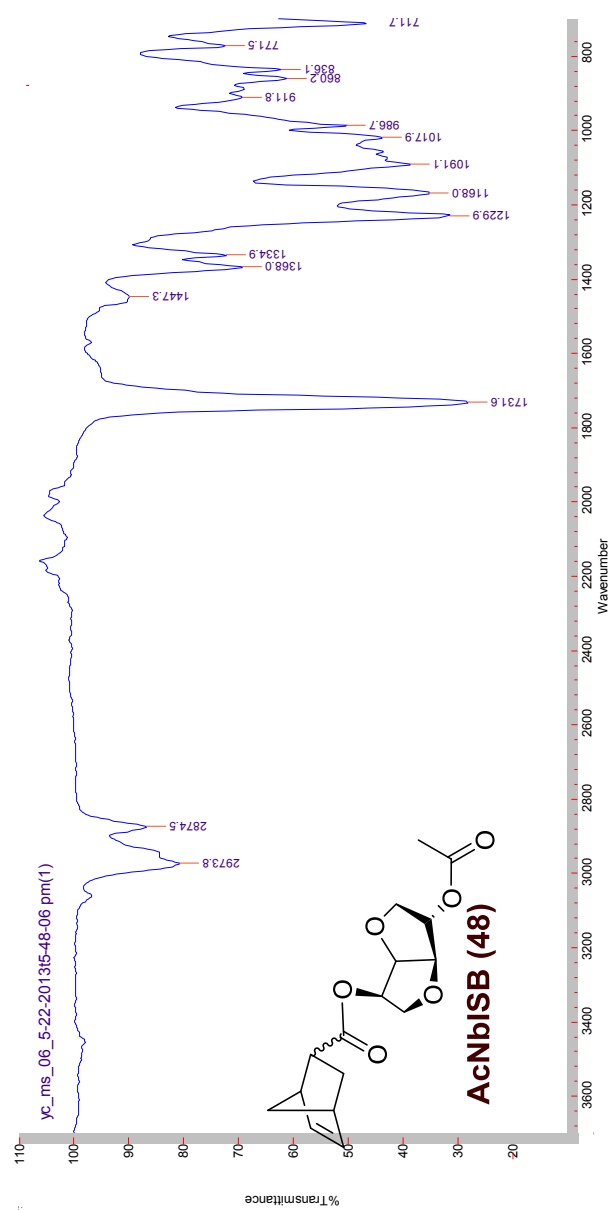


Figure A.4 FT-IR spectrum of [(2-*exo*-acetyl)-5-*endo*-D-isosorbyl]-di-5-norbornen-2-carboxylate (AcNbISB) (48)

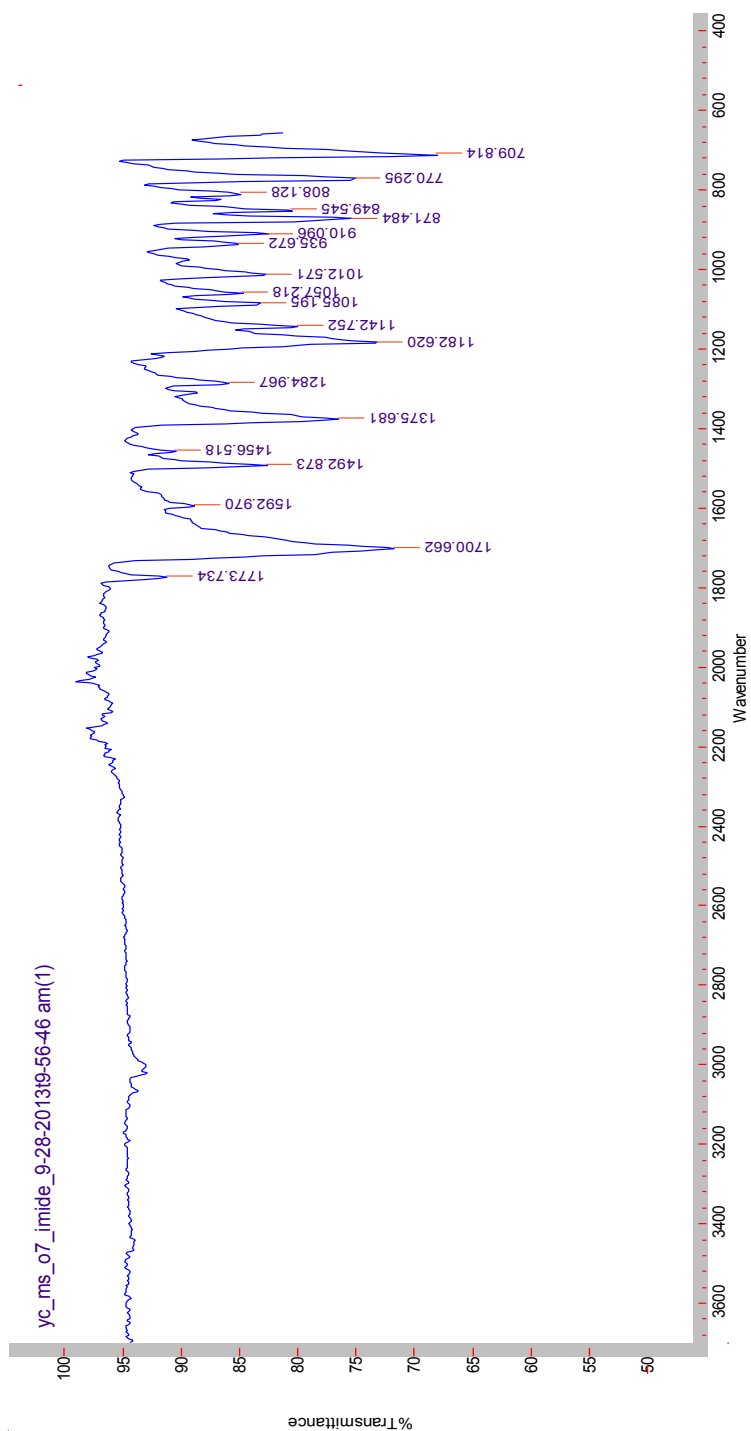


Figure A.5 FT-IR spectrum of *exo*-*N*-Phenyl-7-oxanorbornene-5,6-dicarboximide (NbIMPh) (51).

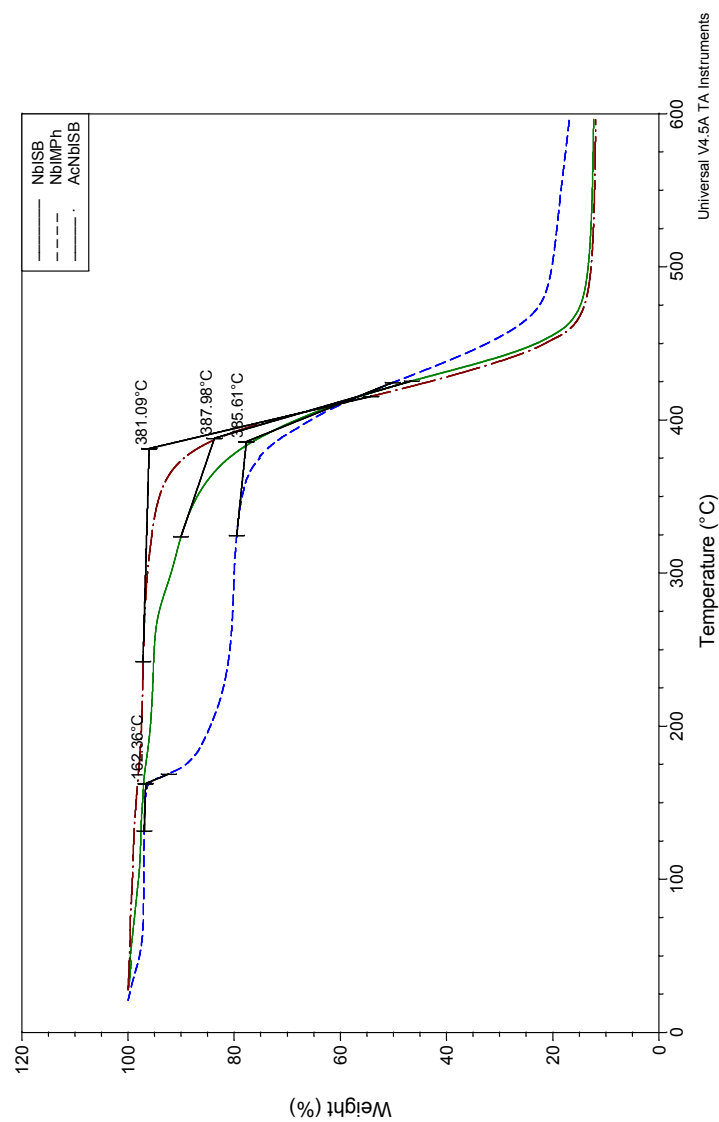


Figure A.6 TGA analysis of NbISB (64), AcNbISB (65) and NbIMPh (66).

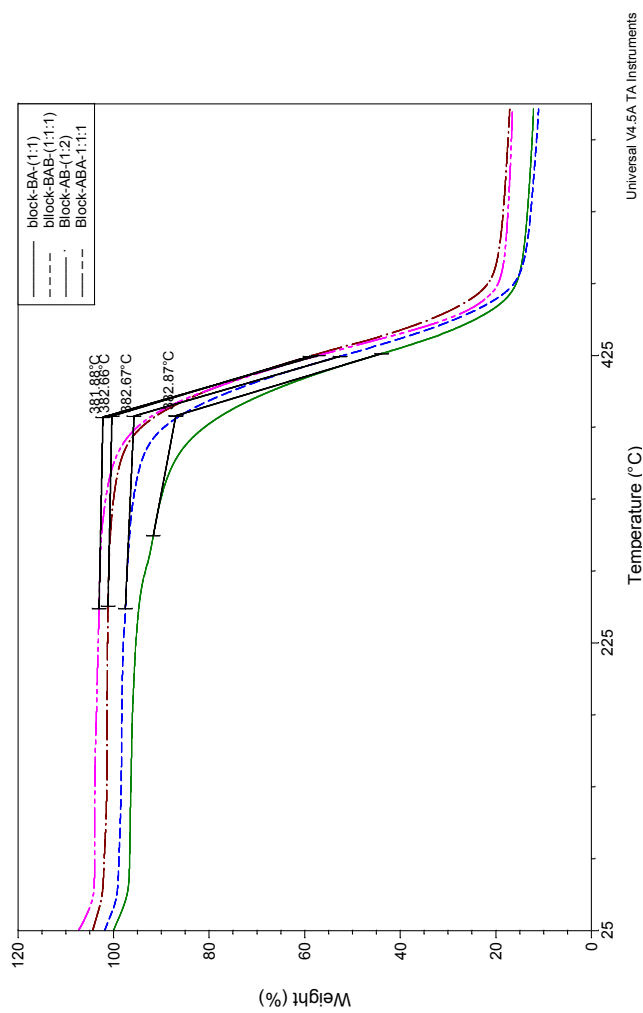


Figure A.7 TGA analysis of block polymers AB (82), BA (84), ABA (87) and BAB (90).

All the block polymers showed similar onset of degradation.

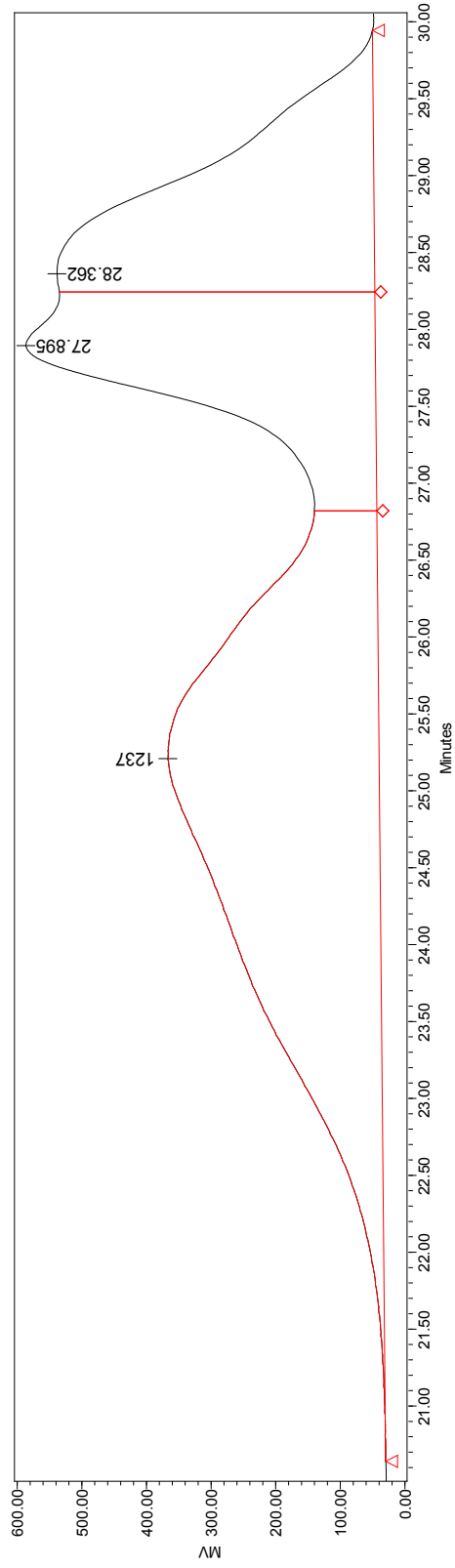


Figure A.8 GPC trace of sample, ADMET polymer **52** with 3 peaks identified, and only one peak lies on the calibration curve.

16 The two other peaks are outside of the calibration.

Table A.2 The processed data for the above GPC trace with the different molecular weights, elution time, peak area, and peak height.

Retention Time (min)	Mn (Da)	Mw (Da)	MP (Da)	Mz (Da)	Mz+1 (Da)	Polydispersity	Mz/Mw	Mz+1/Mw	Area (mV*min)	% Area	Height (mV)	% Height
25.209	1194	2899	1237	6442	10868	2.427376	2.222206	3.748856	55630229	51.17	327025	24.06
27.895									26422349	24.31	540704	39.78
28.362									26656509	24.52	491579	36.16